NACA

RESEARCH MEMORANDUM

[redacted] ubject

THE ORIGIN AND DISTRIBUTION OF SUPERSONIC STORE INTERFERENCE FROM MEASUREMENT OF INDIVIDUAL FORCES ON SEVERAL WING-FUSELAGE-STORE CONFIGURATIONS

IV.- DELTA-WING HEAVY-BOMBER CONFIGURATION WITH LARGE STORE. MACH NUMBER, 1.61

By Odell A. Morris

Langley Aeronautical Laboratory
Langley Field, Va.

NATIONAL ADVISORY COMMITTEE
FOR AERONAUTICS

WASHINGTON
December 15, 1955

NACA RM L55I27a

NATIONAL ADVISORY COMMITTEE FOR AERONAUTICS

RESEARCH MEMORANDUM

THE ORIGIN AND DISTRIBUTION OF SUPERSONIC STORE INTERFERENCE FROM MEASUREMENT OF INDIVIDUAL FORCES ON SEVERAL WING-FUSELAGE-STORE CONFIGURATIONS

IV.- DELTA-WING HEAVY-BOMBER CONFIGURATION WITH LARGE STORE. MACH NUMBER, 1.61

By Odell A. Morris

SUMMARY

A supersonic wind-tunnel investigation of the origin and distribution of store interference has been performed in the Langley 4- by 4-foot supersonic pressure tunnel at a Mach number of 1.6 in which separate forces on a store and on a 60° delta-wing—fuselage combination were measured. The store was separately mounted on its own five-component internal balance and was traversed through a wide range of spanwise, chordwise, and vertical positions. The configuration presented in this report simulates a heavy-bomber delta-wing airplane and has a large external symmetrical store that represents a nacelle having a frontal area equivalent to a twin-engine nacelle.

In general, the results indicated that the interference effects measured for the 60° delta-wing—fuselage combination were similar in character and magnitude to those previously reported for a 45° swept-wing—fuselage combination tested in the presence of the same store. However, the variation of the interference values of lift and drag with store chordwise position produced on the store by the 60° delta-wing—fuselage combination was somewhat smaller than the variation shown for the 45° swept-wing—fuselage combination. Also, the interference drag on the store produced by the presence of the wing and fuselage is explained in a qualitative way by using the "buoyancy" method which considers the pressure field of the wing and fuselage and the resultant buoyant forces on the store.

INTRODUCTION

At transonic and supersonic speeds, research on external stores and nacelles has shown that interference between the various components may incur large performance penalties (ref. 1). However, very little force breakdown data have been obtained from which the problem of store interferences might be understood. In order to furnish such information, a detailed experimental investigation of store interference has been undertaken in the Langley 4- by 4-foot supersonic pressure tunnel. Reference 2 describes in detail the investigation and presents the first phase of the program which includes store tests made in the presence of a 45° swept wing.

The results of store tests in the presence of a 60° delta-wing—fuselage combination at a Mach number of 1.6 are presented herein and include the aerodynamic characteristics of the semispan model (four components) and the individual forces and moment (five components) on the store. The semispan wing-fuselage model and store simulate a delta-wing heavy-bomber configuration with a large external store (a body of revolution having an equivalent frontal area of a twin-engine nacelle with no provision for internal flow). As in reference 2, the data are presented with a somewhat limited analysis in order to expedite publication.

SYMBOLS

$C_{D_{wf}}$ drag coefficient of wing-fuselage combination, $\frac{\text{Drag}}{qS}$

$C_{L_{wf}}$ lift coefficient of wing-fuselage combination, $\frac{\text{Lift}}{qS}$

$C_{m_{wf}}$ pitching-moment coefficient of wing-fuselage combination about $0.625\bar{c}$, $\frac{\text{Pitching moment}}{qS\bar{c}}$

$C_{l_{wf}}$ wing bending moment of wing-fuselage combination, $\frac{\text{Bending moment}}{qS\frac{b}{2}}$

C_{D_s} drag coefficient of store, $\frac{\text{Drag}}{qF}$

$C_{D_{B_s}}$ base drag coefficient of store, $P_{B_s}\frac{A}{F}$

[redacted]

C_{L_s} lift coefficient of store, $\frac{\text{Lift}}{qF}$

C_{m_s} pitching-moment coefficient of store about store nose or store midpoint as indicated, $\frac{\text{Pitching moment}}{qFl}$

C_{Y_s} side-force coefficient of store, $\frac{\text{Side force}}{qF}$

C_{n_s} yawing-moment coefficient of store about store nose or store midpoint as indicated, $\frac{\text{Yawing moment}}{qFl}$

C_{L_t} total lift coefficient of complete configuration (wing and fuselage plus store) based on wing area, $C_{L_{wf}} + C_{L_s}\left(\frac{F}{S}\right)$

C_{D_t} total drag coefficient of complete configuration (wing and fuselage plus store) based on wing area, $C_{D_{wf}} + C_{D_s}\left(\frac{F}{S}\right)$

$C_{L_{s_\alpha}}$ slope of variation of store lift coefficient with wing-fuselage angle of attack

$C_{Y_{s_\alpha}}$ slope of variation of store side-force coefficient with wing-fuselage angle of attack

P_{B_s} pressure coefficient on store base

$\bar{c}$ mean aerodynamic chord of wing, in.

α angle of attack measured with respect to free airstream, deg

S total area of wing semispan, 0.543 sq ft

F maximum frontal area of store, 0.0123 sq ft

A area of store base, 0.005 sq ft

q dynamic pressure, lb/sq ft

b/2 wing semispan, 9.5 in.

l store length, 12 in.

x chordwise position of store midpoint, measured from nose of fuselage (see fig. 1), in.

y spanwise position of store center line, measured from fuselage center line, in.

z vertical position of store center line, measured from wing chord plane, in.

β cotangent of Mach angle, $\sqrt{M^2 - 1}$

M Mach number

Subscripts:

f fuselage

w wing

s store

APPARATUS AND TESTS

Models and Equipment

The principal dimensions of the models and the general arrangement of the test setup are shown in figure 1. A list of the pertinent model dimensions is given in table I. The semispan wing-fuselage combination was designed to simulate a delta-wing heavy bomber-type airplane. The 60° delta wing and fuselage were constructed of metal and were mounted on a boundary-layer bypass plate $10\frac{3}{4}$ inches from the tunnel wall.

The fuselage and store are the same used in previous store tests and are described in detail in reference 2 together with a description of the test equipment, methods, and remarks on support interference. The delta-wing—fuselage model angle of attack was varied from 0° to 4° with the store angle of attack remaining constant at 0°. Tests were made with the store in the presence of the wing-fuselage model at various spanwise and chordwise positions and for vertical heights z of 1.15 inches, 1.67 inches, and 2.09 inches as shown in figure 1. All tests were run with boundary-layer transition fixed as described in reference 2, and with no store-support pylons or model tail surfaces.

The tests were performed in the 4- by 4-foot supersonic pressure tunnel at a Mach number of 1.61 and a corresponding Reynolds number per foot of 4.20×10^6.

[redacted]

Accuracy of Data

An estimate of the relative accuracy of the present data as determined from an inspection of repeat test points and static-deflection calibrations is presented below:

Store position:	
x, in.	±0.025
y, in.	±0.05
z, in.	±0.05
Store characteristics:	
C_{D_s}	±0.005
C_{L_s}	±0.010
C_{m_s}	±0.005
C_{Y_s}	±0.010
C_{n_s}	±0.005
α_s, deg	±0.2
Wing-fuselage:	
$C_{D_{wf}}$	±0.0005
$C_{L_{wf}}$	±0.005
$C_{m_{wf}}$	±0.002
$C_{l_{wf}}$	±0.002
α_{wf}, deg	±0.1

RESULTS AND DISCUSSION

Basic Data

Isolated store and wing-fuselage data.- The lift, drag, and pitching-moment coefficients for the isolated store at angles of attack up to 10° were obtained from references 2 and 3 and are presented in figure 2(a). Data are shown for tests made with the store pitched both in the plane of the normal-force beam and in the plane of the side-force beam; for as was pointed out in ref. 2, the store was rolled as the values of vertical height z were changed. The data thus obtained are shown to be within the stated accuracy of the tests. Also, the pitching-moment data are presented computed about the store nose and about the store midpoint; for the referenced interference data have been presented about both points.

Figure 2(b) presents the lift, drag, and pitching moment for the isolated fuselage and the isolated wing-fuselage combination for angles of attack up to 4°.

Chordwise plots of force coefficients.- The basic data for the store in the presence of the wing-fuselage combination are presented in figures 3 to 8. All store drag data have been corrected for free-stream static pressure at the base. Figures 9 to 14 show the corresponding basic data for the wing-fuselage combination in the presence of the store. The data are presented in the form of plots of coefficients against a chordwise position parameter $x - By$ which is a function of the position of the store midpoint and the inclination of the free-stream Mach line. A horizontal Mach line offset, which was discussed in detail in reference 2, permits the curves of the chordwise coefficient variation to be faired as a "family," and thus results in a more systematic fairing between test points. Offset vertical scales are used so that data for the 11 spanwise positions can be shown on a single figure. On the right and left margins, the zero for each curve is identified with the line symbol corresponding to the spanwise position. The spanwise or chordwise store positions at which measurements were obtained are identified by the appropriate symbol in a sketch drawn to scale on each figure.

Contour Plots

Contour plots of the aerodynamic forces and moments for selected configurations have been prepared from the basic data (figs. 3 to 14) and are presented in figures 15 to 25. For all the contour plots, the force or moment coefficient involved is plotted at the store midpoint for the various store locations.

Store drag.- Figure 15 shows the drag of the store (coefficient based on store frontal area) in the presence of the wing-fuselage combination. The influence of the wing-fuselage combination on the drag of the store is shown (fig. 15(a)) to increase the drag of the store about 60 percent in the vicinity of the wing midchord inboard positions. When the store is moved rearward toward the wing trailing edge and outboard toward the wing tip, the store drag values decrease toward the isolated store values. Favorable interference reduces the store drag behind the wing trailing edge. Figure 15(b) shows that increases in vertical displacement between the store and wing, in general, decrease the store drag for all store positions in the region of the wing plan form. Increasing the wing-fuselage angle of attack increases the store drag near the wing trailing edge when $z = 2.09$ (fig. 15(c)).

Store lift.- Contour plots of the store lift in the presence of the wing fuselage are presented in figure 16. In the vicinity of the wing

[redacted]

plan form, the data show large increases in store lift (fig. 16(a)), particularly for store positions inboard on the span. The increase in the store lift is probably caused by the negative pressure region beneath the wing plan form. The store lift forward and rearward of the wing plan form decreases and for some store positions becomes negative.

In general, increasing the displacement between the store and wing shows small decreases in store lift (fig. 16(b)). Effects of angle of attack on store lift indicate a small reduction in store lift inboard on the wing and an increase near the tip (fig. 16(c)).

Store pitching moment.- Contour plots of the store pitching moments in the presence of the wing and fuselage are presented in figure 17. Since the pitching moments for this figure are calculated about the store nose, the pitching-moment values shown are largely a result of lift on the store and, in general, show the same trends as previously described for lift.

Store side force.- The data of figure 18 show a contour plot of the store side force in the presence of the wing and fuselage. The data of figure 18(a) show a positive (inward) side force for all store positions on the wing plan form, except along the wing trailing edge. Increasing the vertical displacement between the store and wing shifts the region of negative side-force coefficients forward on the wing plan form somewhat (fig. 18(b)) but no major effects of vertical displacement are noted.

However, increasing the wing angle of attack (fig. 18(c)) causes large increases in store side force which will be discussed in more detail in subsequent figures.

Store yawing moment.- Contour plots of the store yawing-moment coefficients in the presence of the wing fuselage are presented in figure 19. The yawing-moment coefficients for this figure are also computed about the store nose and are largely a result of side force.

Wing-fuselage drag.- Contour plots of the wing-fuselage drag in the presence of the store are presented in figure 20 (coefficients based on wing area). The drag of the wing and fuselage shows an increase of approximately 0.0010 to 0.0015 due to store interference for both store vertical heights (figs. 20(a) and (b)) which is about a 13-percent drag increase over the isolated wing-fuselage drag (0.0115). Increasing the angle of attack to 4° (fig. 20(c)) raises the drag level due to angle-of-attack loading; however, the wing-fuselage drag due to store interference was about the same for store positions forward of the wing plan form with small increases shown for positions in the vicinity of the wing trailing edge.

Figure 21 shows the total drag for the complete configuration (wing and fuselage plus store). In the region of the wing plan form, the total drag varied from about 0.017 to 0.022 with the minimum values shown for store positions along the wing trailing edge and around the wing tip (fig. 21(a)). Maximum total drag is shown for store positions in the vicinity of the wing midchord inboard stations. Since the total drag for the isolated store and the isolated wing and fuselage is only 0.0172, at $\alpha = 0^\circ$ the maximum total drag (0.022) corresponds to an increase of approximately 28 percent due to mutual interference.

Increasing the vertical displacement between the store and wing lowers the increase in total drag for store positions in the region of the wing root (fig. 21(b)). Changing the angle of attack to 4° (fig. 21(c)) affects the total drag in a manner similar to the effects previously discussed for wing-fuselage drag.

Wing-fuselage lift.- The lift of the wing-fuselage combination in the presence of the store is presented in figure 22. With the store near the wing surface (fig. 22(a)), a positive lift interference occurs for all store positions rearward of about the wing center (about $0.5\bar{c}$) with maximum values shown inboard along the wing trailing edge. For store positions near the forward portion of the wing, negative lift-interference values were obtained. Increasing the vertical displacement between the wing and store tends to shift the negative lift-interference region forward somewhat (fig. 22(b)), but the magnitudes of the lift values remain about the same. Changes in lift interference due to angle of attack appear to be relatively small (fig. 22(c)).

Figure 23 shows the total lift of the complete configuration (wing and fuselage plus store). These data show only small variations from the results previously shown for the wing-fuselage lift, and thus indicate that the effects of store lift on total lift are relatively small.

Wing-fuselage pitching moments.- The data of figure 24 present the contour plots of the wing-fuselage pitching moments in the presence of the store (data computed about $0.625\bar{c}$). Figure 24(a) shows that for store positions in the proximity of the wing ($z = 1.15$) maximum positive pitching moments occur in the vicinity of the inboard midchord stations. For store positions along the wing trailing edge and forward of the wing leading edge, the pitching moments decrease to zero. Increasing the store vertical height (fig. 24(b)) decreases the magnitude of the pitching moments and shifts the region of maximum values forward somewhat. The pitching moments were increased approximately 0.026 due to 4° angle-of-attack loading (fig. 24(c)), but the effects of store interference on the pitching moments remained about the same.

Wing-root bending moments.- Contour plots of the wing-root bending moments are shown in figure 25 (data computed about model center line).

[redacted]

The bending-moment contours (fig. 25(a)) are similar to the wing-fuselage lift contours insofar as positive bending moments occur for store positions rearward of about the wing center and change to negative bending moments on the forward portion of the wing. Increasing the store vertical displacement (fig. 25(b)) tends to move the region of positive interference forward on the wing, but the magnitudes of the bending moments show only small differences. The peak values of bending moments shown, about 0.024, correspond to that produced by approximately 1° angle of attack. The contour plot of figure 25(c) shows that increasing the angle of attack to 4° causes no appreciable changes in the incremental bending-moment values for store positions in the vicinity of the wing plan form.

Pressure Field Analysis

As indicated in reference 2, there is a need for more experimental and theoretical studies of the interferences of actual airplane configurations. Therefore, it appears that a simple understanding of the sources and distribution of the interference effects of specific configurations would be useful, particularly with regard to drag. Thus, the drag data have been analyzed accordingly by using the qualitative "buoyancy" method outlined in reference 2.

Store drag in presence of wing fuselage.- The effect of the wing-fuselage pressure field on store drag for two spanwise stations may be seen in figure 26. The only static-pressure measurements taken in the flow field were at the base of the store. The difference between base pressure of the store in presence of the wing and fuselage and that of the isolated store is indicative of the mutual interference effects at the base. The incremental pressures obtained at the base of the store were found to vary approximately as the theoretical flow field pressures for isolated delta wings in reference 4; so these incremental pressures were used for the present qualitative study of the store interference effects. The variation of the store plus interference drag can be shown by simply mapping this flow field into positive and negative pressure-coefficient regions as shown in figure 26. The increase or decrease in the store-drag curve over or below that of the isolated store drag can be explained in a qualitative way by simple "buoyancy considerations." That is, the values of store drag above the isolated store values are a result of the presence of the store afterbody in a region of negative pressure and the presence of the store nose in a region of positive pressure with peak drag values resulting from a combination of these pressures on the store. The values of drag below those for the isolated store can similarly be explained by negative pressures on the store nose or positive pressures on the store afterbody.

An attempt was made to compute the store drag by the buoyancy method of reference 2 using the pressure-field information of figure 26. The

store drag values calculated for the spanwise stations of figure 26 ($y = 5.4$ and $y = 7.8$) showed poor agreement with the measured store drag, and therefore the values are not shown. No extensive calculations were attempted because the pressure-field information was somewhat limited. Thus, it appears that a more complete survey of the flow field than was obtained in these tests, preferably obtained by more exact methods of measurement, would be required to predict the store drag with any degree of accuracy.

Drag of wing and fuselage in presence of store.- The variation of the wing-fuselage drag with chordwise store position for four spanwise stations is shown in figure 27. The position of the local wing section with respect to the store and its pressure field (ref. 2) for a number of points on the curve is shown in the sketches. As before, the drag of the wing and fuselage above or below the isolated value is explained by the position of the local wing-chord section in the positive or negative pressure field of the store. In general, high drags are a result of positive pressures over the forward portion of the wing section, or negative pressures over the rearward portion of the wing section, or a combination of both. Although only local chordwise effects are illustrated, the same observations can be made by mapping the flow field over that part of the wing plan form affected by the store pressure field.

Thus, it is shown that the method used in reference 2 to explain the mutual interference drag of a swept wing and a store is also applicable to the case of the delta-wing configuration.

Effect of Store Vertical Displacement and Wing-Fuselage Angle of Attack

Effect of store vertical displacement z.- The effects of vertical displacement between the store and wing on the store and wing forces and moments are summarized in figure 28 to 37 for four spanwise stations. The store moments for these figures were calculated about the store midpoint. As was previously noted in the discussion of the contour plots, figures 28 to 37 indicate that the effects of store vertical height on the measured store and wing-fuselage forces and moments are relatively small or negligible except for store drag and store lift which showed significant changes for some store positions. Similar results due to the effects of store vertical displacement were also shown in references 2 and 3 for the swept-wing configuration.

Effect of wing-fuselage angle of attack.- The effects of the wing-fuselage angle of attack on the store forces and moments are presented in figures 38 to 44. It should be noted that the store angle of attack remained at 0° when the wing-fuselage angle of attack was changed. The

values of the store data, therefore, represent only the interference values; and thus in applying these data for angles of attack other than zero, the effects of store angle of attack must also be considered.

Figure 38 shows that increasing the wing angle of attack to 4° increases the store interference drag considerably for store position along the wing trailing edge. However, for inboard store positions on the forward portion of the wing plan form, increasing the angle of attack decreases the store drag somewhat.

The effects of angle of attack of the wing-fuselage combination on store lift are shown in figure 39. Increasing the angle of attack to 4° (fig. 39) decreases the store lift considerably for inboard spanwise store positions on the wing plan form. This result, as pointed out in reference 2, was probably due to increased intensity in the positive pressure region ahead of the wing leading edge which is to be expected with increased angle of attack.

The contour map of $C_{L_{s_\alpha}}$ in figure 40 for angles of attack up to 4° (linear variation between 0° and 4°) shows that wing lift changes store interference lift in a negative direction for store positions over a range slightly larger than the wing plan form except for store positions in the vicinity of wing tip. For the region around the wing tip, some increase in store lift was noted which probably resulted from the effects of tip vortices.

The data of figures 41 and 42 indicate large increases in store side force with increases in angle of attack. The contour plot $C_{Y_{s_\alpha}}$ (linear variation between 0° and 4°) shows that the maximum increase in side force occurs in the vicinity of the wing tip. This is as expected since the intensity of the spanwise flow increases toward the tip. The small change in vertical height which occurs when the wing-fuselage angle of attack is changed is small and has little effect upon the side-force loads now being considered.

Although the contour plot $C_{Y_{s_\alpha}}$ (fig. 42) was prepared from data limited to 4° angle of attack, these data indicate that, for higher angles of attack, the side-force loads on the store or pylon would continue to increase and become critical. This has been shown to be true for a similar delta-wing configuration tested in the 9- by 12-inch blowdown tunnel for angles of attack up to 10° (ref. 5). A comparison of the data of the two investigations was made in figure 9 of reference 6 and showed good agreement between the results. Also, as was pointed out in reference 6, the comparison indicated that the side-force data from the present tests might be cautiously extrapolated to higher angles of attack using the 9- by 12-inch blowdown tunnel data as a guide.

Figures 43 and 44 show the effect of angle of attack on store pitching moment and yawing moment, respectively, to be measurable, but small. Figure 44 also shows but little variation of store yawing moment with store chordwise or spanwise positions. However, the store yawing-moment data of reference 3 for tests on a 45° swept wing also indicated similar results.

The data of figures 45 and 46 show the effects of angle of attack on wing-fuselage drag and total drag (wing and fuselage plus store), respectively. Figures 47 to 49 illustrate the effects of angle of attack on wing-fuselage lift, total lift (wing and fuselage plus store), and pitch, respectively. Although the data for each of these figures show that the curves were displaced considerably due to angle-of-attack loading, the variations with store chordwise position are similar in shape and in magnitudes of changes shown. Thus, in general, the figures show that the interferences of the store on the wing-fuselage combination are little affected by wing angle of attack and appear to depend primarily upon store position. A similar result was found for the swept wing of reference 3.

Relative Contribution of the Store and the Wing and Fuselage Toward Total Drag and Lift

Figures 50 and 51 show the drag and lift for the store (based on wing area), the wing-fuselage combination, and the sum of these two which is the total for the complete model plotted against store chordwise position. The data of figure 50 show that the maximum drag for both the store and the wing and fuselage occurs at about the same store chordwise positions (between $x = 20$ to 24), thus causing high peaks in the total drag curves. Similar results were also noted in reference 2 for the swept-wing configuration; however, the drag-curve peaks were somewhat more pronounced and slightly farther rearward (about stations $x = 24$ to $x = 28$). Figure 51 shows that the store lift (based on wing area) is very small and consequently it contributes only a small part toward the total lift.

Comparison of Store and Wing-Fuselage Forces for the Swept- and Delta-Wing Combinations

Figure 52 shows a comparison of the contour plots of the store drag and total drag ($\alpha = 0°$, $z = 2.09$) for the 60° delta-wing combination and a 45° swept-wing combination (refs. 2 and 3). Although the wing plan forms differed markedly in sweep, aspect ratio, and thickness ratio, the interference values of store drag produced on the store by both model

[redacted]

combinations were of comparable magnitudes and, in general, showed similar trends. The maximum store drag for store positions in the vicinity of the wing occurred for both models inboard on the wing plan form. However, the data of reference 2 for the swept wing indicated that the fuselage has a significant effect on the store interference drag for some inboard store positions, and thus should not be neglected in making comparisons. The contour plots for total drag show a considerably higher drag level for the 45° swept wing, and the magnitudes of the incremental drag variation due to store interferences are approximately twice the incremental values shown by the delta wing in the vicinity of the wing plan forms. Also, the variation of total drag with store spanwise position appears to be somewhat larger for the 45° swept wing.

Comparisons of the contour plots of the store lift for the delta and the swept wing are shown in figure 53. The data show that the magnitudes of store lift for both wing-fuselage combinations were of comparable magnitudes; however, the values were slightly larger for some store positions in the presence of the swept wing. Contour plots of the total lift (wing and fuselage plus store) show that maximum total lift interference occurred on both wings for store positions in the vicinity of the wing plan form along the wing trailing edge near the inboard stations. The magnitudes of the maximum total lift interference in this region are slightly larger for the swept wing (about 0.01) as a result of the slightly higher store lift values.

A comparison of the contour plot of the store side-force slope coefficient $C_{Y_{s_\alpha}}$ for the two wings can be found in reference 6 (z = 2.09). These data indicate that the highest side-force loads are obtained at the tip for both wings and the coefficients show values of comparable magnitudes. Further, the comparison showed the chordwise variation of $C_{Y_{s_\alpha}}$ to be essentially zero in the case of the delta wing, whereas the swept wing showed considerable chordwise variation of $C_{Y_{s_\alpha}}$.

CONCLUSIONS

A supersonic wind-tunnel investigation has been conducted in the Langley 4- by 4-foot supersonic pressure tunnel at a Mach number of 1.6 in which separate forces were measured on a store and on a 60° delta-wing—fuselage combination for a wide range of store positions. The results are compared with similar tests of the store in the presence of a 45° swept-wing—fuselage combination (refs. 2 and 3) and indicate the following conclusions:

[redacted]

1. Large changes in store and wing-fuselage forces and moments may occur for both wing-fuselage combinations with small changes in store spanwise or chordwise positions.

2. The store positions for high drag with both complete configurations (wing and fuselage plus store) were in the vicinity of the wing inboard spanwise stations.

3. The interference drag on the store produced by the presence of the wing and fuselage is explained in a qualitative way by using the "buoyancy" method which considers the pressure field of the wing and fuselage and the resultant buoyant forces on the store.

4. Increasing the wing-fuselage angle of attack caused large changes in store lift and side force with both wing-fuselage combinations, but resulted in only small changes on the measured store moments. The interferences of the store on the wing-fuselage combinations were little affected by wing-fuselage angle of attack and appear to depend primarily upon store position.

5. The interference values produced on the store by the delta-wing— and swept-wing—fuselage combinations were of comparable magnitudes at 0° angle of attack for lift and for drag. However, the variation of these forces with store chordwise position was greater for the swept-wing combination.

Langley Aeronautical Laboratory,
National Advisory Committee for Aeronautics,
Langley Field, Va., September 12, 1955.

[redacted]

REFERENCES

1. Smith, Norman F., Bielat, Ralph P., and Guy, Lawrence D.: Drag of External Stores and Nacelles at Transonic and Supersonic Speeds. NACA RM L53I23b, 1953.

2. Smith, Norman F., and Carlson, Harry W.: The Origin and Distribution of Supersonic Store Interference From Measurement of Individual Forces on Several Wing-Fuselage-Store Configurations. I.- Swept-Wing Heavy-Bomber Configuration With Large Store (Nacelle). Lift and Drag; Mach Number, 1.61. NACA RM L55A13a, 1955.

3. Smith, Norman F., and Carlson, Harry W.: The Origin and Distribution of Supersonic Store Interference From Measurement of Individual Forces on Several Wing-Fuselage-Store Configurations. II.- Swept-Wing Heavy-Bomber Configuration With Large Store (Nacelle). Lateral Forces and Pitching Moments; Mach Number, 1.61. NACA RM L55E26a, 1955.

4. Roper, G. M.: The Pressure Distribution, (According to the Linear Theory), on the Ground Due to a Delta Wing in Steady Level Supersonic Flight. Tech. Note No. Aero 2332, British R. A. E., Nov. 1954.

5. Guy, Lawrence D.: Loads on External Stores at Transonic and Supersonic Speeds. NACA RM L55E13b, 1955.

6. Smith, Norman F., and Carlson, Harry W.: Some Effects of Configuration Variables on Store Loads at Supersonic Speeds. NACA RM L55E05, 1955.

TABLE I.- PERTINENT MODEL DIMENSIONS

Store:	
Maximum diameter, in.	1.5
Maximum frontal area, sq ft	0.0123
Base diameter, in.	0.96
Base area, sq ft	0.005
Overall length, in.	12
Nose fineness ratio	3
Afterbody fineness ratio	1.82
Overall fineness ratio	8
Ratio of wing area to store maximum frontal area	44.2
Fuselage:	
Maximum diameter, in.	2.75
Maximum frontal area (semicircle), sq ft	0.0206
Base diameter, in.	1.372
Base area (semicircle), sq ft	0.0051
Overall length, in.	35.75
Nose fineness ratio	4.75
Afterbody fineness ratio	3
Overall fineness ratio	13
60° Delta Wing:	
Semispan, in.	9.5
Mean aerodynamic chord, in.	10.97
Area (semispan), sq ft	0.543
Aspect ratio	2.31
Center-line chord, in.	16.454
Section	NACA 65A-004

[redacted]

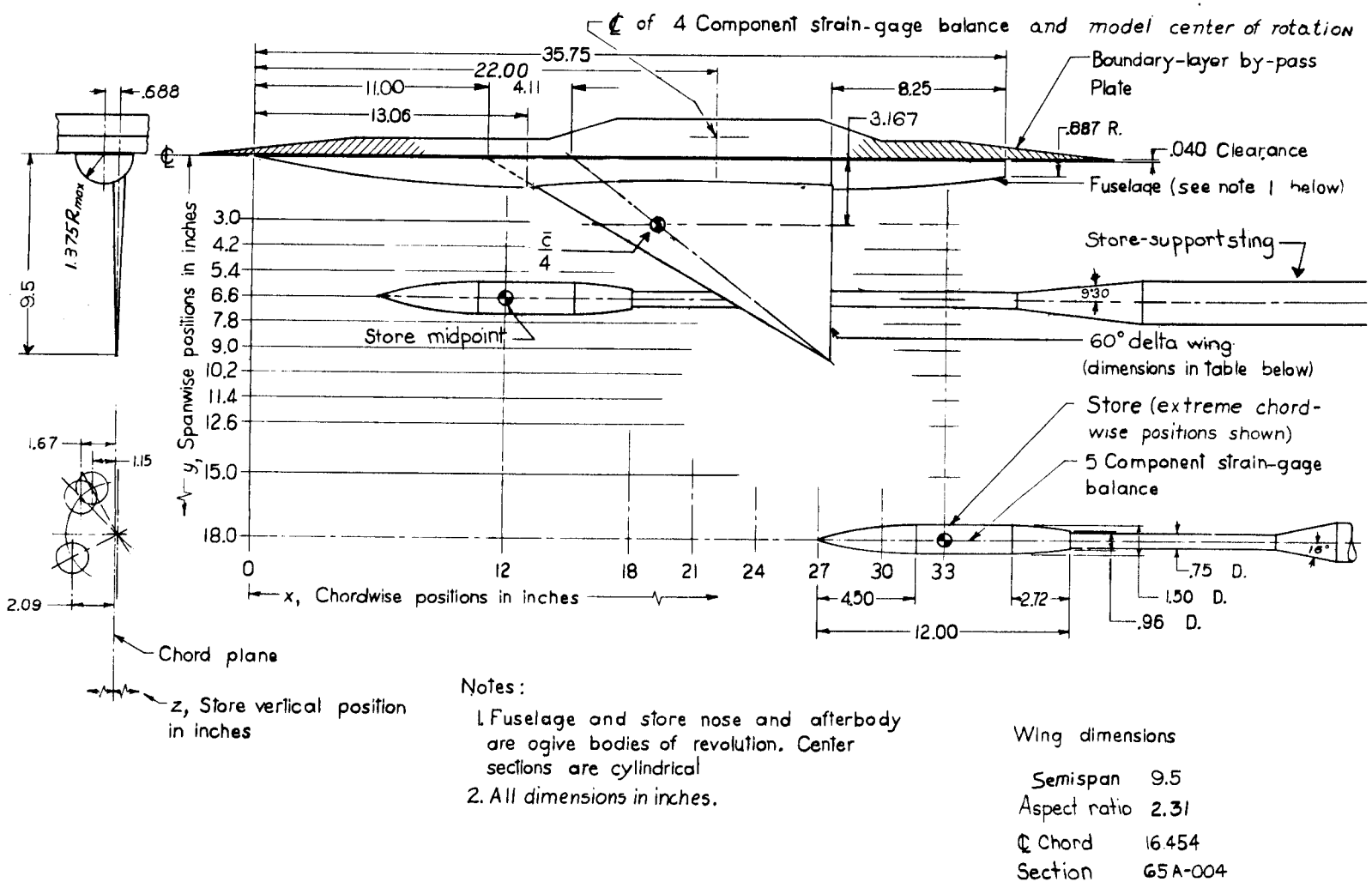

Notes:

1. Fuselage and store nose and afterbody are ogive bodies of revolution. Center sections are cylindrical
2. All dimensions in inches.

Wing dimensions

Semispan	9.5
Aspect ratio	2.31
℄ Chord	16.454
Section	65A-004

Figure 1.- Layout of models showing dimensions of components and ranges of store positions investigated.

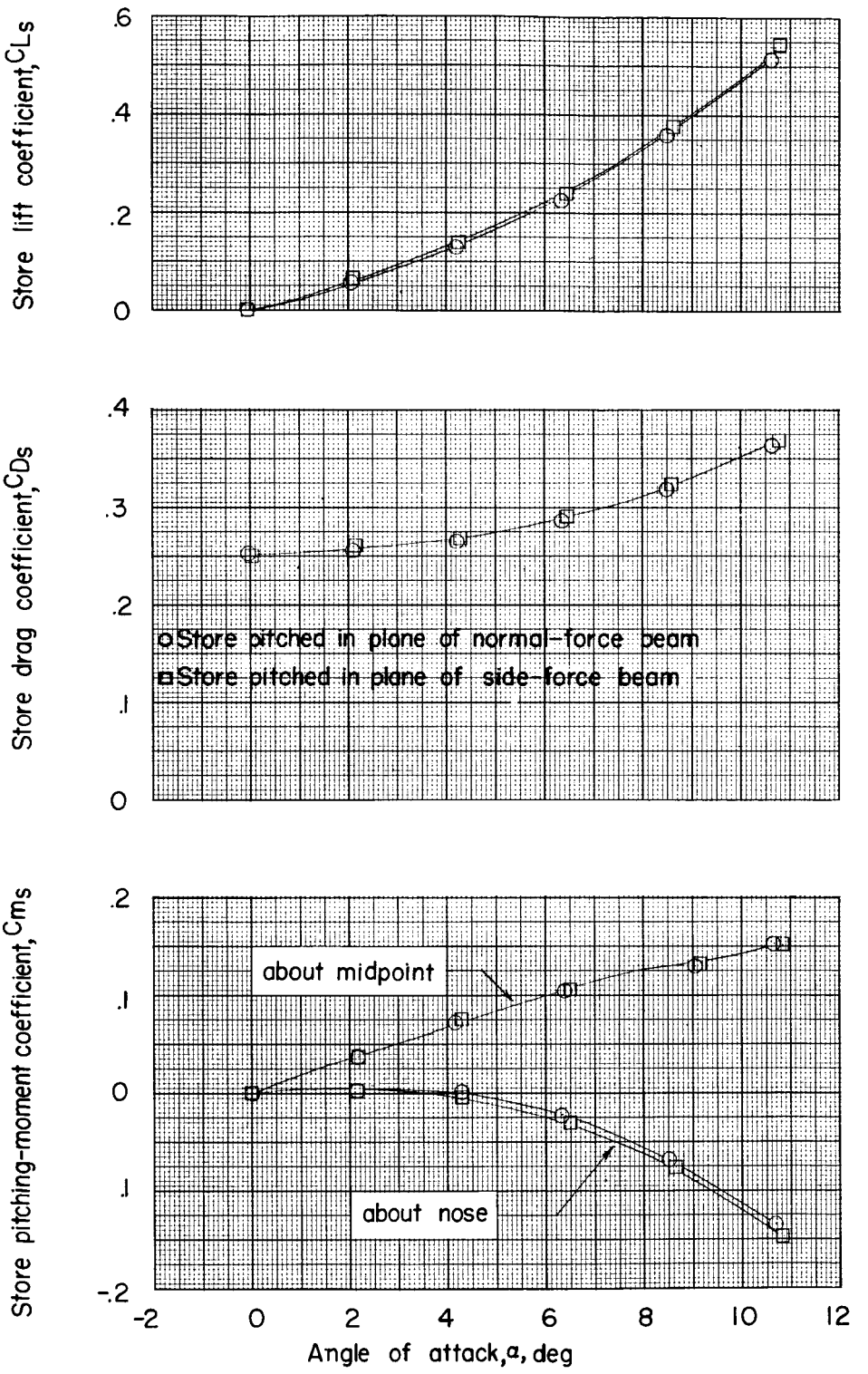

(a) Store lift, drag, and pitching moment.

Figure 2.- Aerodynamic characteristics of the isolated configuration components.

[redacted]

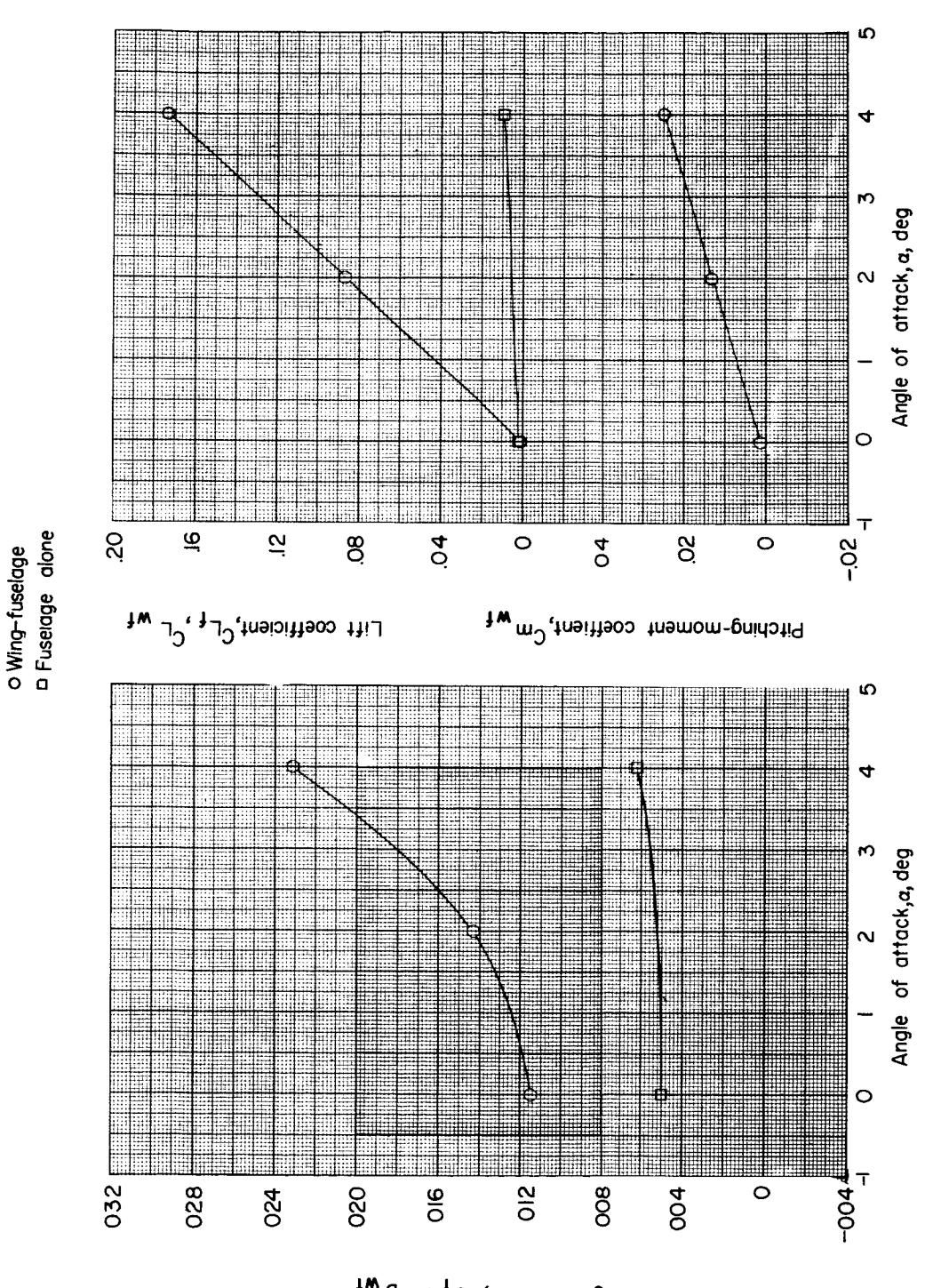

(b) Fuselage and wing-fuselage drag, lift, and pitching moment.

Figure 2.- Concluded.

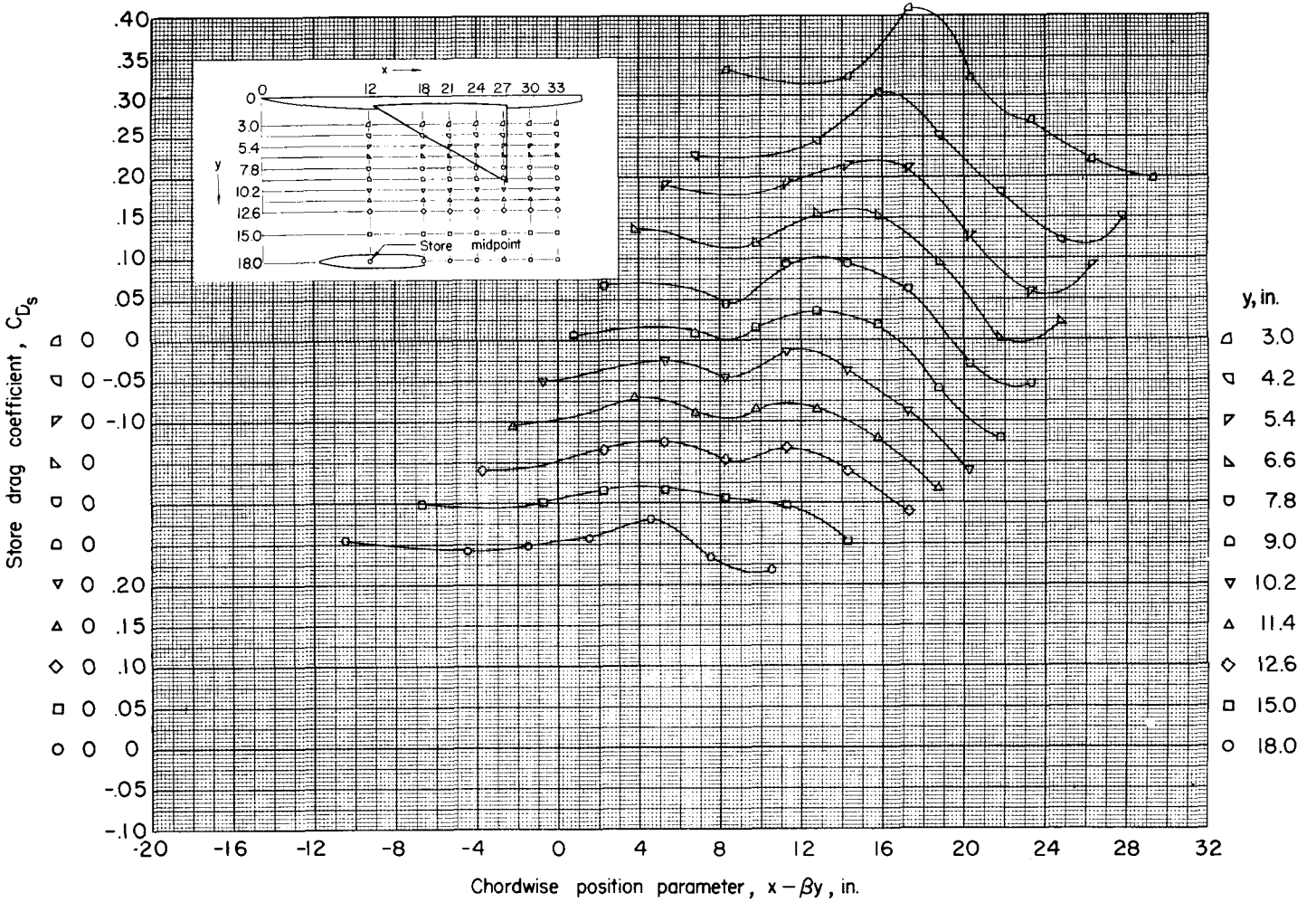

(a) z = 1.15 inches; $\alpha = 0^{\circ}$.

Figure 3.- Drag of store in presence of wing-fuselage combination. M = 1.61.

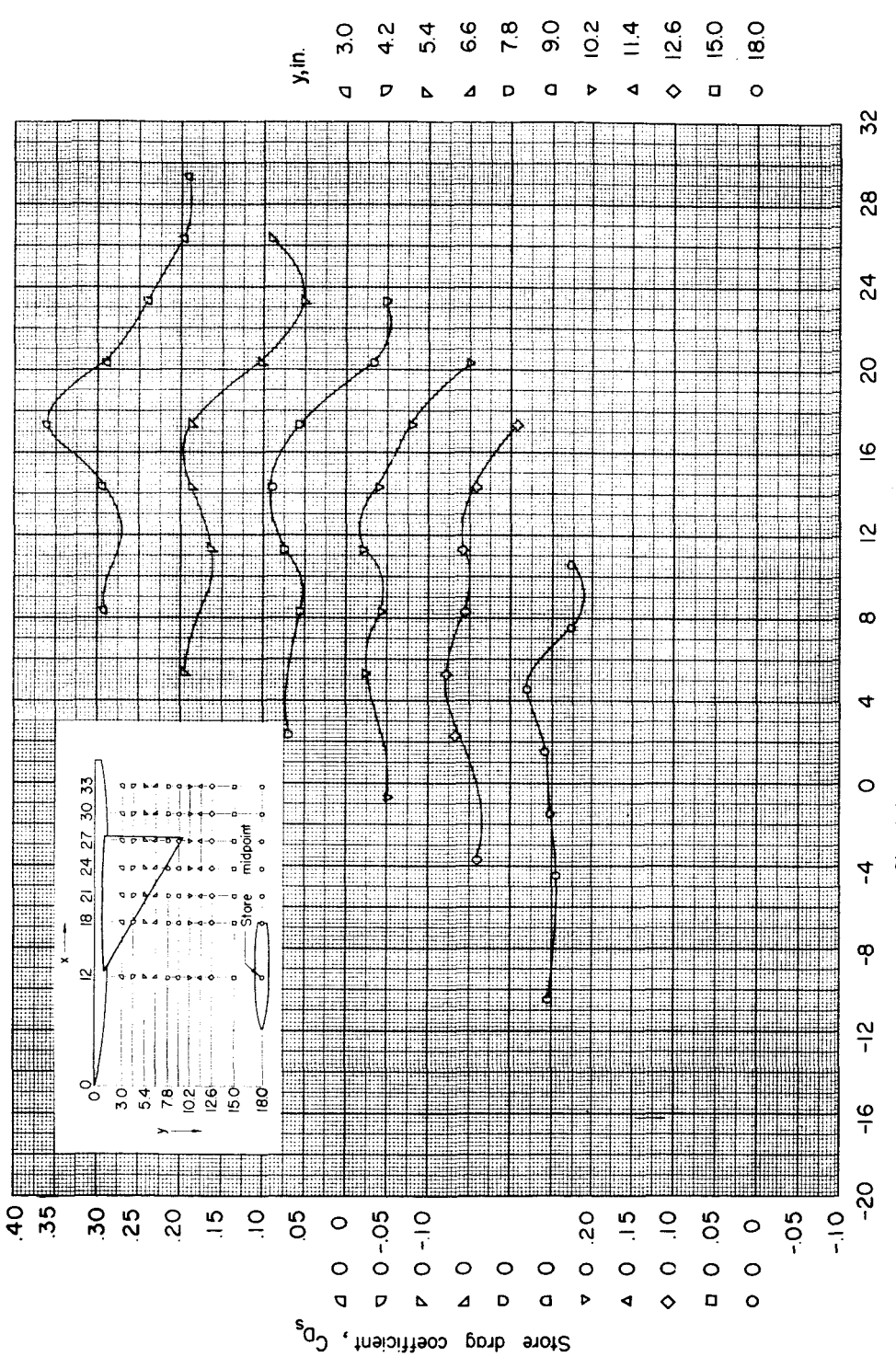

(b) $z = 1.67$ inches; $\alpha = 0^{\circ}$.

Figure 3.- Continued.

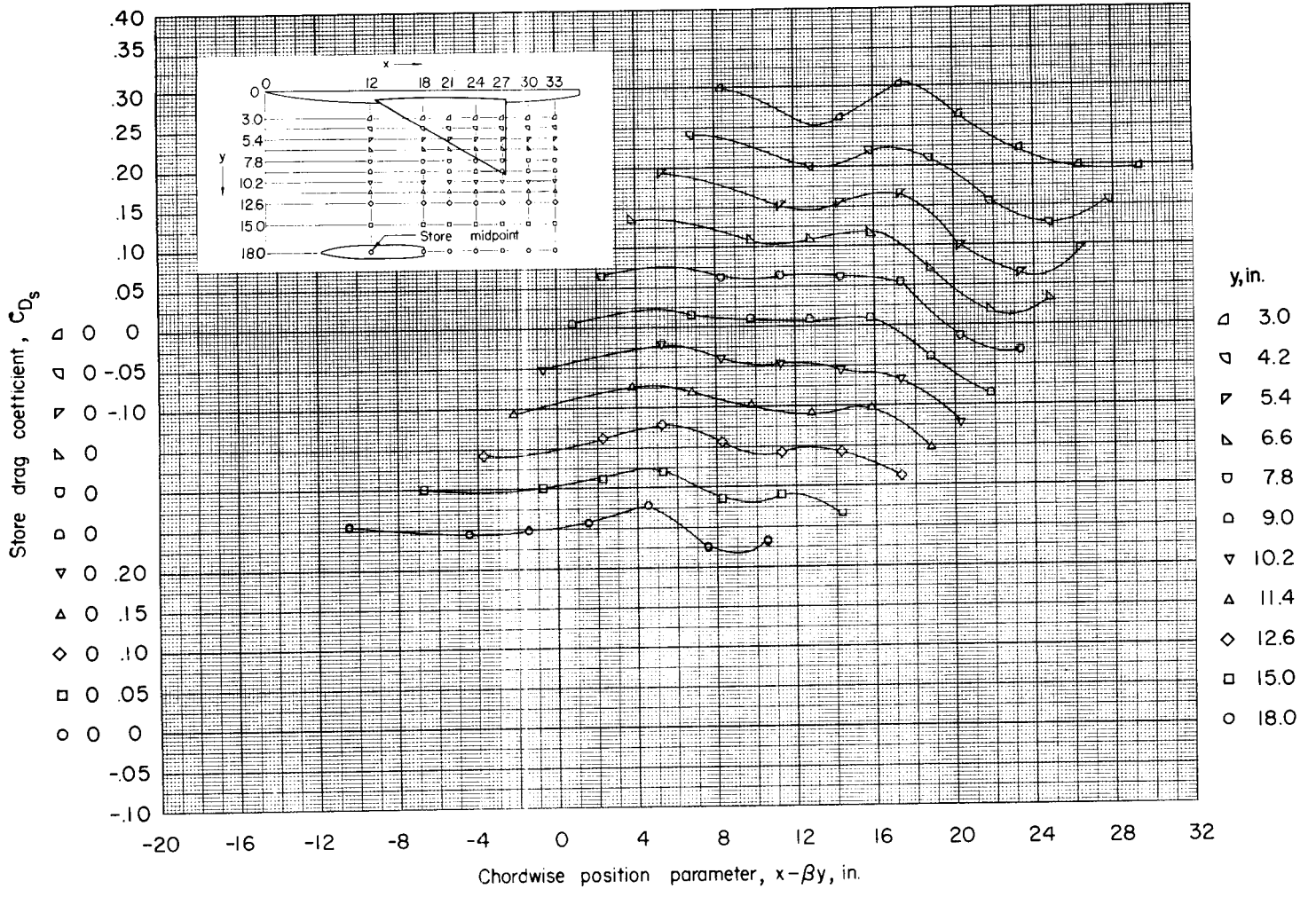

(c) z = 2.09 inches; $\alpha = 0^{\circ}$.

Figure 3.- Continued.

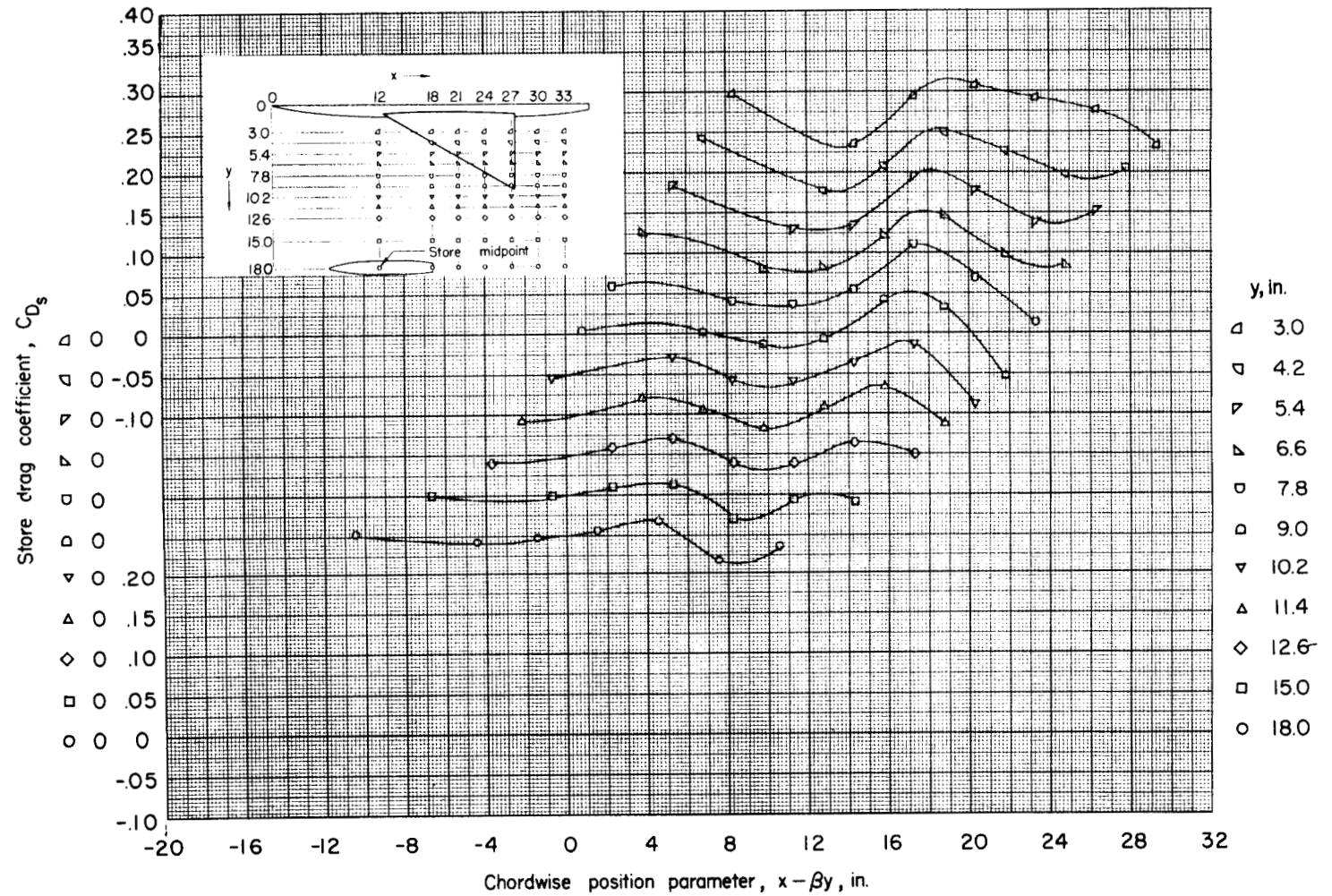

(d) z = 2.09 inches; $\alpha = 4^{\circ}$.

Figure 3.- Concluded.

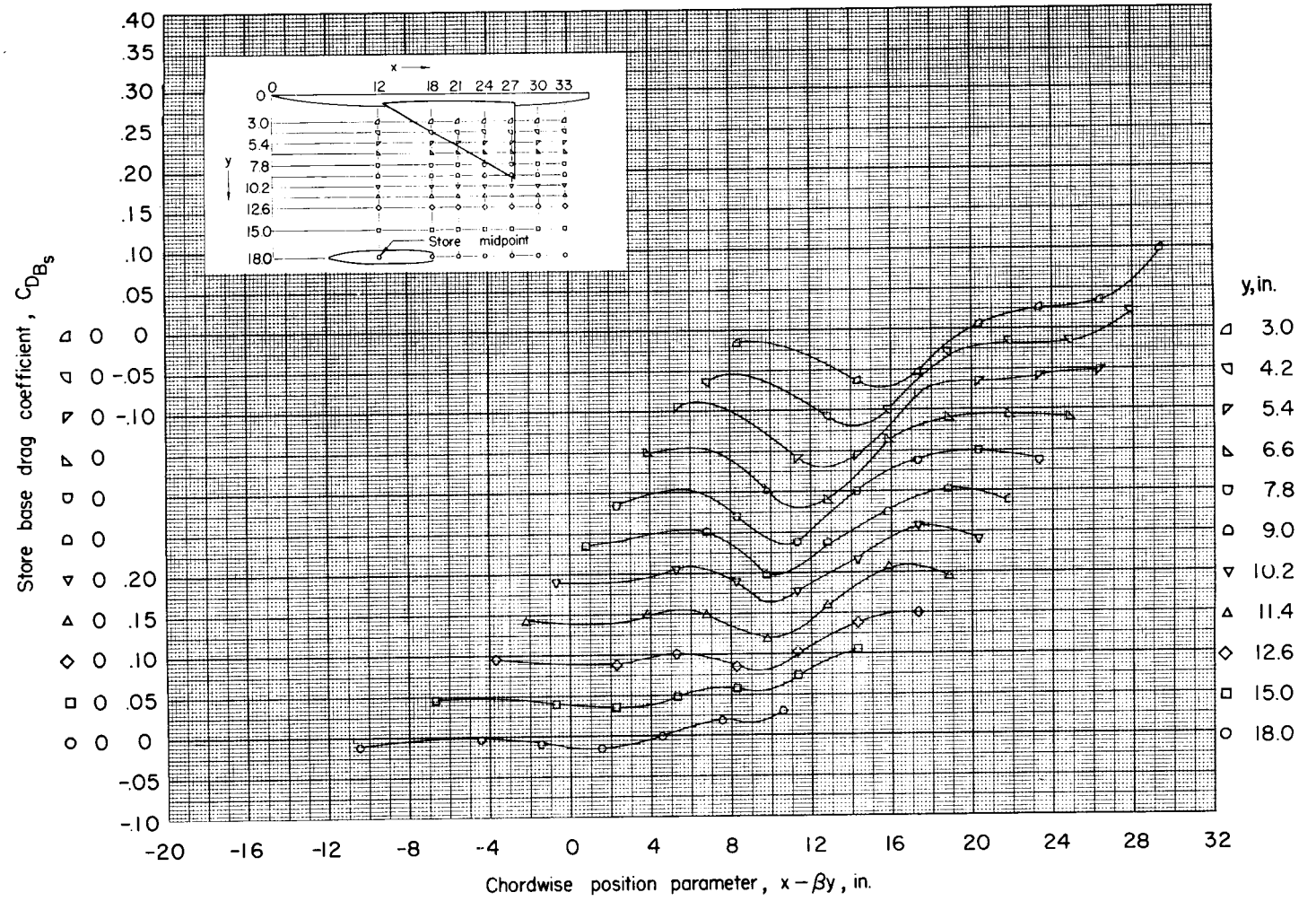

(a) z = 1.15 inches; $\alpha = 0^{\circ}$.

Figure 4.- Base drag of store in presence of wing-fuselage combination. M = 1.61.

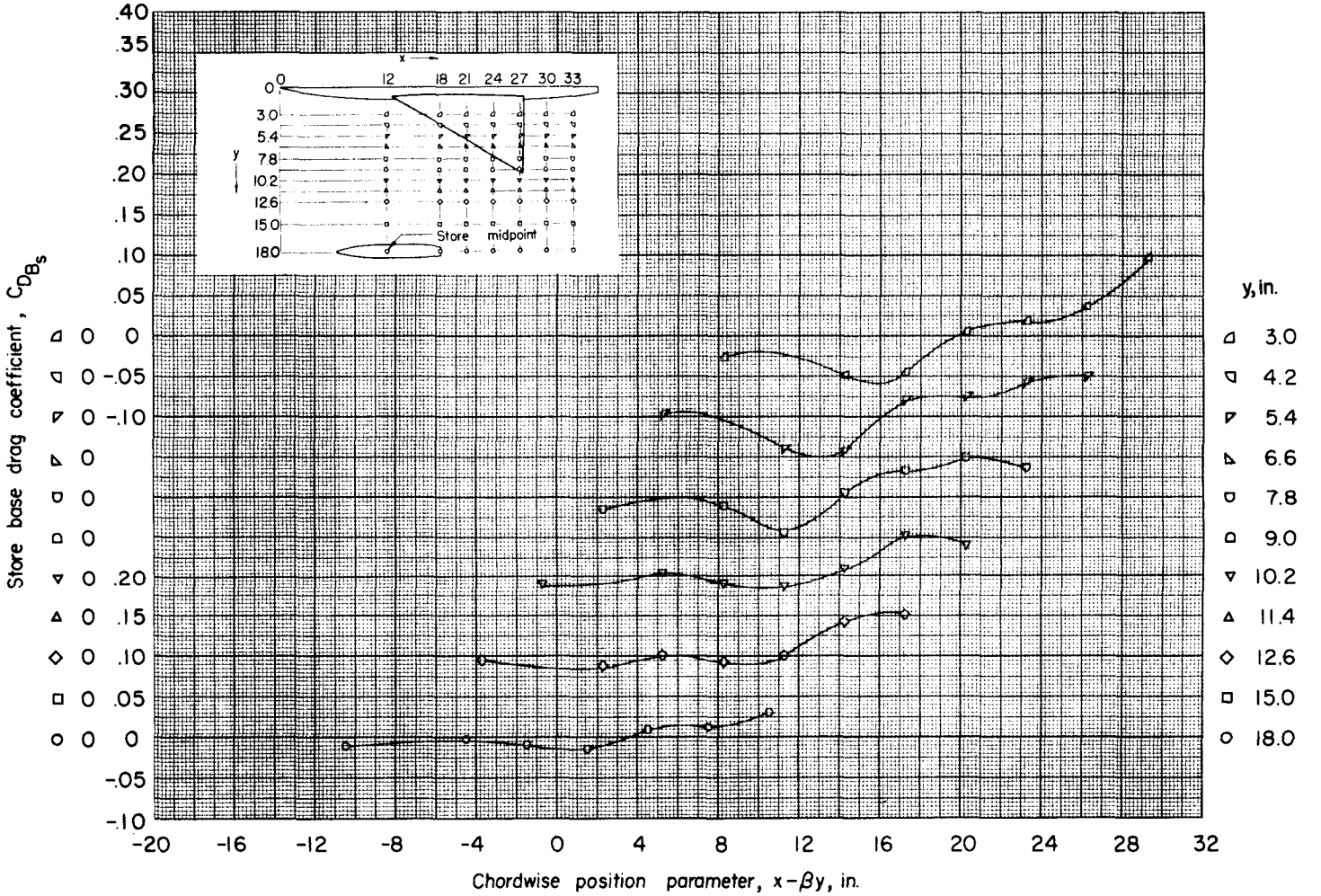

(b) $z = 1.67$ inches; $\alpha = 0^\circ$.

Figure 4.- Continued.

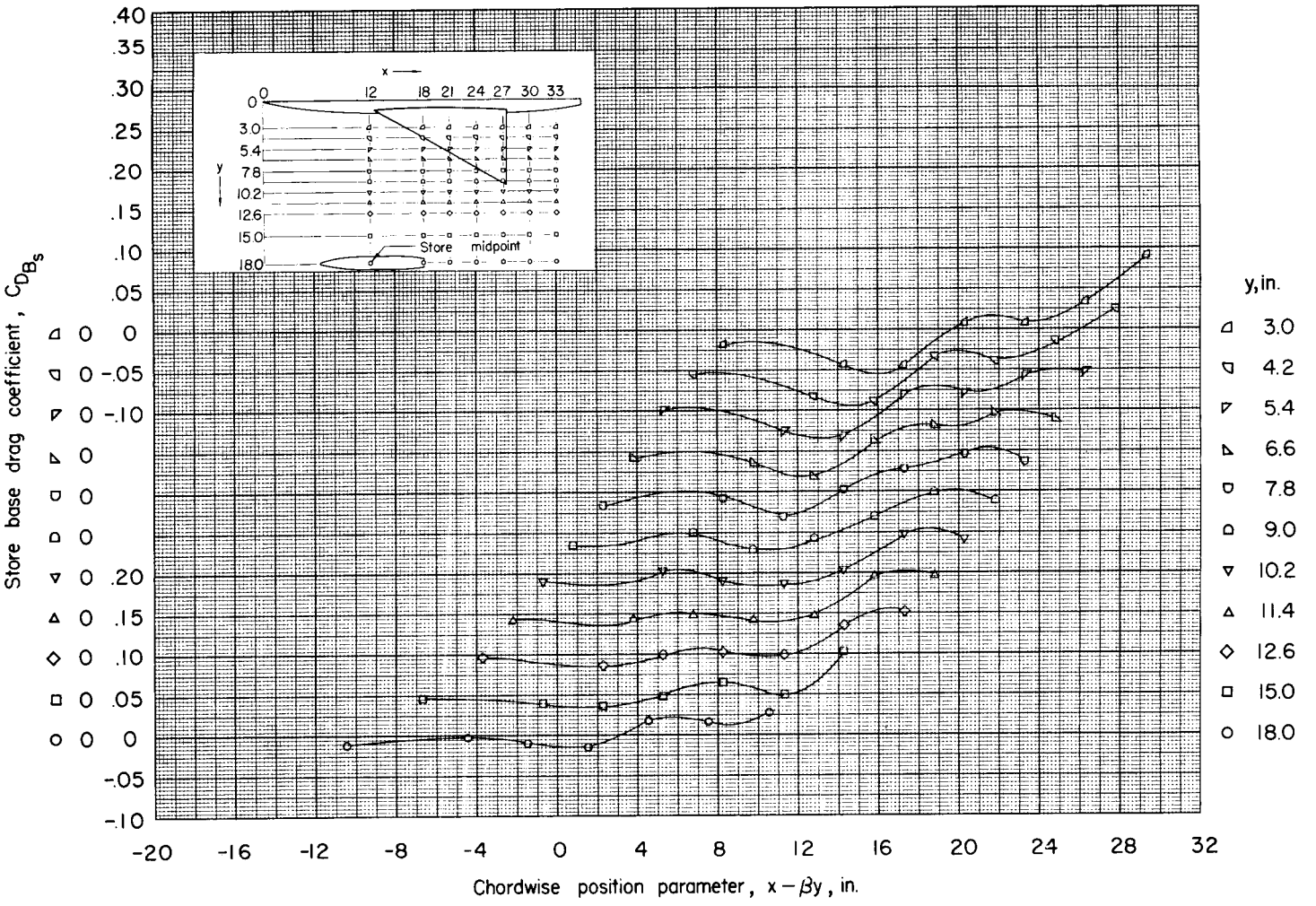

(c) z = 2.09 inches; $\alpha = 0^{\circ}$.

Figure 4.- Continued.

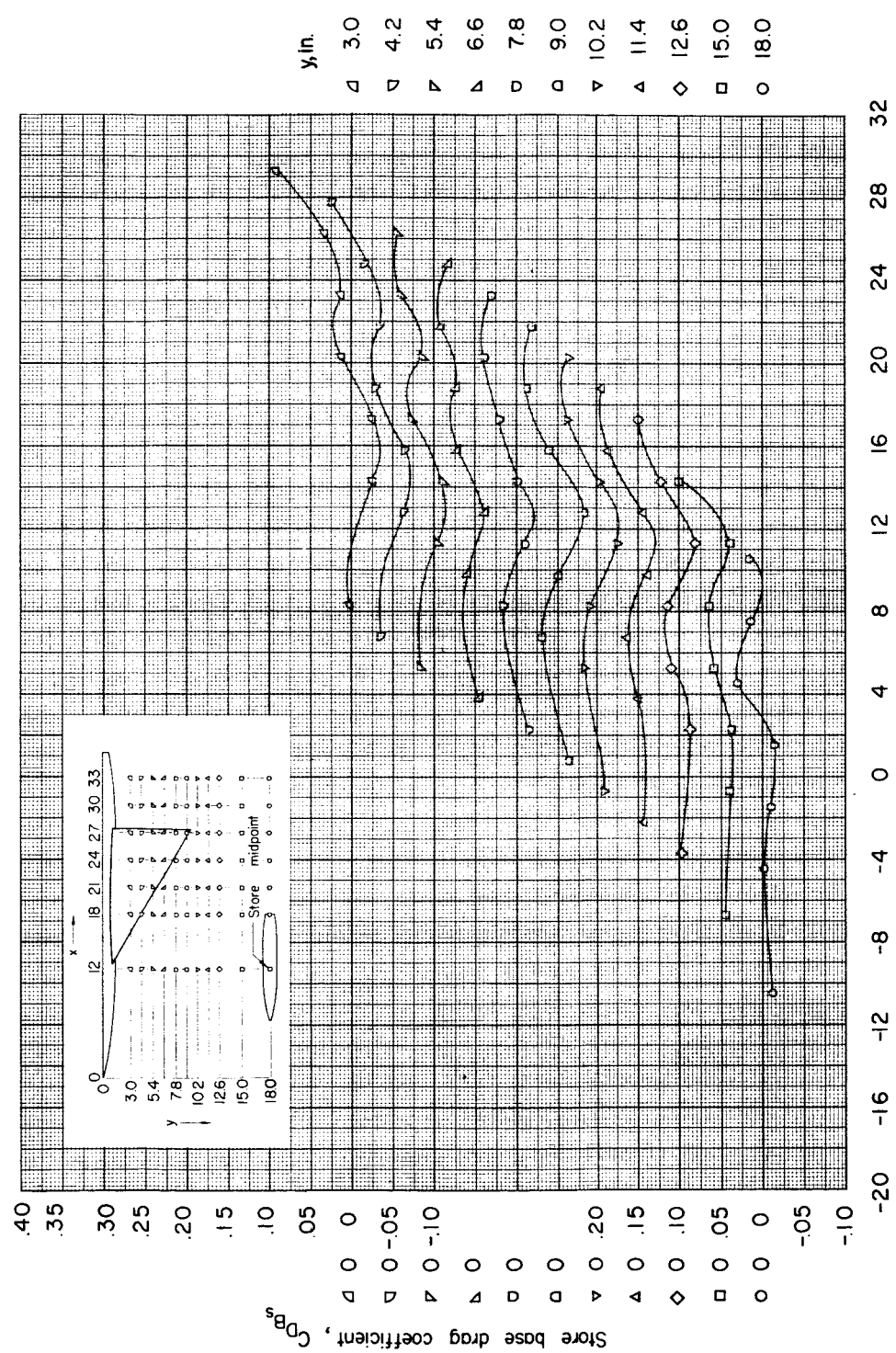

(d) $z = 2.09$ inches; $\alpha = 4^\circ$.

Figure 4.- Concluded.

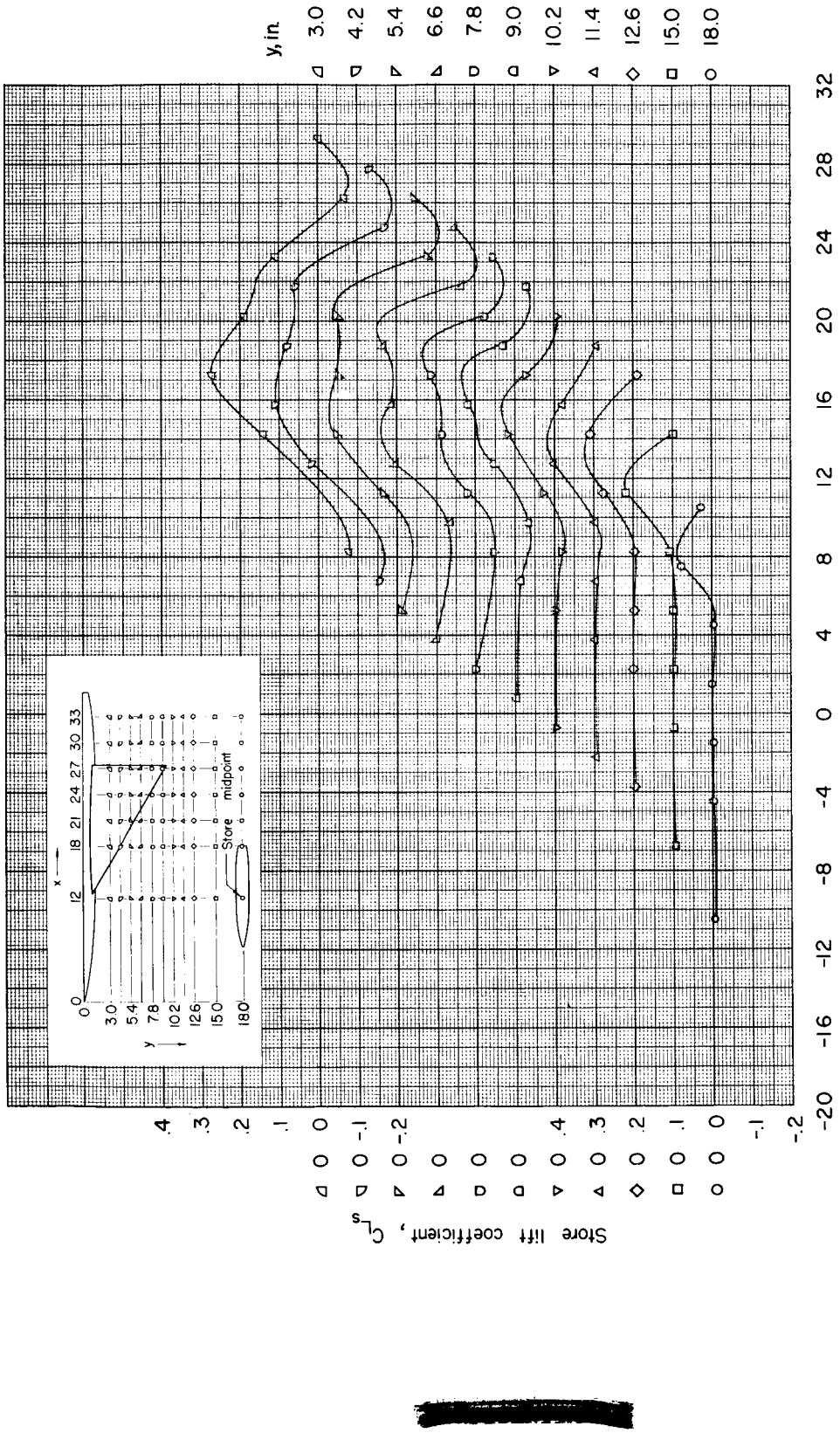

(a) $z = 1.15$ inches; $\alpha = 0^\circ$.

Figure 5.- Lift of store in presence of wing-fuselage combination. $M = 1.61$.

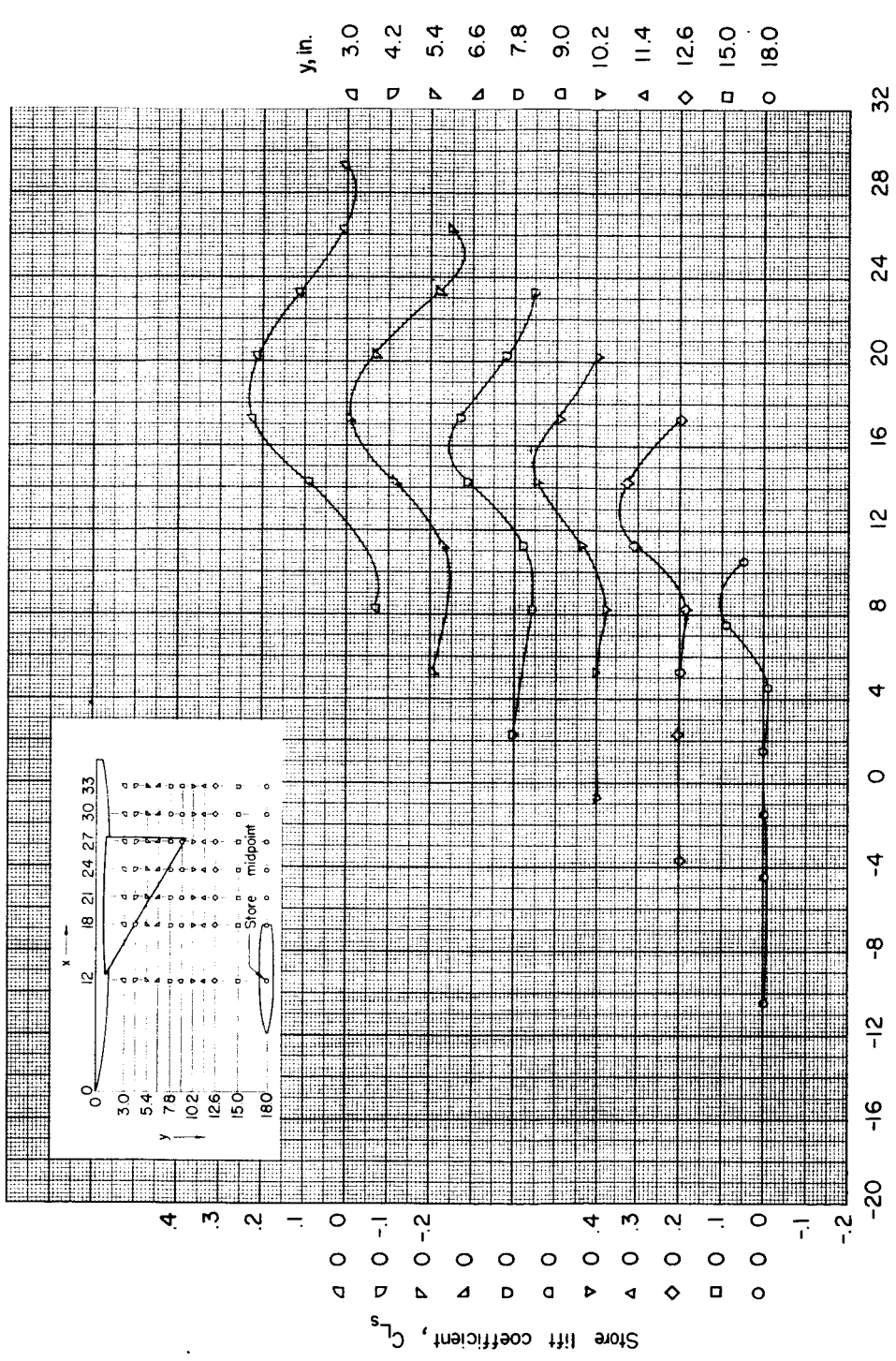

(b) $z = 1.67$ inches; $\alpha = 0^{\circ}$.

Figure 5.- Continued.

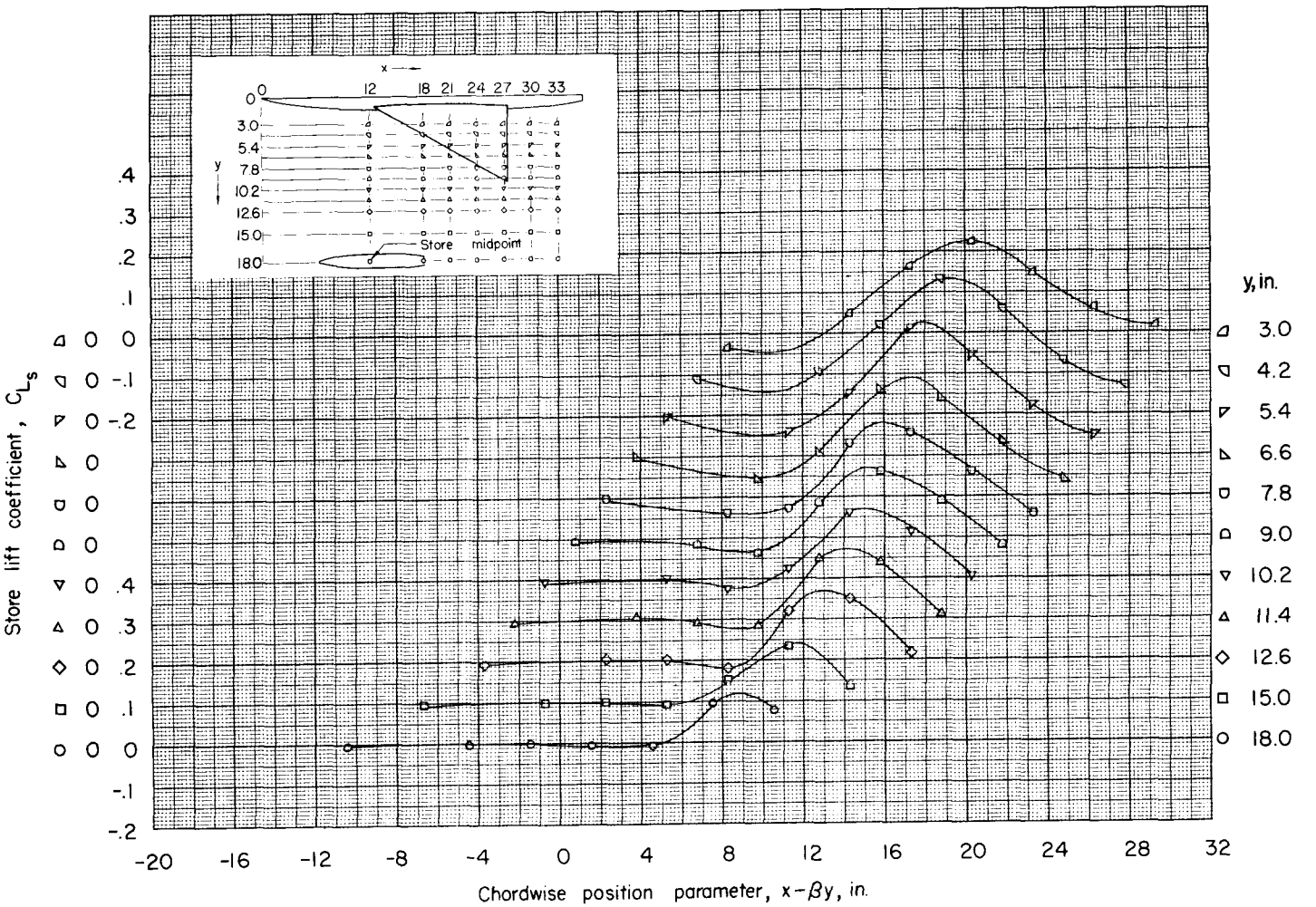

(c) z = 2.09 inches; $\alpha = 0^{\circ}$.

Figure 5.- Continued.

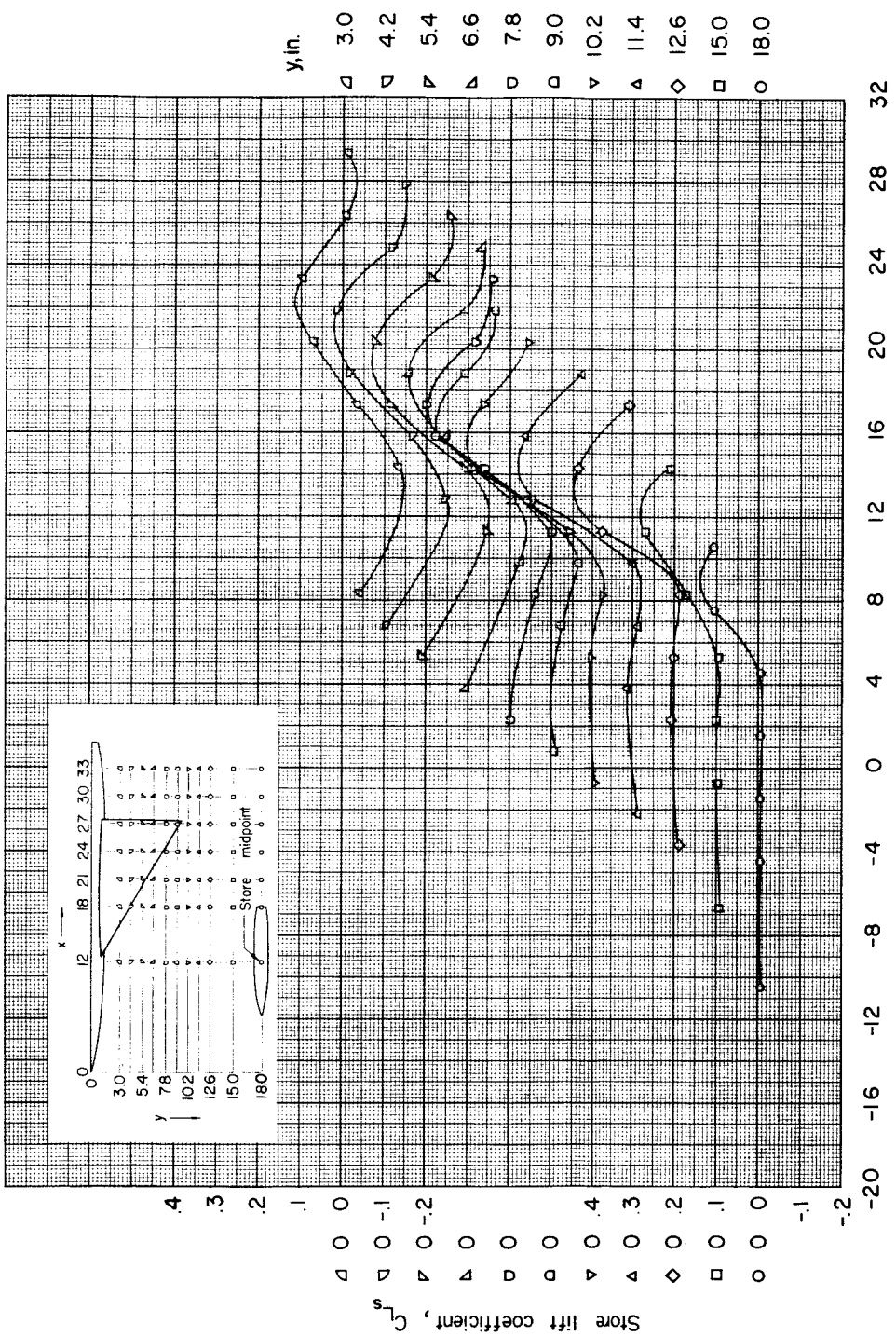

(d) $z = 2.09$ inches; $\alpha = 4^{\circ}$.

Figure 5.- Concluded.

(a) $z = 1.15$ inches; $\alpha = 0^{\circ}$.

Figure 6.- Pitching moment of store in presence of wing-fuselage combination (computed about store nose). $M = 1.61$.

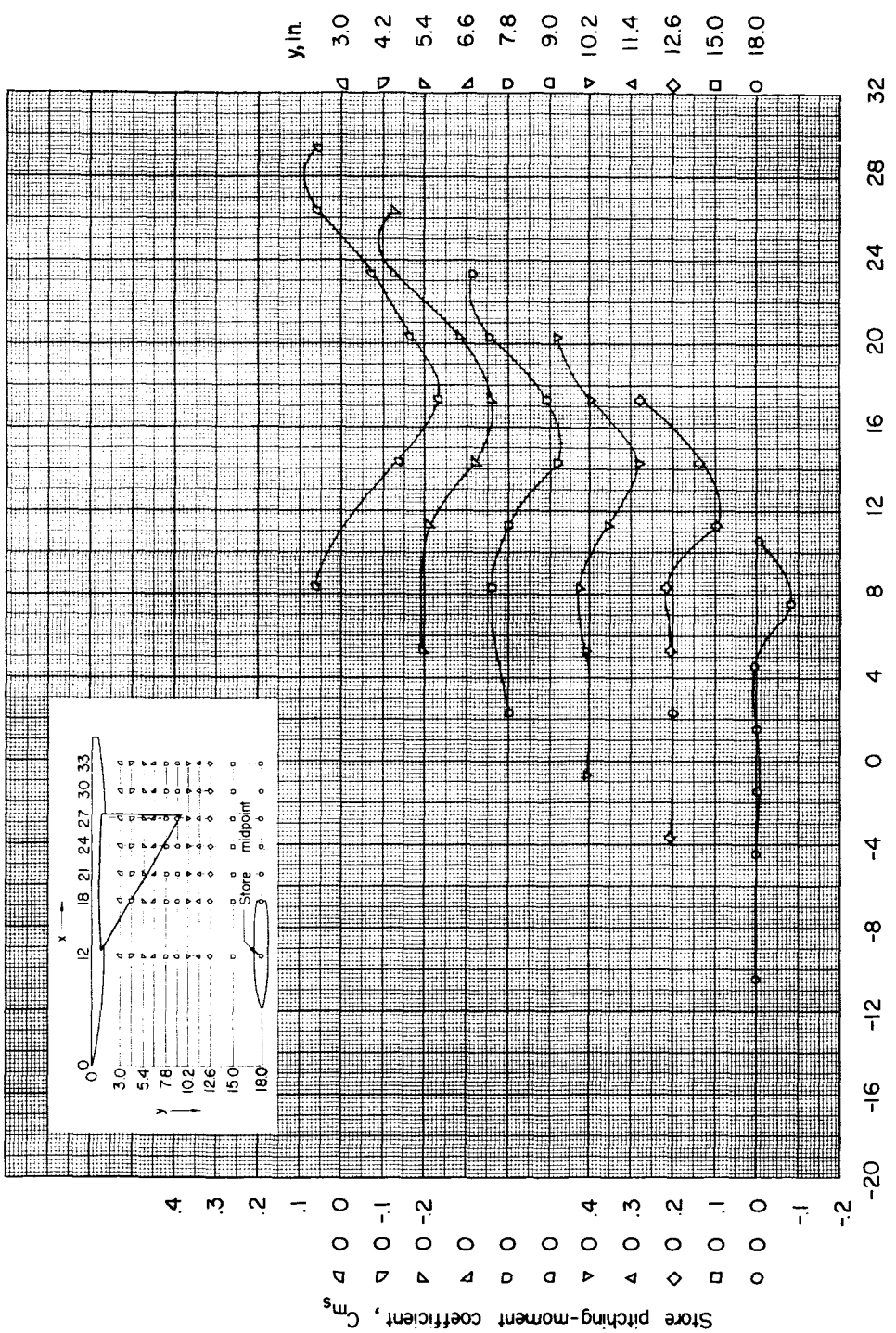

(b) z = 1.67 inches; $\alpha = 0^{\circ}$.

Figure 6.- Continued.

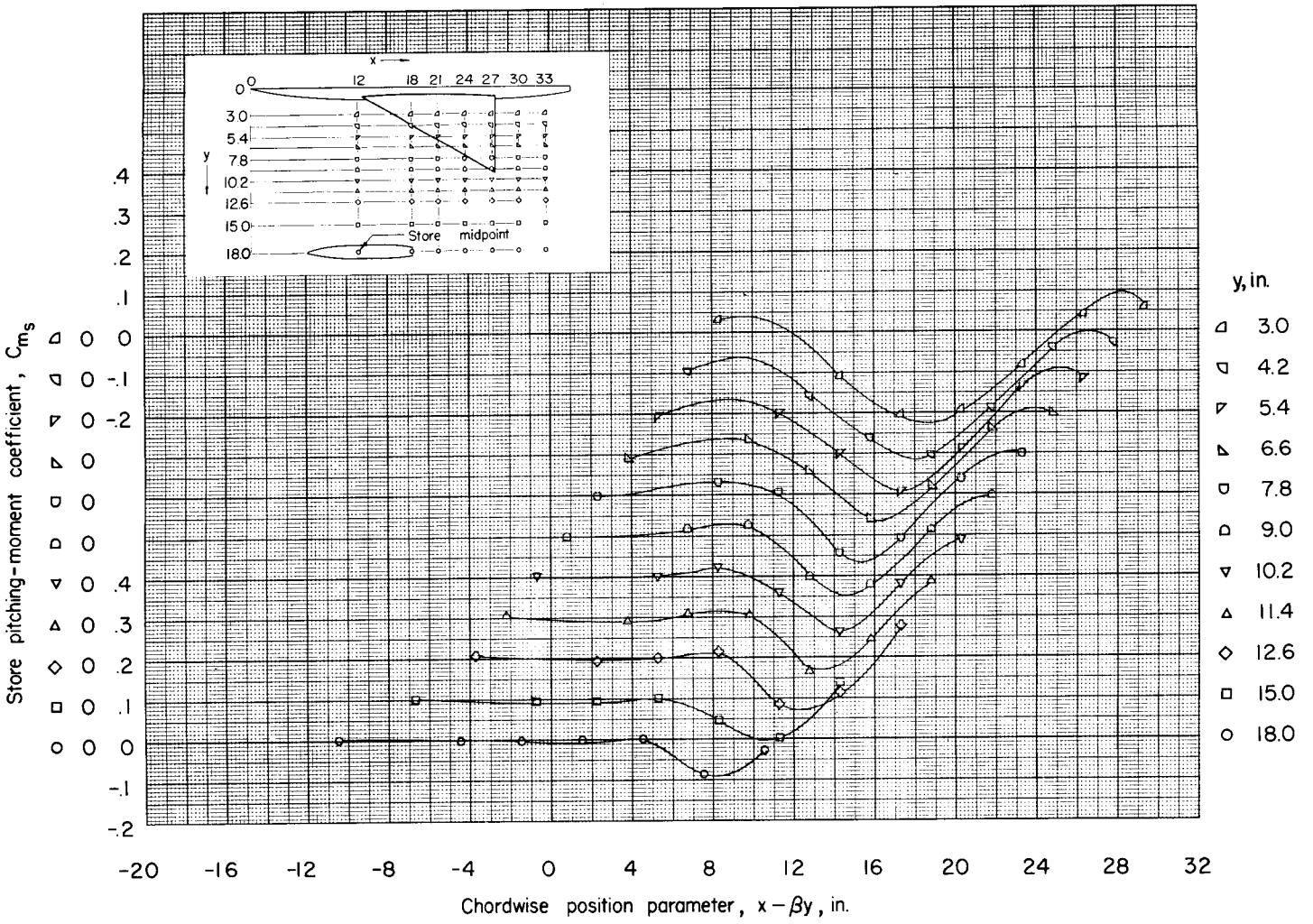

(c) z = 2.09 inches; $\alpha = 0^{\circ}$.

Figure 6.- Continued.

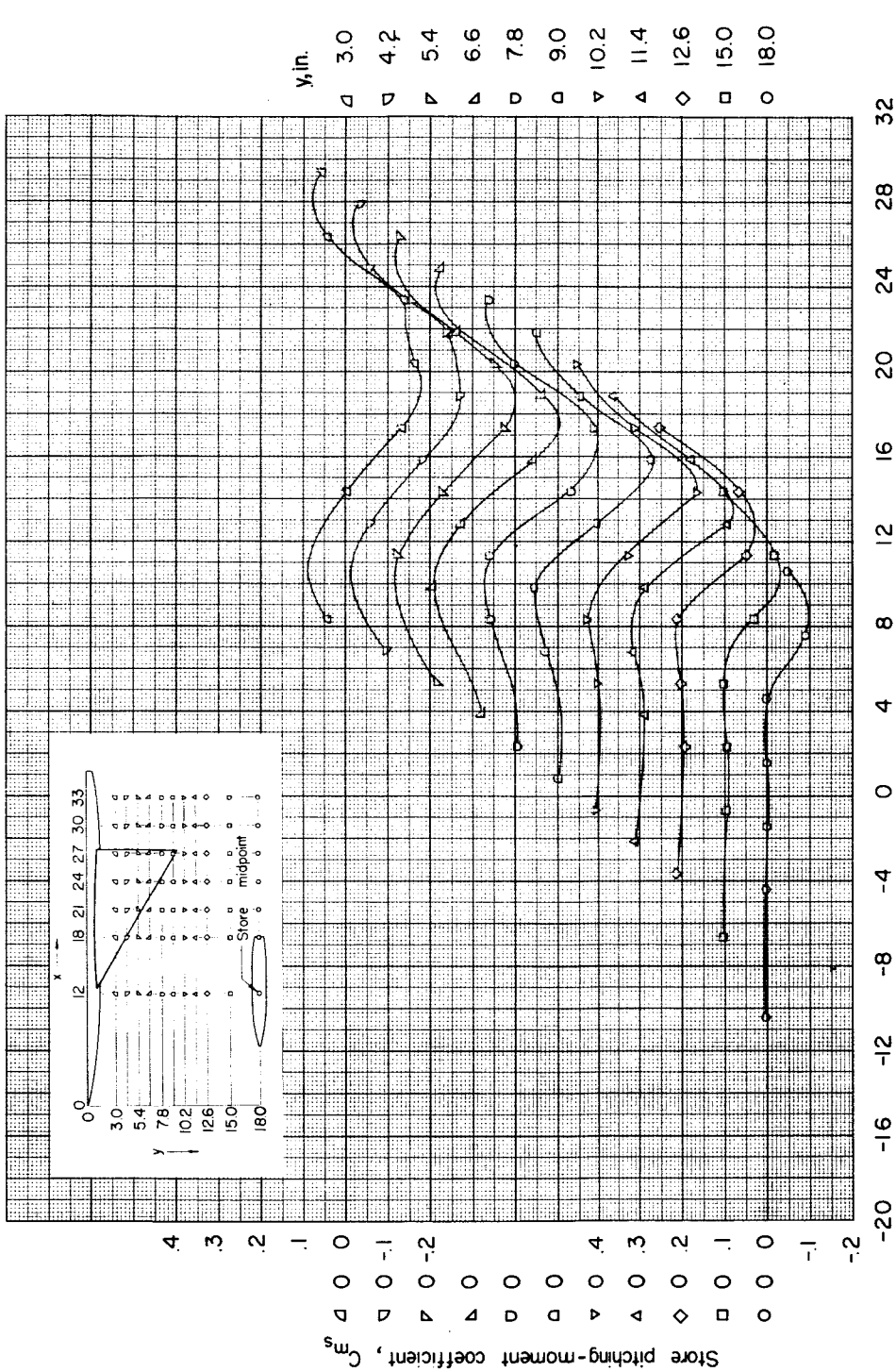

(d) $z = 2.09$ inches; $\alpha = 4^{\circ}$.

Figure 6.- Concluded.

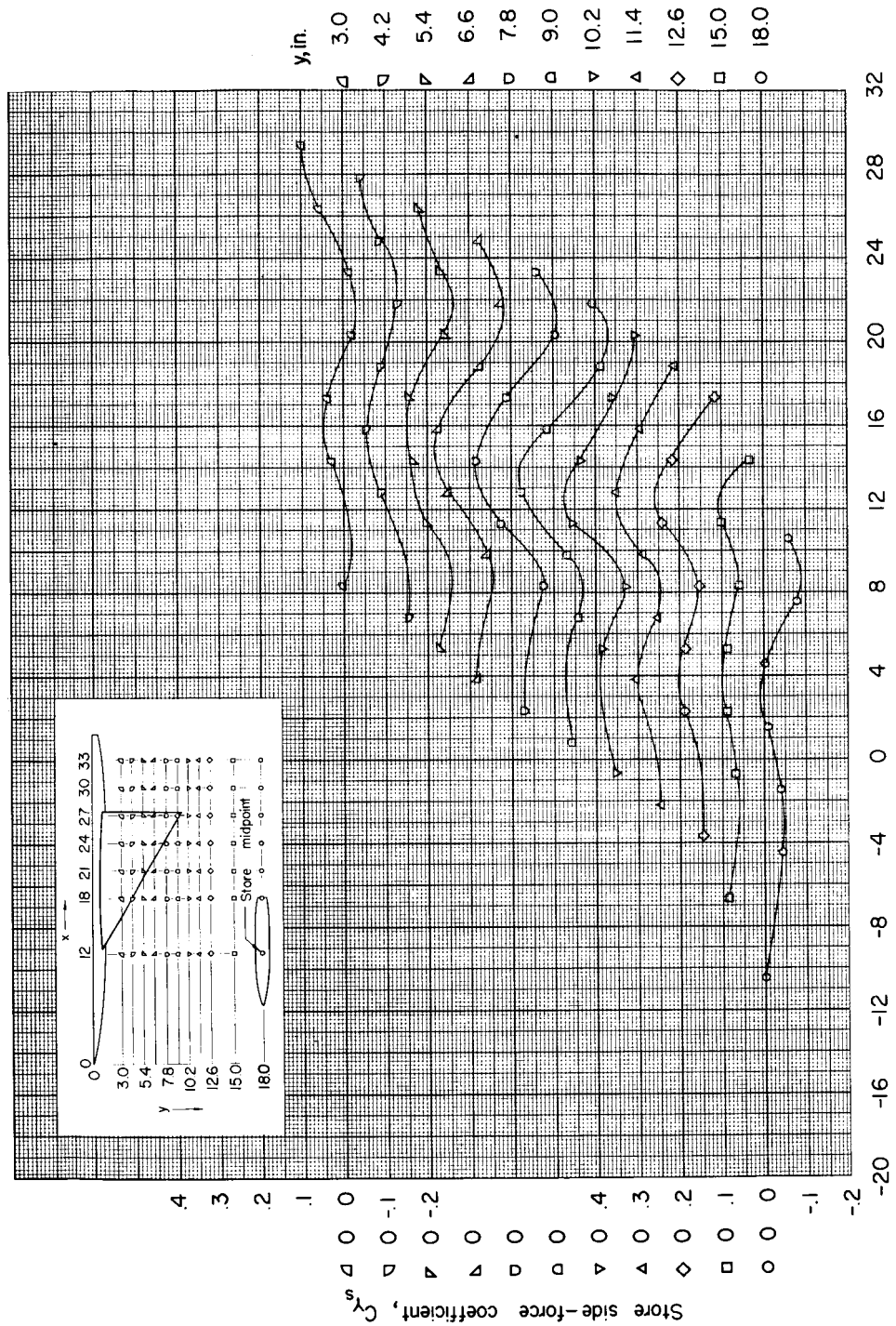

(a) $z = 1.15$ inches; $\alpha = 0^{\circ}$.

Figure 7.- Side force of store in presence of wing-fuselage combination. $M = 1.61$.

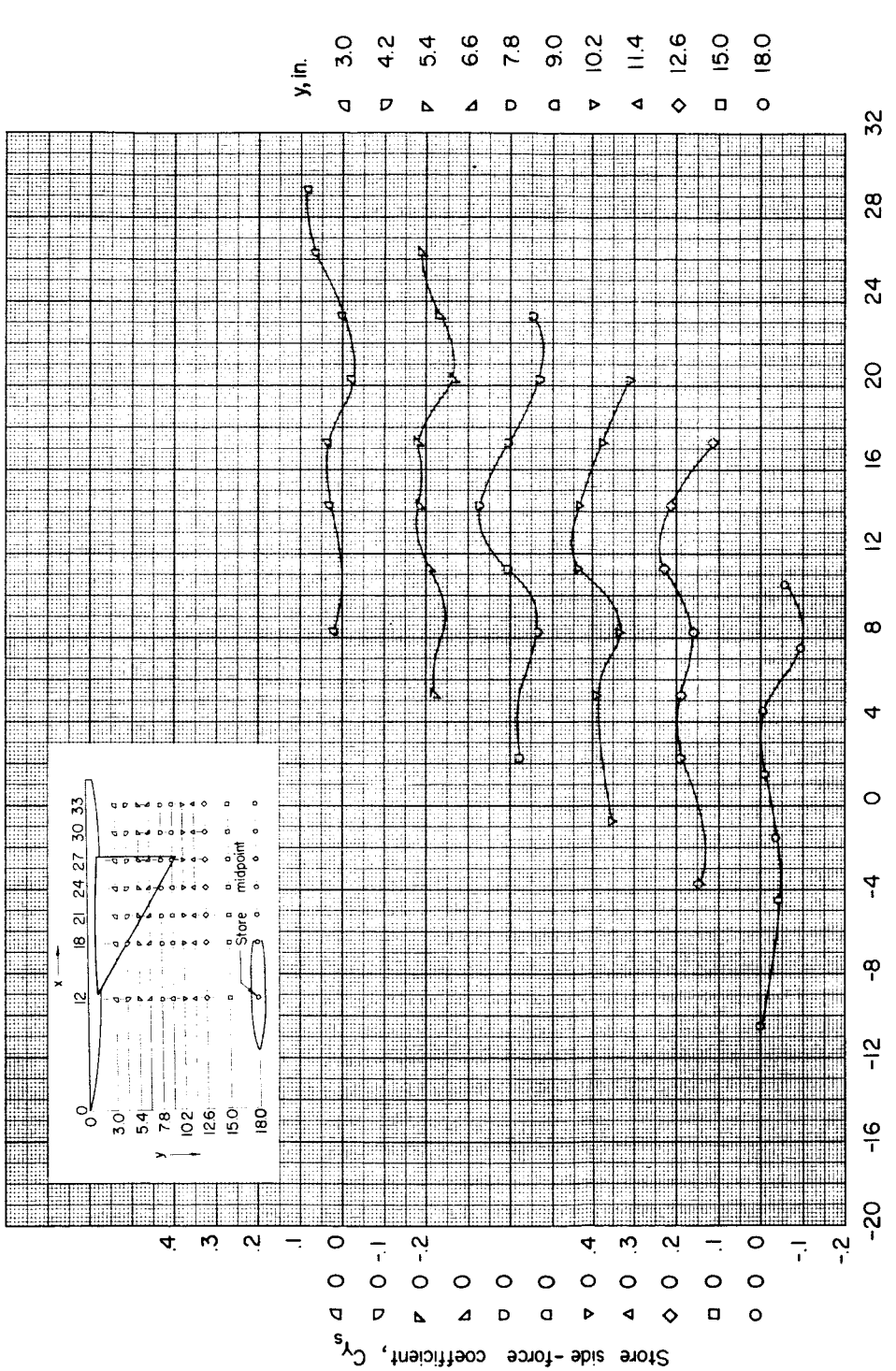

(b) $z = 1.67$ inches; $\alpha = 0^{\circ}$.

Figure 7.- Continued.

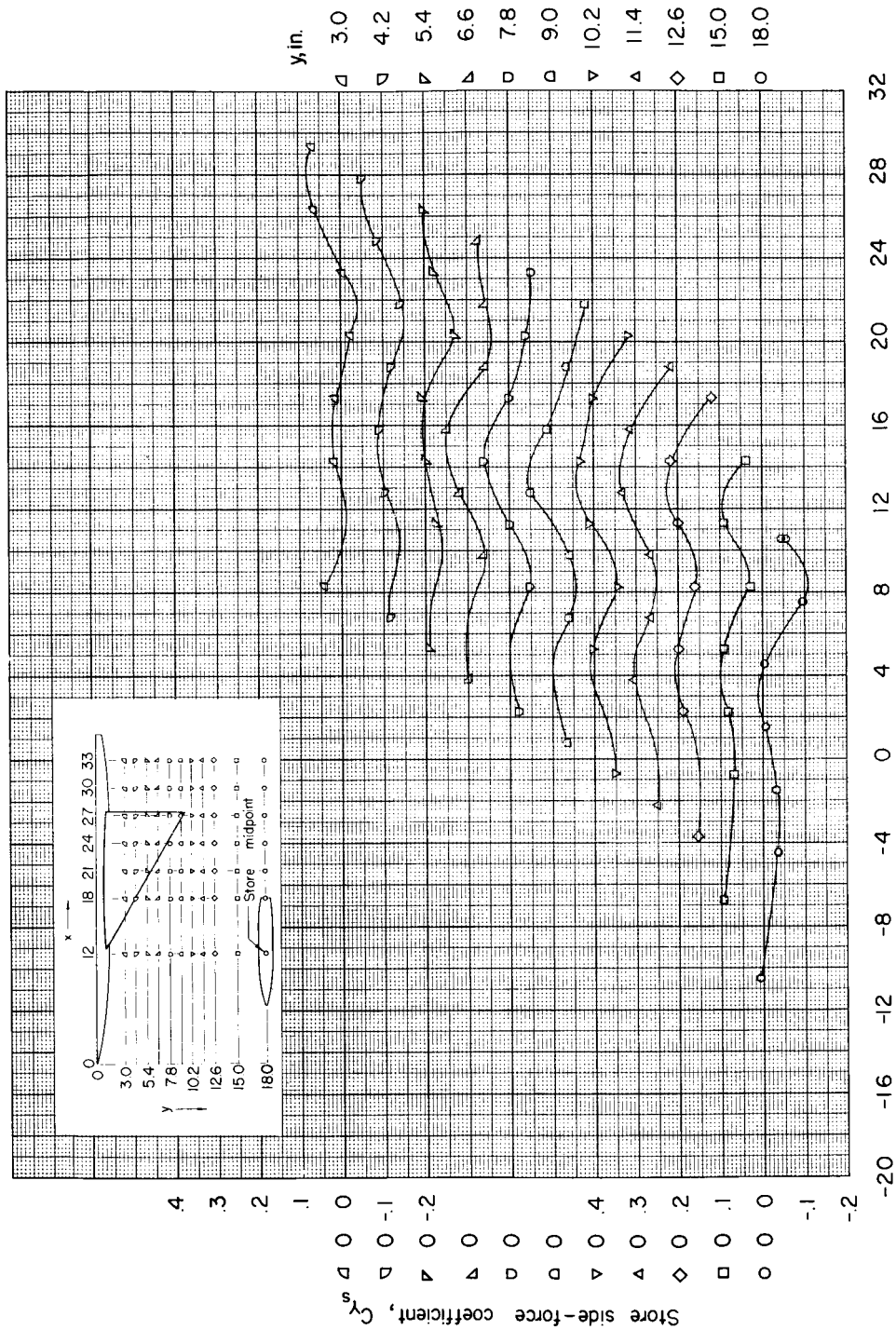

(c) z = 2.09 inches; $\alpha = 0^{\circ}$.

Figure 7.- Continued.

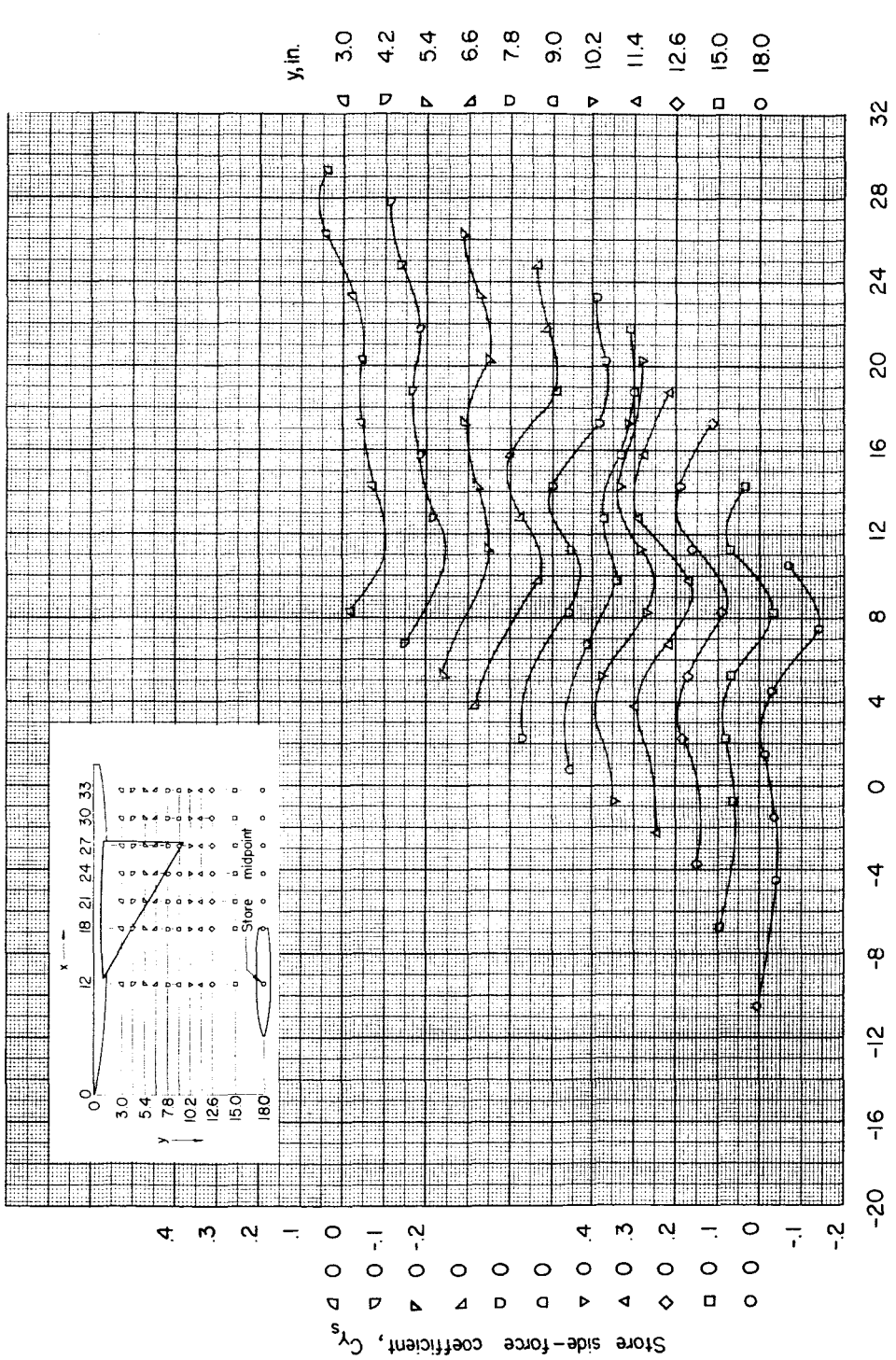

(d) $z = 2.09$ inches; $\alpha = 4^{\circ}$.

Figure 7.- Concluded.

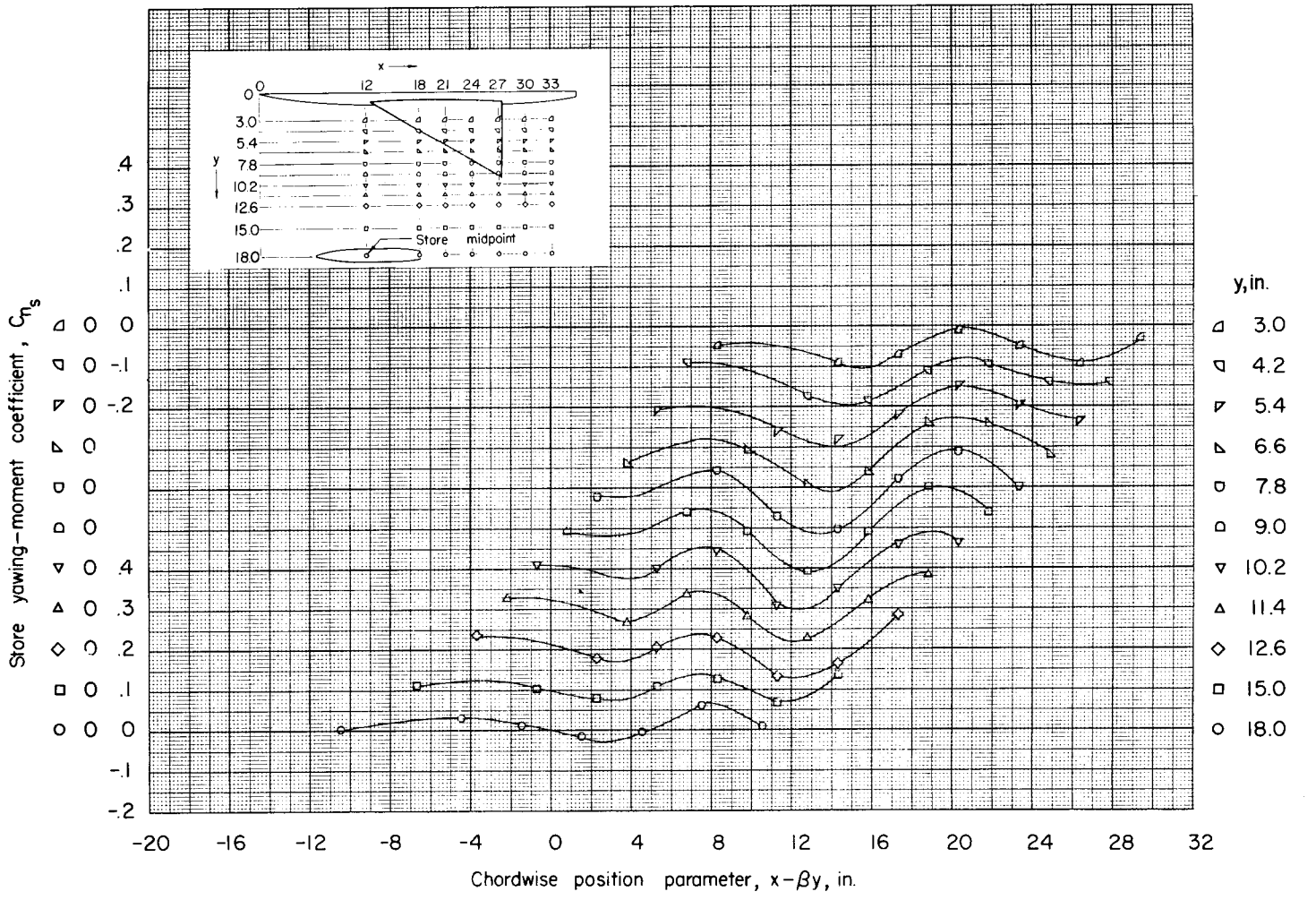

(a) z = 1.15 inches; $\alpha = 0^{\circ}$.

Figure 8.- Yawing moment of store in presence of wing-fuselage combination (computed about store nose). M = 1.61.

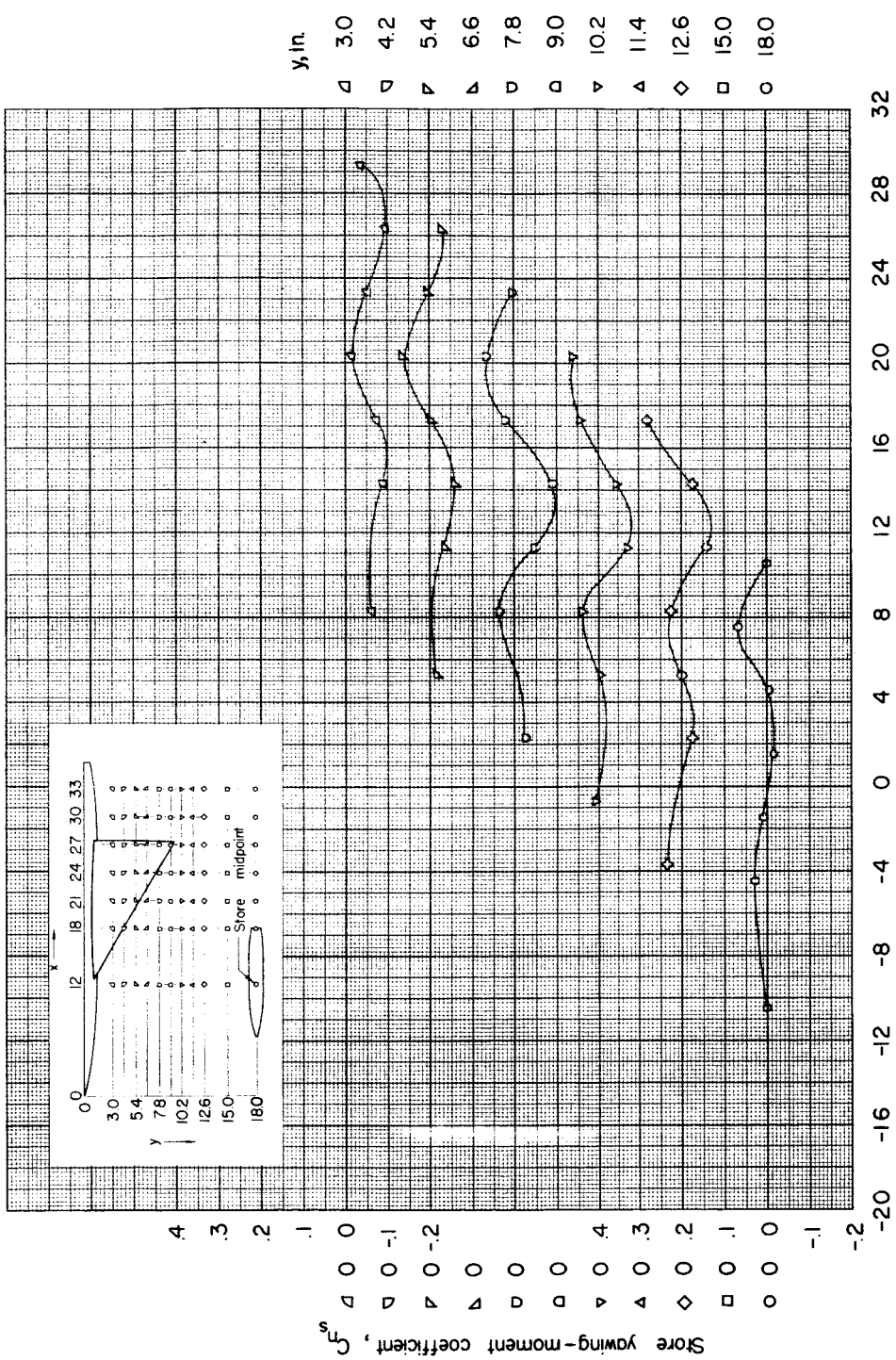

(b) z = 1.67 inches; $\alpha = 0^{\circ}$.

Figure 8.- Continued.

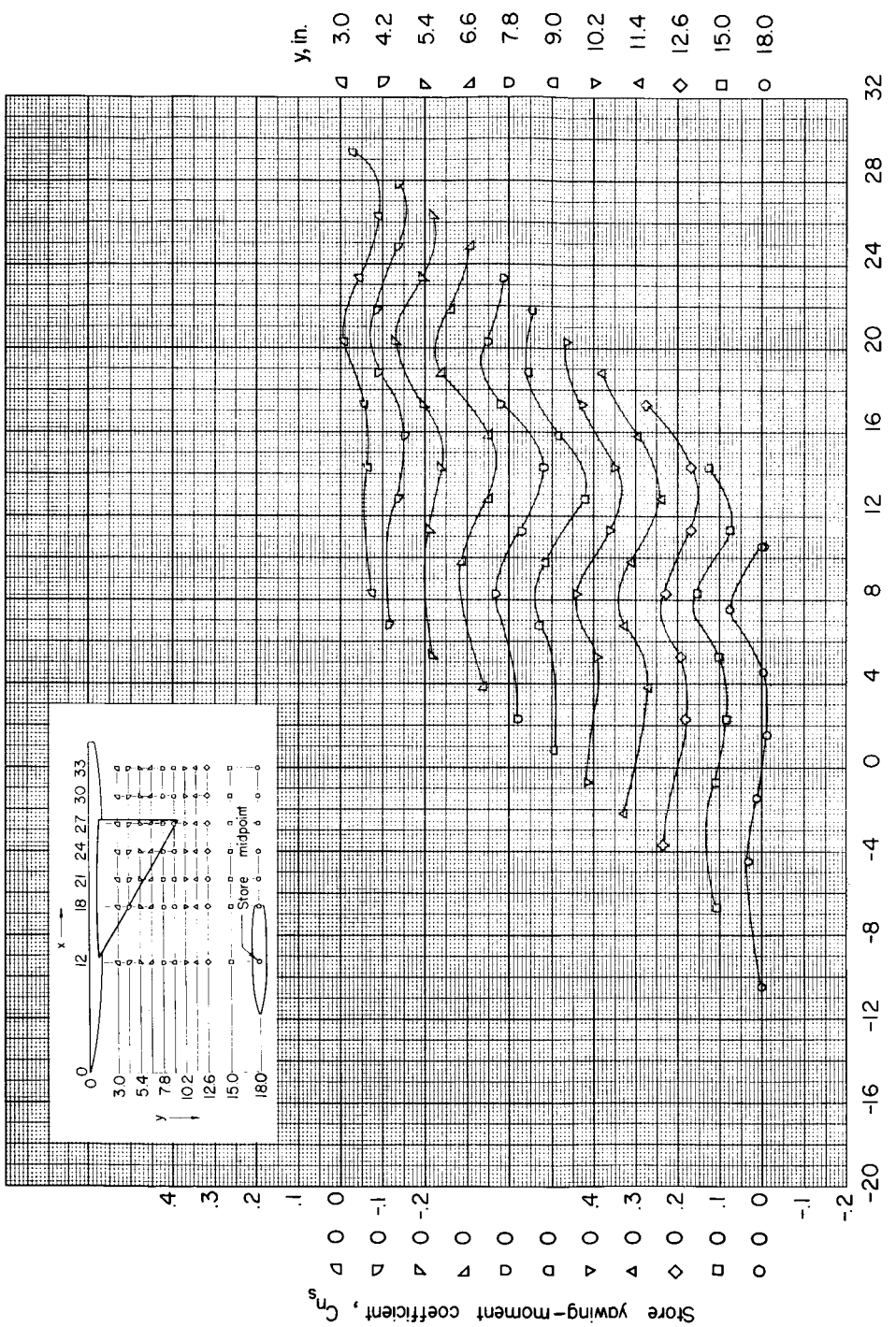

(c) z = 2.09 inches; $\alpha = 0^{\circ}$.

Figure 8.- Continued.

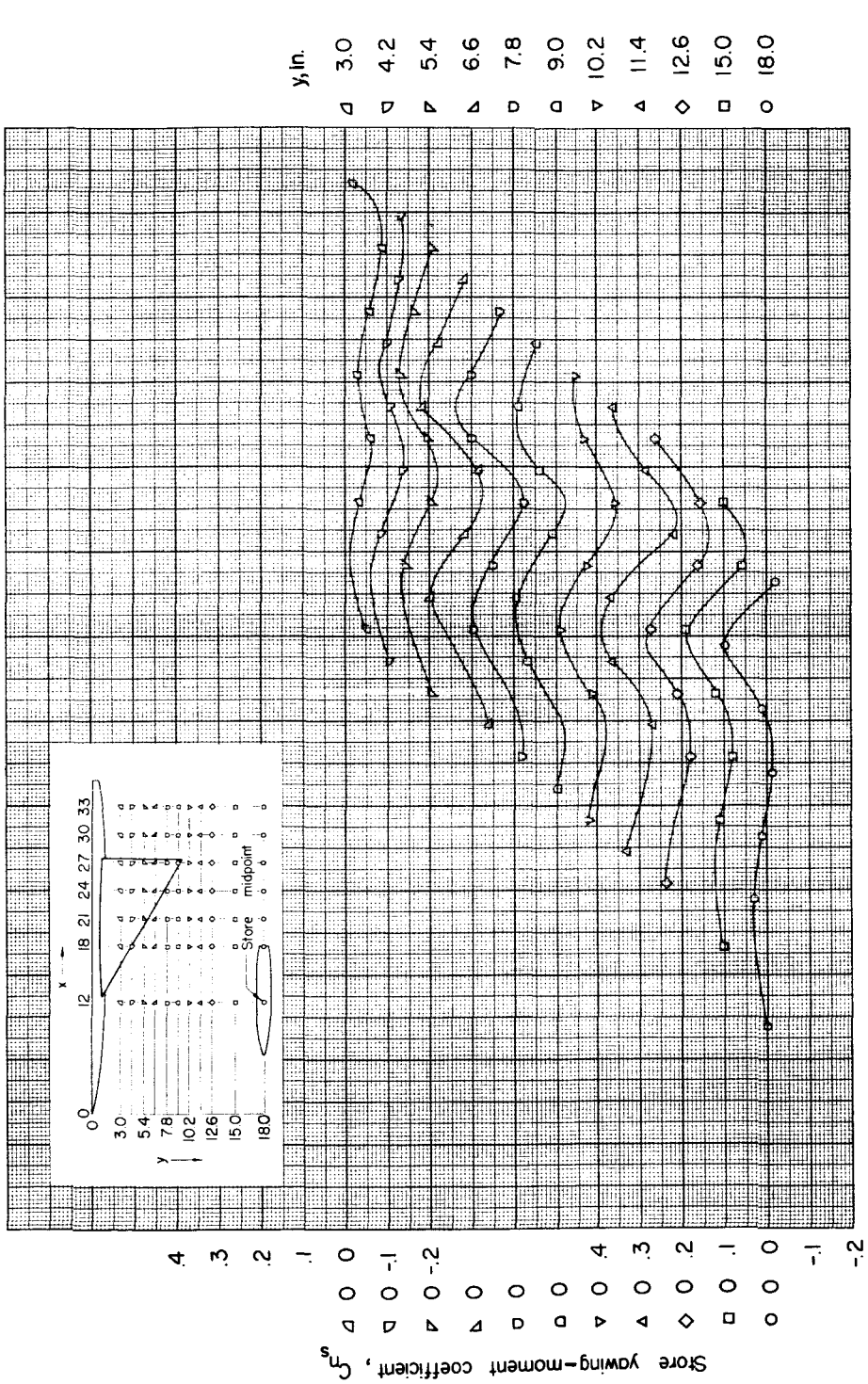

(d) $z = 2.09$ inches; $\alpha = 4^{\circ}$.

Figure 8.- Concluded.

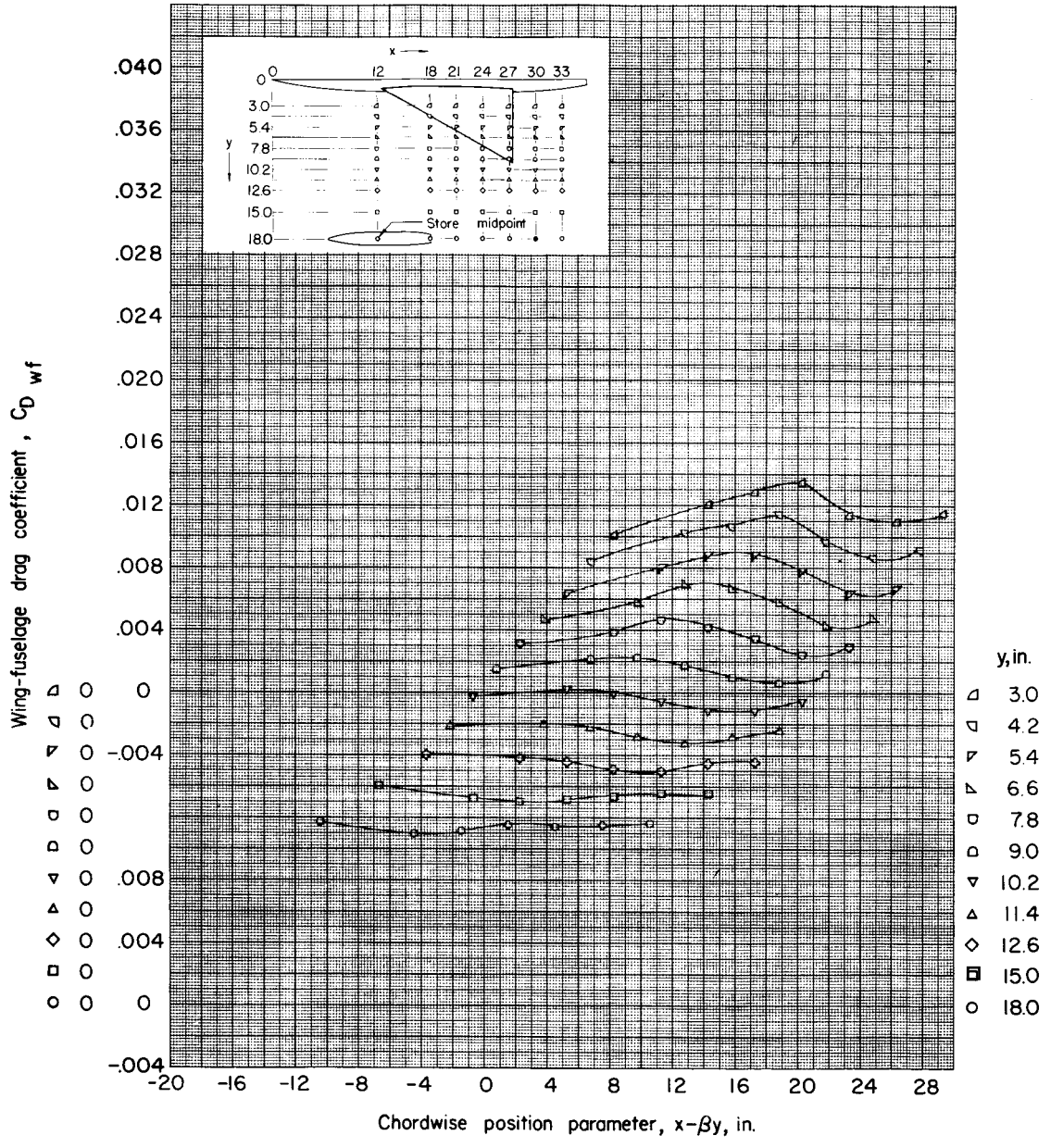

(a) $z = 1.15$ inches; $\alpha = 0^{\circ}$.

Figure 9.- Drag of wing-fuselage combination in presence of store. $M = 1.61$.

[redacted]

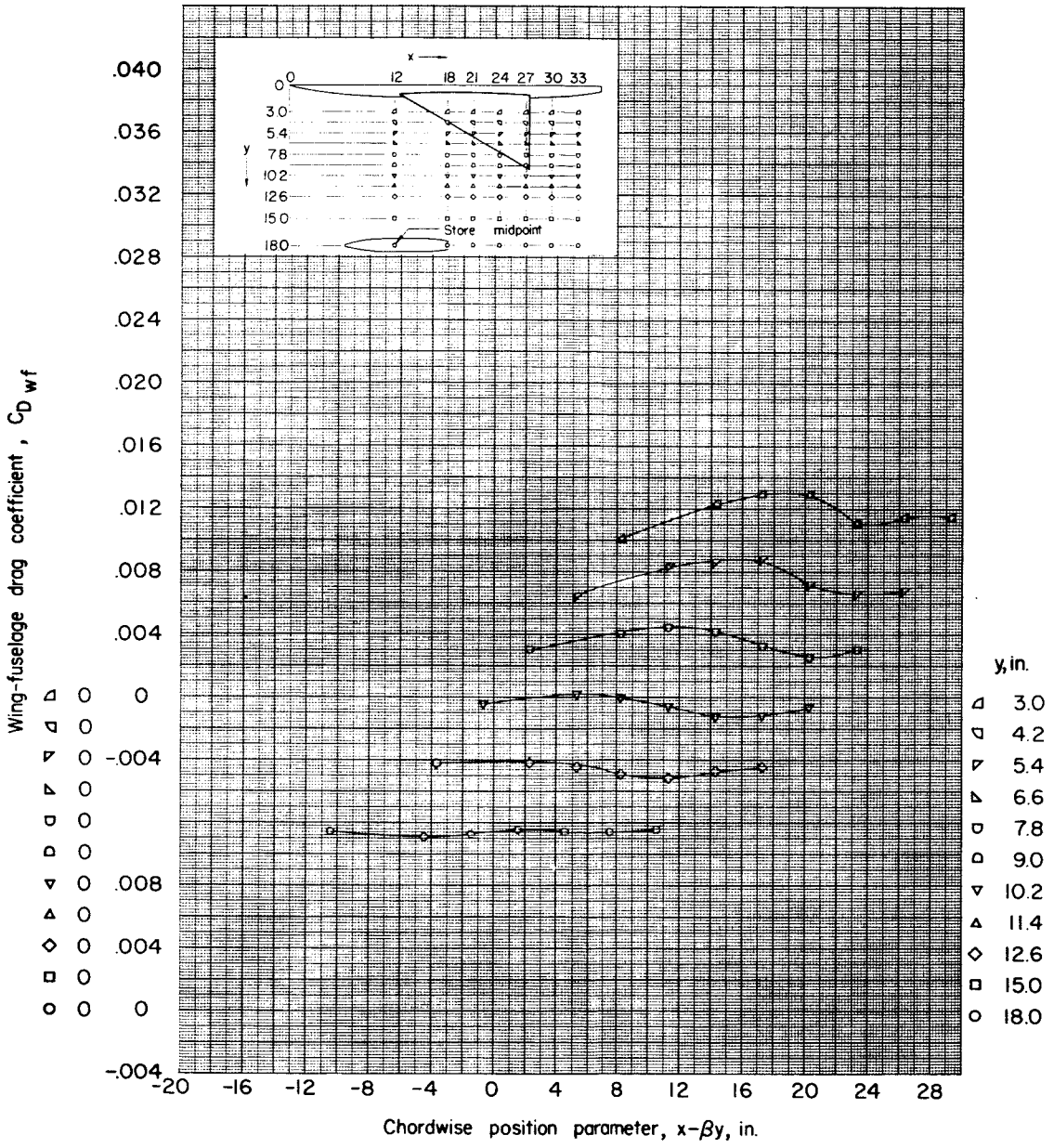

(b) z = 1.67 inches; $\alpha = 0^{\circ}$.

Figure 9.- Continued.

[redacted]

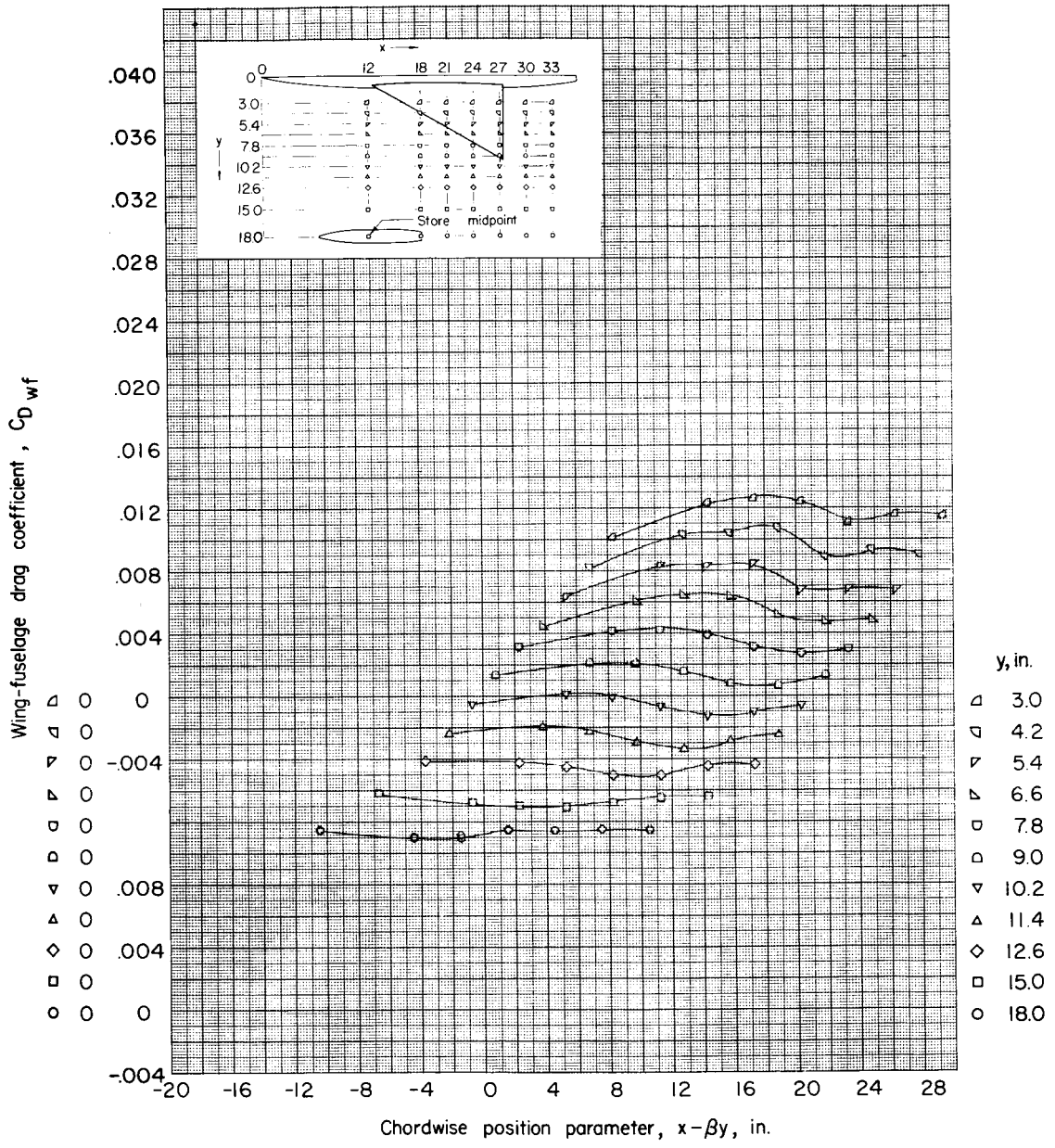

(c) z = 2.09 inches; $\alpha = 0^{\circ}$.

Figure 9.- Continued.

[redacted]

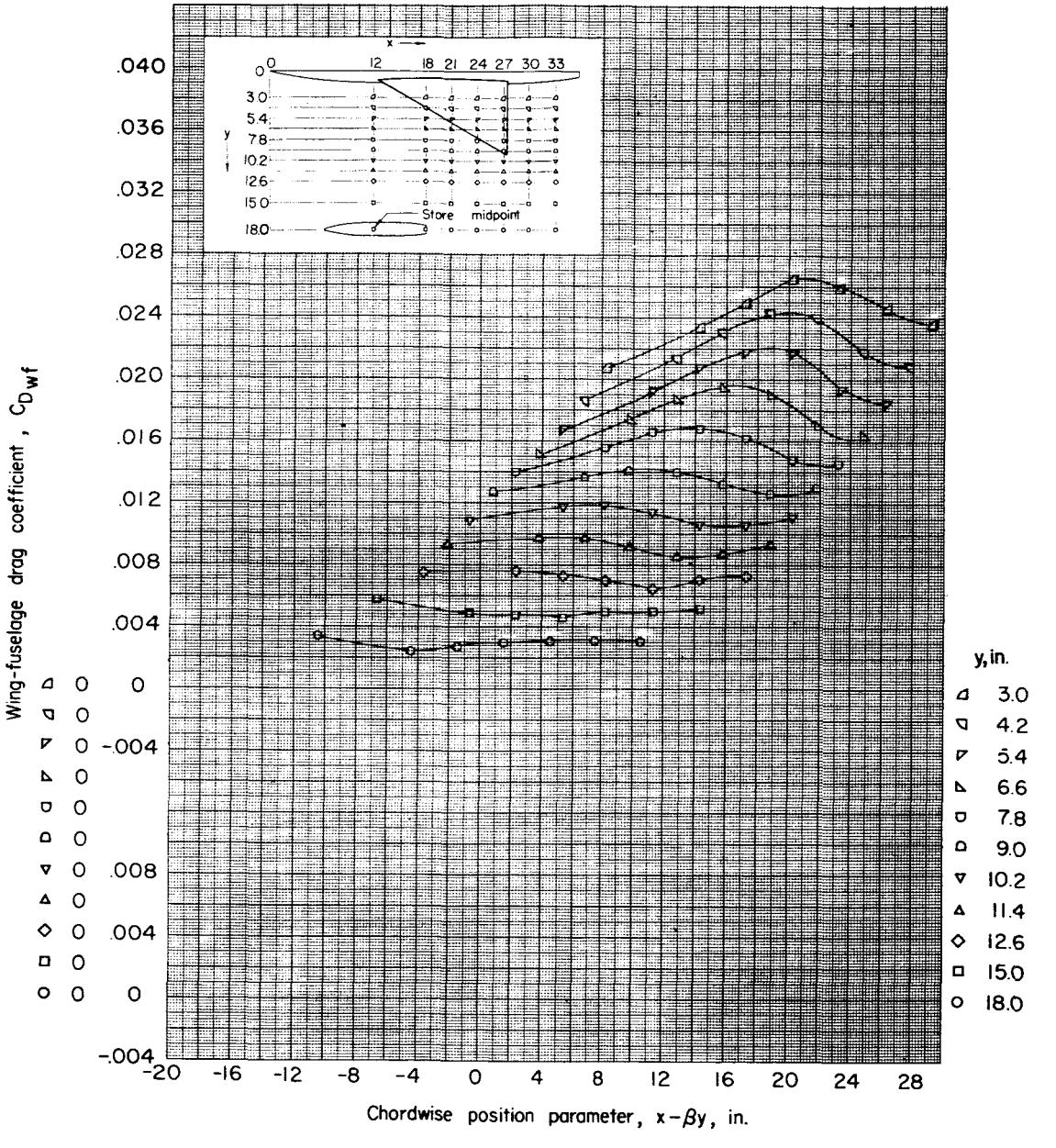

(d) z = 2.09 inches; $\alpha = 4^{\circ}$.

Figure 9.- Concluded.

[redacted]

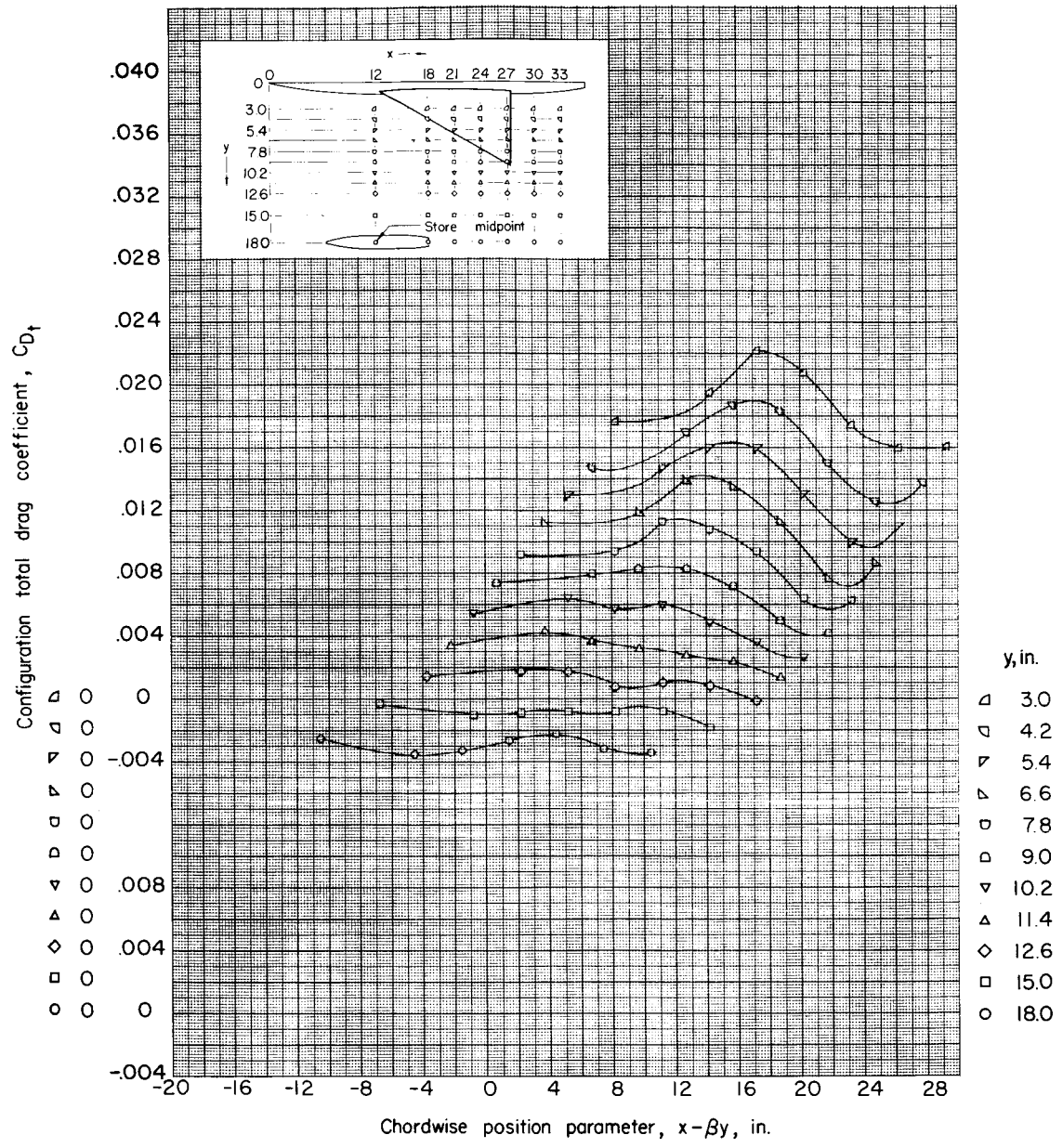

(a) z = 1.15 inches; $\alpha = 0^{\circ}$.

Figure 10.- Total drag of the complete configuration (wing and fuselage plus store). M = 1.61.

[redacted]

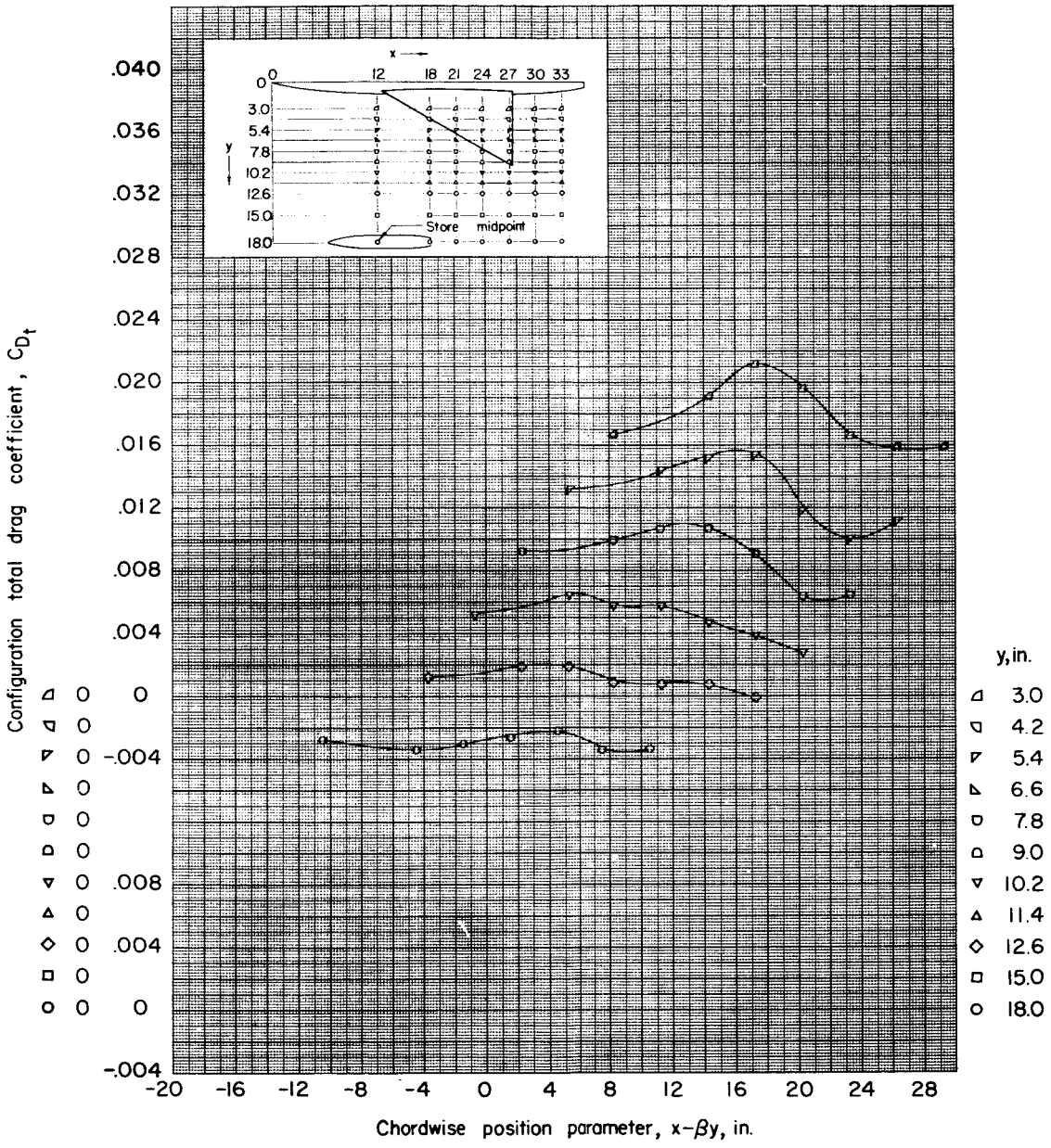

(b) z = 1.67 inches; $\alpha = 0^{\circ}$.

Figure 10.- Continued.

[redacted]

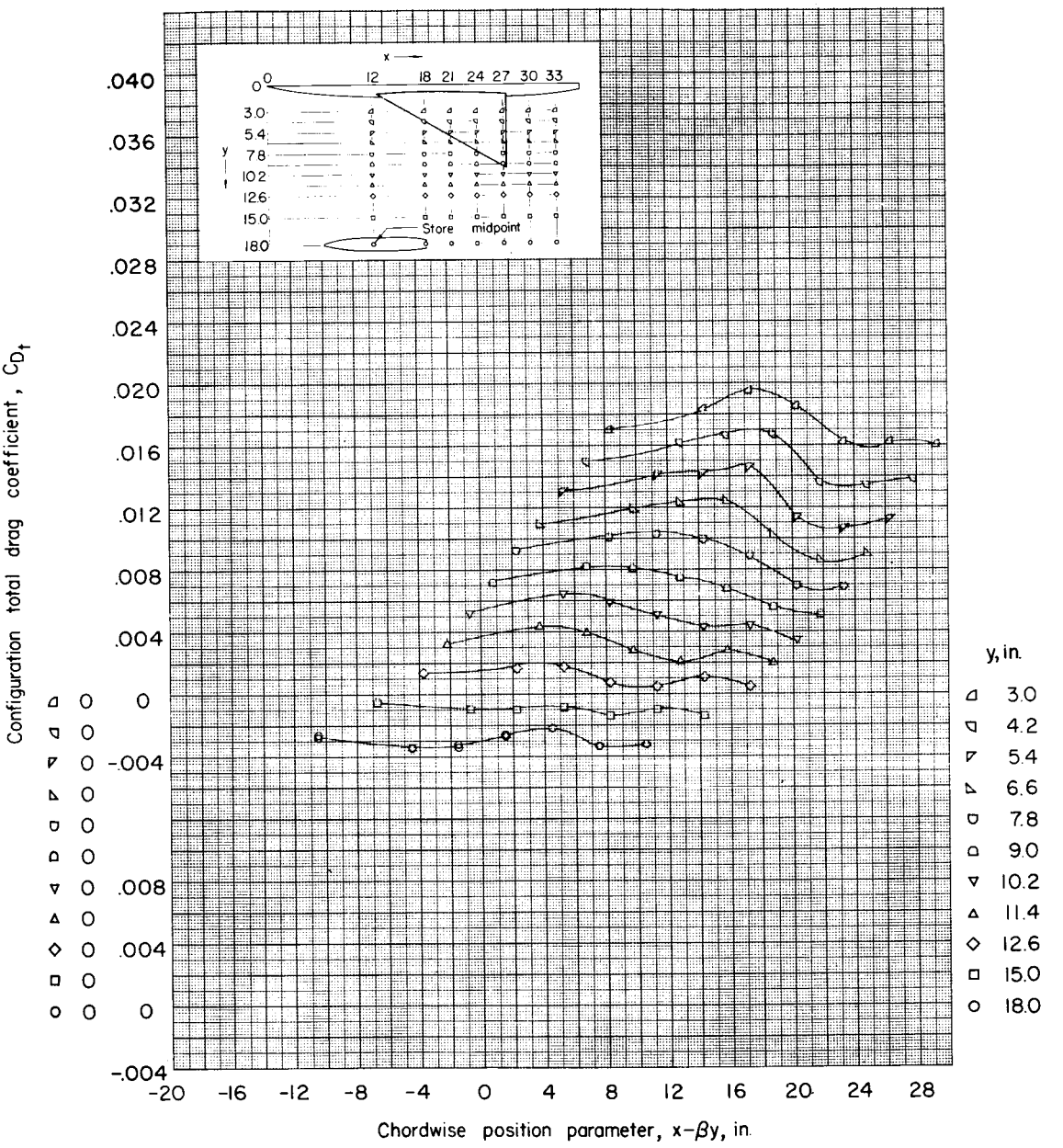

(c) z = 2.09 inches; $\alpha = 0^{\circ}$.

Figure 10.- Continued.

[redacted]

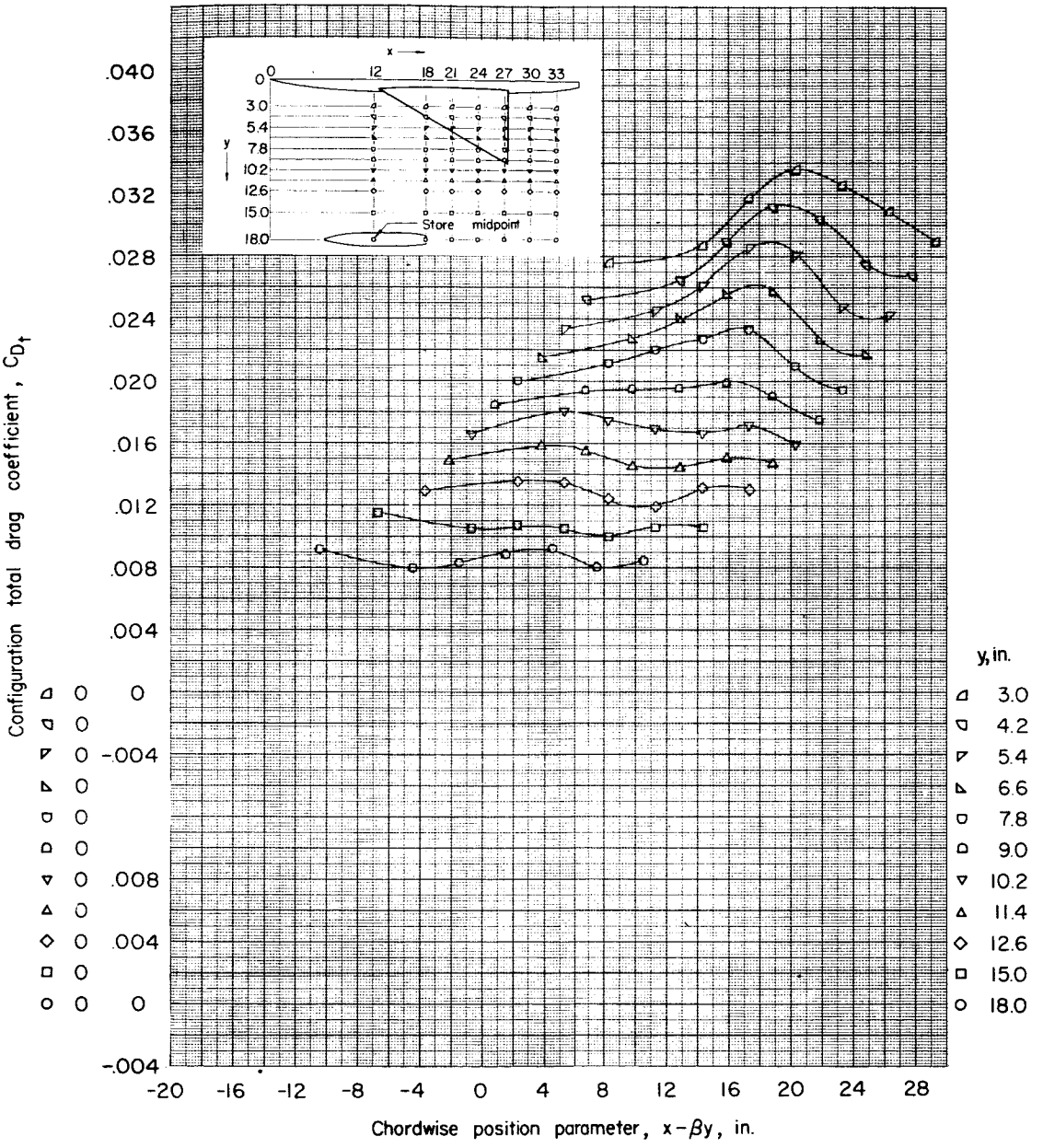

(d) z = 2.09 inches; $\alpha = 4^{\circ}$.

Figure 10.- Concluded.

[redacted]

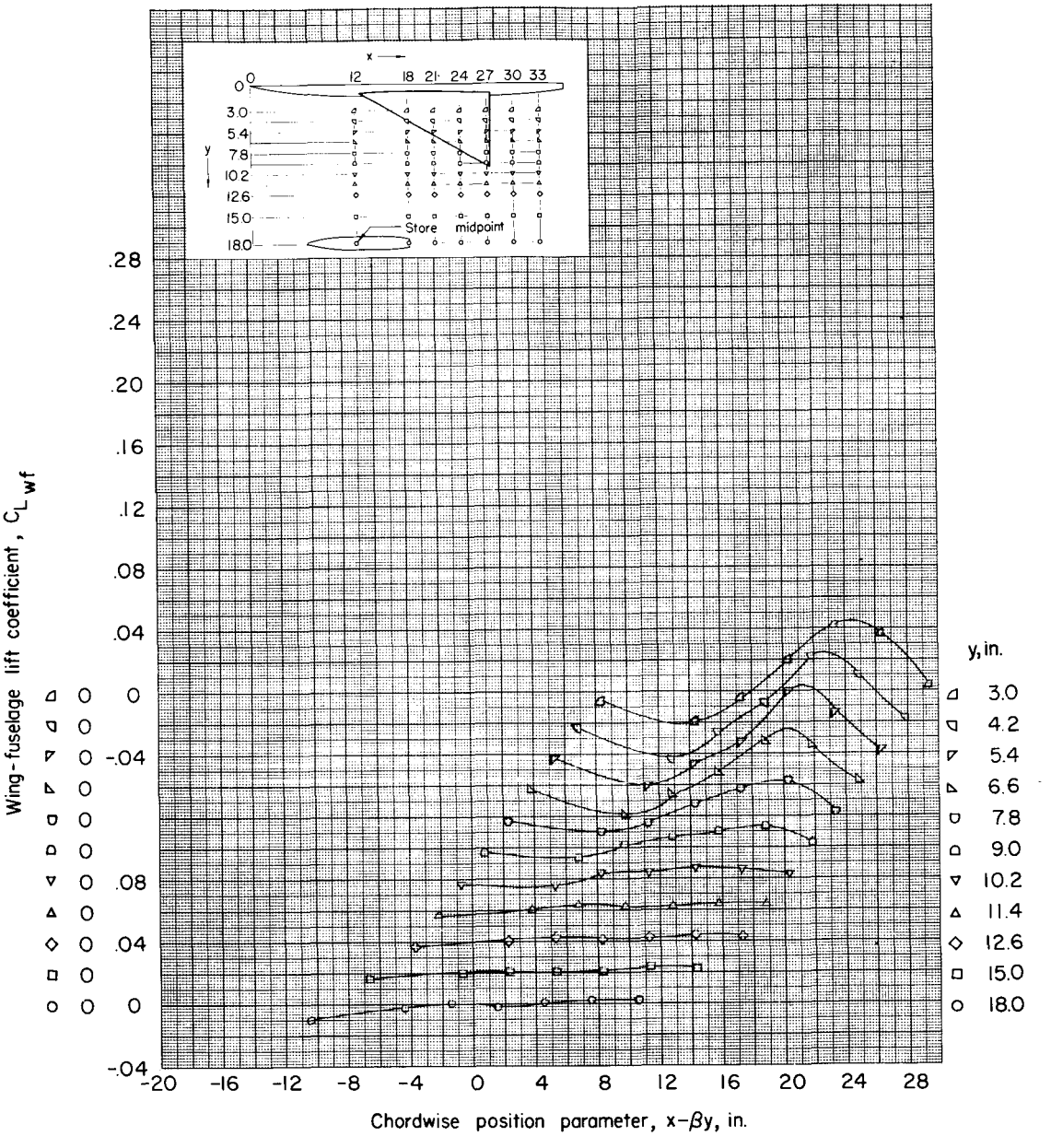

(a) z = 1.15 inches; $\alpha = 0^{\circ}$.

Figure 11.- Lift of wing-fuselage combination in presence of store. M = 1.61.

[redacted]

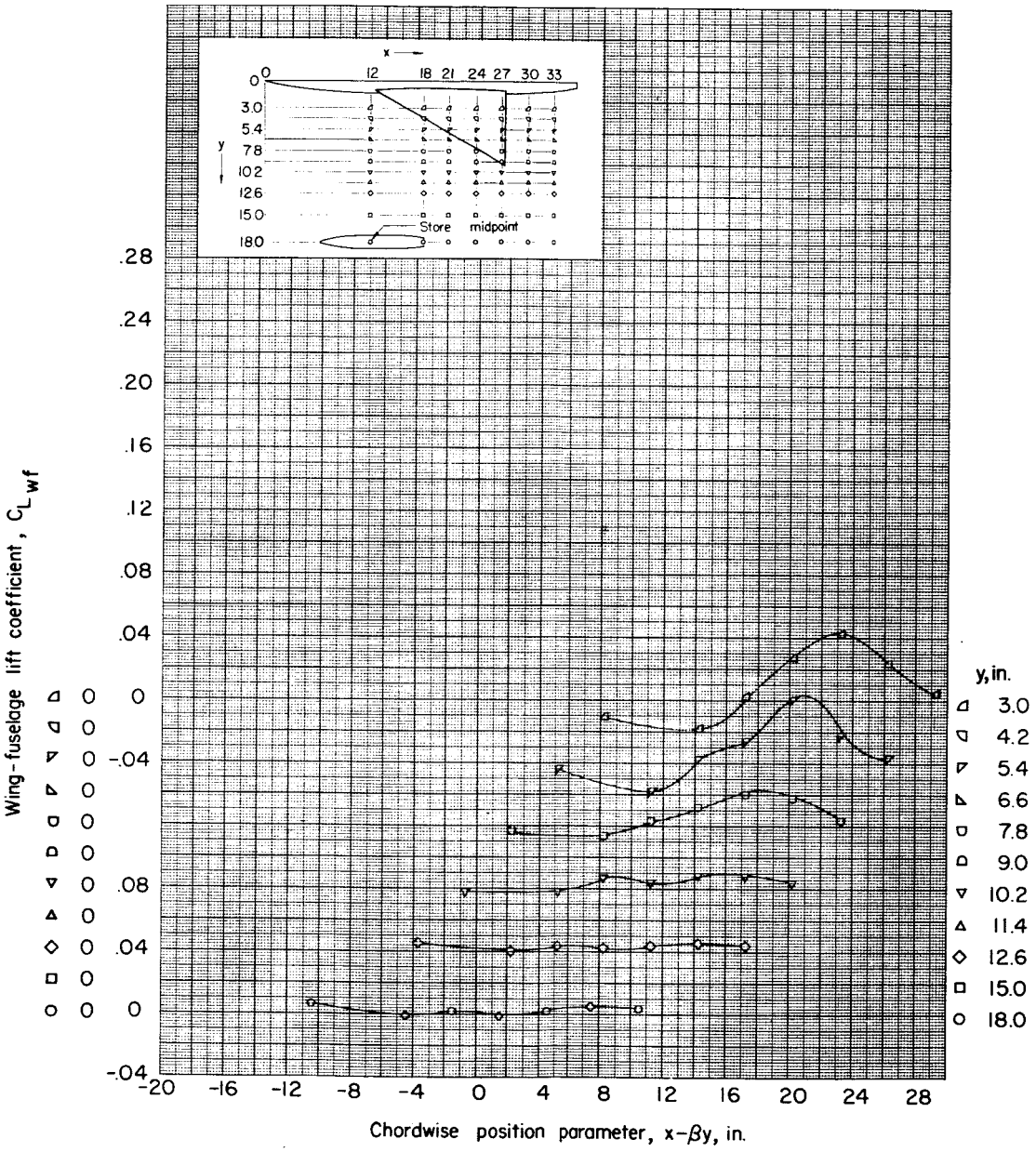

(b) z = 1.67 inches; $\alpha = 0^{\circ}$.

Figure 11.- Continued.

[redacted]

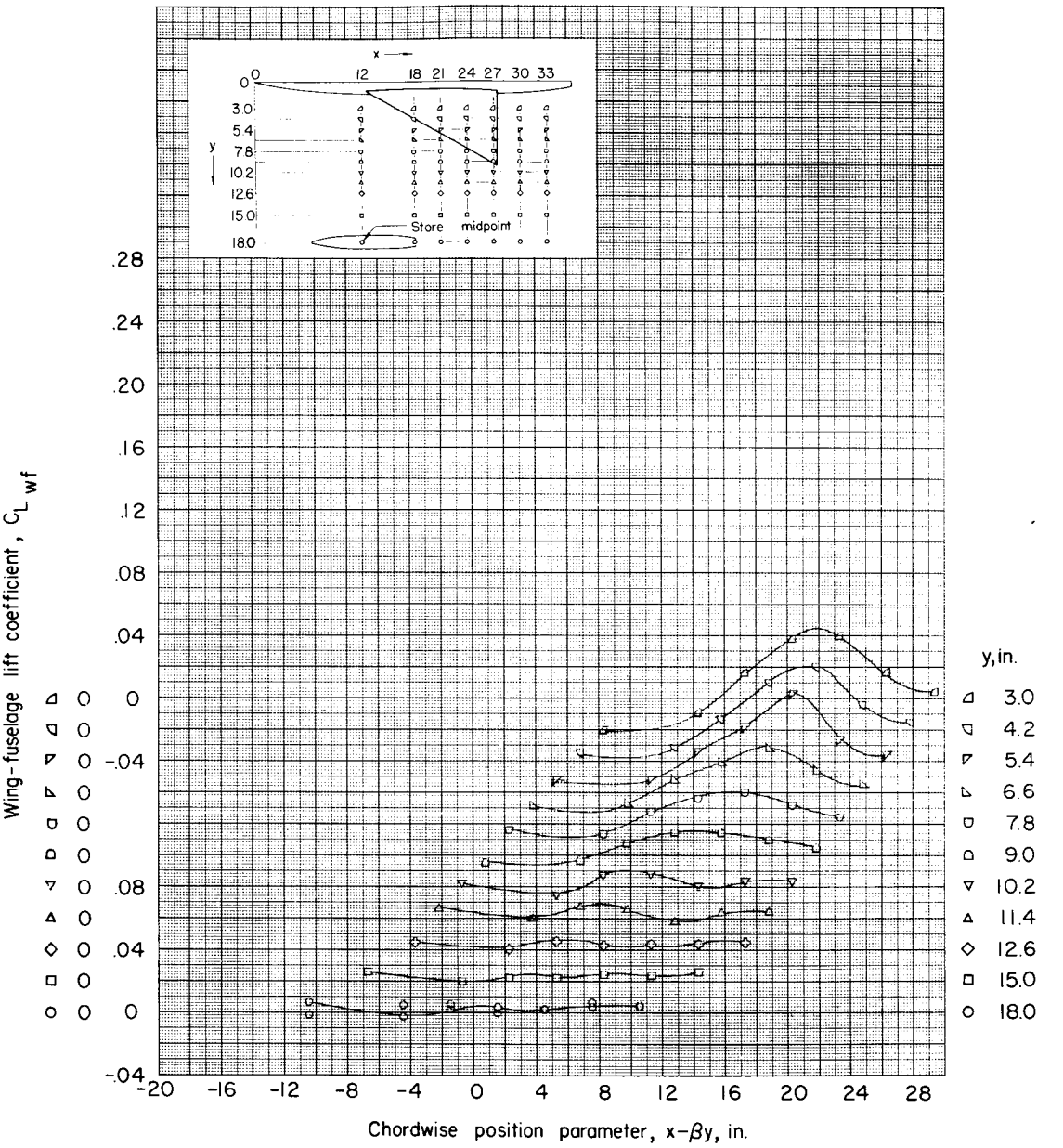

(c) z = 2.09 inches; $\alpha = 0^{\circ}$.

Figure 11.- Continued.

[redacted]

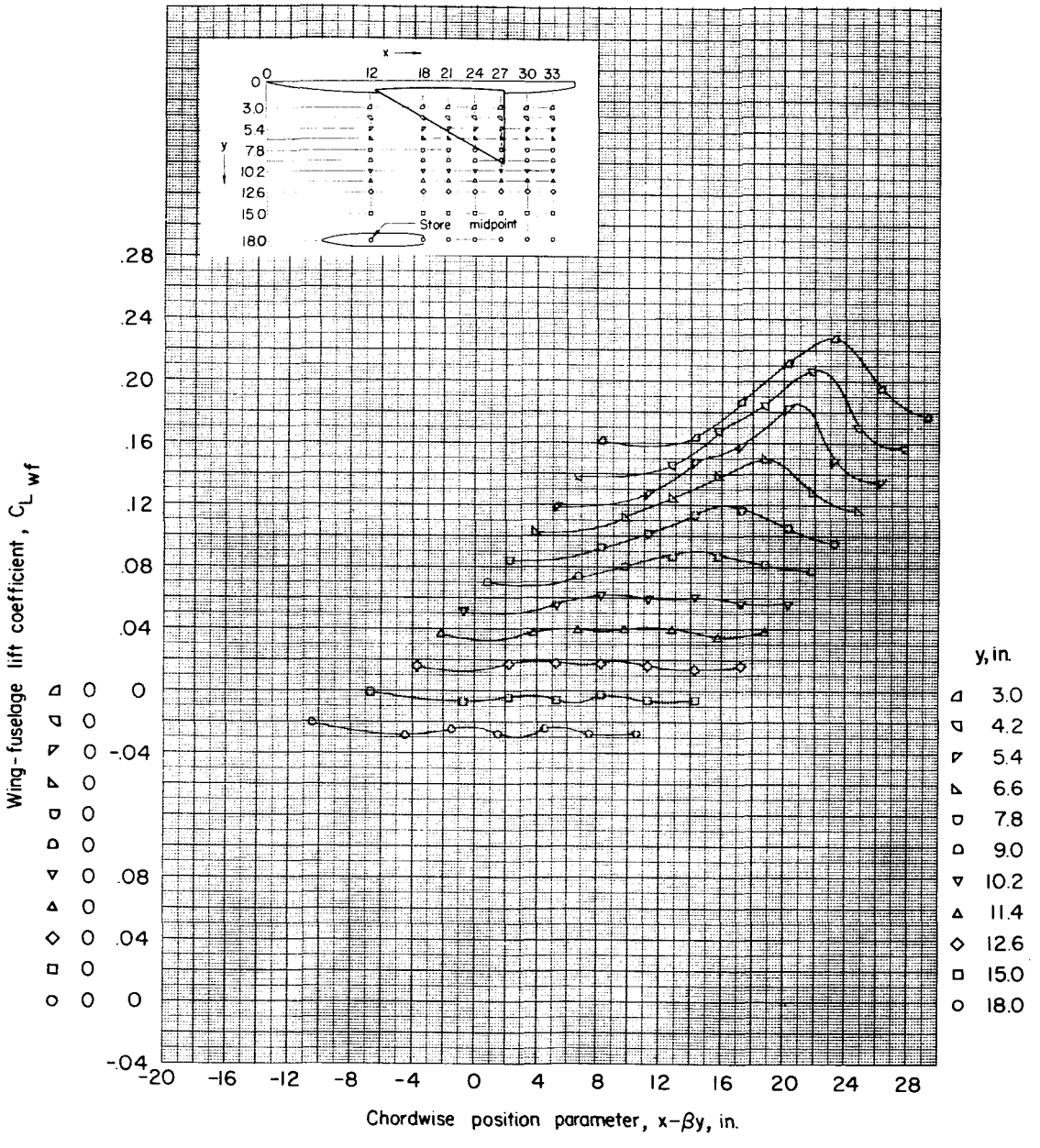

(d) z = 2.09 inches; $\alpha = 4^{\circ}$.

Figure 11.- Concluded.

[redacted]

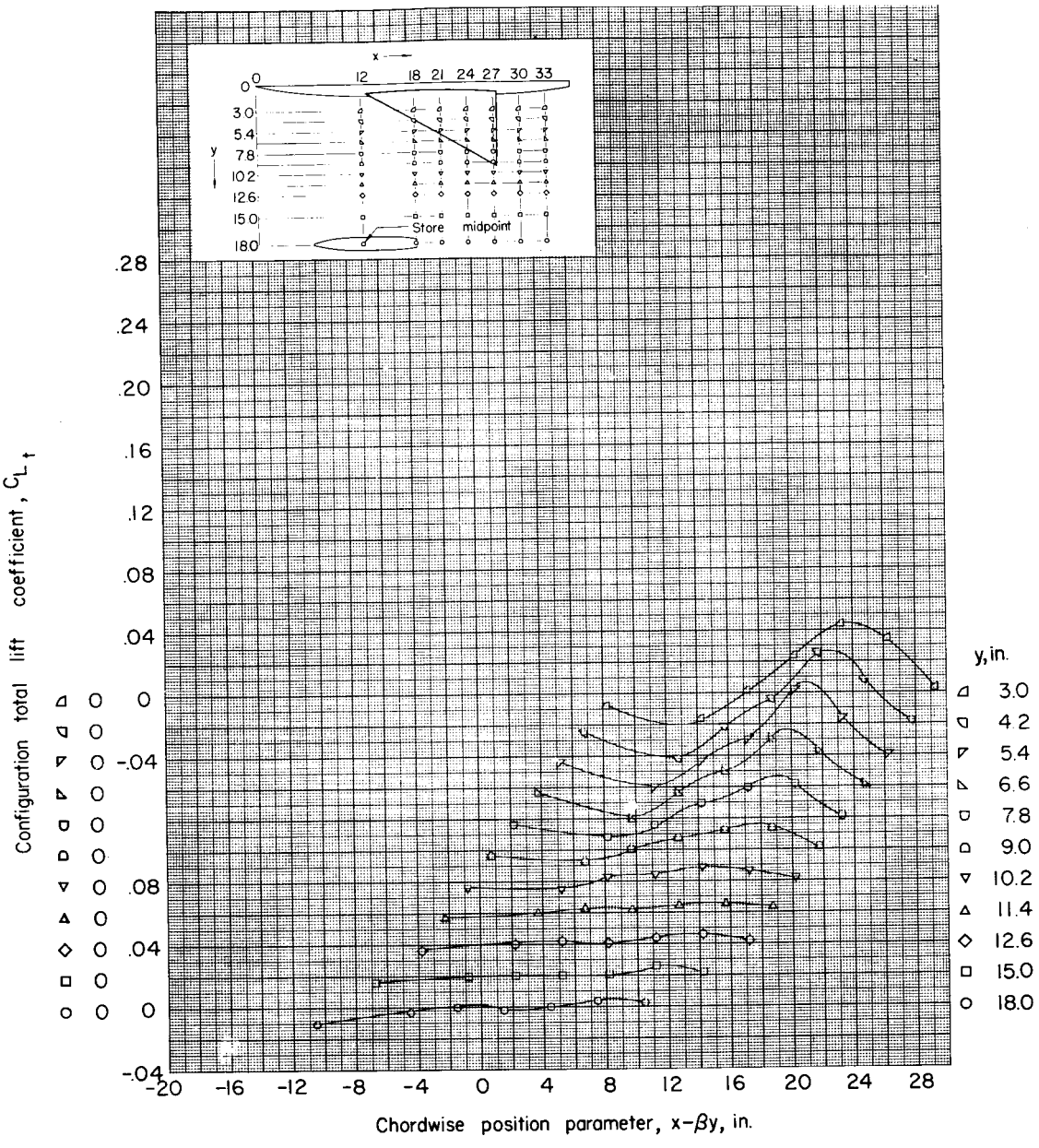

(a) z = 1.15 inches; $\alpha = 0^{\circ}$.

Figure 12.- Total lift of the complete configuration (wing and fuselage plus store). M = 1.61.

[redacted]

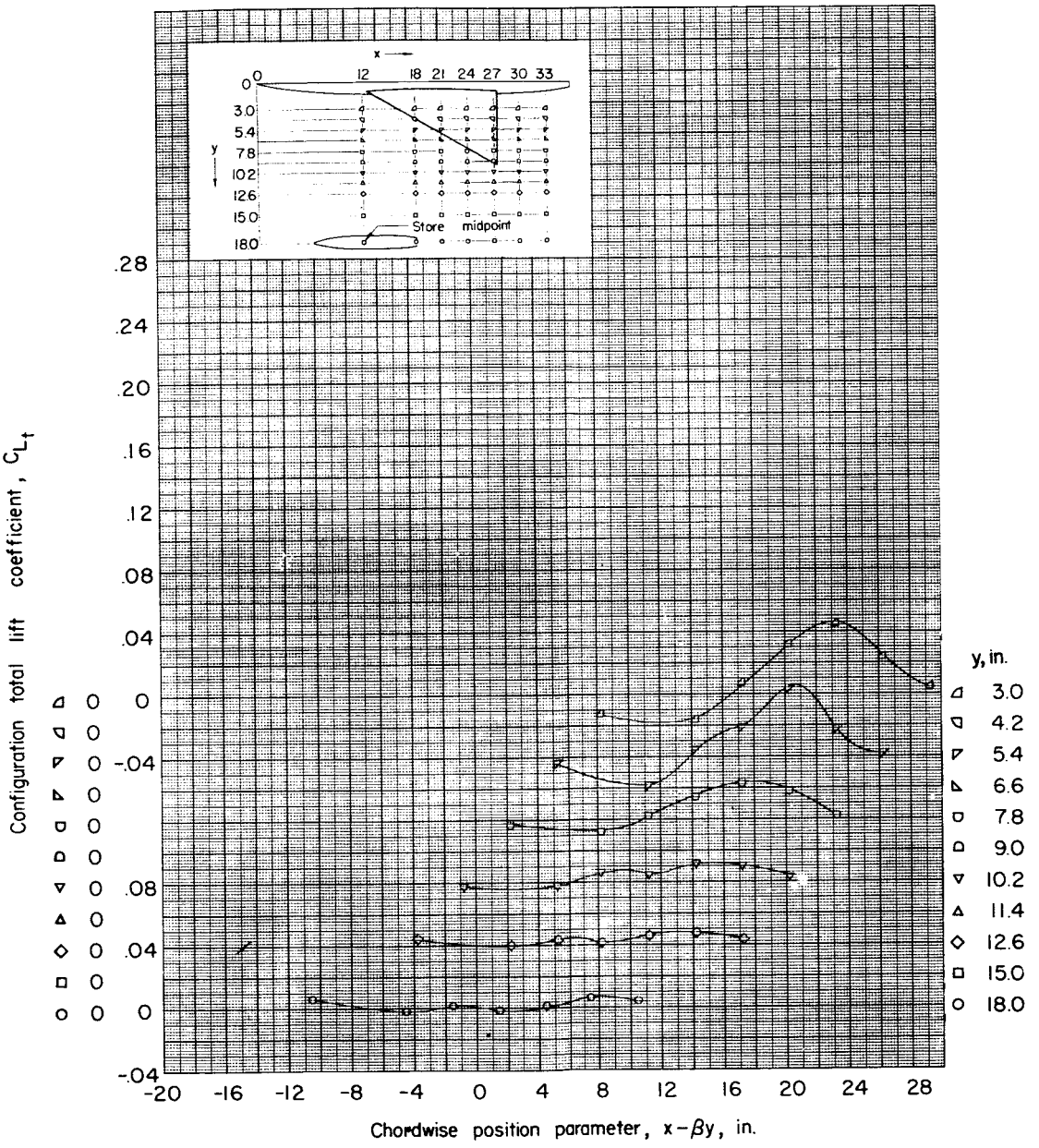

(b) z = 1.67 inches; $\alpha = 0^{\circ}$.

Figure 12.- Continued.

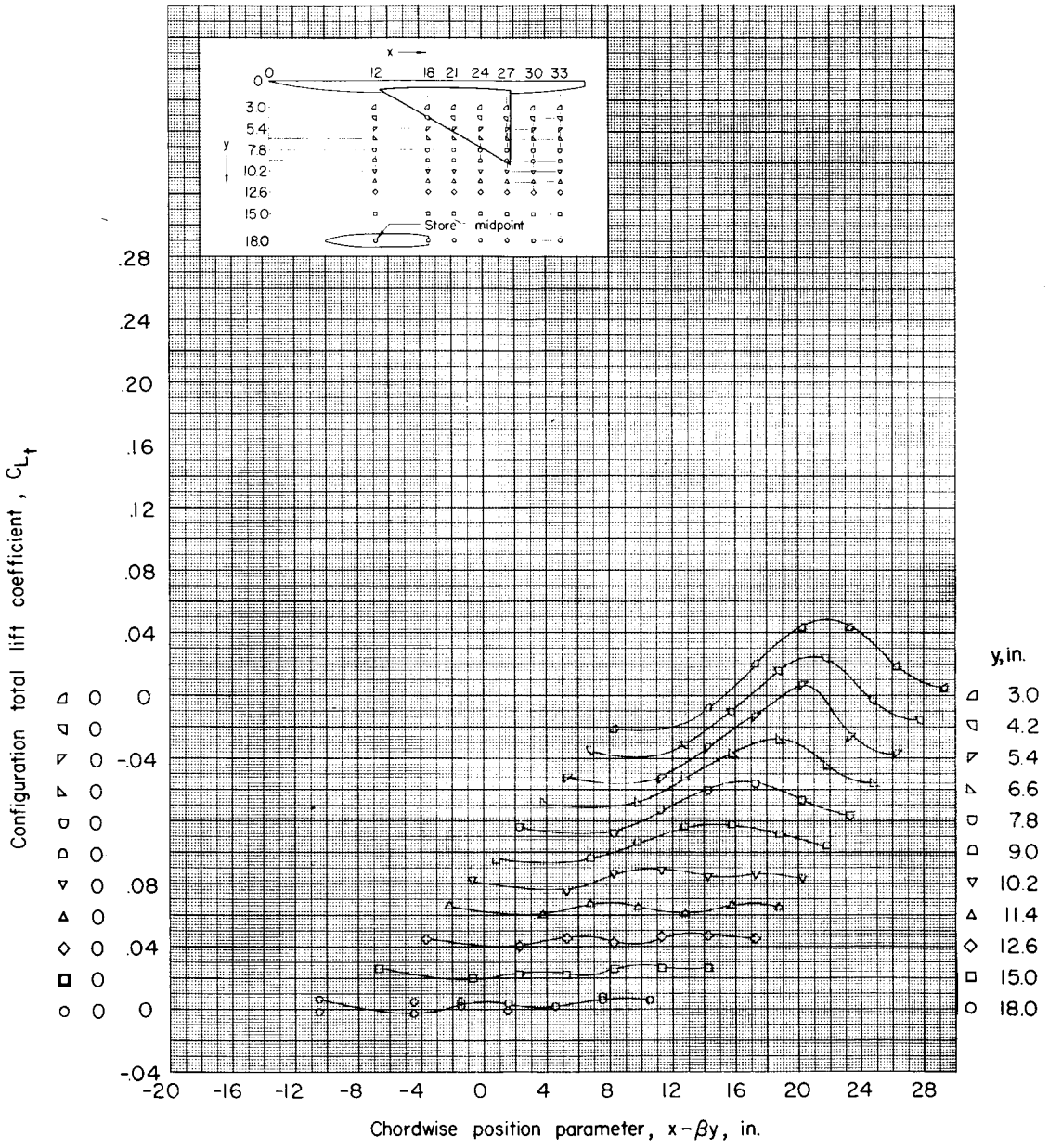

(c) z = 2.09 inches; $\alpha = 0^{\circ}$.

Figure 12.- Continued.

[redacted]

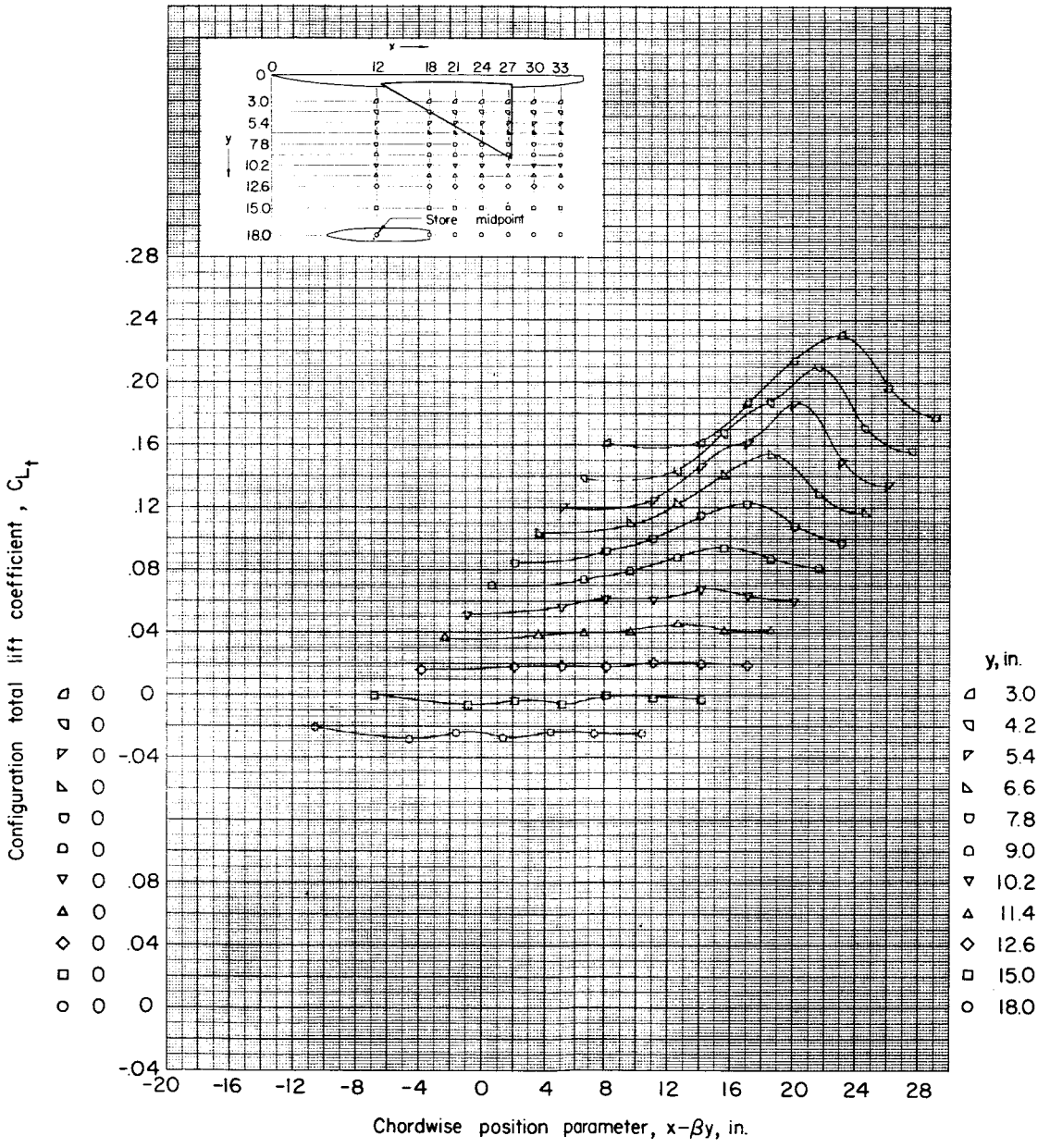

(d) z = 2.09 inches; $\alpha = 4^{\circ}$.

Figure 12.- Concluded.

[redacted]

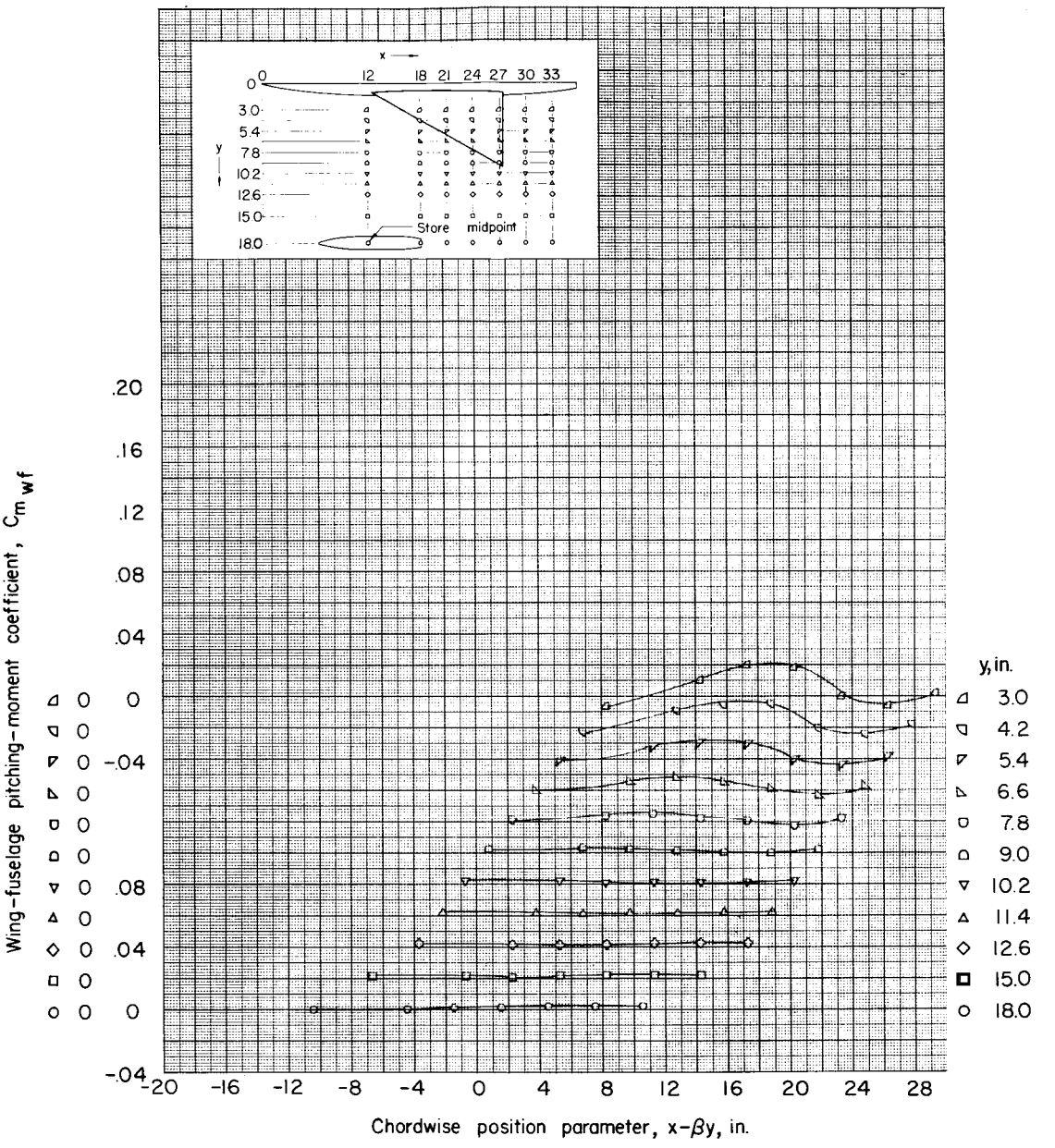

(a) $z = 1.15$ inches; $\alpha = 0^\circ$.

Figure 13.- Pitching moment of wing-fuselage combination in presence of store (computed about $0.625\bar{c}$). $M = 1.61$.

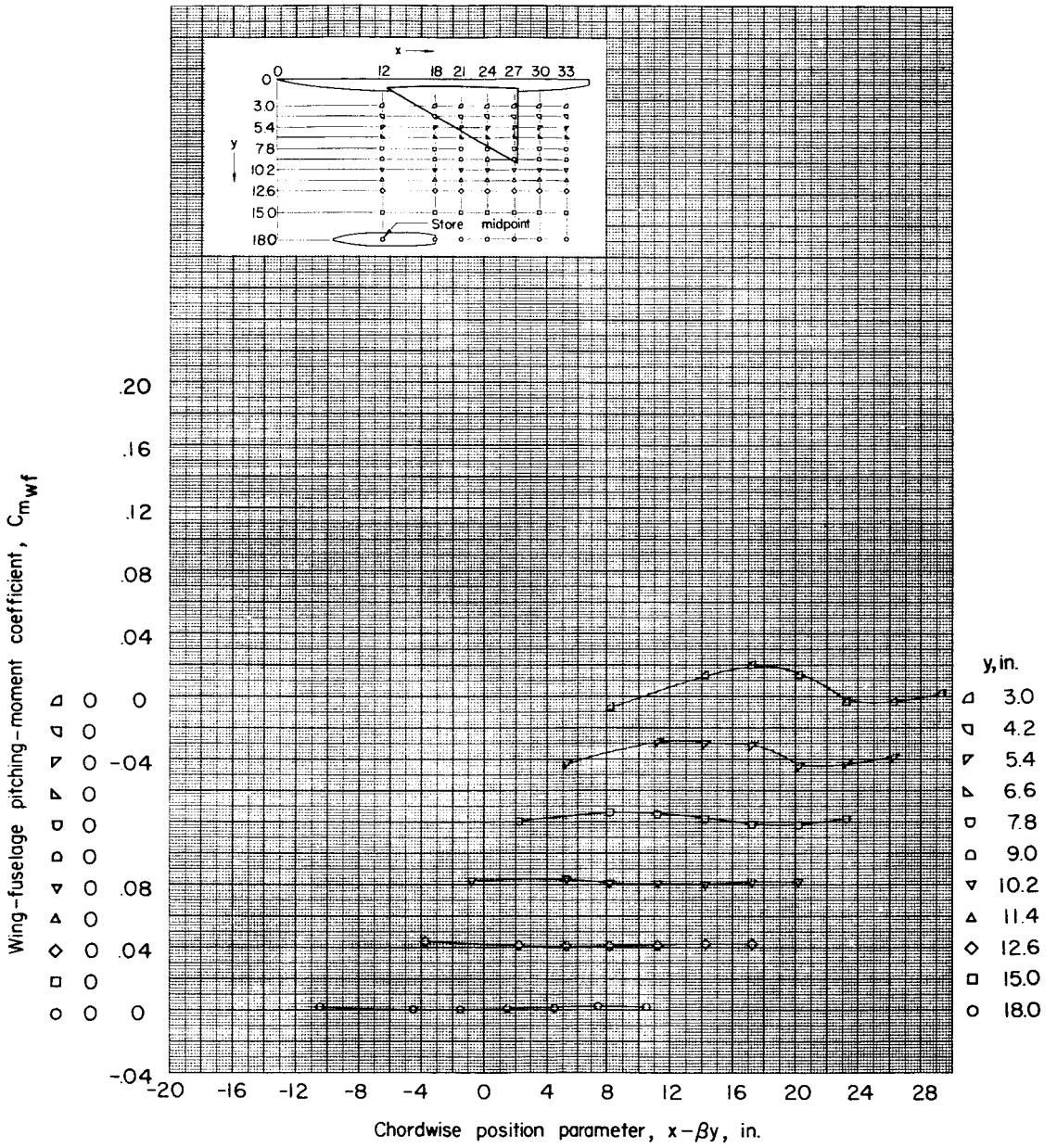

(b) z = 1.67 inches; $\alpha = 0^{\circ}$.

Figure 13.- Continued.

[redacted]

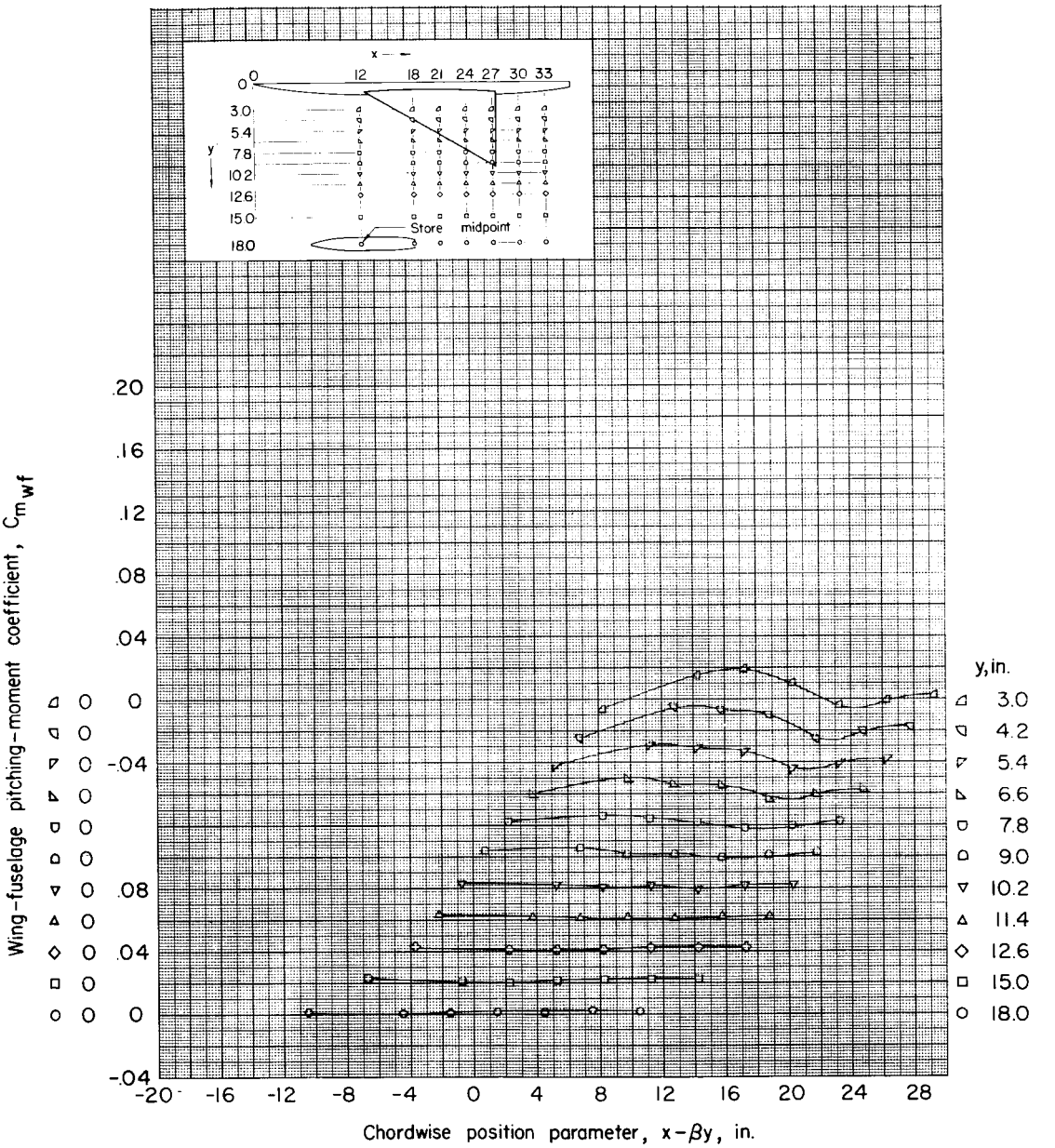

(c) z = 2.09 inches; $\alpha = 0^{\circ}$.

Figure 13.- Continued.

[redacted]

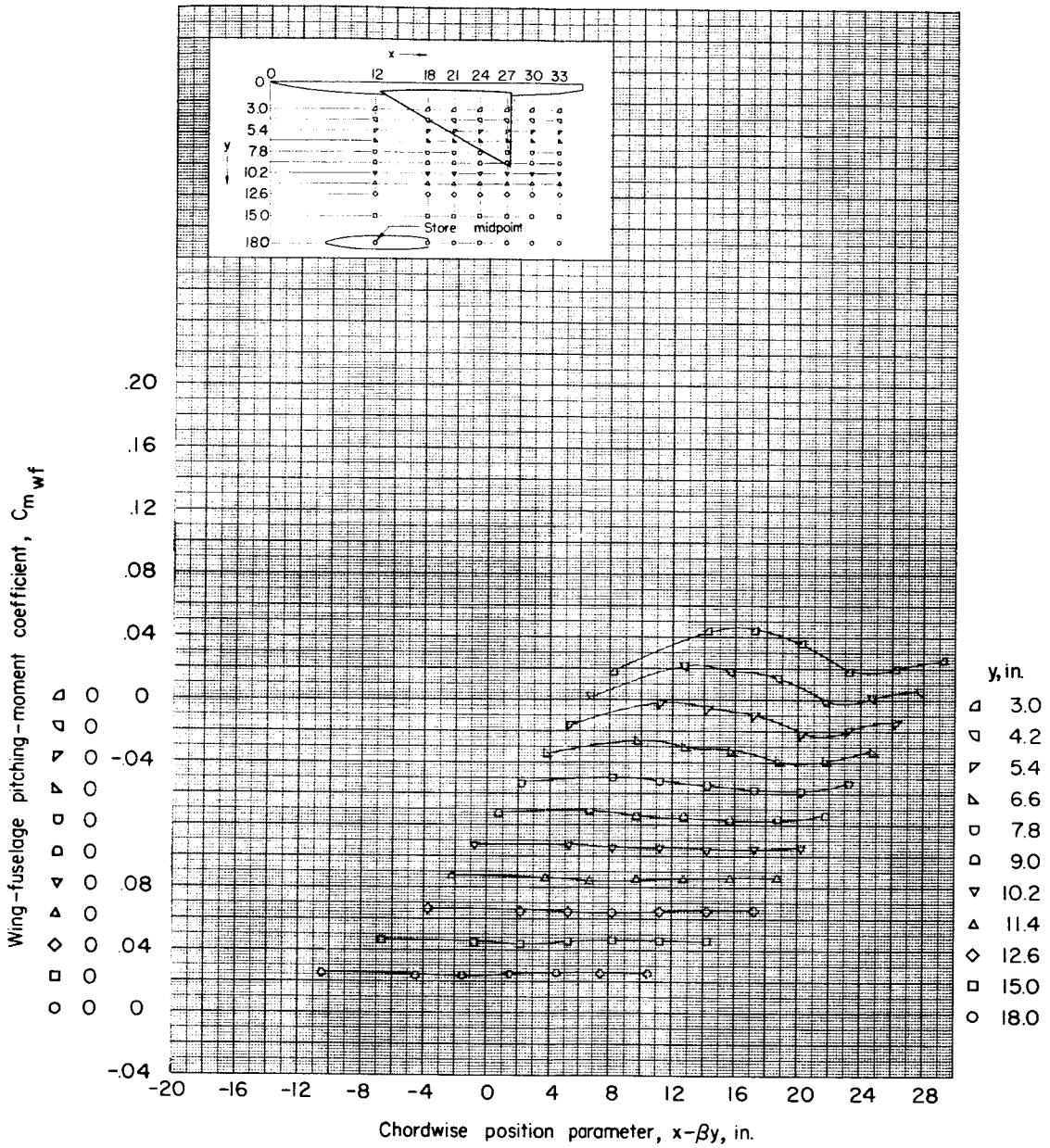

(d) z = 2.09 inches; $\alpha = 4^{\circ}$.

Figure 13.- Concluded.

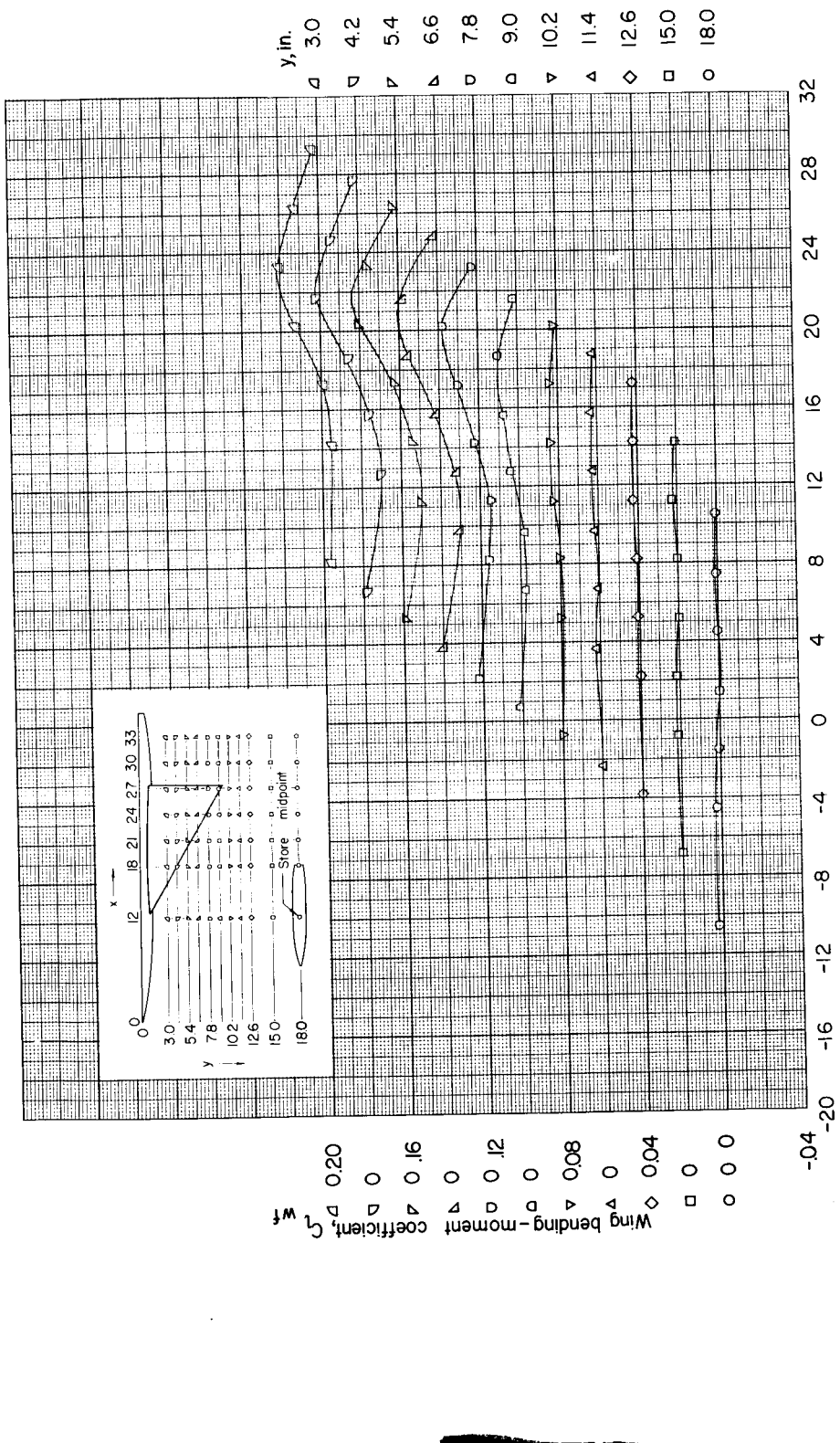

(a) $z = 1.15$ inches; $\alpha = 0^{\circ}$.

Figure 14.- Wing bending moment for wing-fuselage combination in presence of store.

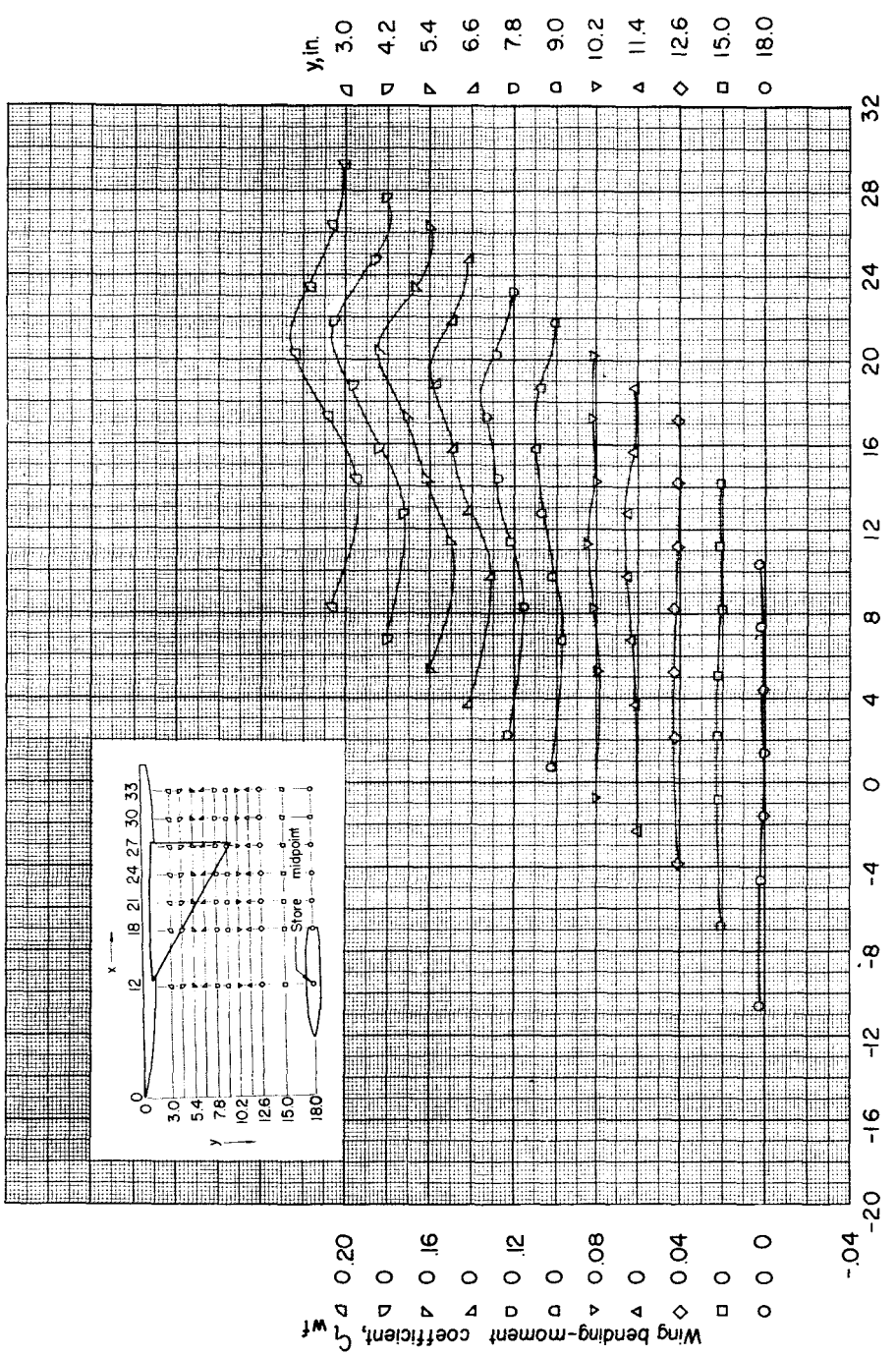

(b) z = 2.09 inches; $\alpha = 0^{\circ}$.

Figure 14.- Continued.

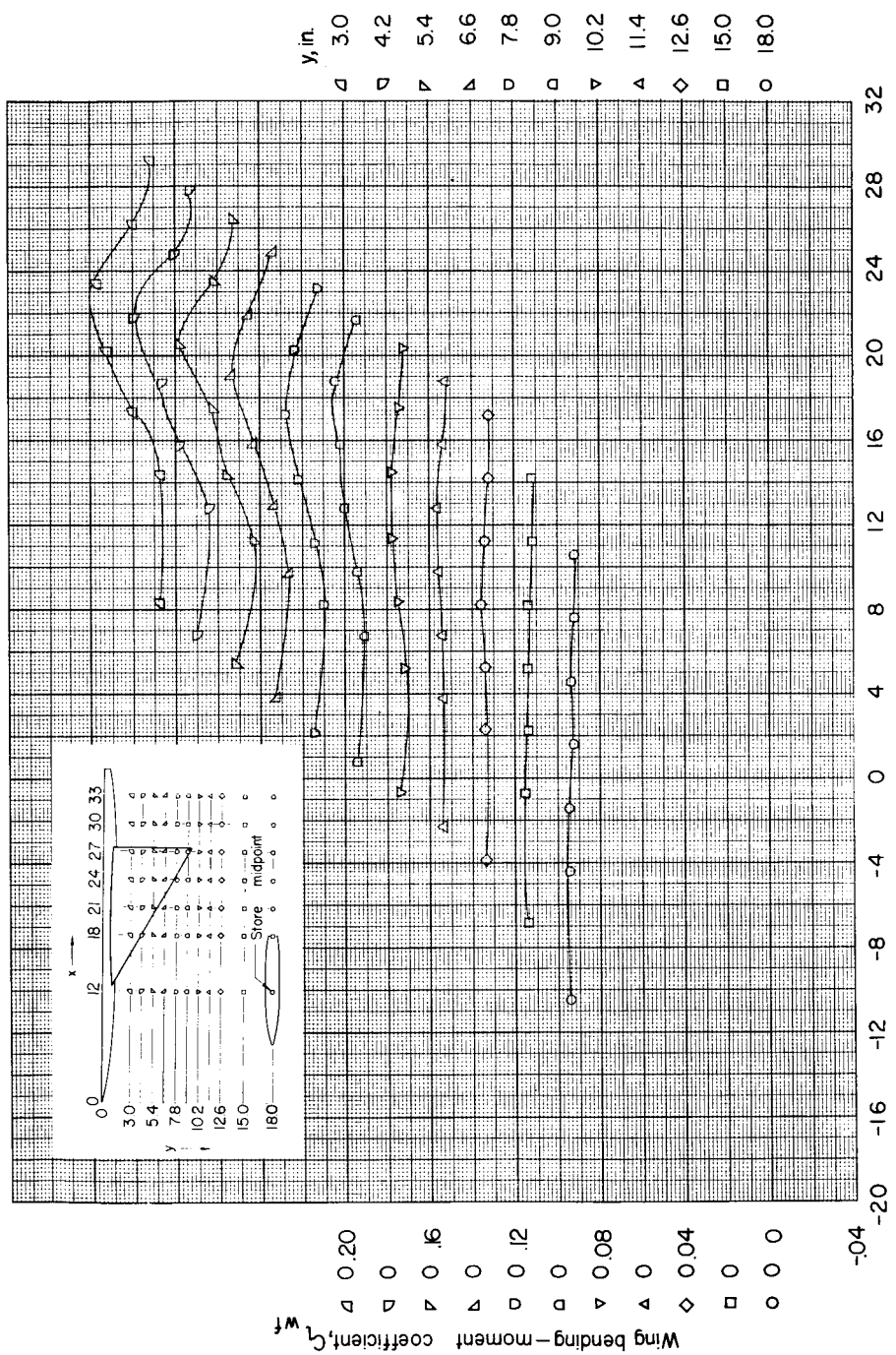

(c) $z = 2.09$ inches; $\alpha = 4^{\circ}$.

Figure 14.- Concluded.

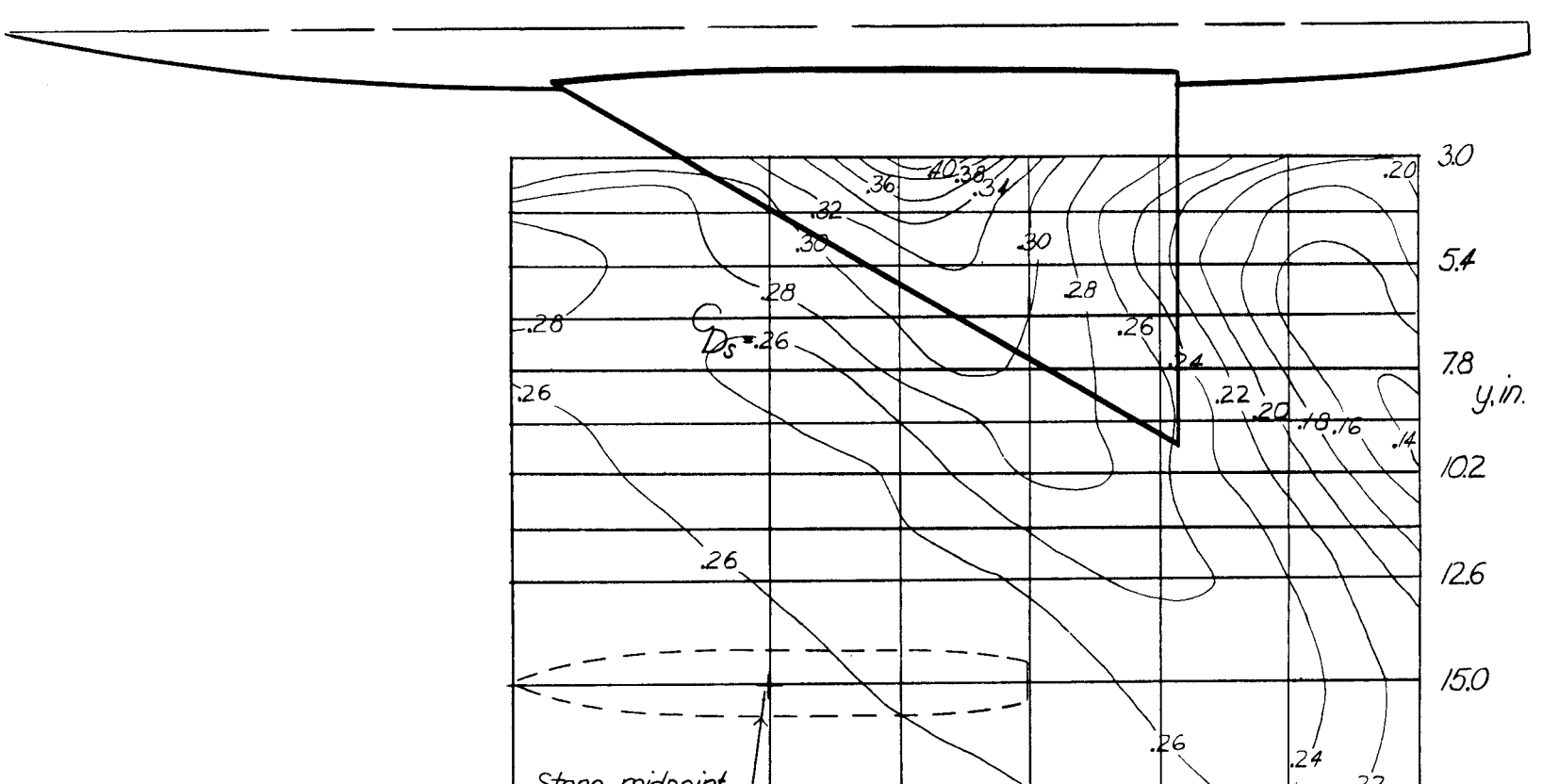

(a) z = 1.15 inches; $\alpha = 0^{\circ}$.

Figure 15.- Contour plot of the drag of store in presence of wing-fuselage combination. Drag coefficient of isolated store is 0.252.

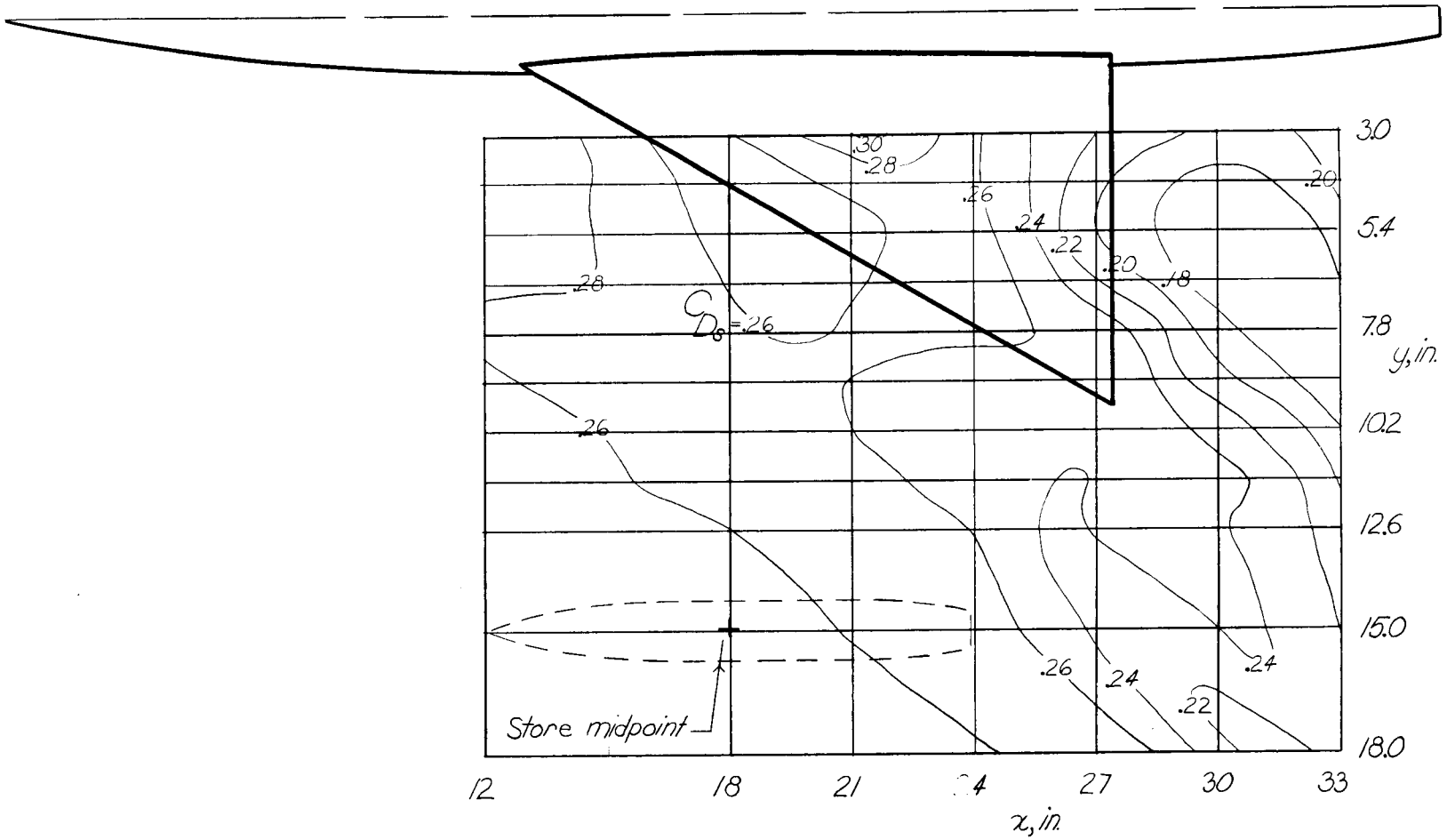

(b) z = 2.09 inches; $\alpha = 0^\circ$.

Figure 15.- Continued.

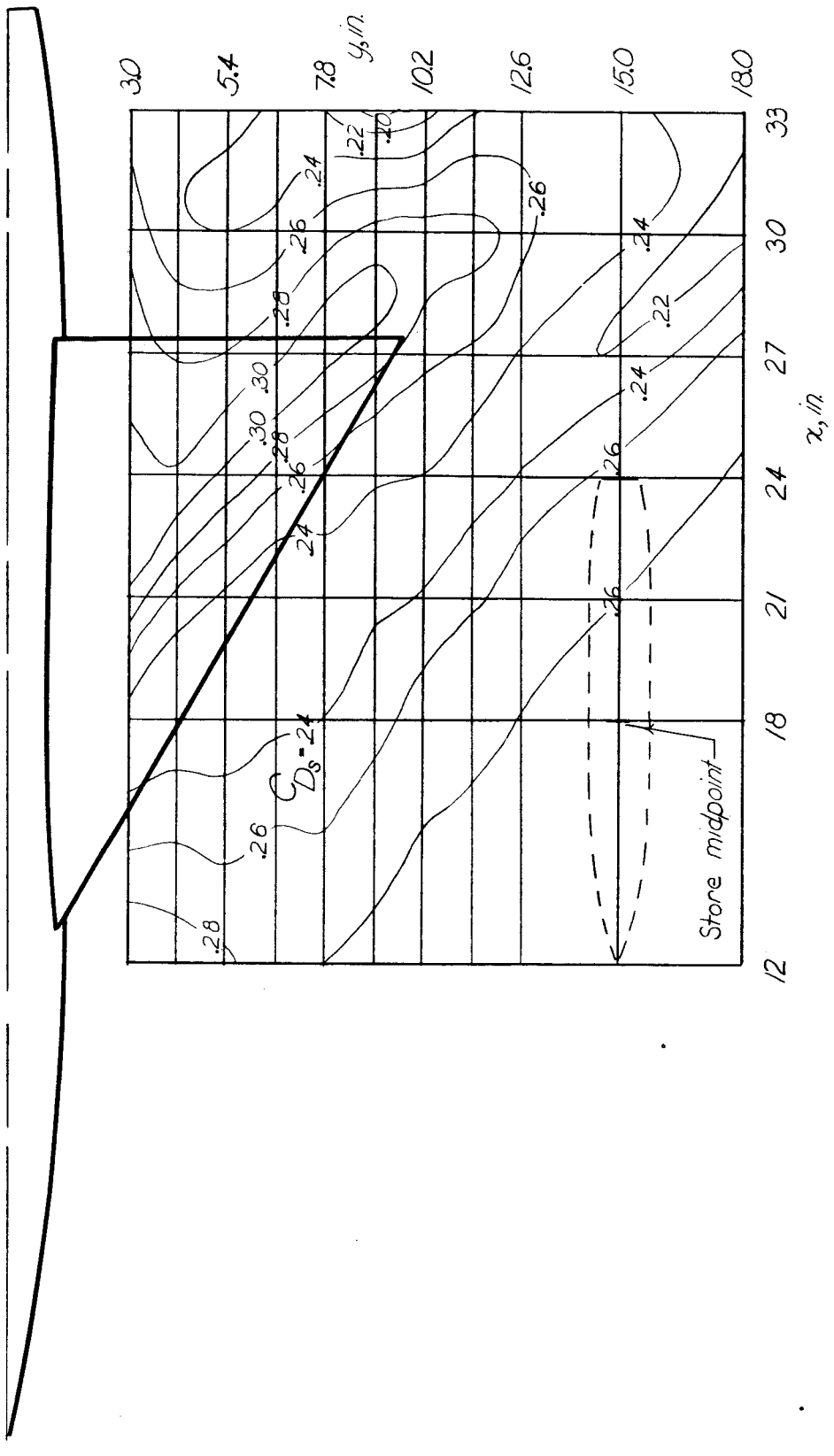

(c) z = 2.09 inches; $\alpha = 4^\circ$.

Figure 15.- Concluded.

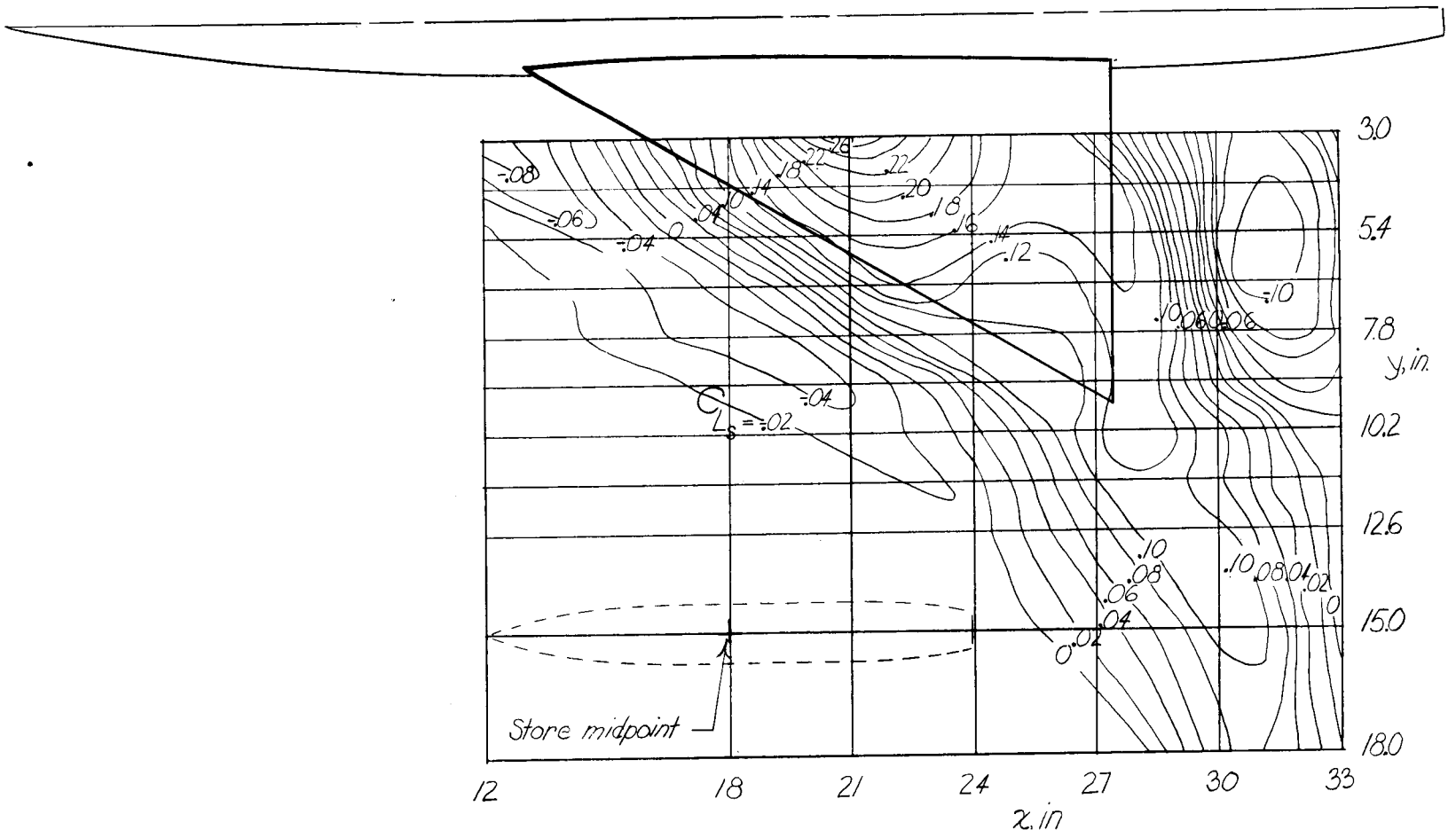

(a) z = 1.15 inches; $\alpha = 0^{\circ}$.

Figure 16.- Contour plot of lift of store in presence of wing-fuselage combination.

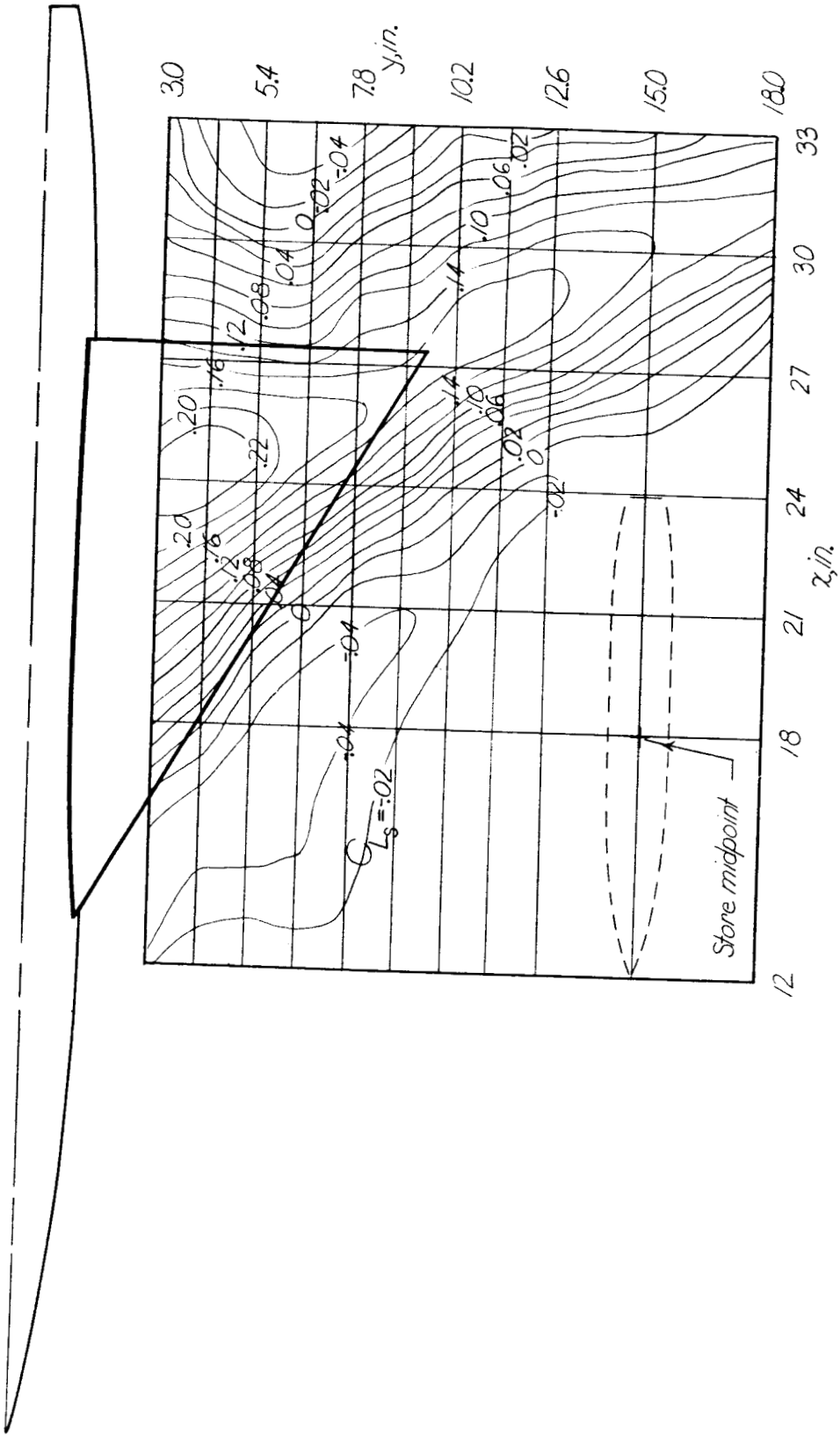

(b) z = 2.09 inches; α = 0°.

Figure 16.- Continued.

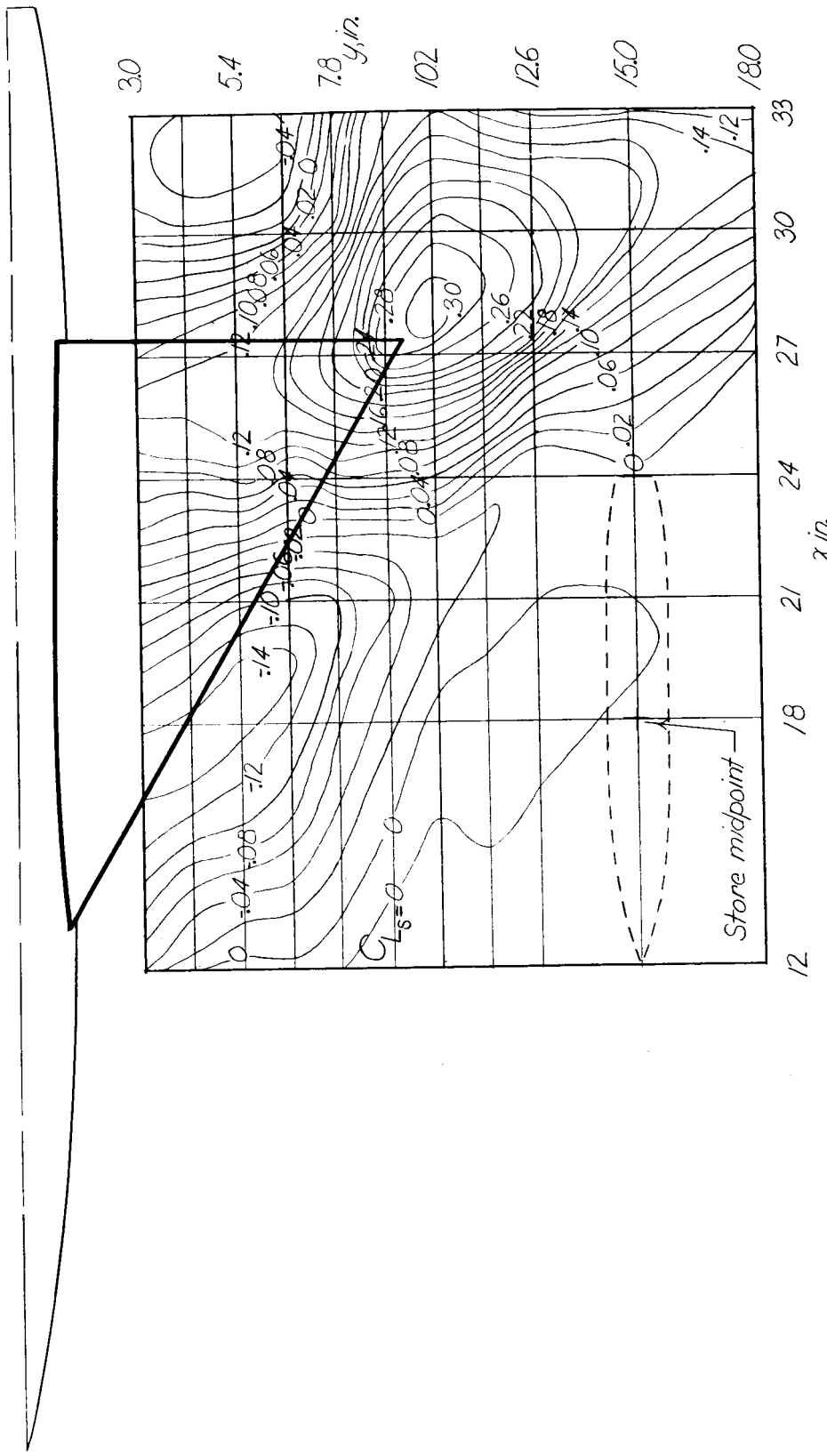

(c) z = 2.09 inches; $\alpha = 4^{\circ}$.

Figure 16.- Concluded.

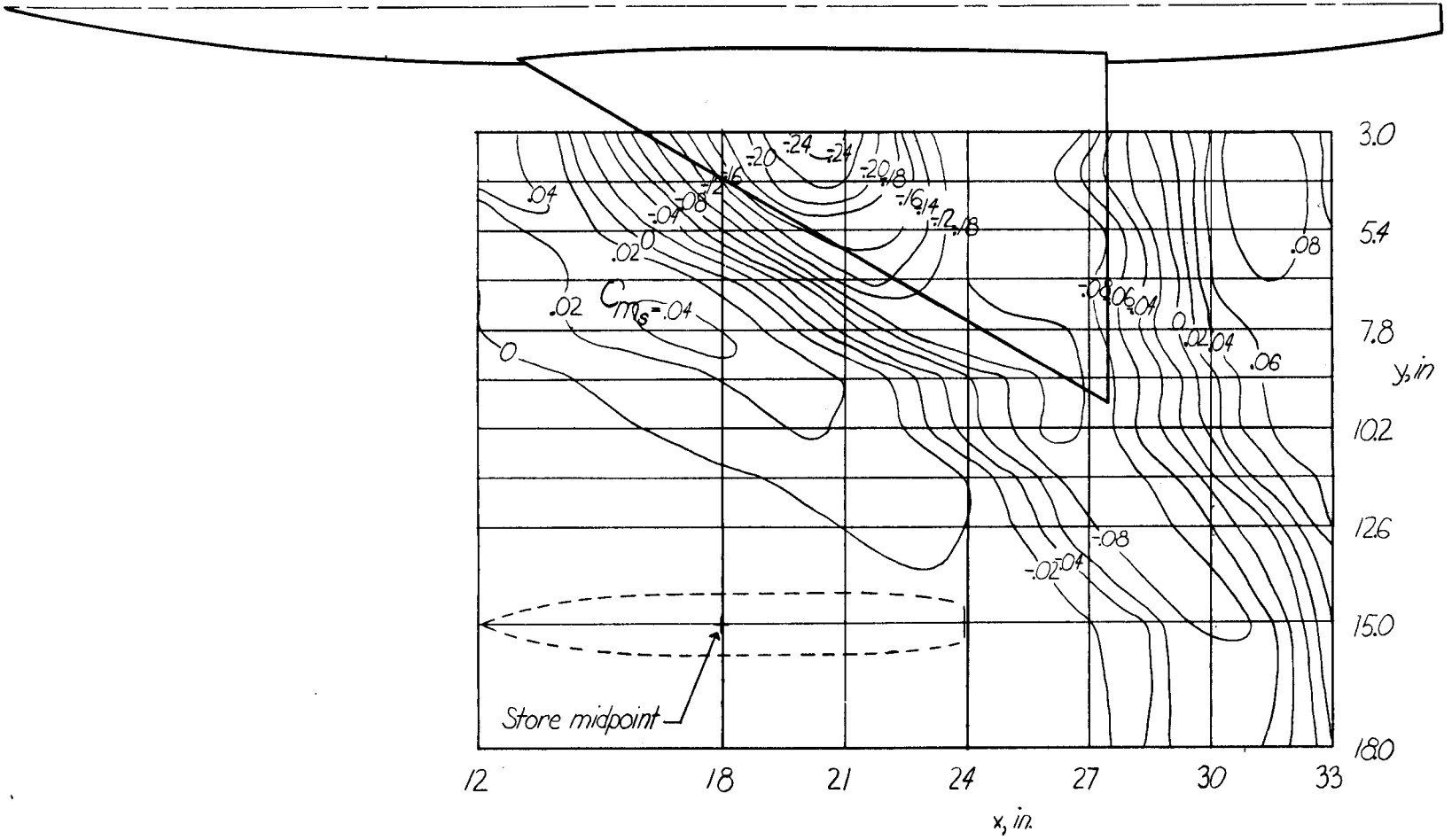

(a) z = 1.15 inches; $\alpha = 0^{\circ}$.

Figure 17.- Contour plot of pitching moment of store in presence of wing-fuselage combination (computed about store nose). M = 1.61.

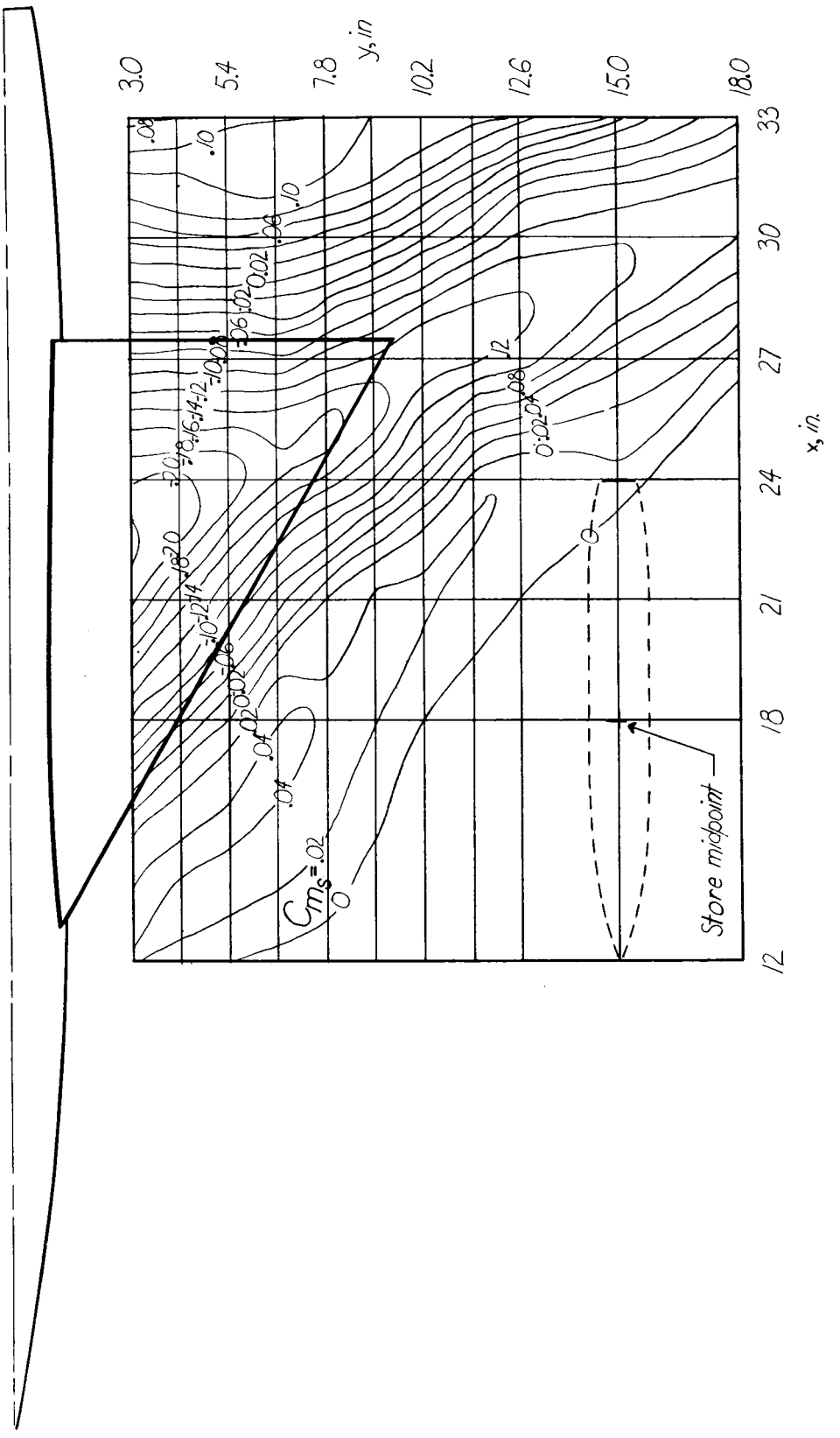

(b) z = 2.09 inches; $\alpha = 0^{\circ}$.

Figure 17.- Continued.

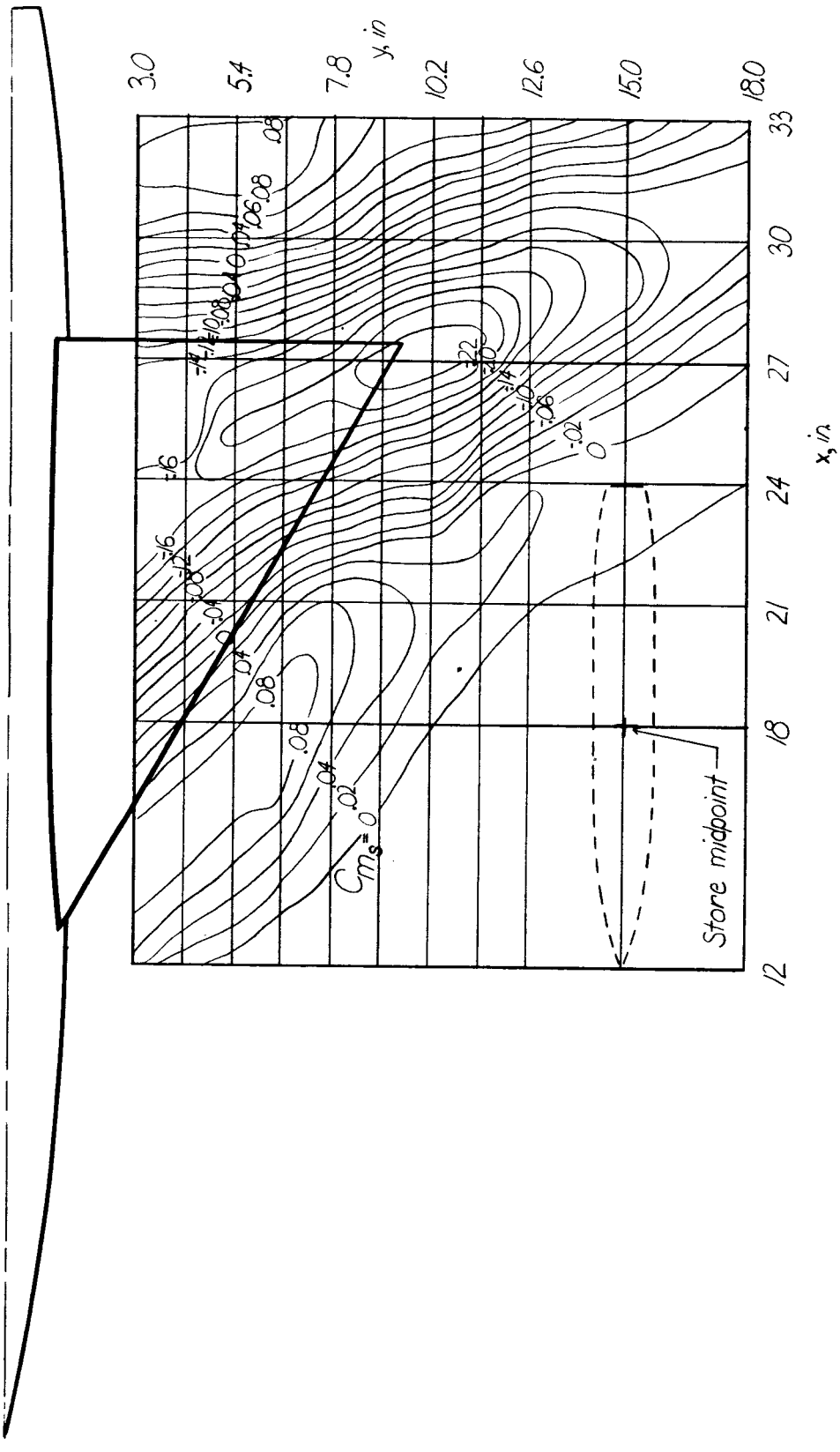

(c) z = 2.09 inches; $\alpha = 4^\circ$.

Figure 17.- Concluded.

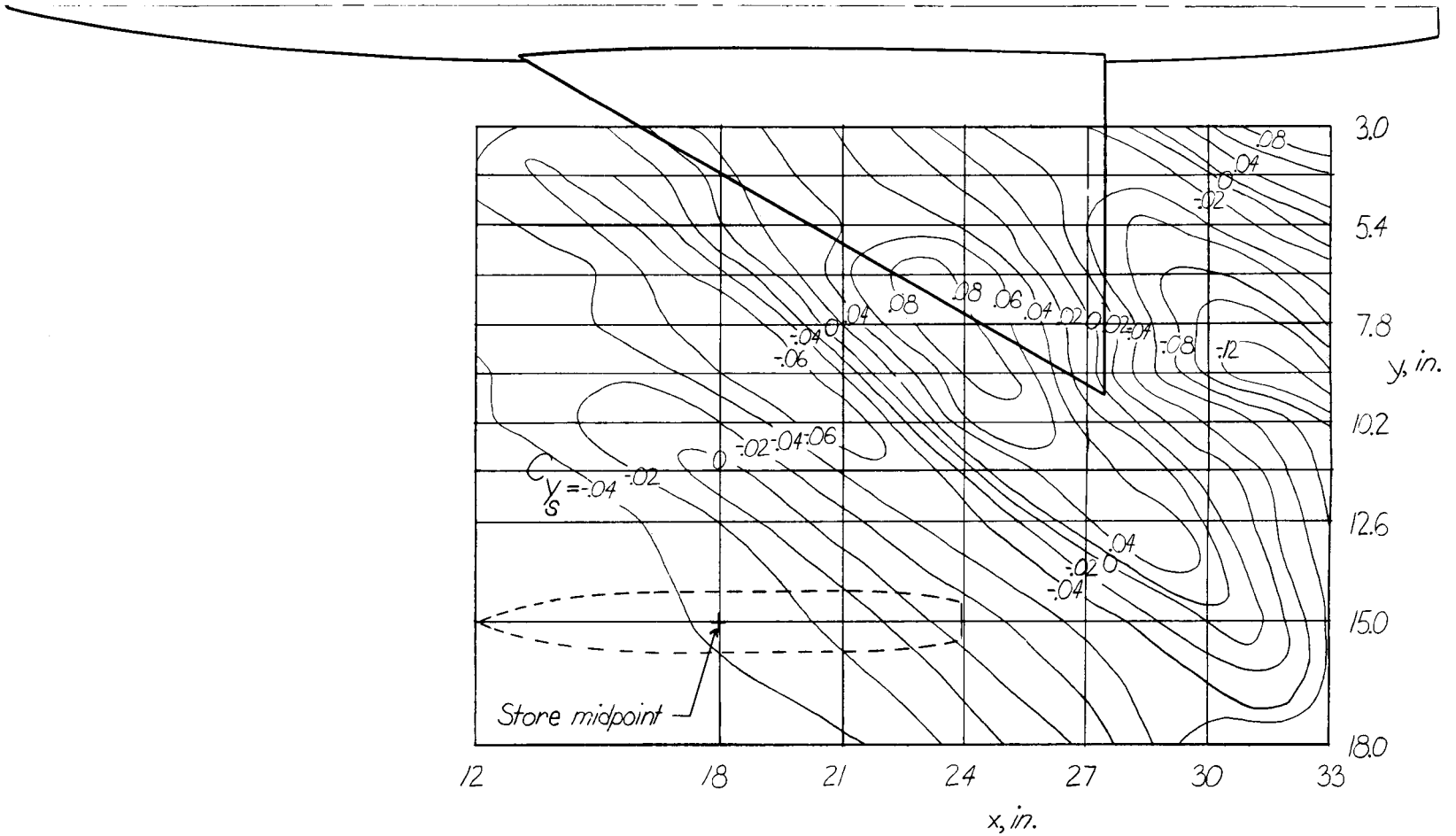

(a) z = 1.15 inches; $\alpha = 0^\circ$.

Figure 18.- Contour plot of side force of store in presence of wing-fuselage combination.

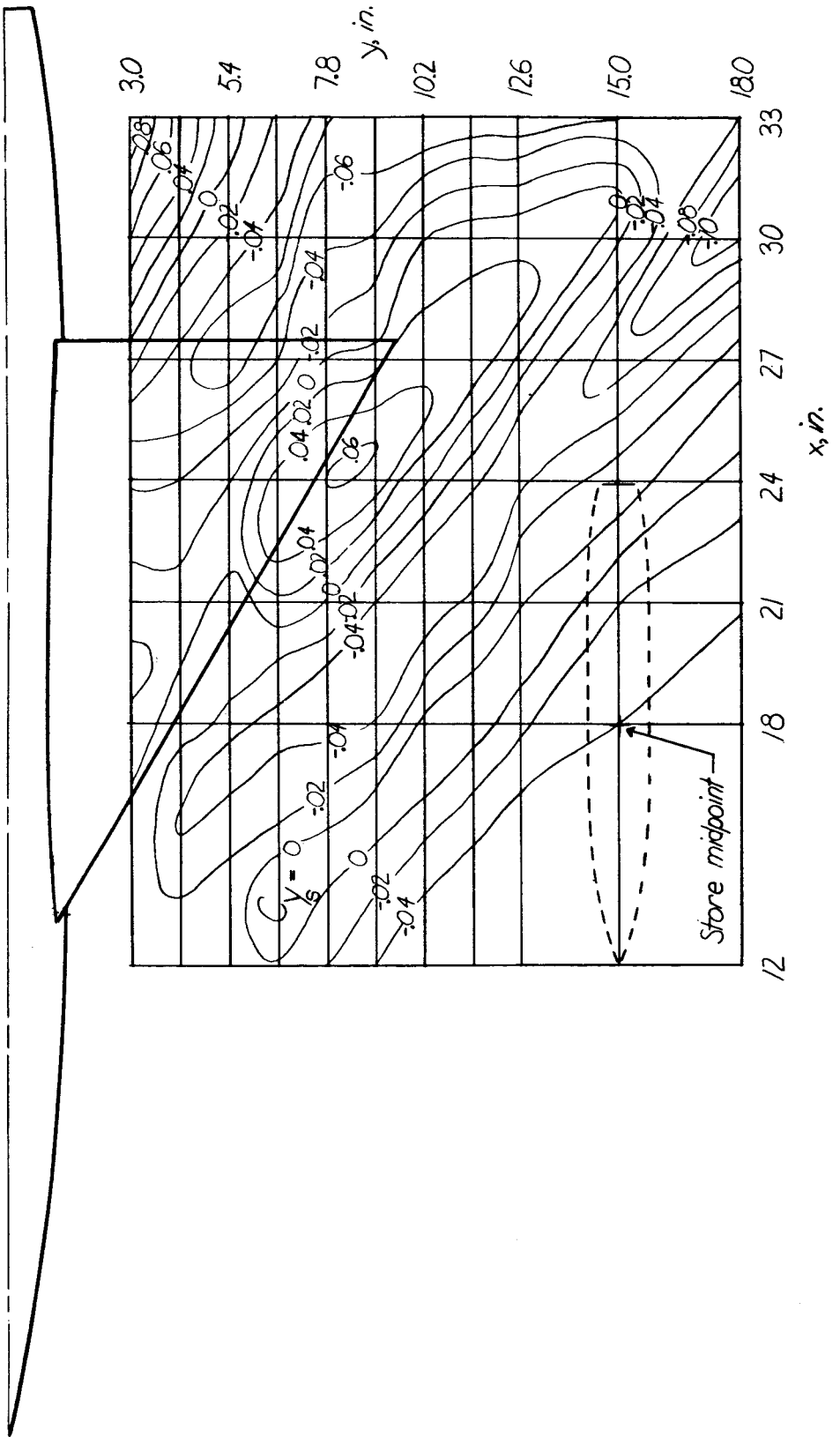

(b) z = 2.09 inches; α = 0°.

Figure 18.- Continued.

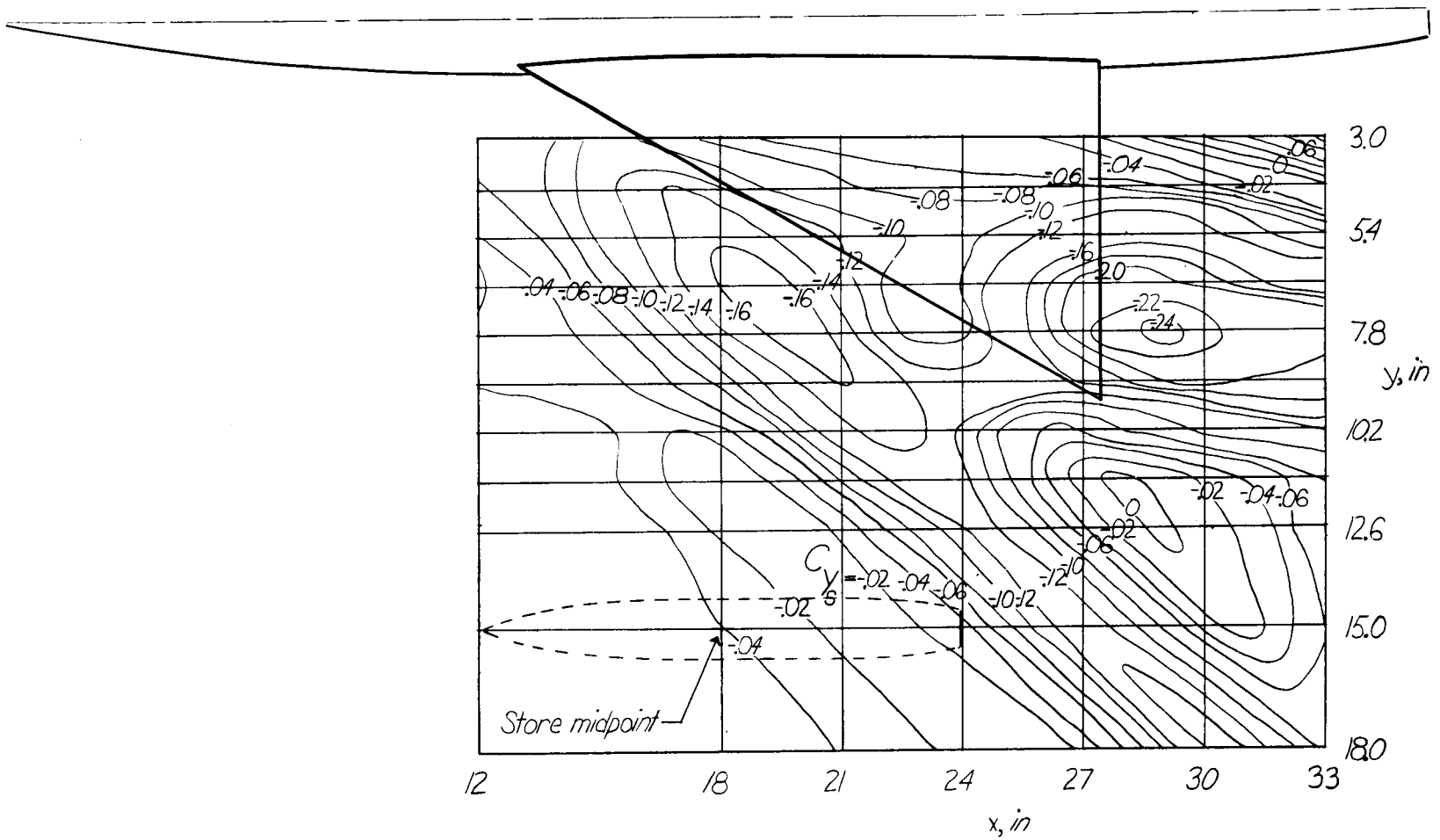

(c) z = 2.09 inches; $\alpha = 4^{\circ}$.

Figure 18.- Concluded.

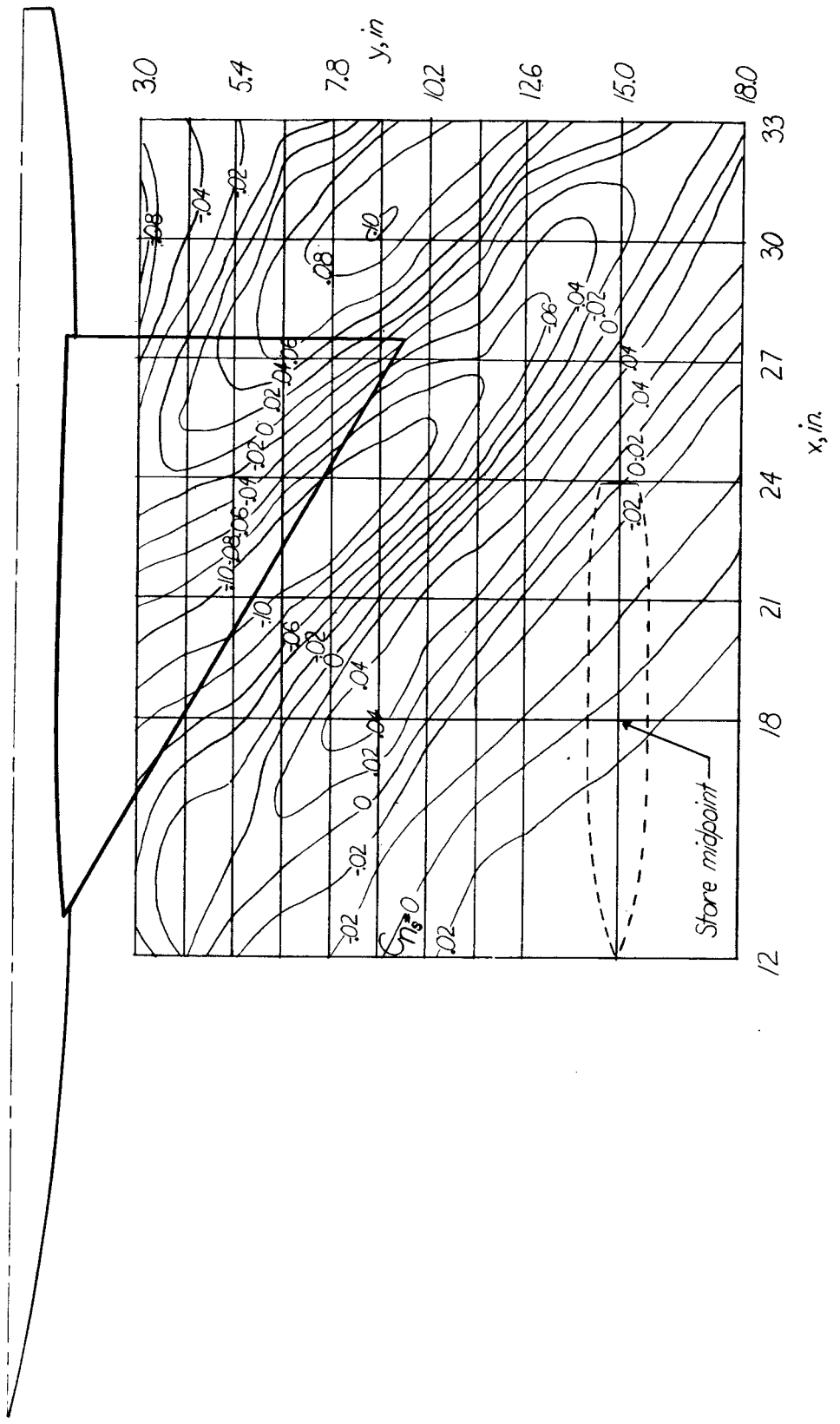

(a) z = 1.15 inches; α = 0°.

Figure 19.- Contour plot of yawing moment of store in presence of wing-fuselage combination (computed about store nose).

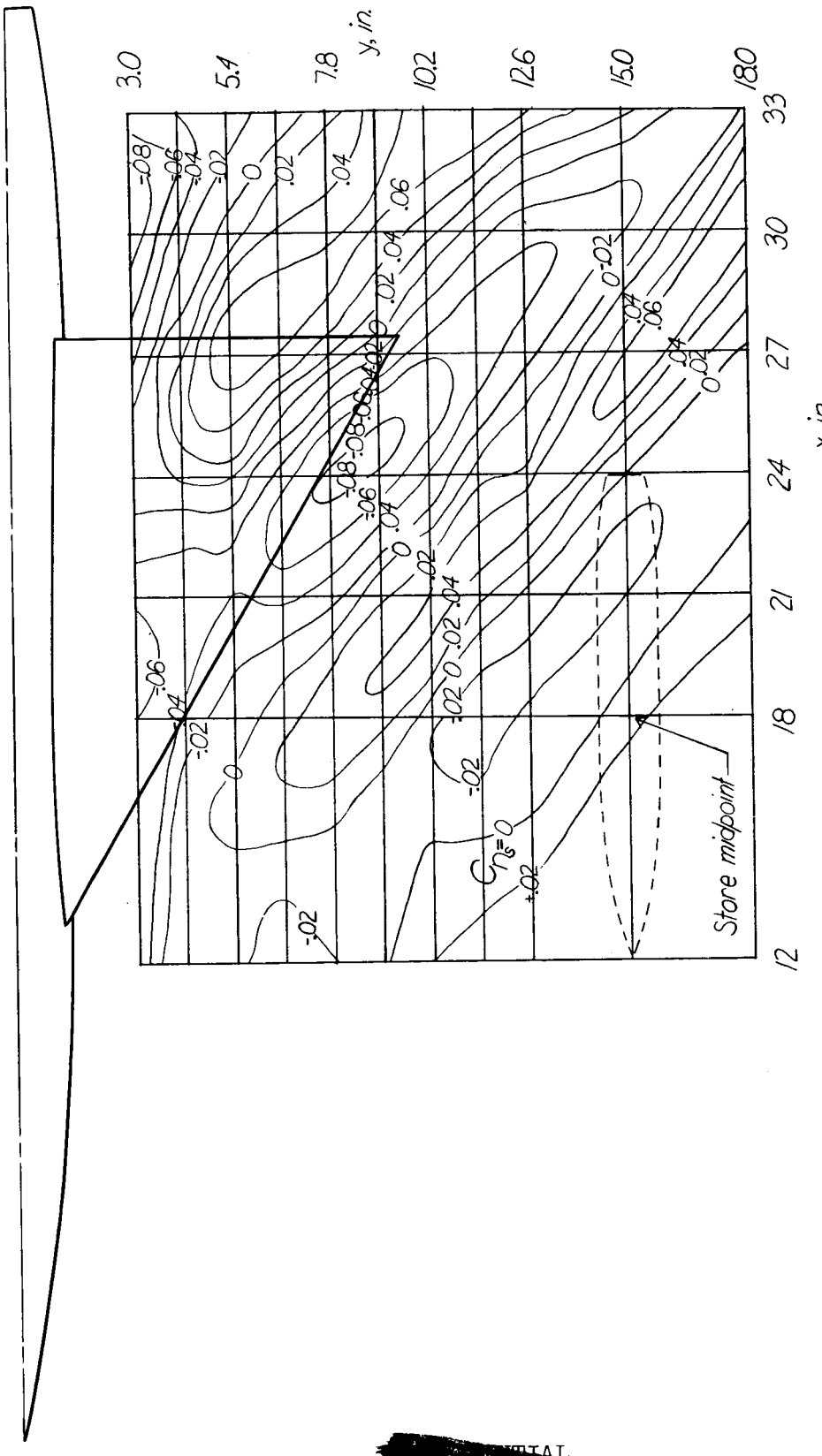

(b) z = 2.09 inches; $\alpha = 0^\circ$.

Figure 19.- Continued.

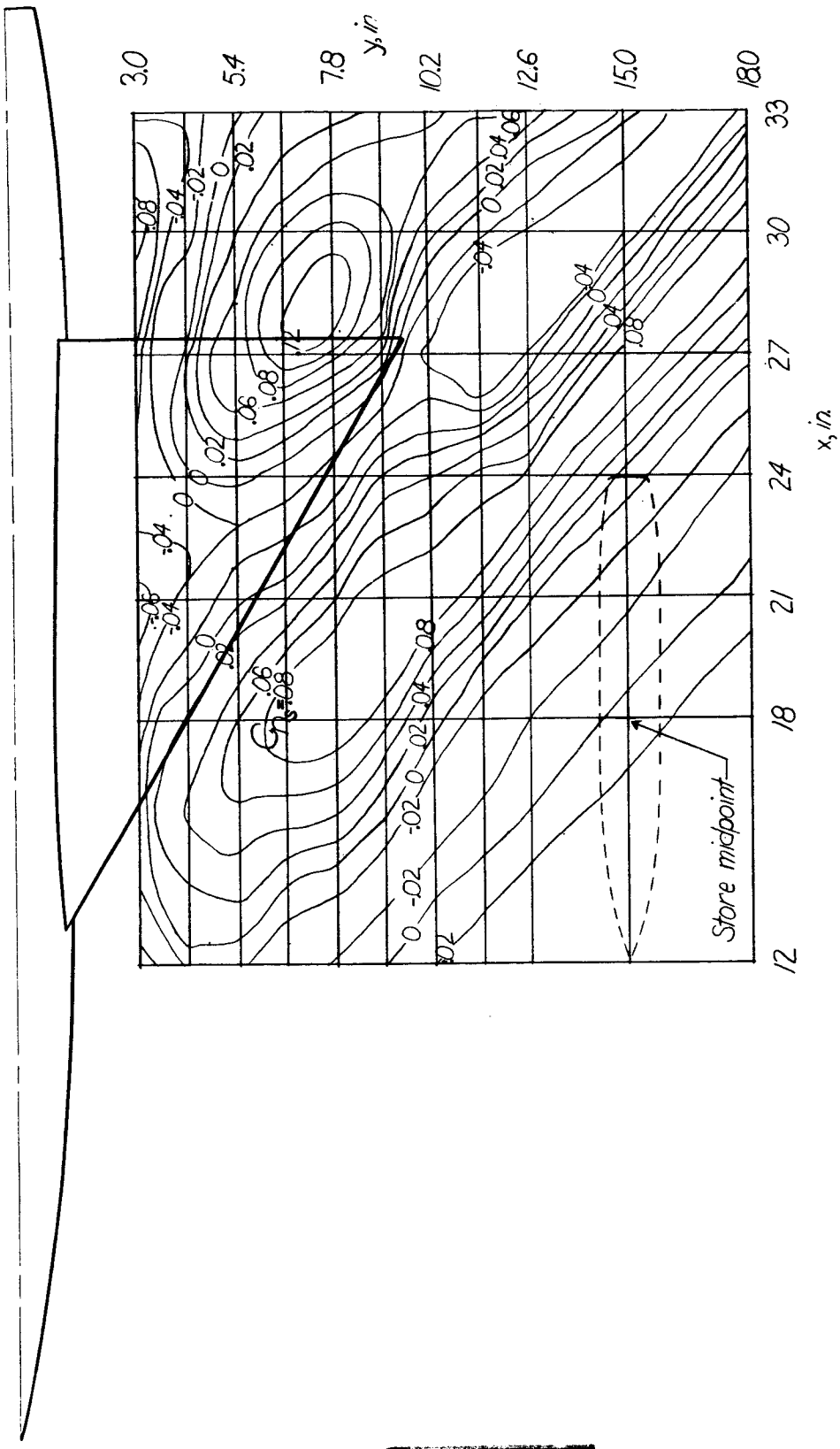

(c) z = 2.09 inches; $\alpha = 4^{\circ}$.

Figure 19.- Concluded.

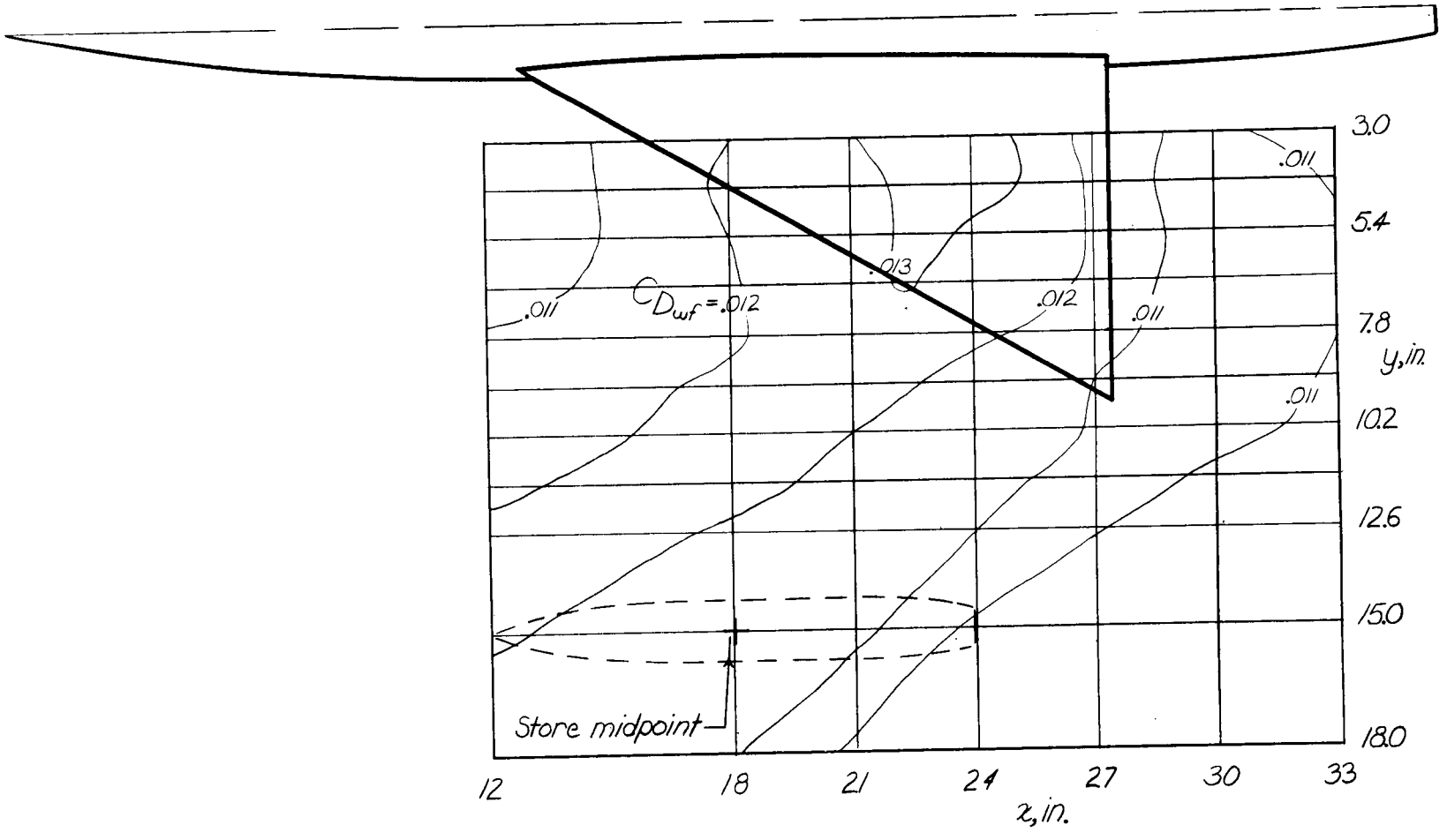

(a) z = 1.15 inches; $\alpha = 0^{\circ}$; isolated $C_{D_{wf}} = 0.0115$.

Figure 20.- Contour plot of drag of wing and fuselage in presence of store.

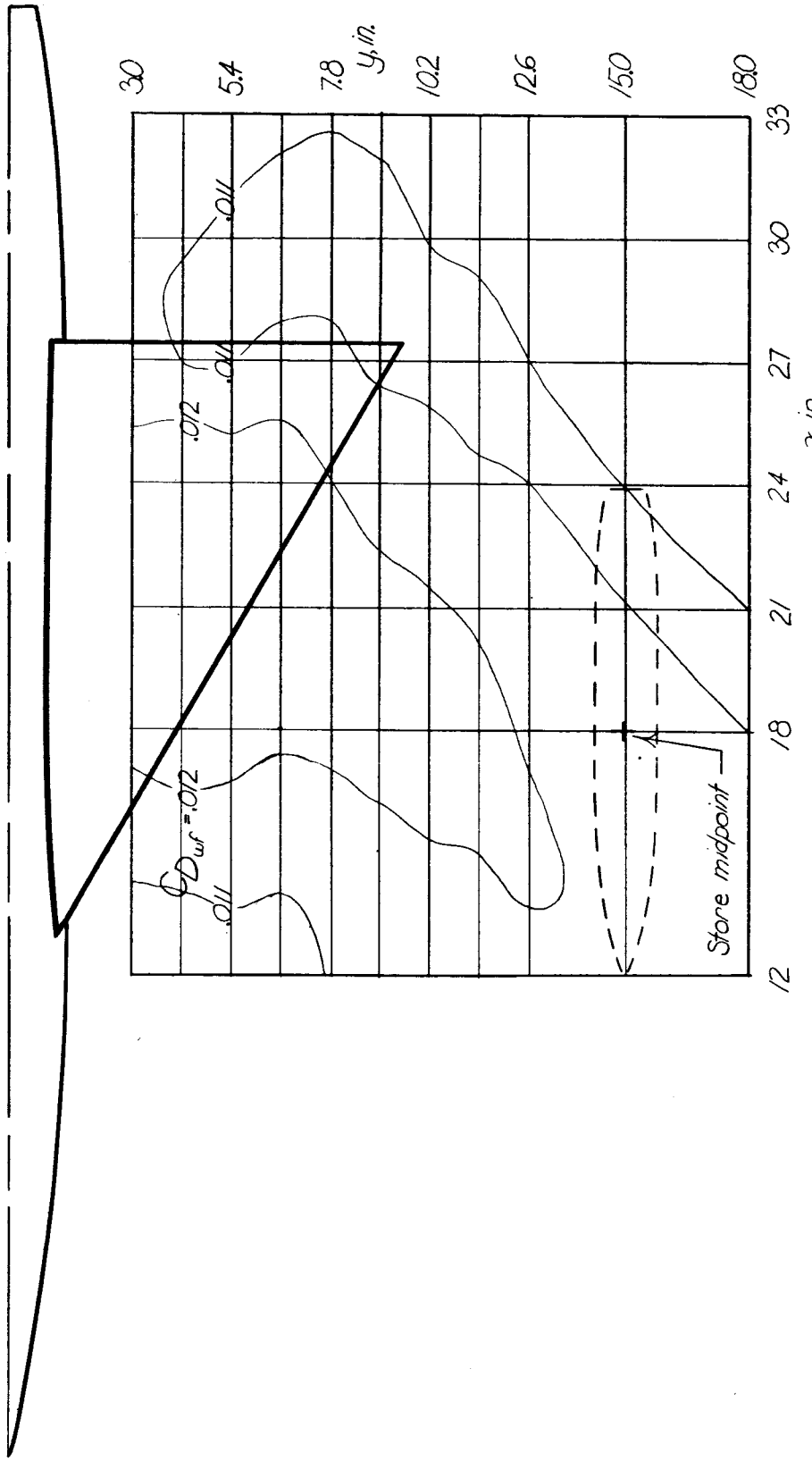

(b) z = 2.09 inches; $\alpha = 0^{\circ}$; isolated $C_{D_{wf}} = 0.0115$.

Figure 20.- Continued.

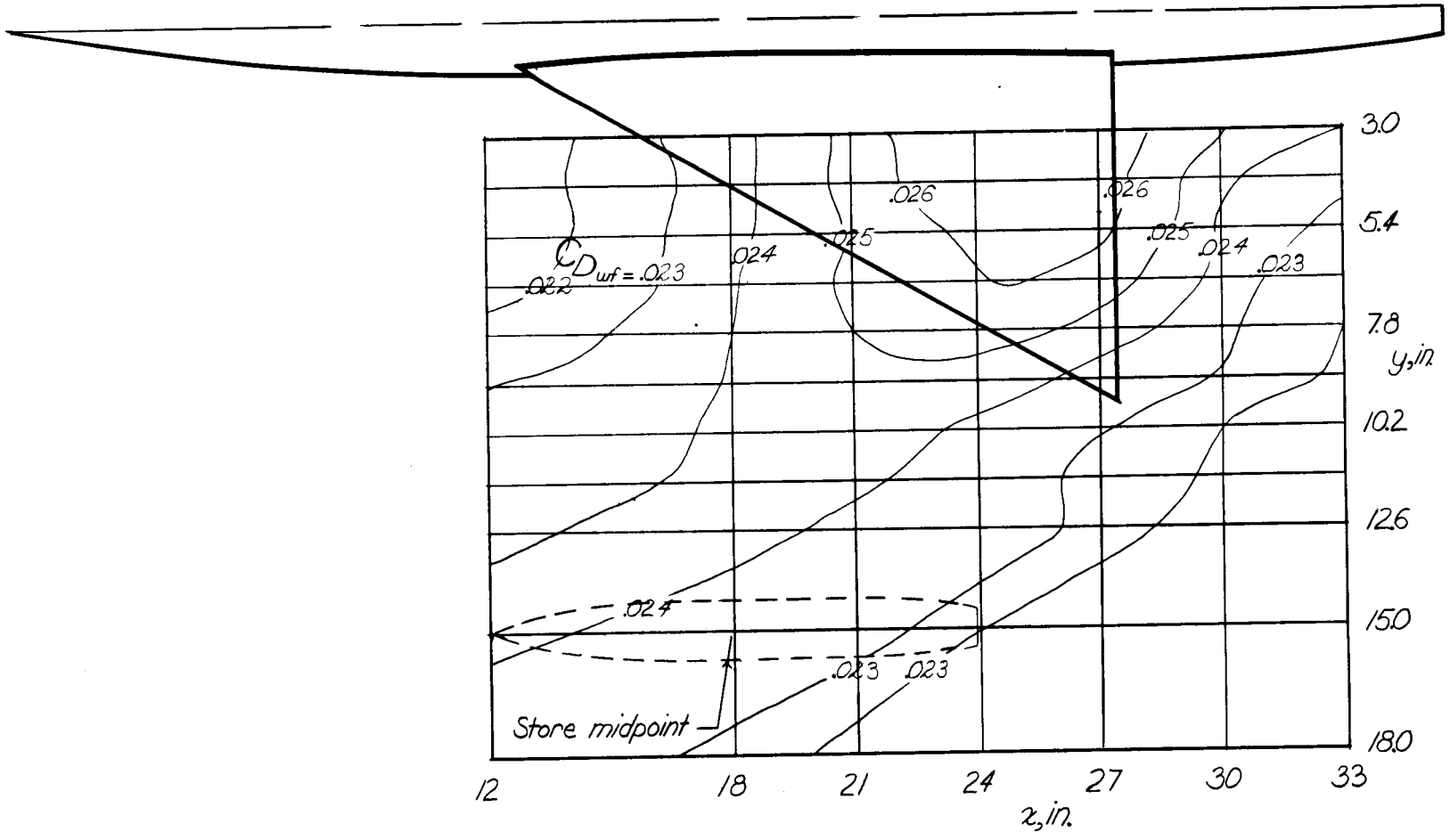

(c) z = 2.09 inches; $\alpha = 4^{\circ}$; isolated $C_{D_{wf}} = 0.0231$.

Figure 20.- Concluded.

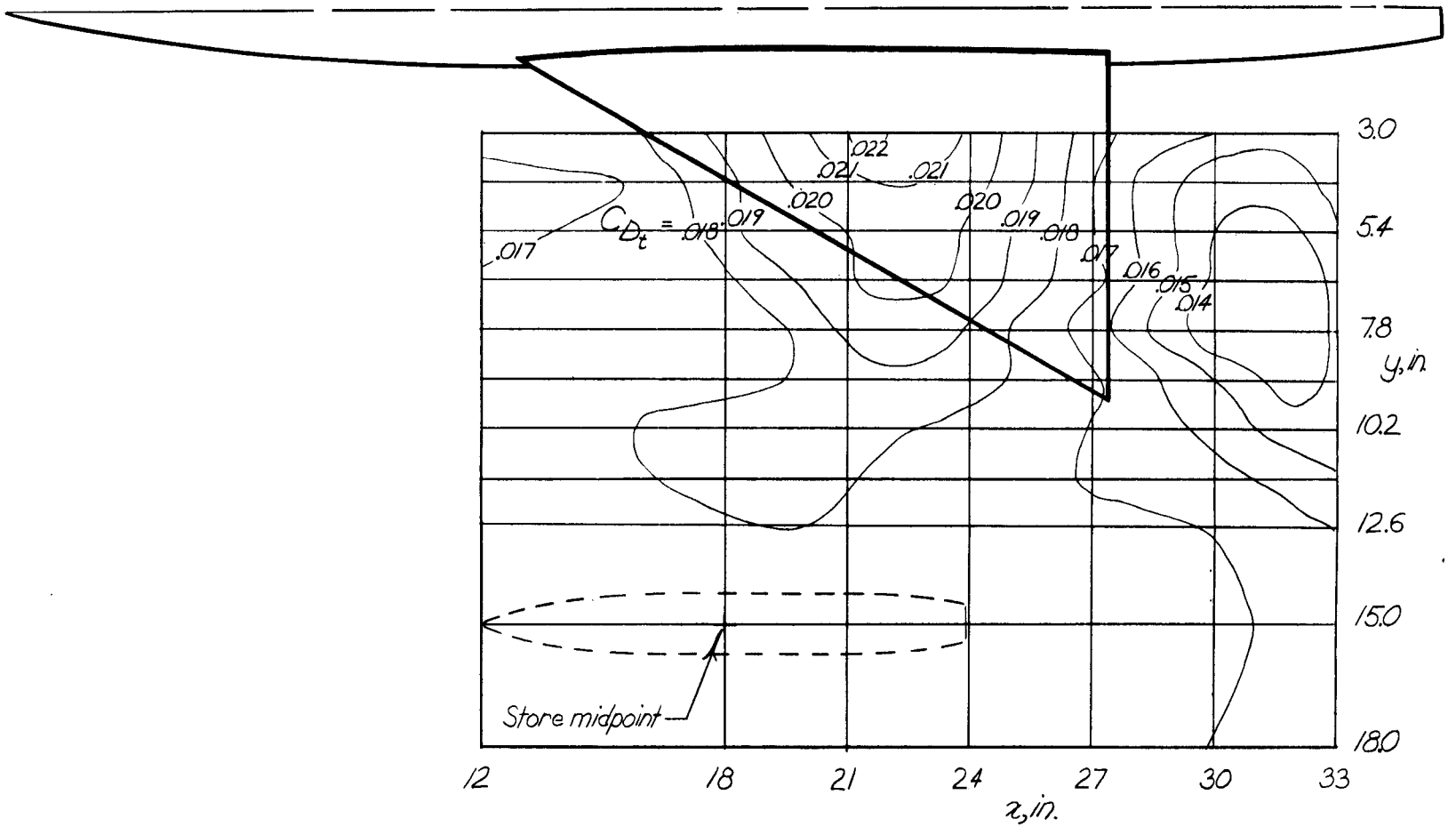

(a) z = 1.15 inches; $\alpha = 0^\circ$; isolated $C_{D_t} = 0.0172$.

Figure 21.- Contour plot of the total drag of the complete configuration (wing and fuselage plus store).

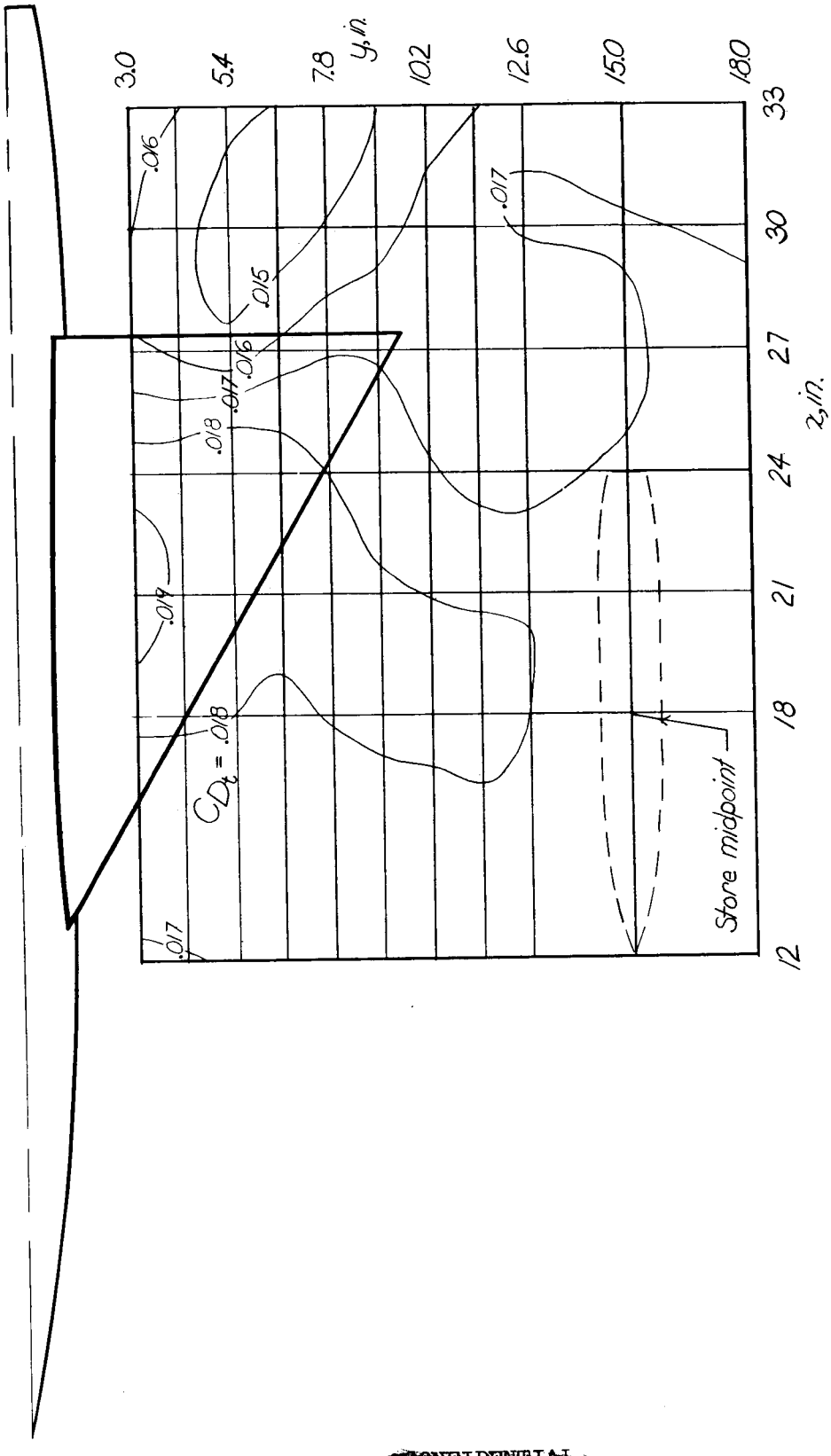

(b) z = 2.09 inches; $\alpha = 0^{\circ}$; isolated $C_{D_t} = 0.0172$.

Figure 21.- Continued.

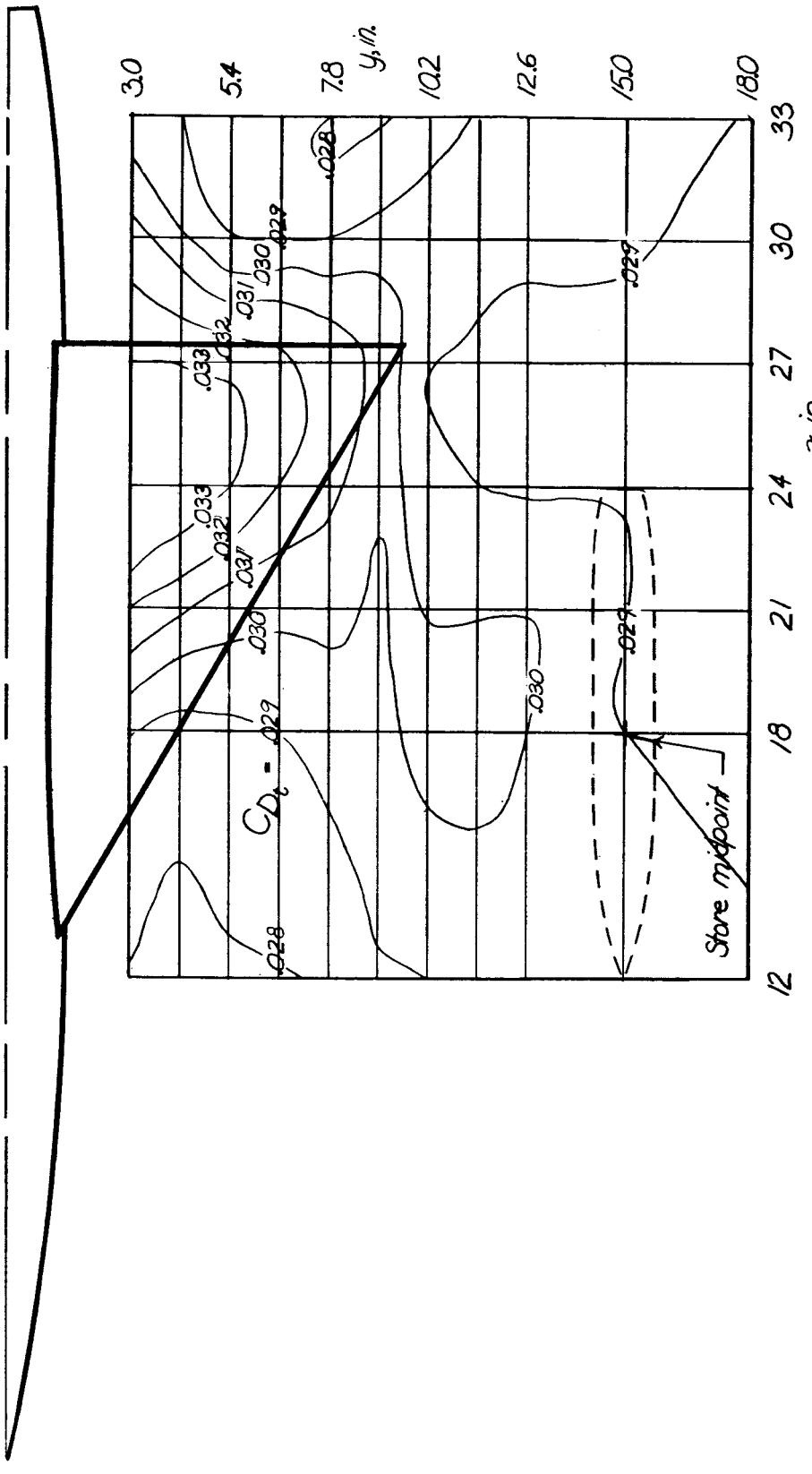

(c) z = 2.09 inches; $\alpha = 4^\circ$; isolated $C_{D_t} = 0.288$.

Figure 21.- Concluded.

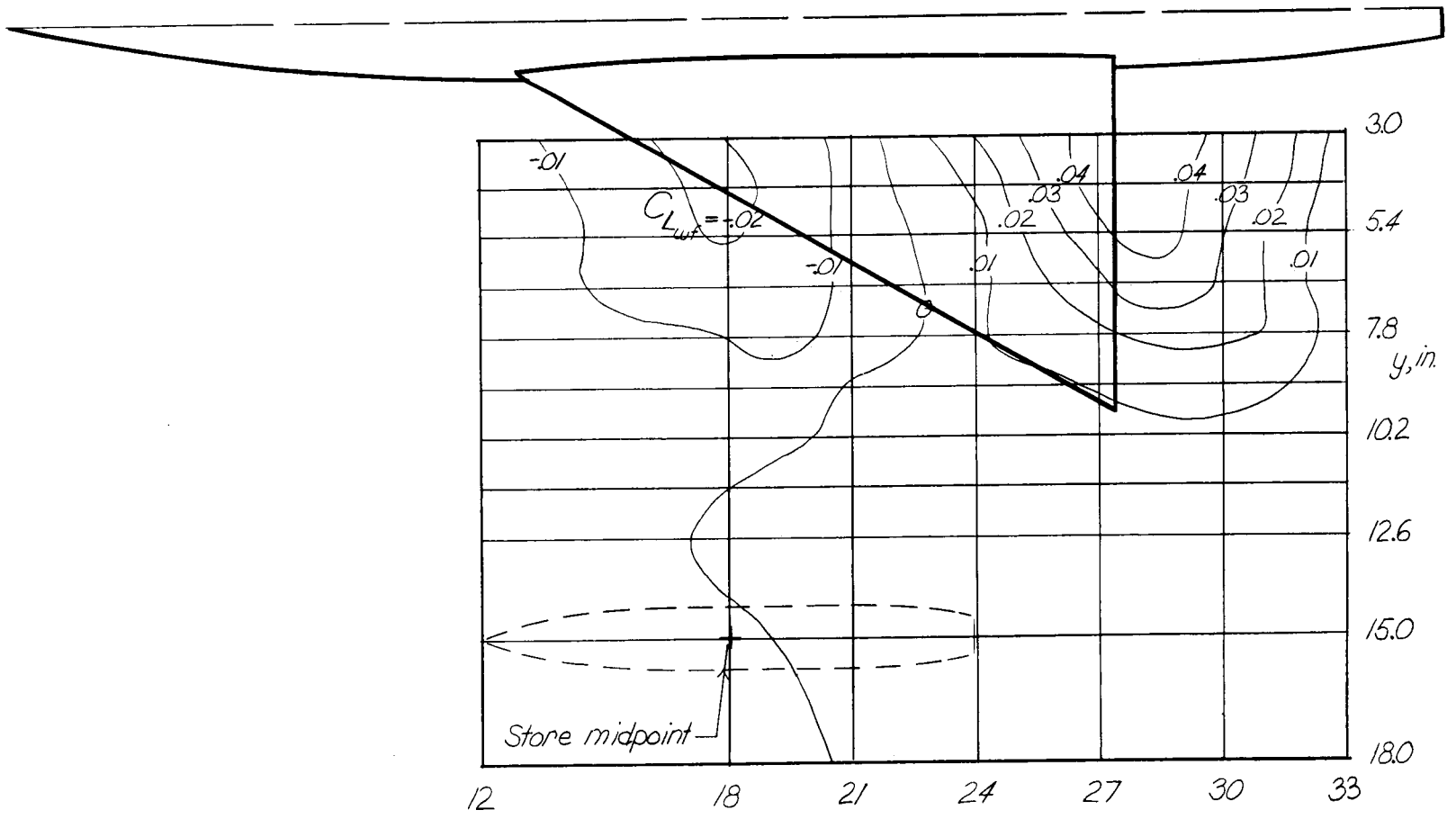

(a) $z = 1.15$ inches; $\alpha = 0^{\circ}$; isolated $C_{L_{wf}} = 0.001$.

Figure 22.- Contour plot of the lift of the wing-fuselage combination in presence of store.

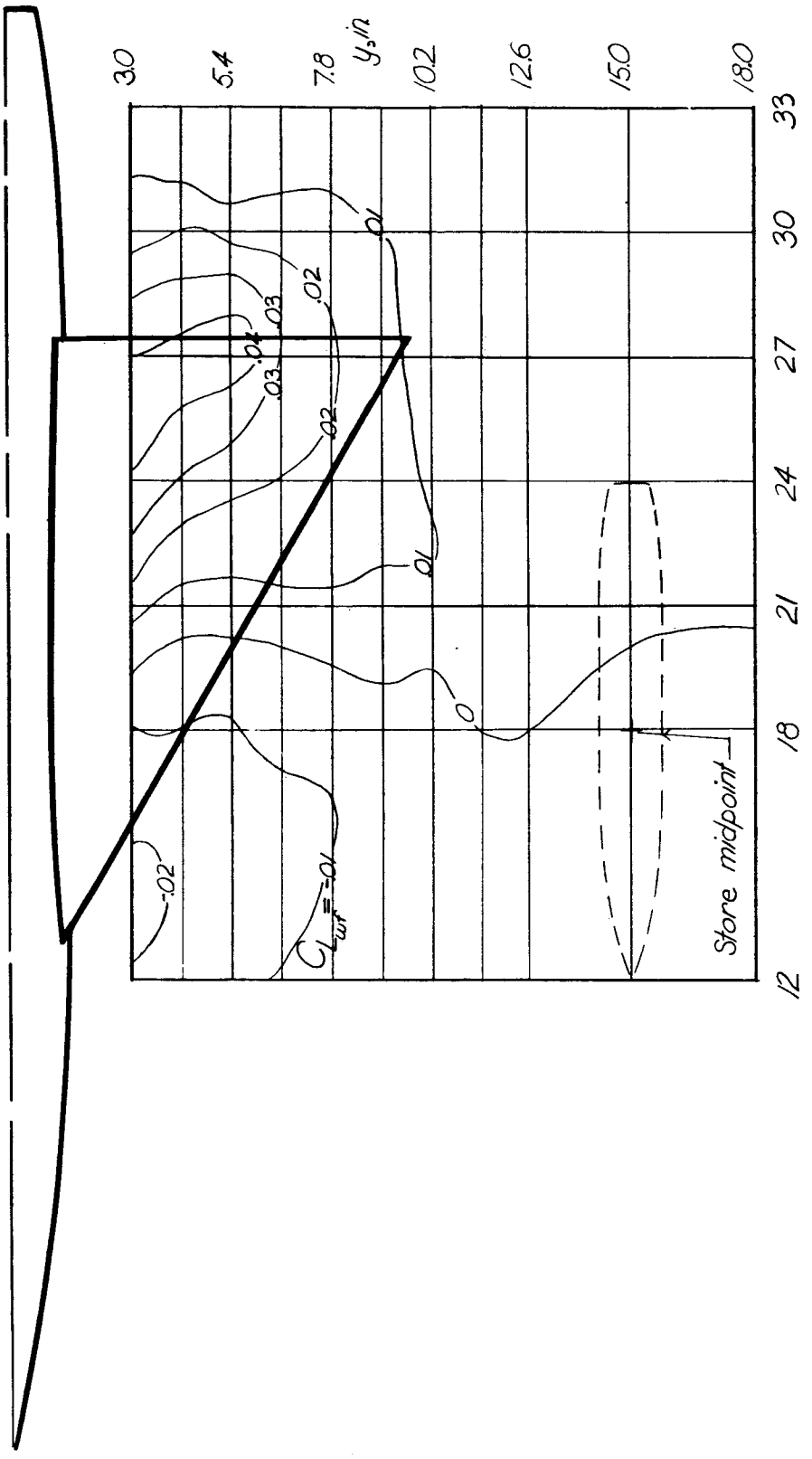

(b) z = 2.09 inches; $\alpha = 0^{\circ}$; isolated $C_{L_{wf}} = 0.001$.

Figure 22.- Continued.

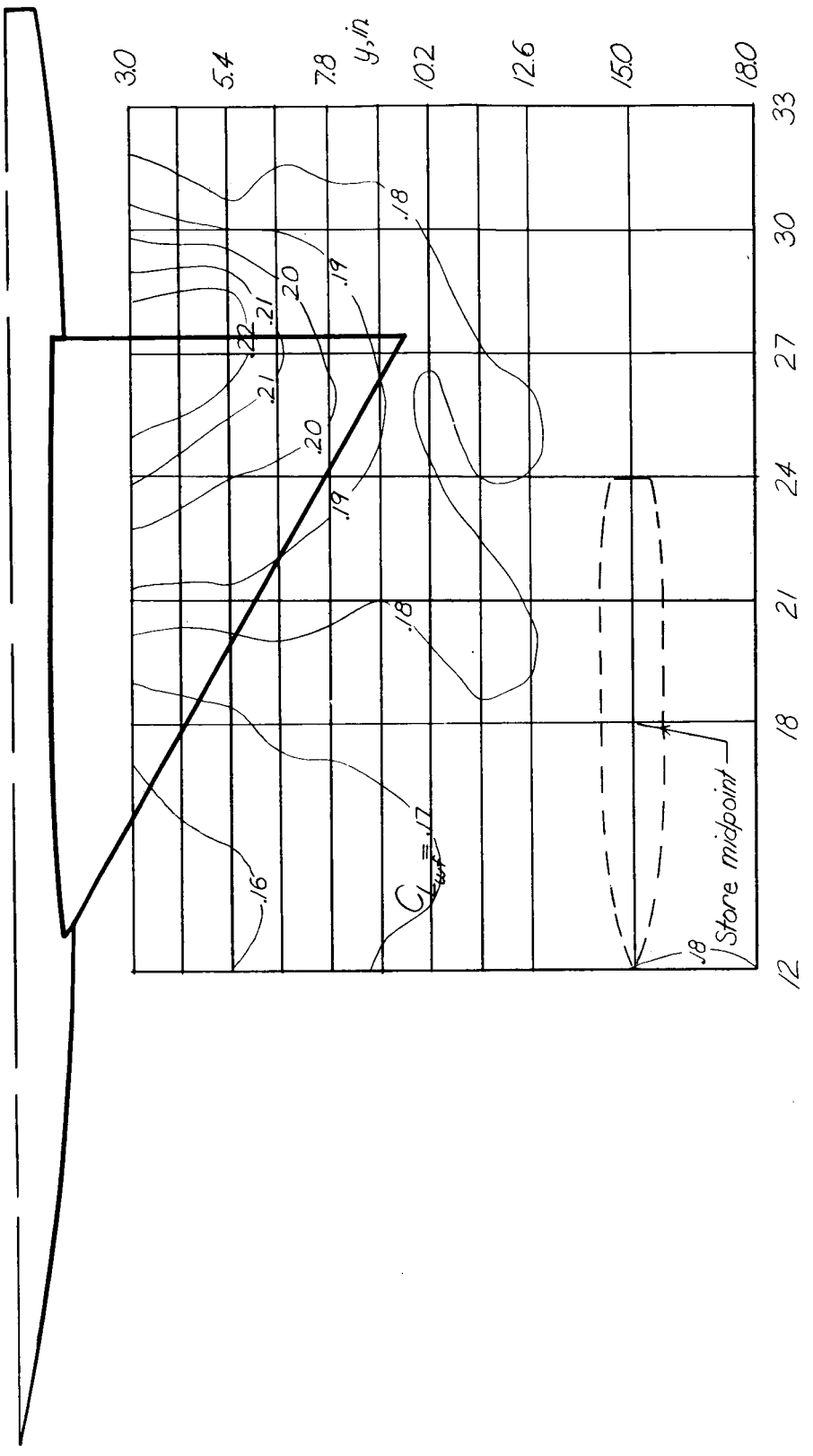

(c) z = 2.09 inches; $\alpha = 4^{\circ}$; isolated $C_{L_{wf}} = 0.175$.

Figure 22.- Concluded.

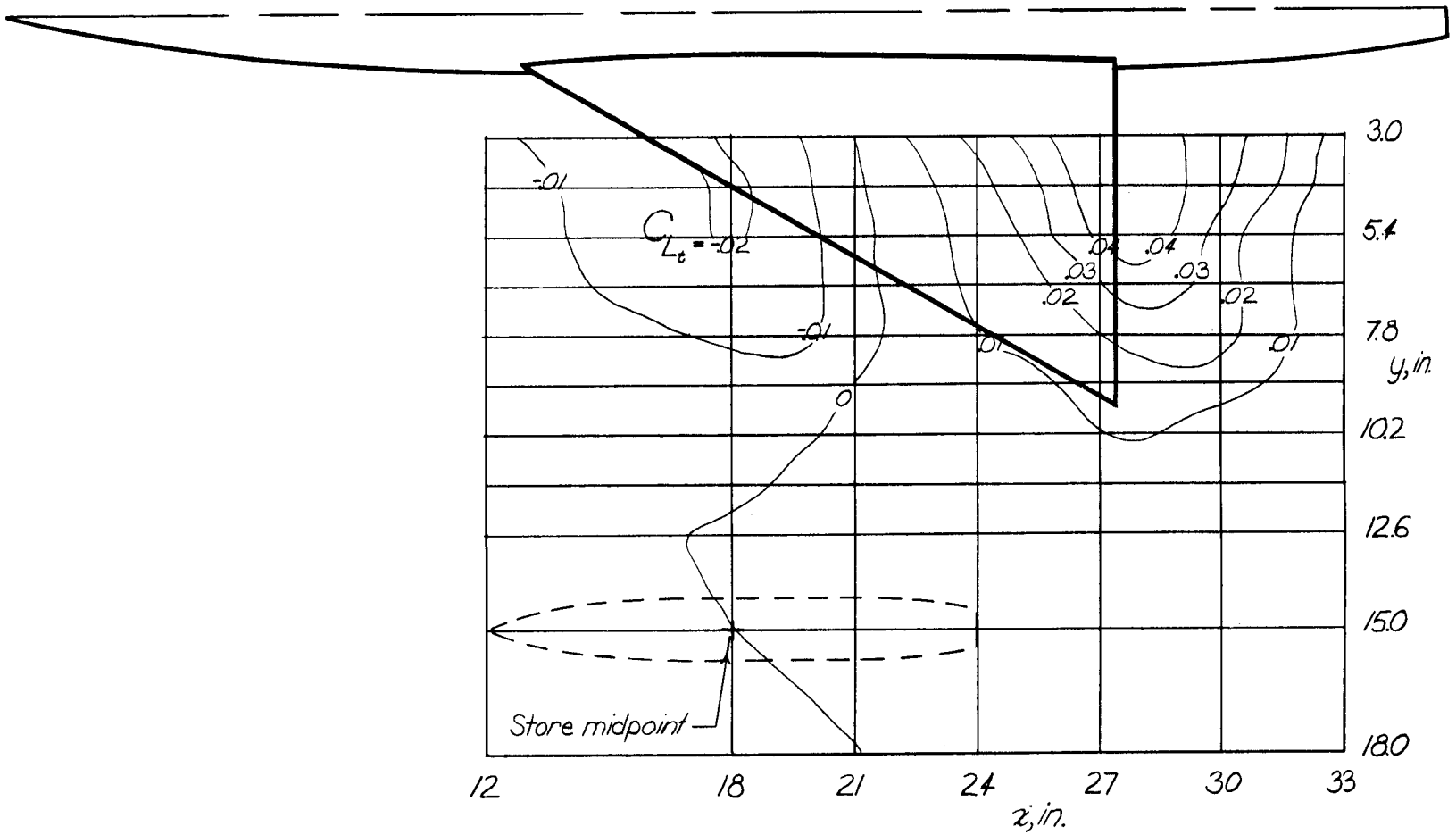

(a) z = 1.15 inches; $\alpha = 0^{\circ}$; isolated $C_{L_t} = 0.001$.

Figure 23.- Contour plot of the total lift of the complete configuration (wing fuselage plus store).

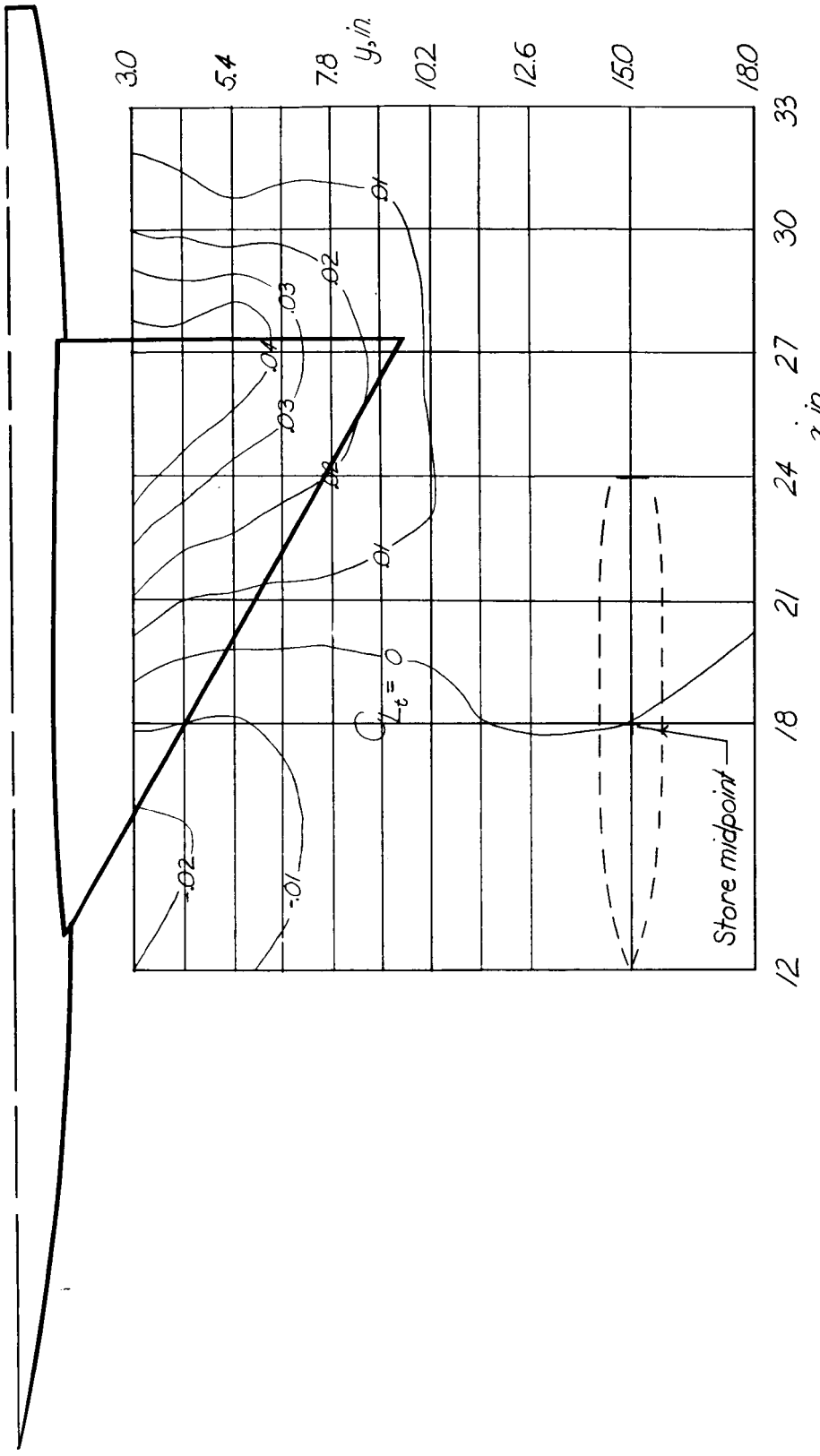

(b) z = 2.09 inches; $\alpha = 0^{\circ}$; isolated $C_{L_t} = 0.001$.

Figure 23.- Continued.

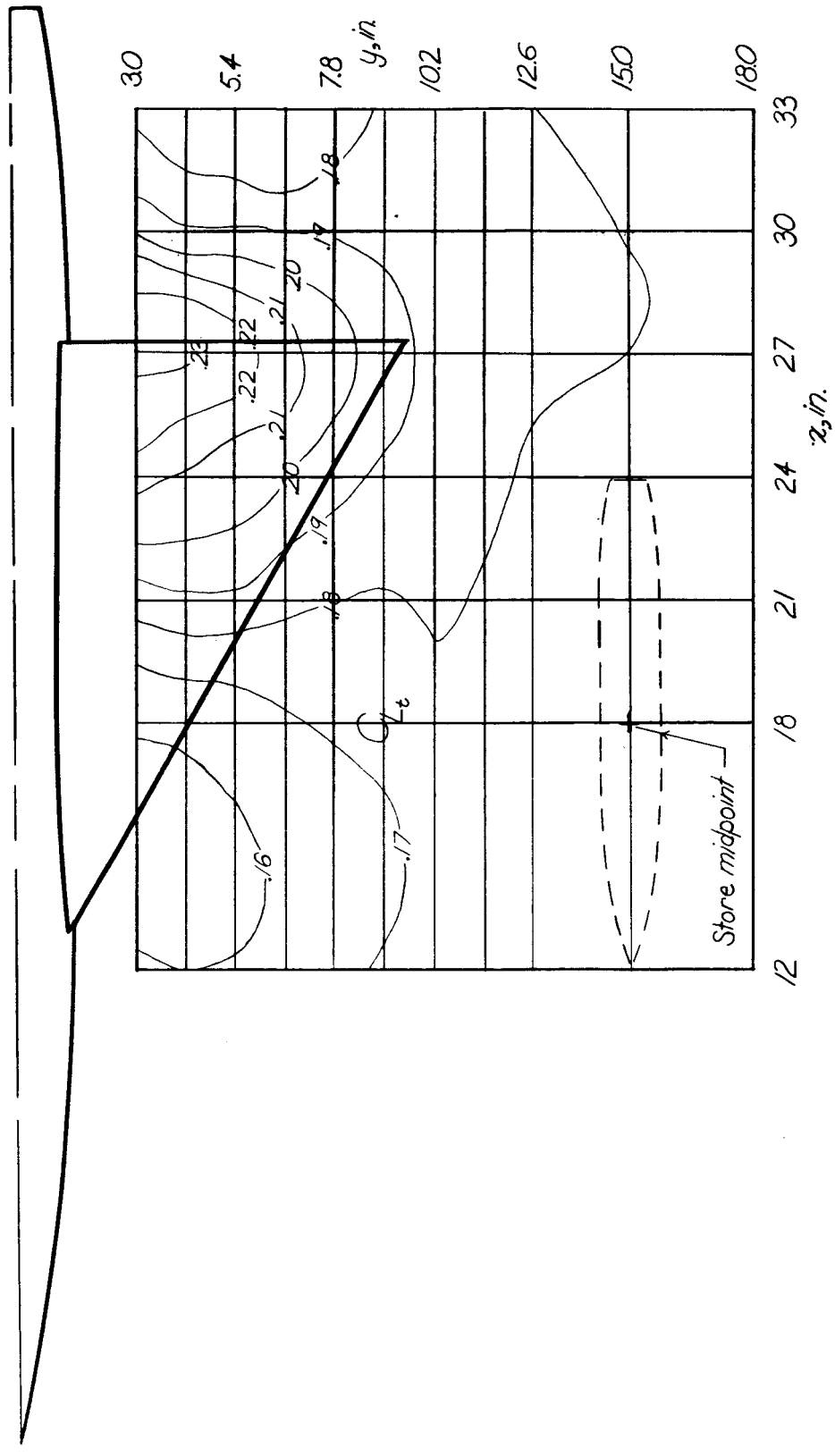

(c) z = 2.09 inches; $\alpha = 4^\circ$; isolated $C_{L_t} = 0.175$.

Figure 23.- Concluded.

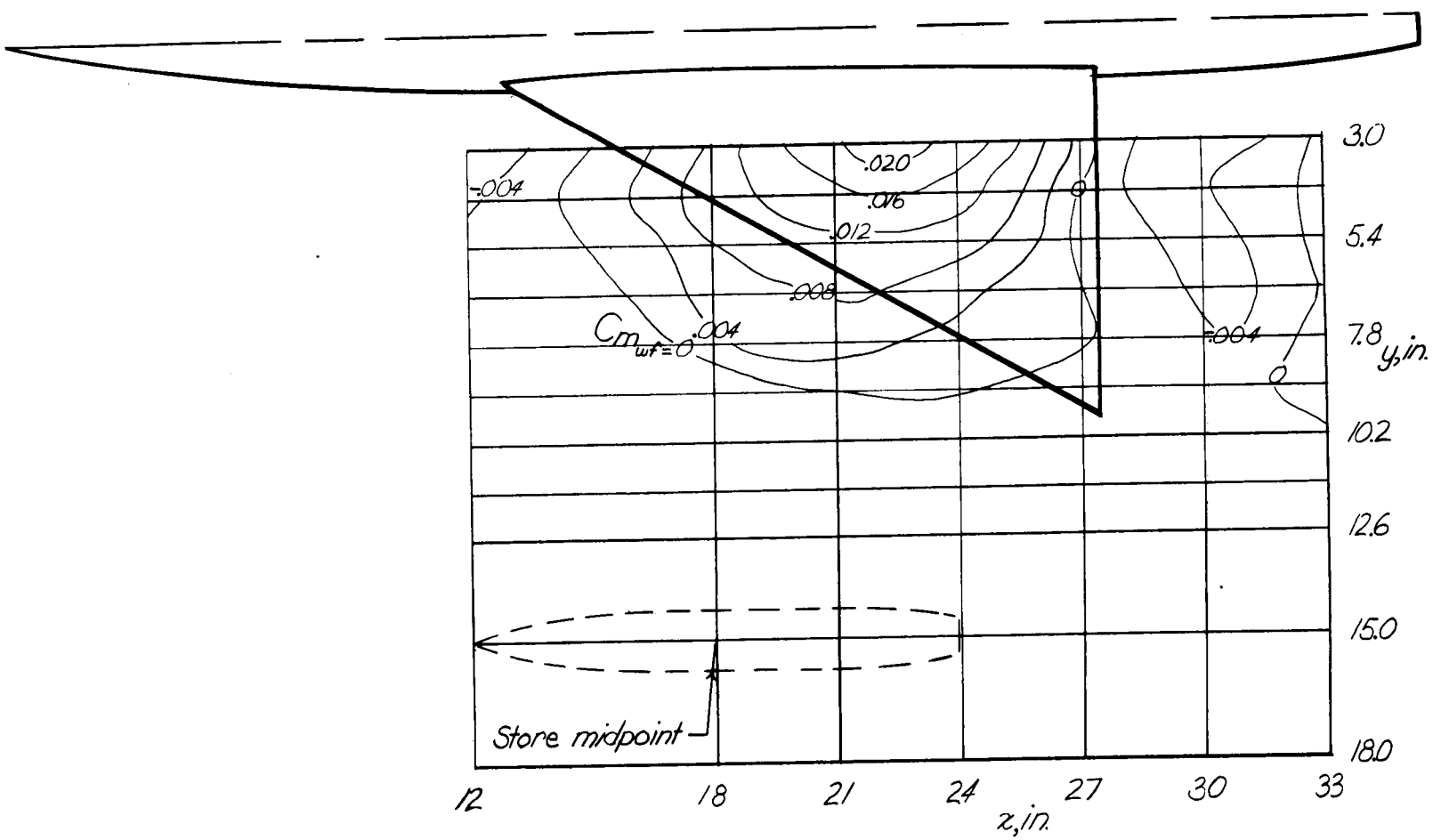

(a) z = 1.15 inches; $\alpha = 0^{\circ}$; isolated $C_{m_{wf}} = 0.001$.

Figure 24.- Contour plot of the pitching moment of the wing-fuselage combination in presence of store (computed about $0.625\bar{c}$). M = 1.61.

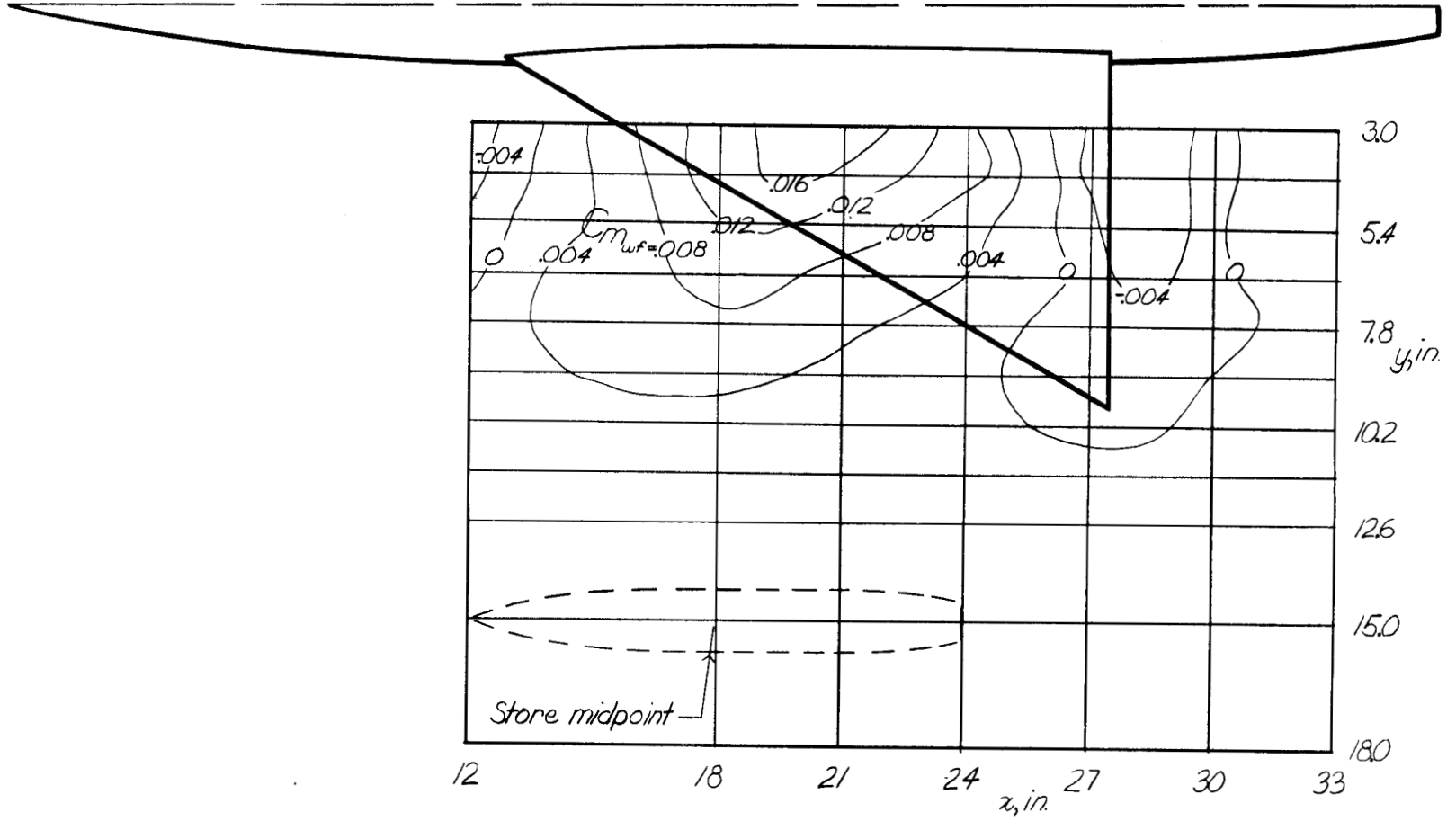

(b) z = 2.09 inches; $\alpha = 0^{\circ}$; isolated $C_{m_{wf}} = 0.001$.

Figure 24.- Continued.

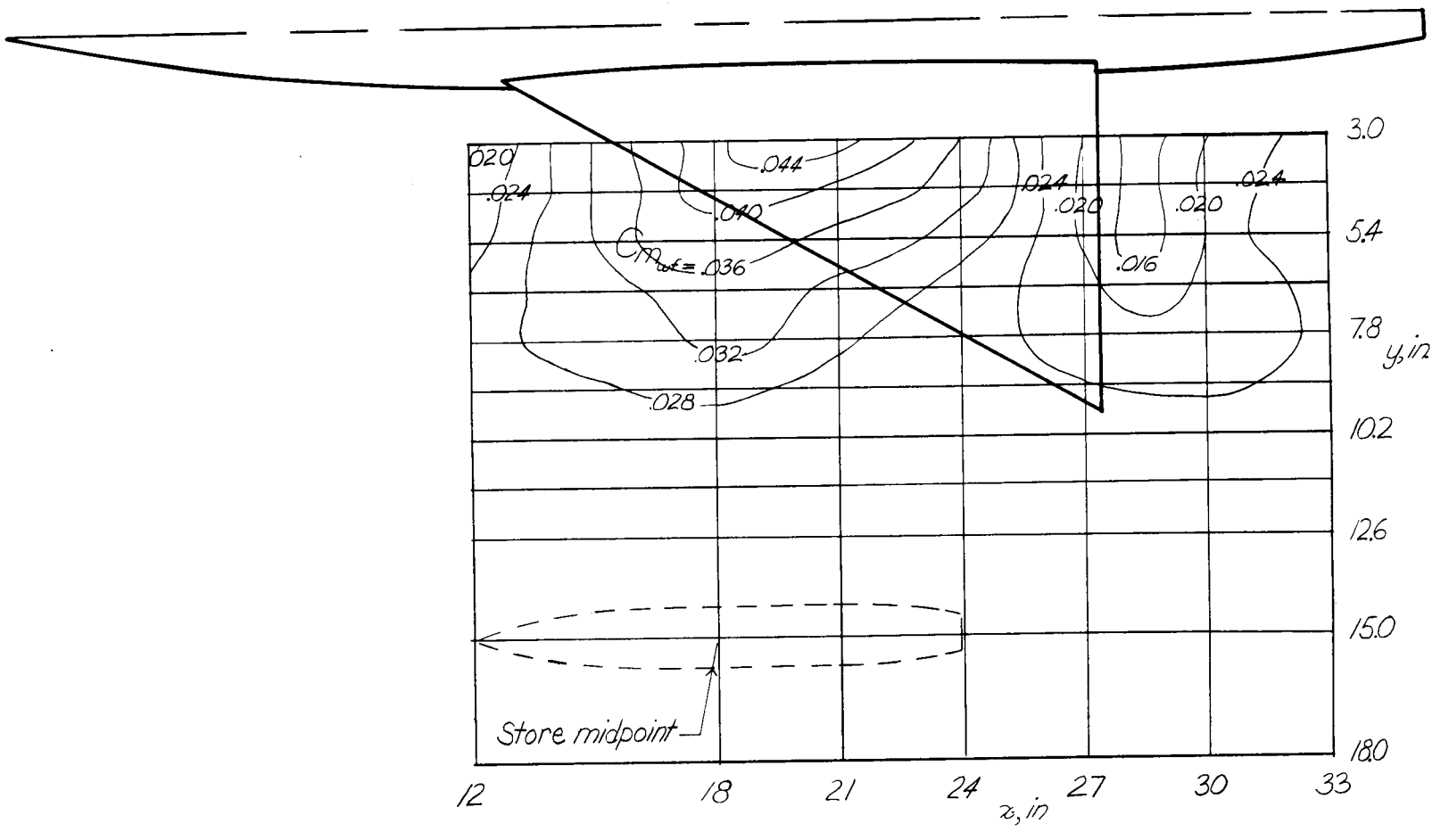

(c) z = 2.09 inches; $\alpha = 4^{\circ}$; isolated $C_{m_{wf}} = 0.025$.

Figure 24.- Concluded.

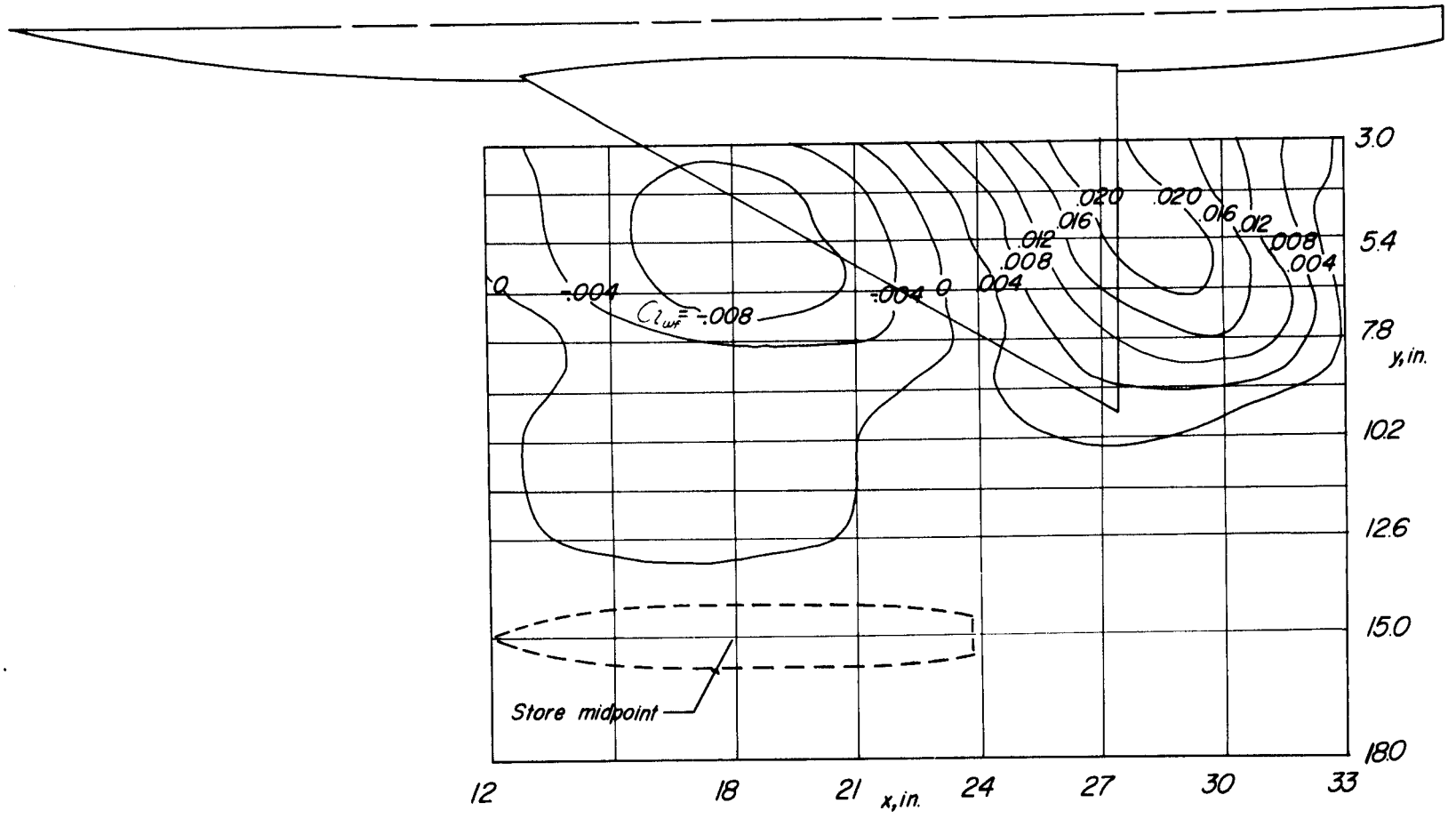

(a) z = 1.15 inches; $\alpha = 0^{o}$; isolated $C_{l_{wf}} = 0$.

Figure 25.- Contour plot of the wing-root bending moment of the wing-fuselage combination in presence of store.

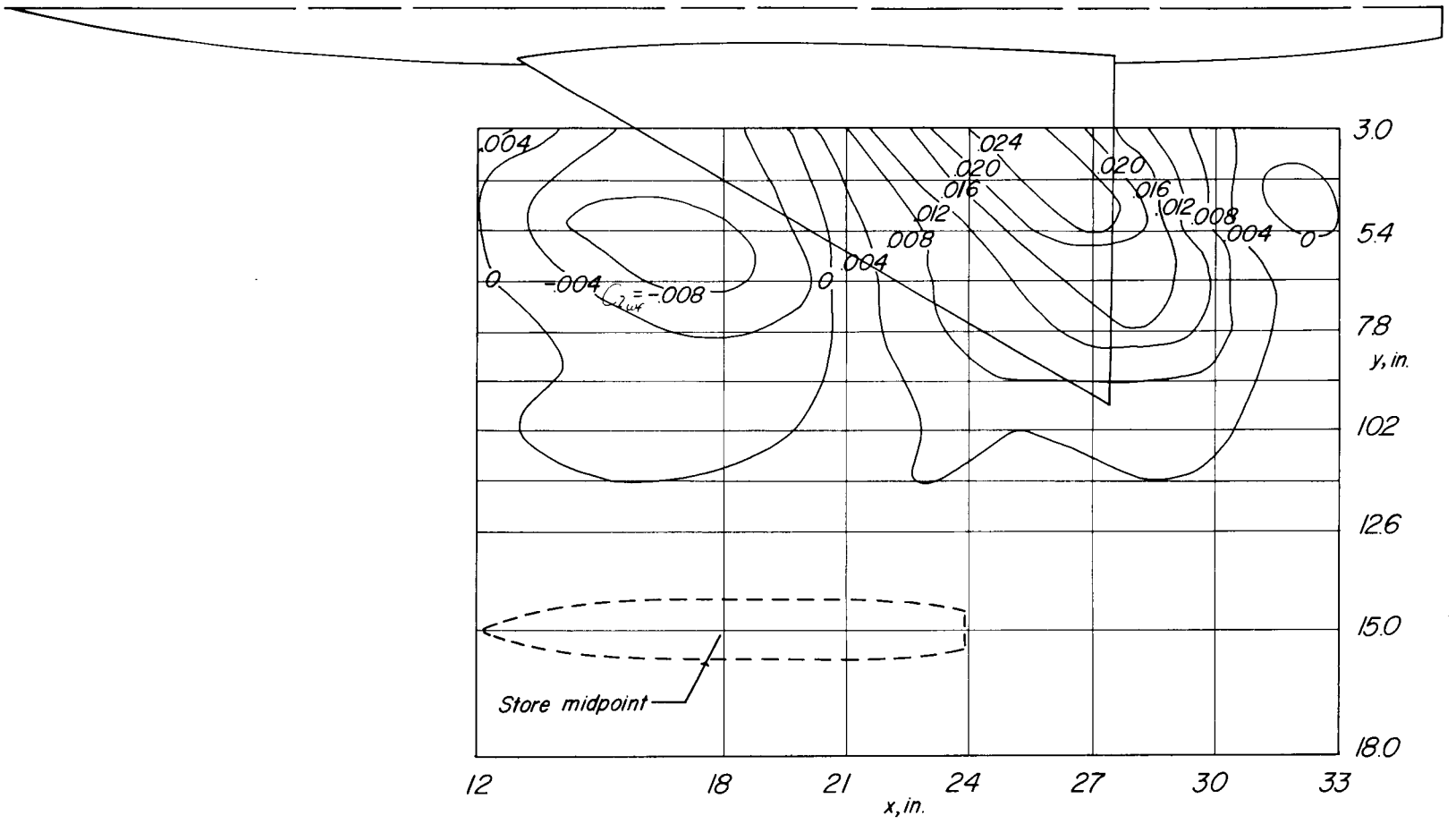

(b) z = 2.09 inches; $\alpha = 0^{\circ}$; isolated $C_{l_{wf}} = 0$.

Figure 25.- Continued.

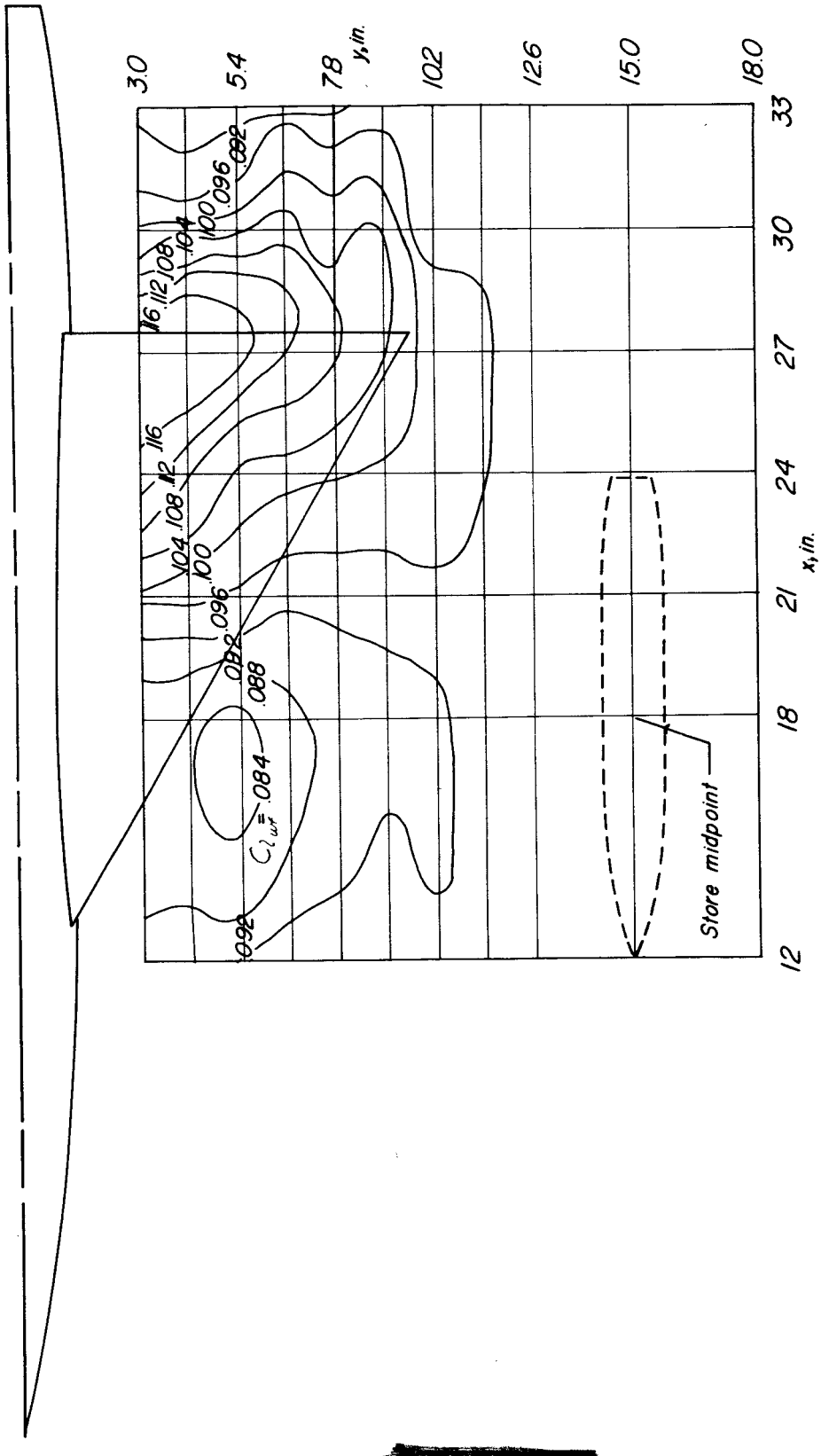

(c) z = 2.09 inches; $\alpha = 4^{\circ}$; isolated $C_{l_{wf}} = 0.094$.

Figure 25.- Concluded.

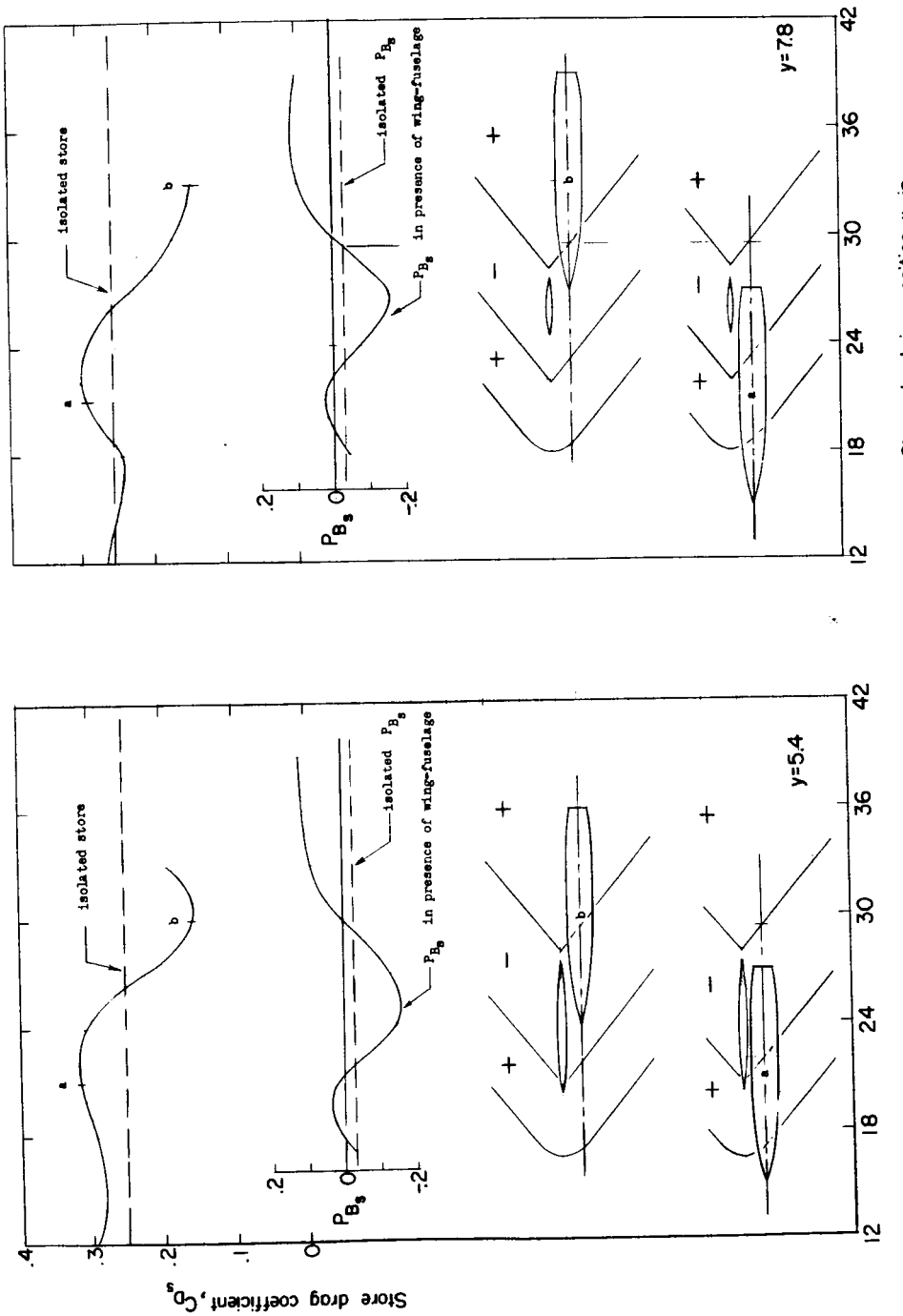

Figure 26.- Effect of wing-fuselage pressure field on store drag. z = 1.15 inches; $\alpha = 0^{\circ}$.

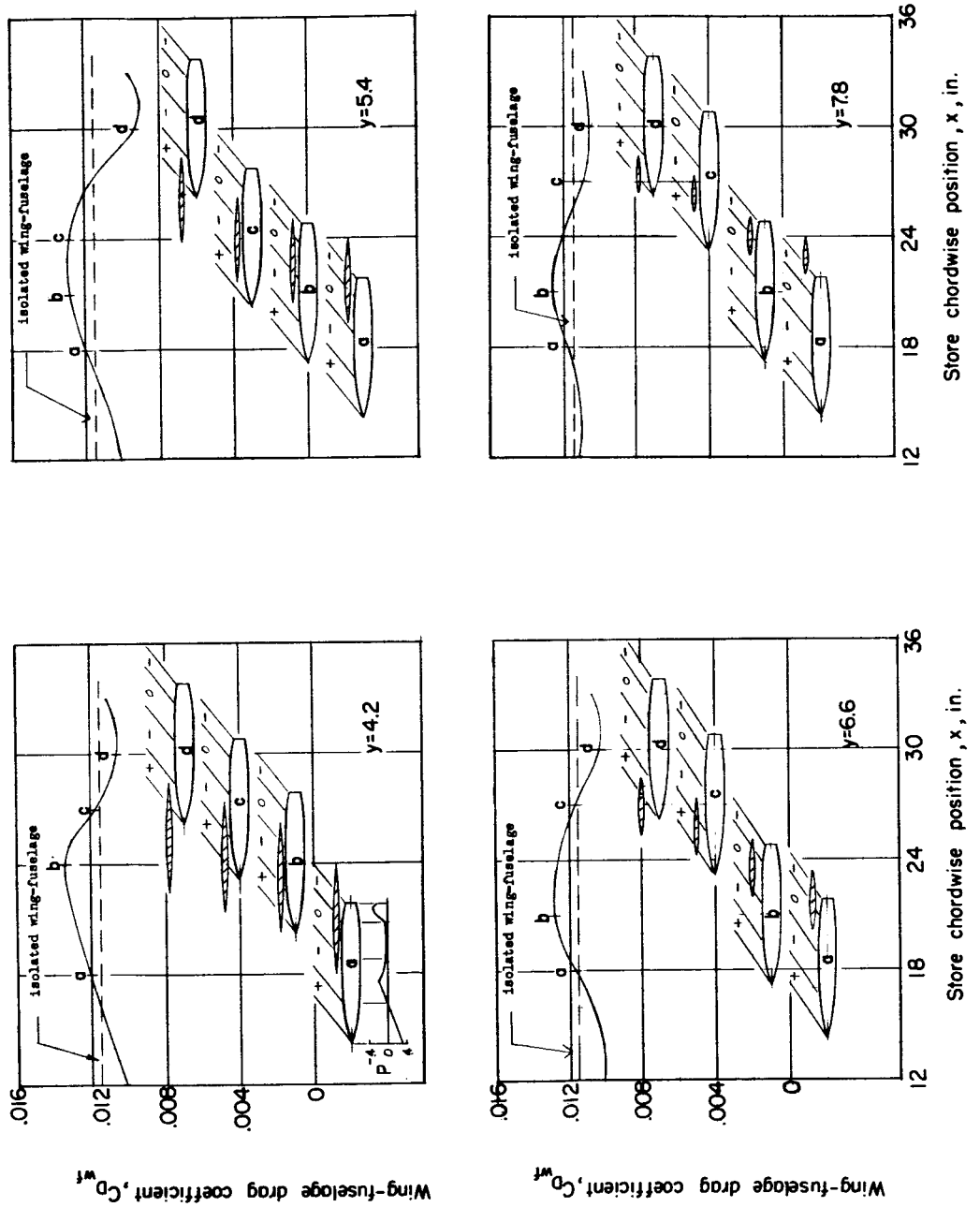

Figure 27.- Effect of store pressure field on drag of the wing and fuselage. $z = 1.15$; $\alpha = 0^{\circ}$.

[redacted]

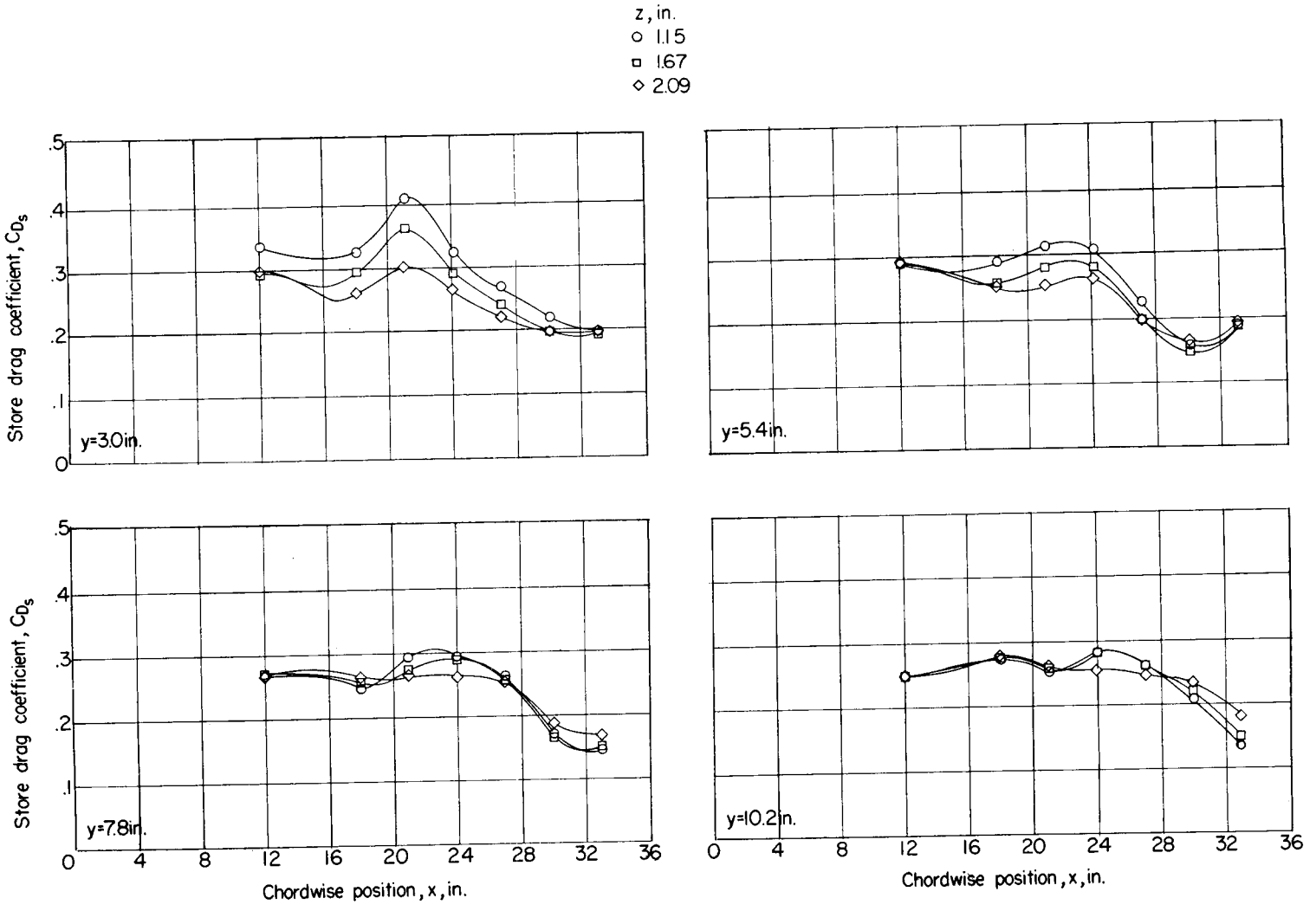

Figure 28.- Effect of vertical position z on store drag (isolated $C_{D_s} = 0.252$). $\alpha = 0^{\circ}$.

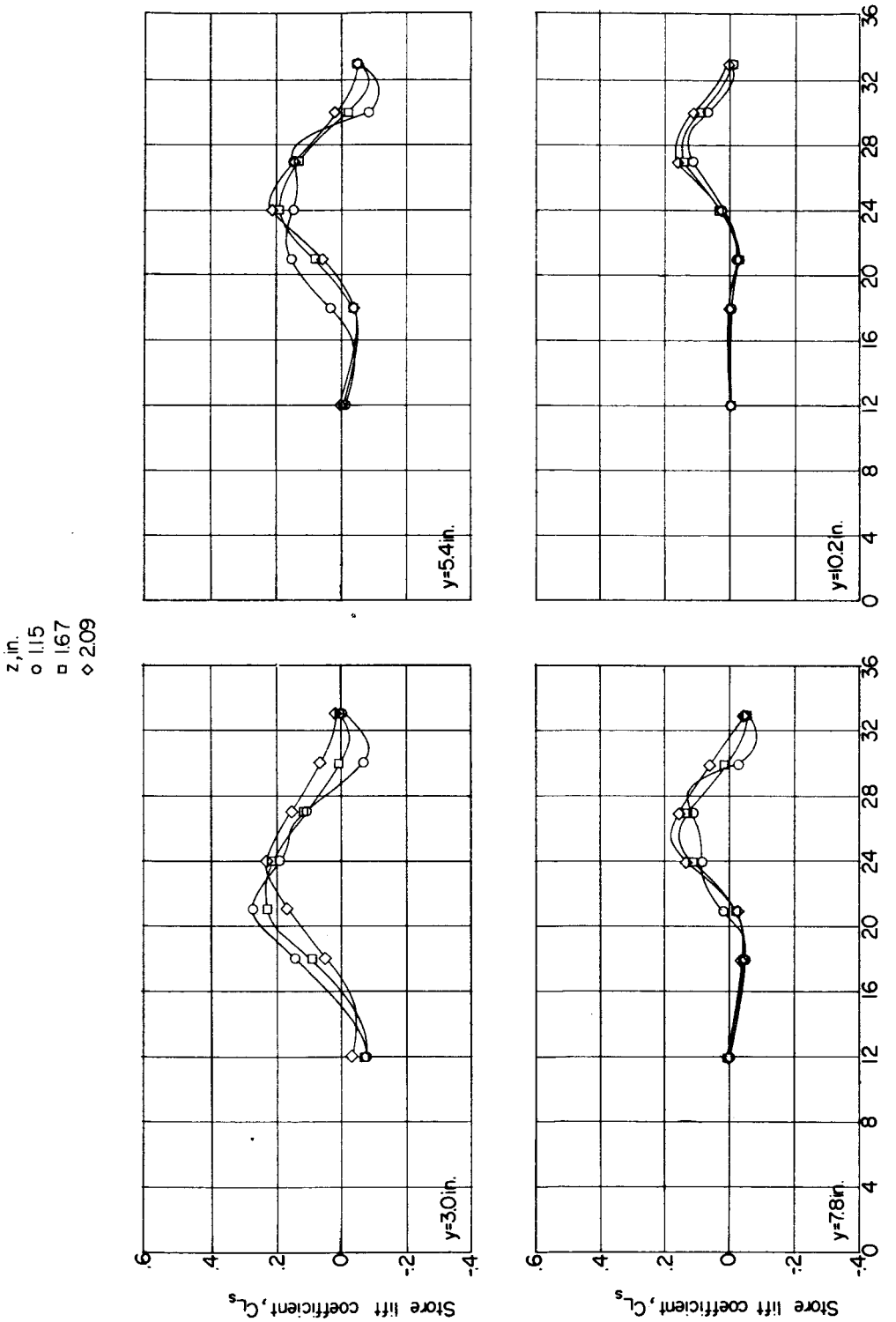

Figure 29.- Effect of vertical position z on store lift. $\alpha = 0^{\circ}$.

[redacted]

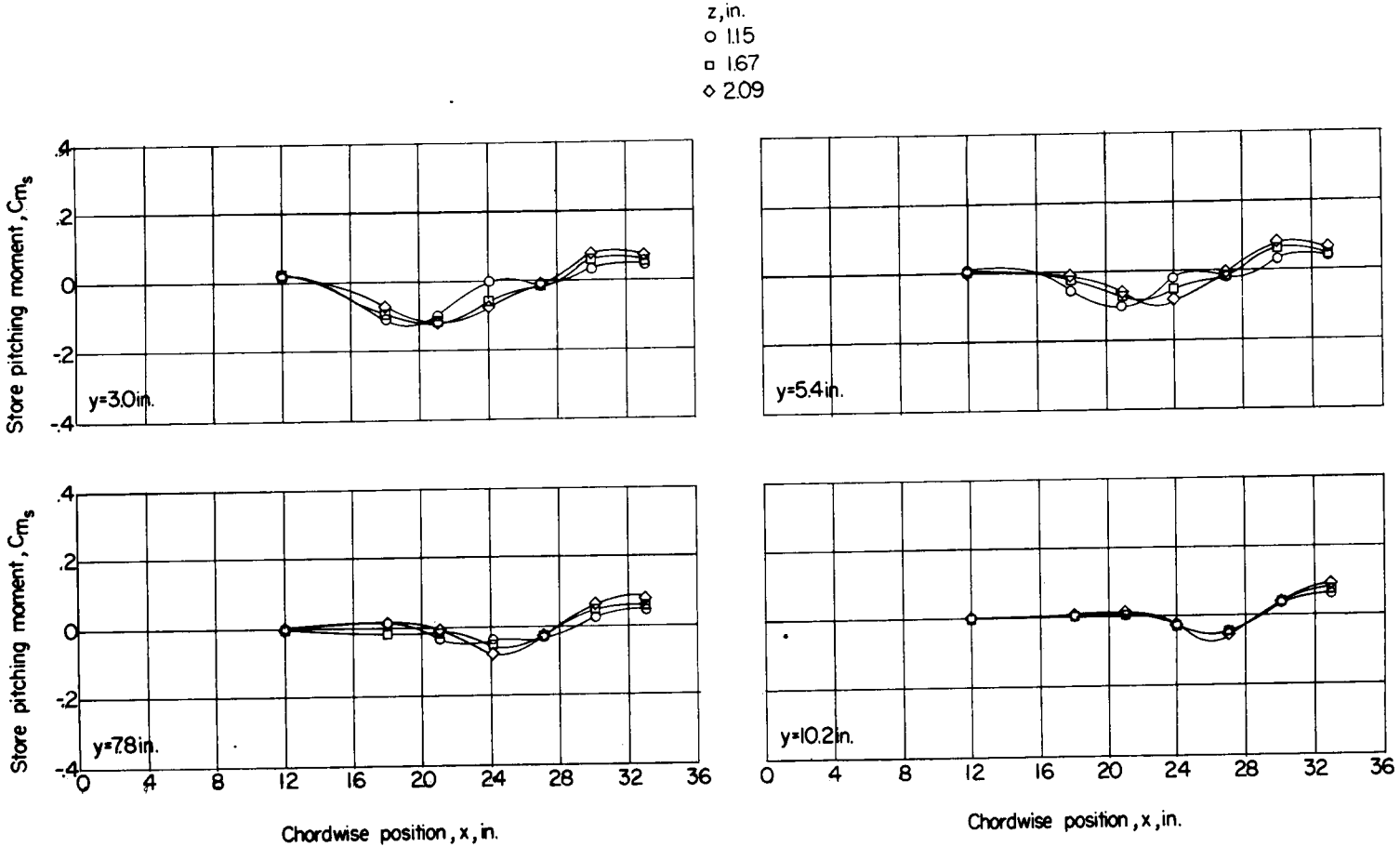

Figure 30.- Effect of store vertical position z on store pitching moment (values recalculated about store midpoint). $\alpha = 0^{\circ}$.

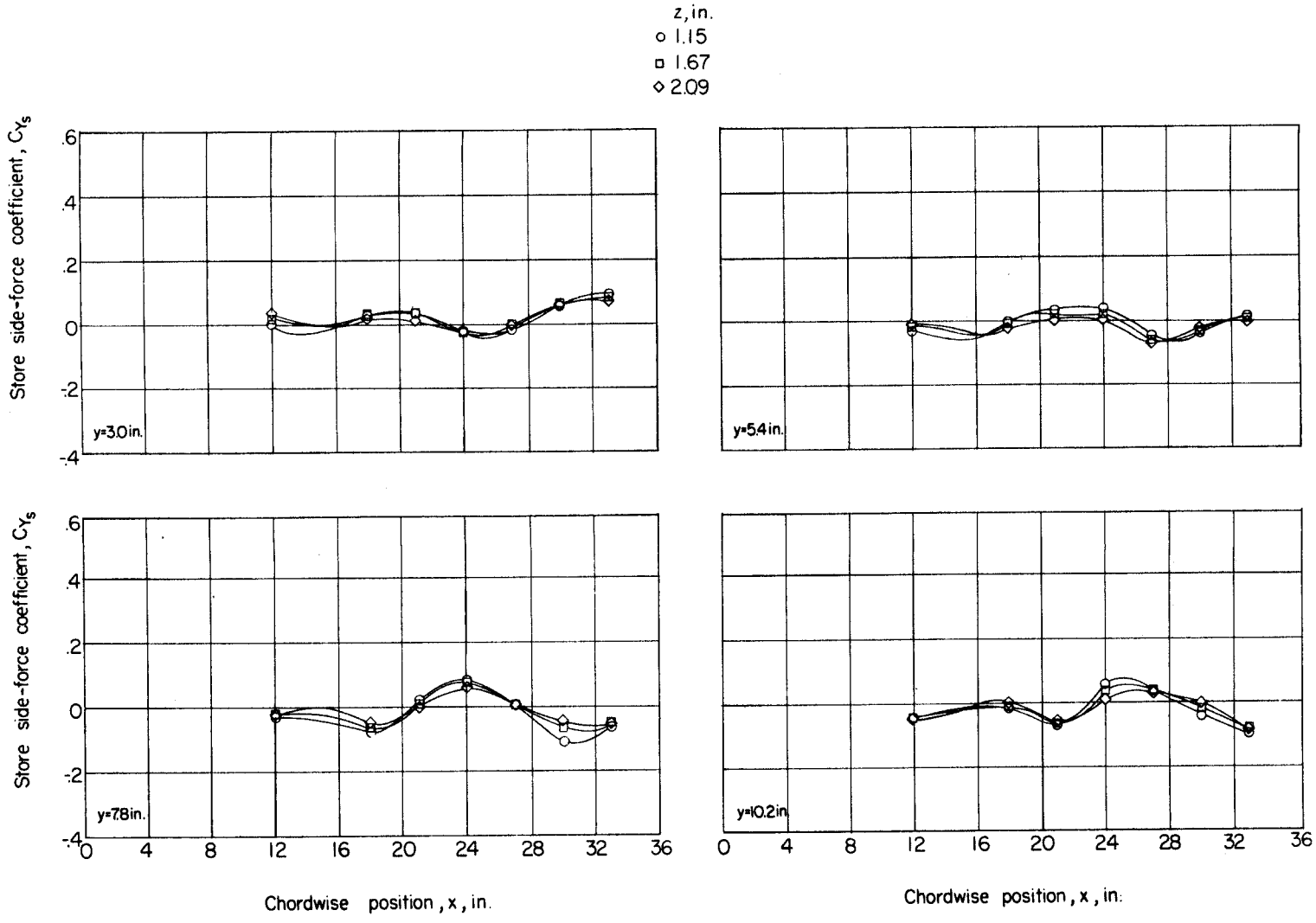

Figure 31.- Effect of store vertical position z on store side force. $\alpha = 0^{\circ}$.

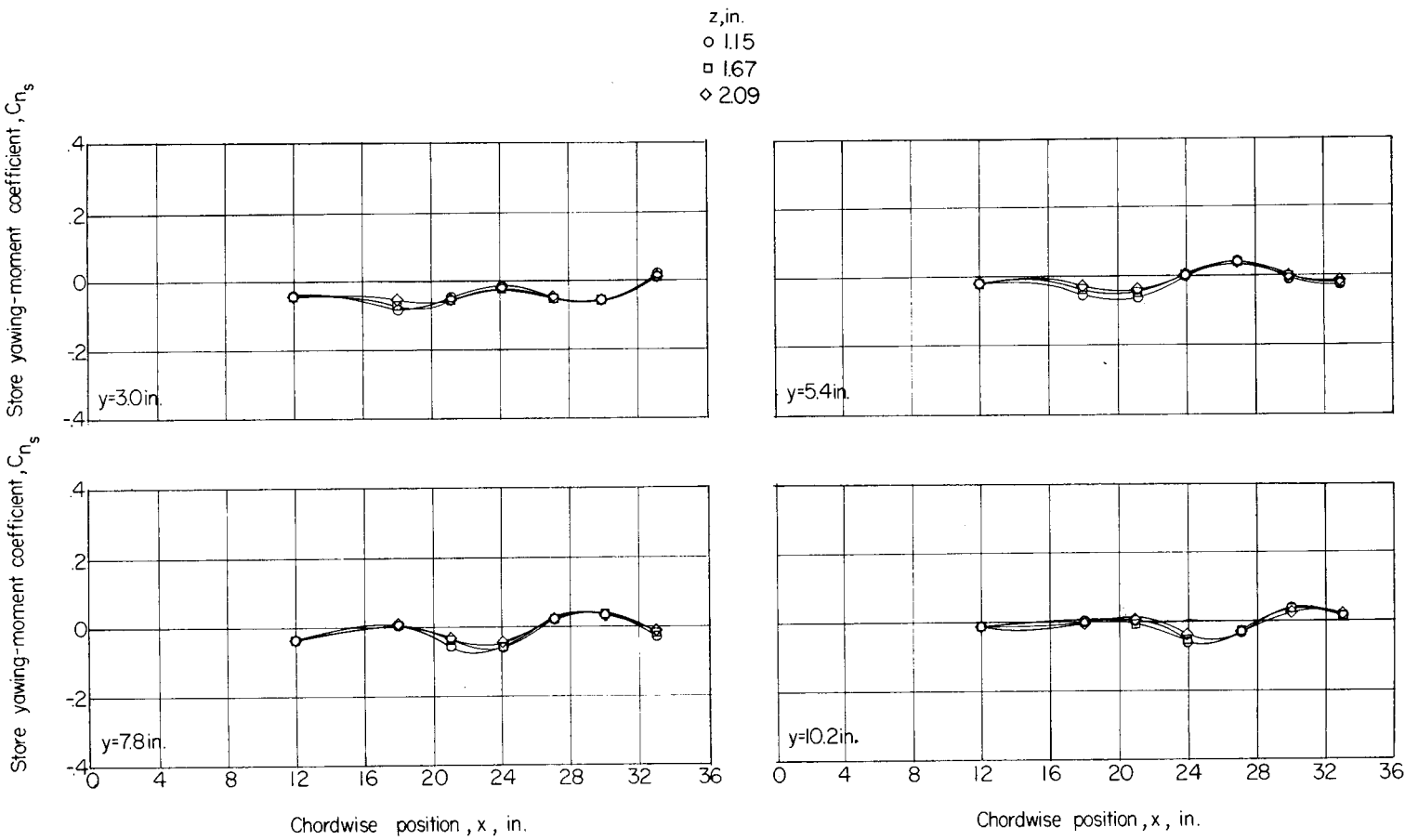

Figure 32.- Effect of store vertical position z on store yawing moment (values recalculated about store midpoint). $\alpha = 0^{\circ}$.

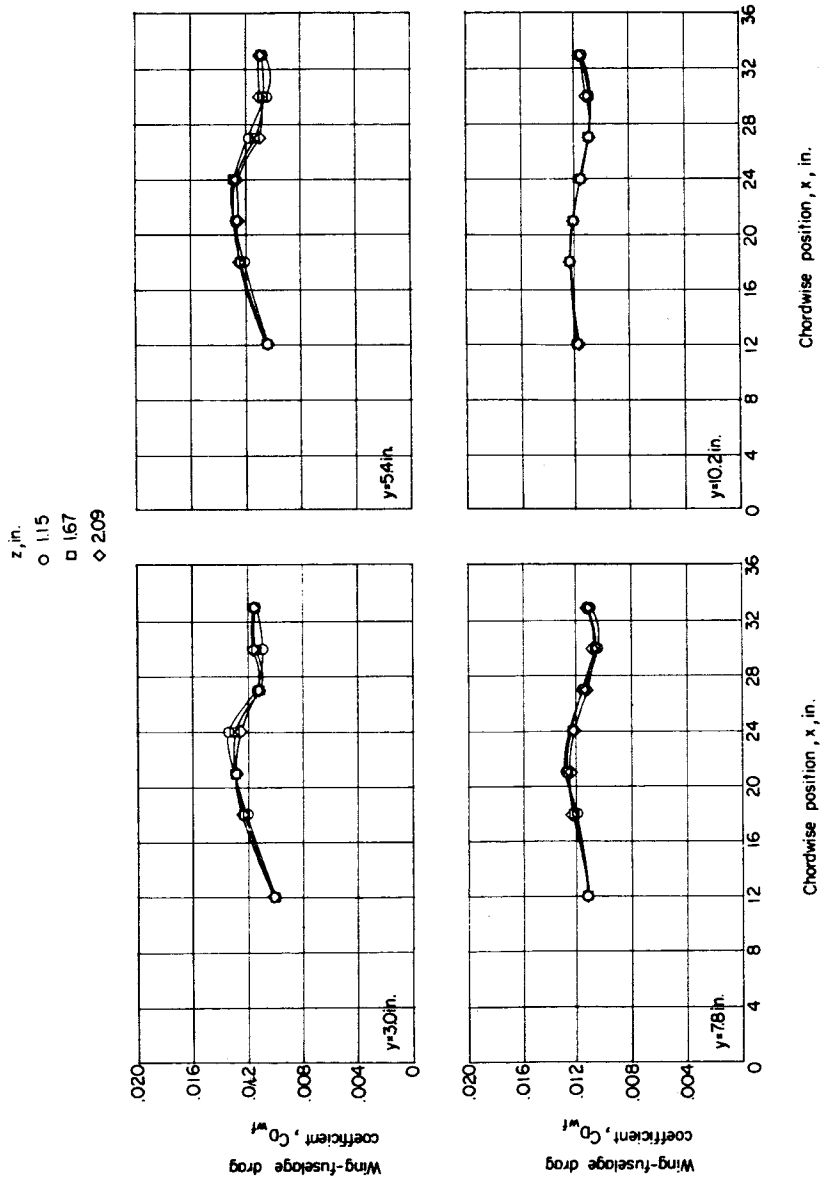

Figure 33.- Effect of store vertical position z on wing-fuselage drag. Isolated $C_{D_{wf}} = 0.0115$; $\alpha = 0^{\circ}$.

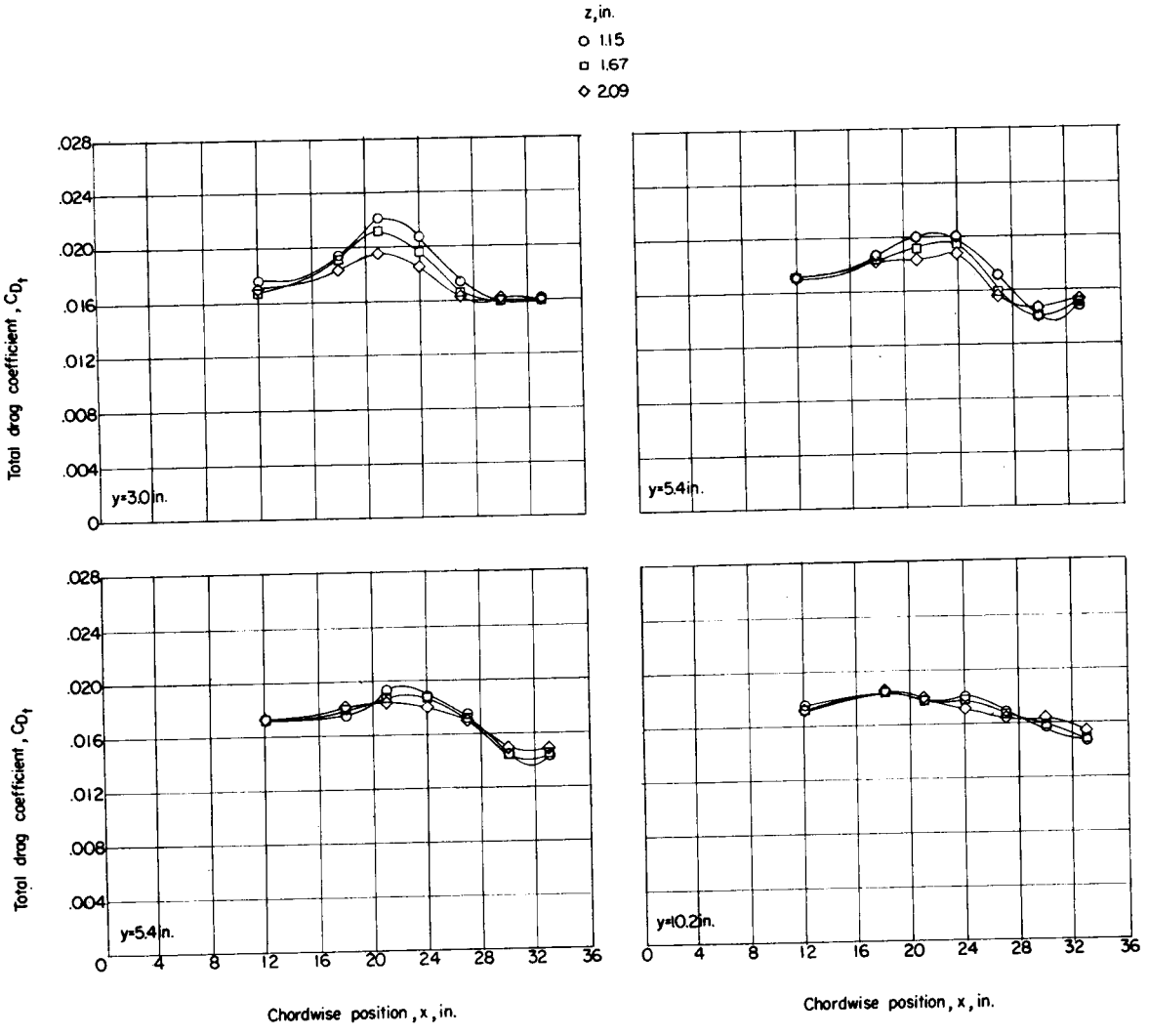

Figure 34.- Effect of store vertical position z on total drag. Isolated $C_{D_t} = 0.0172$; $\alpha = 0^{\circ}$.

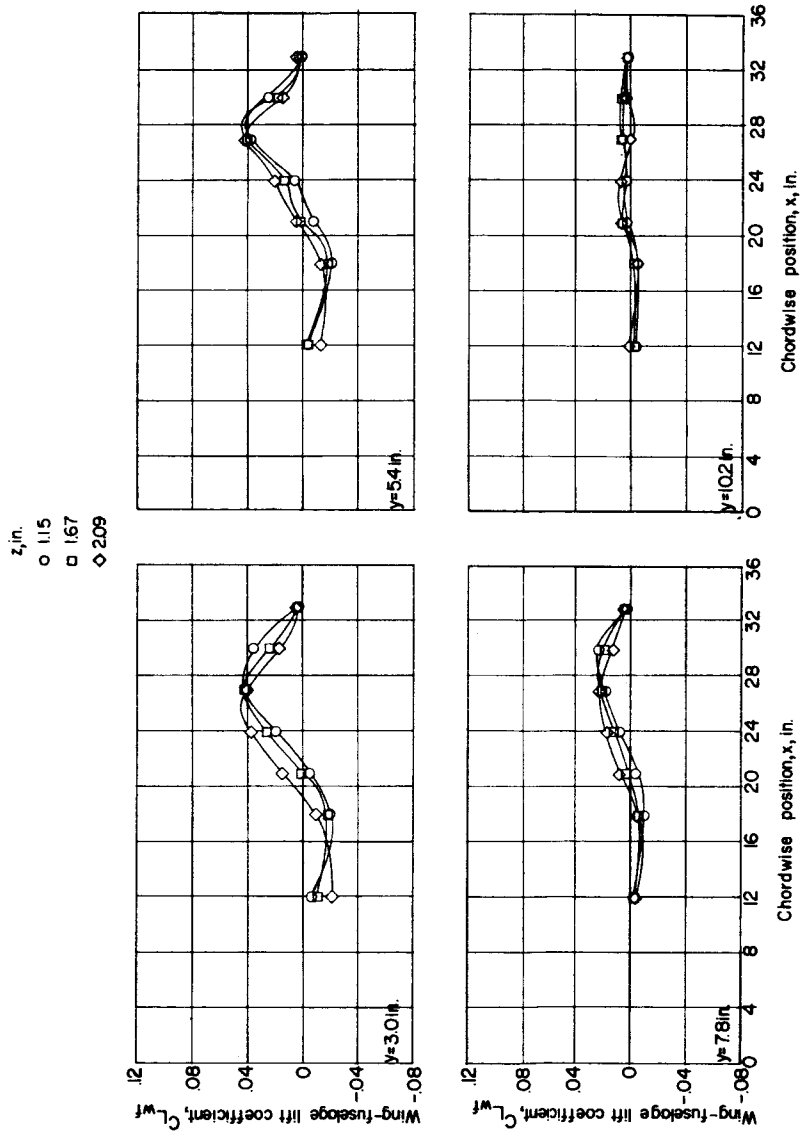

Figure 35.- Effect of store vertical position z on wing-fuselage lift. $\alpha = 0^{\circ}$.

[redacted]

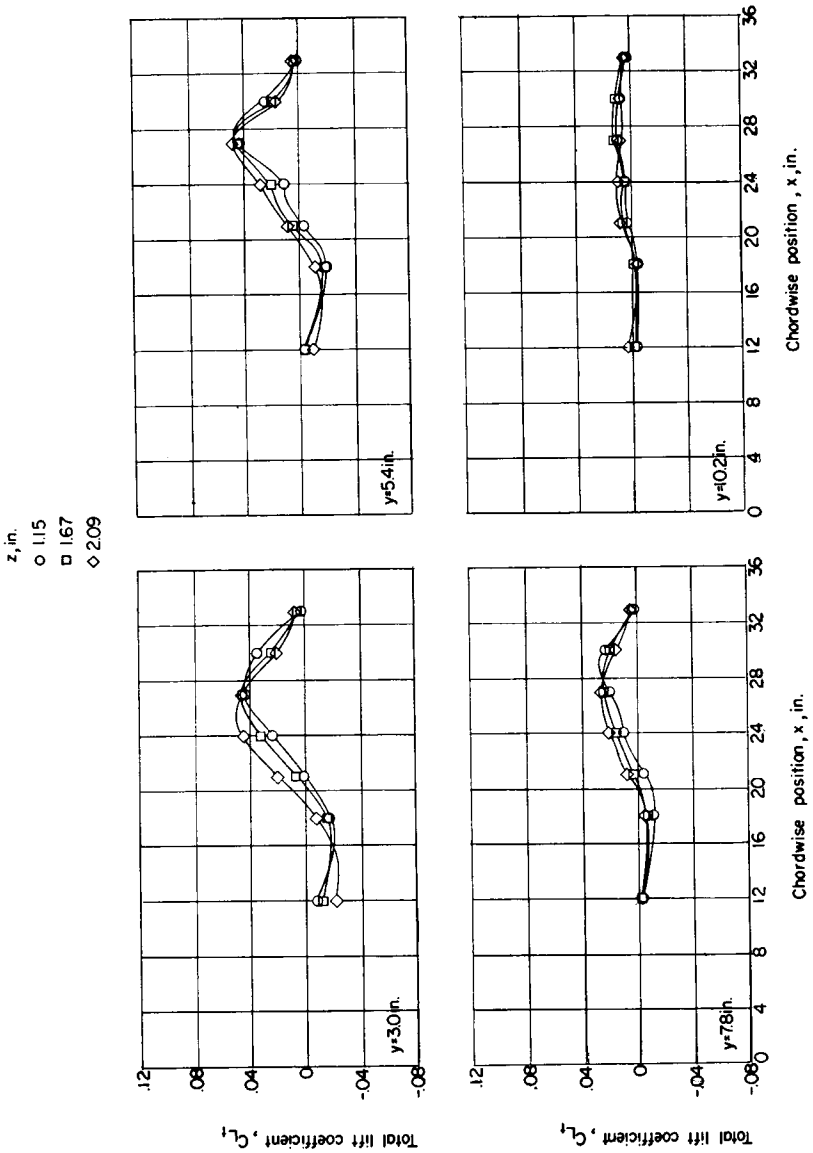

Figure 36.- Effect of store vertical position z on total lift. $\alpha = 0^{\circ}$.

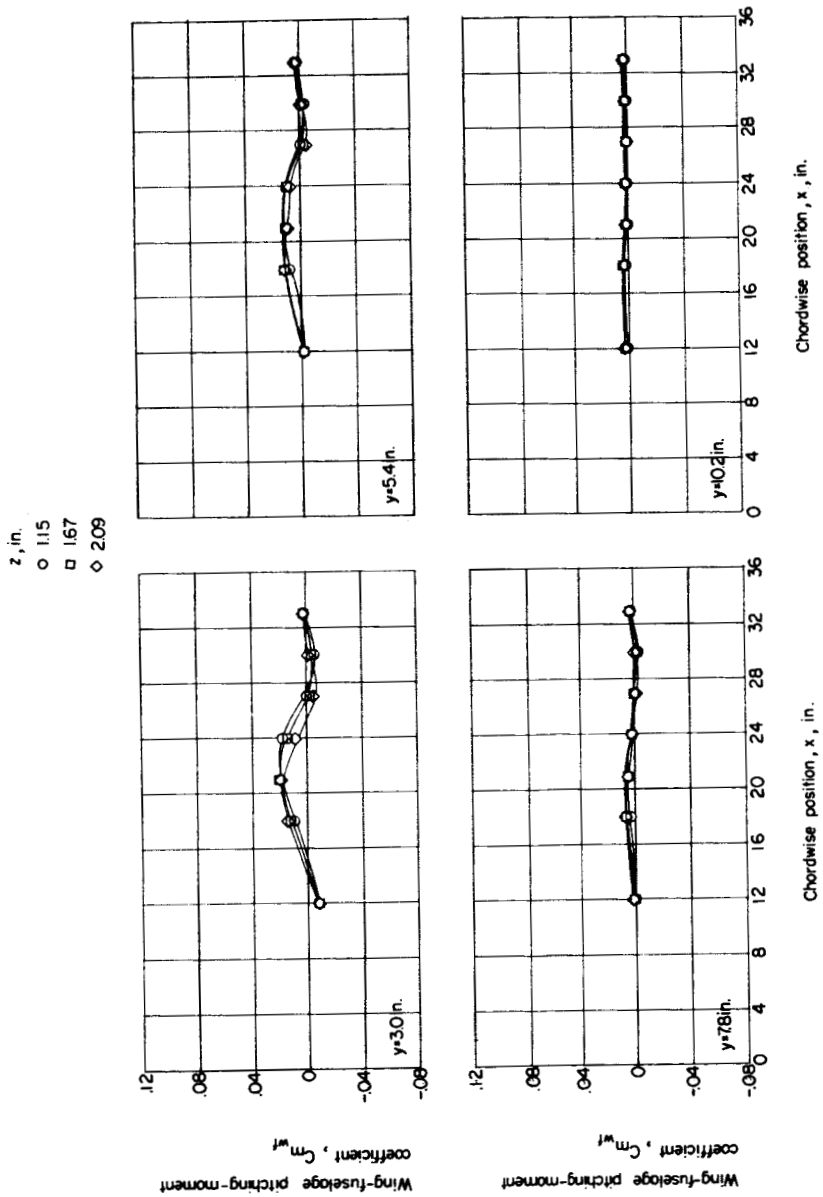

Figure 37.- Effect of vertical position z on wing-fuselage pitching moment (computed about 0.625$\bar{c}$). $\alpha = 0^{\circ}$.

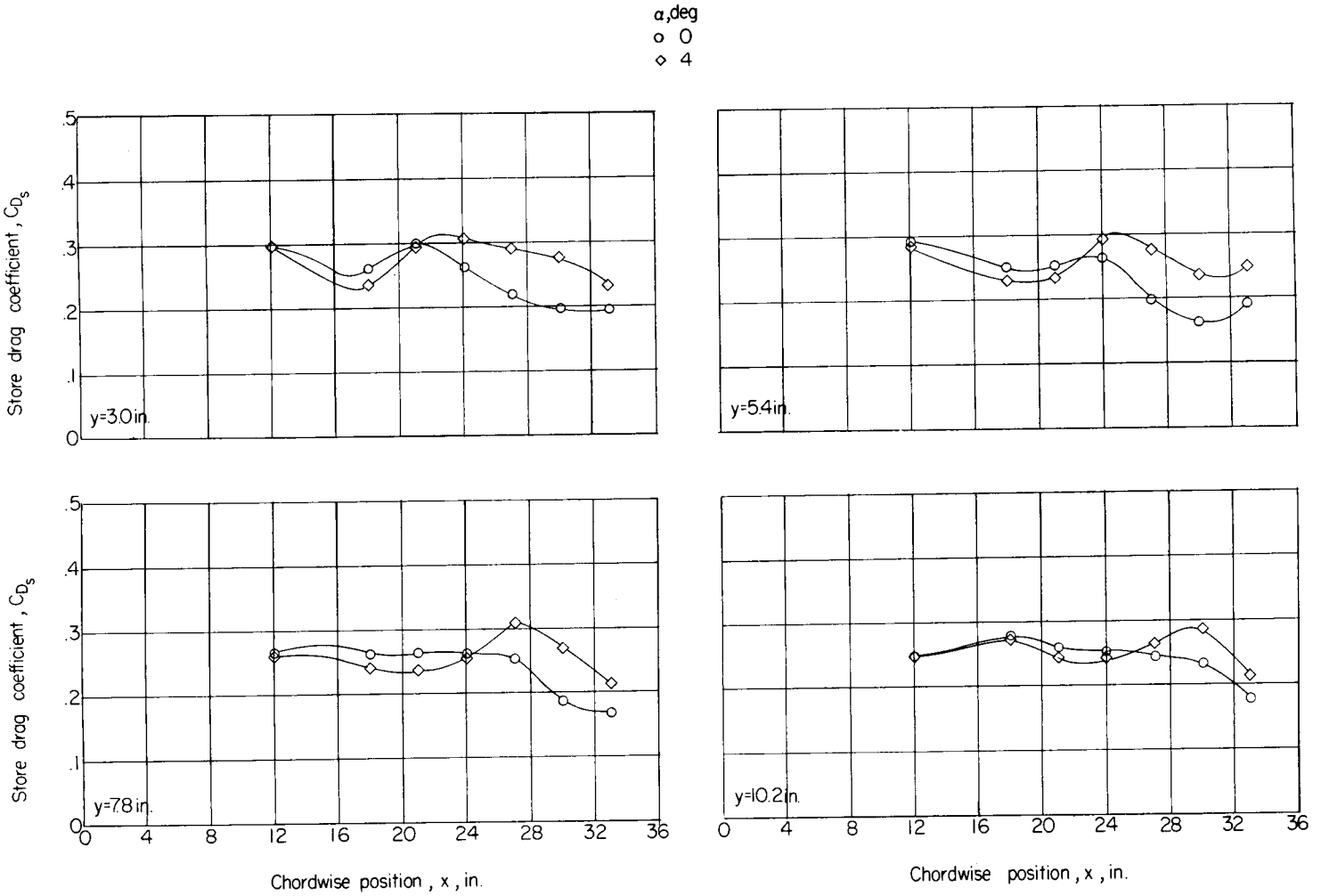

Figure 38.- Effect of angle of attack of wing-fuselage combination on store drag. Isolated C_{D_s} = 0.252; z = 2.09 inches.

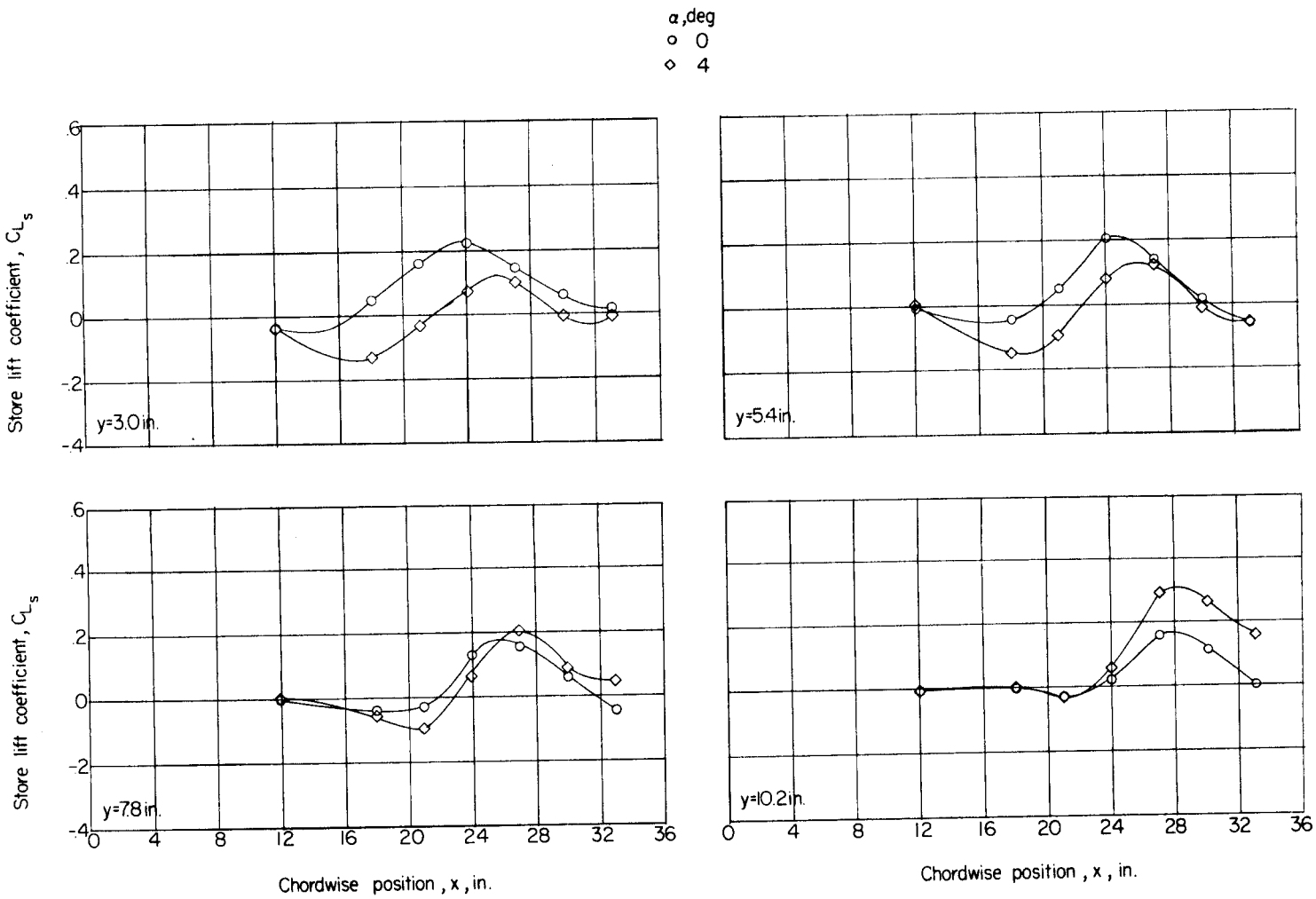

Figure 39.- Effect of angle of attack of wing-fuselage combination on store lift. z = 2.09 inches.

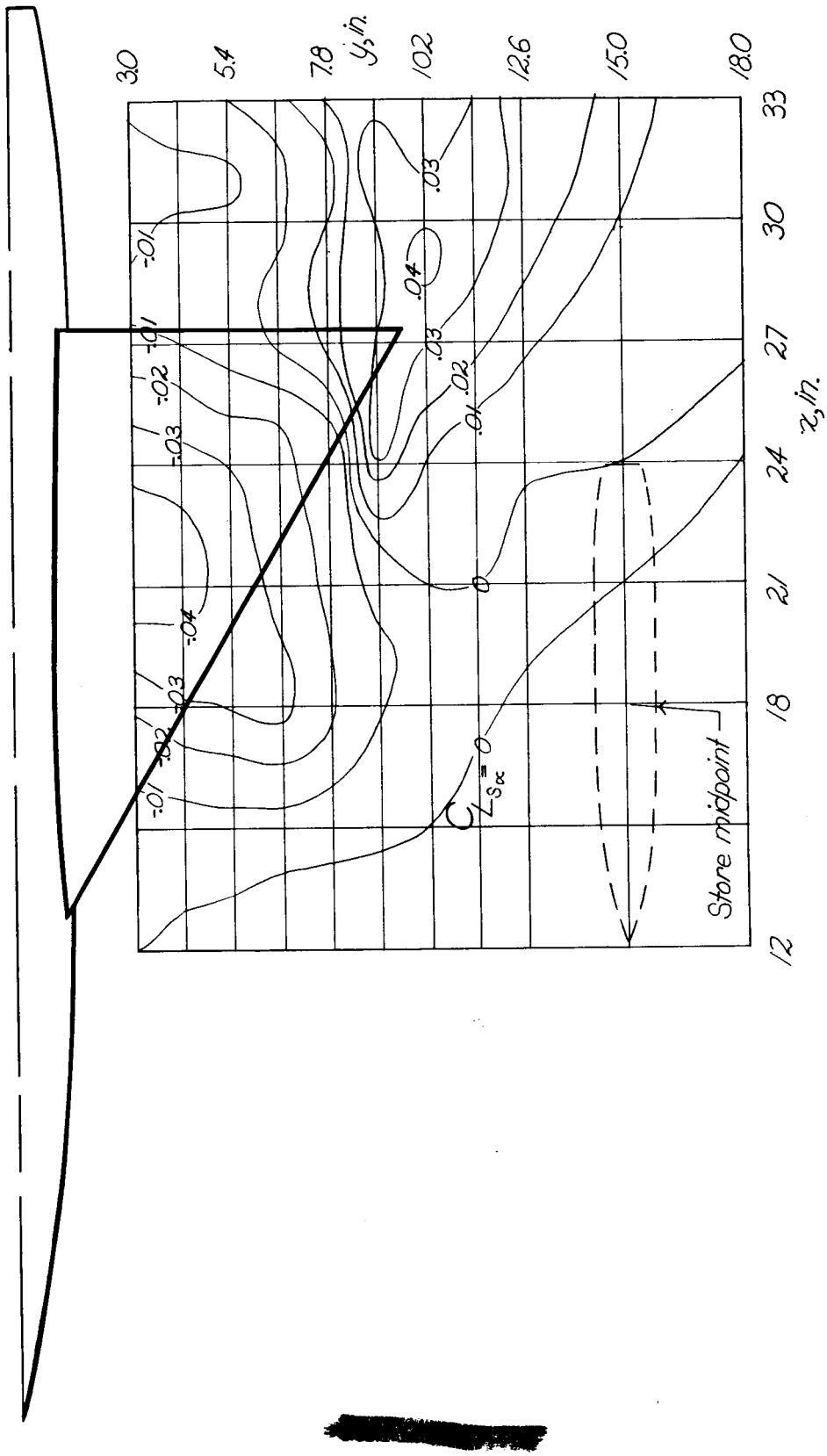

Figure 40.- Contour plot of slope of store lift with wing-fuselage α.
$z = 2.09$ inches.

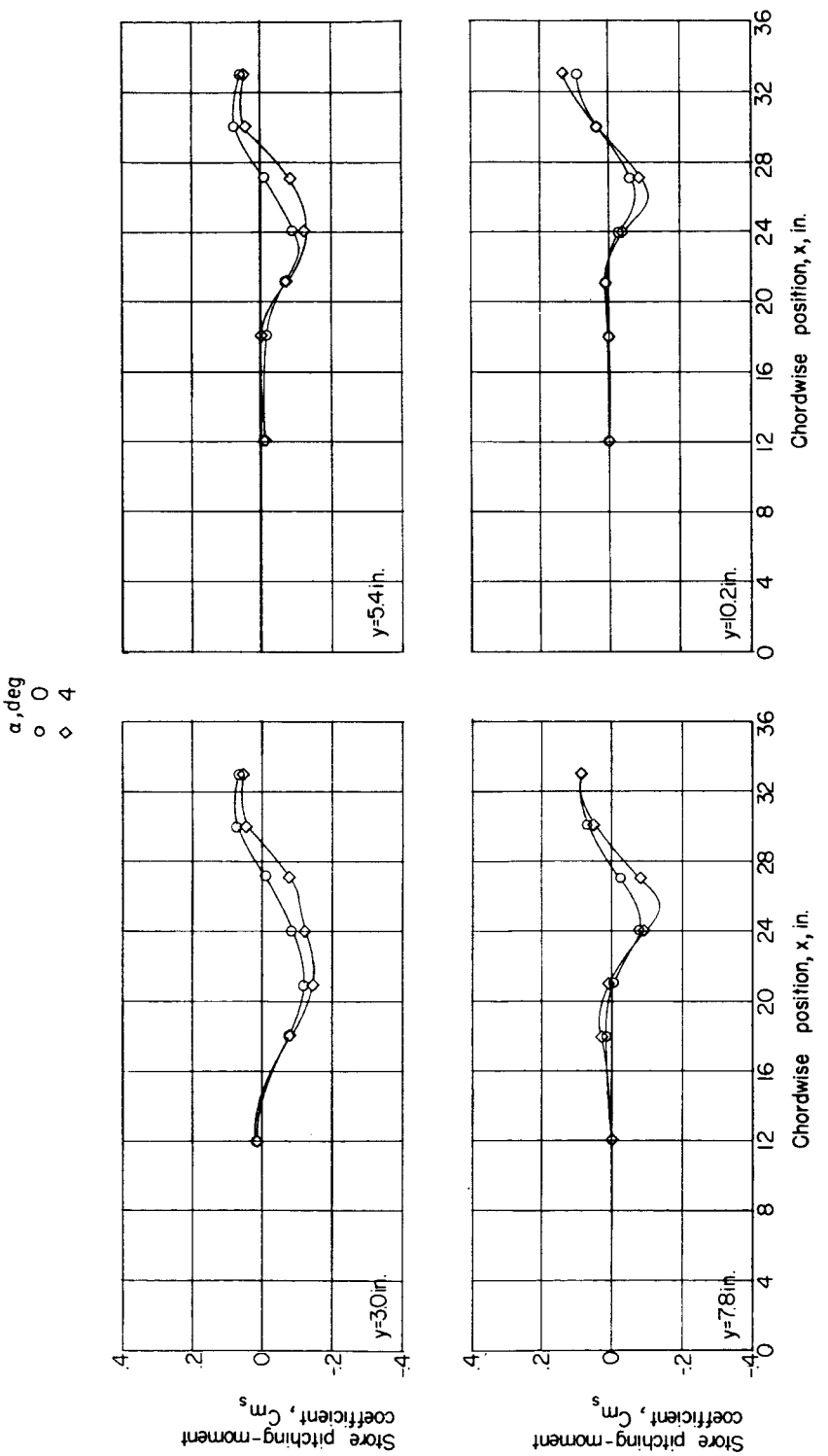

Figure 41.- Effect of angle of attack of wing-fuselage combination on store pitching moment (values recalculated about store midpoint). z = 2.09 inches.

[redacted]

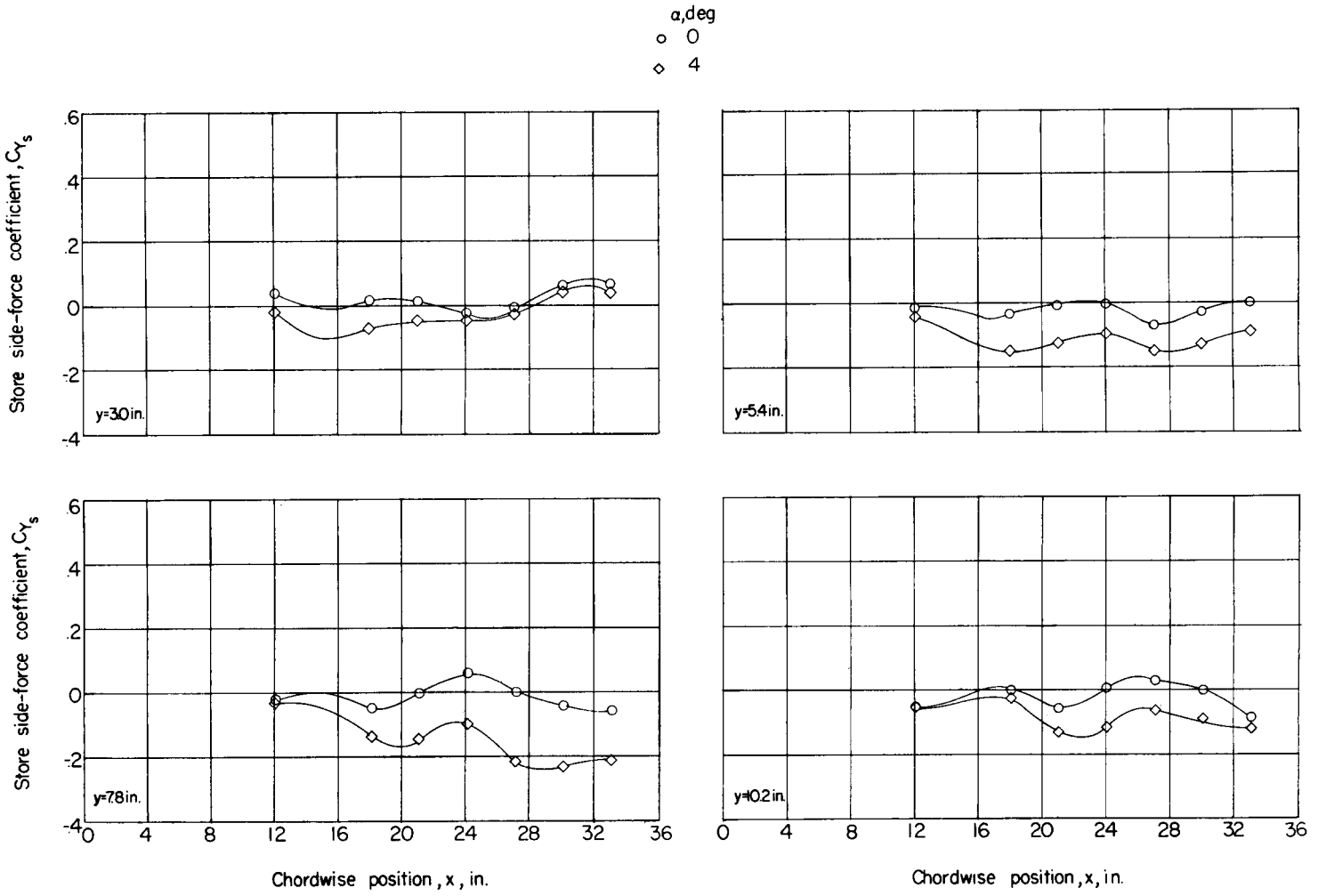

Figure 42.- Effect of α on store side force. z = 2.09 inches.

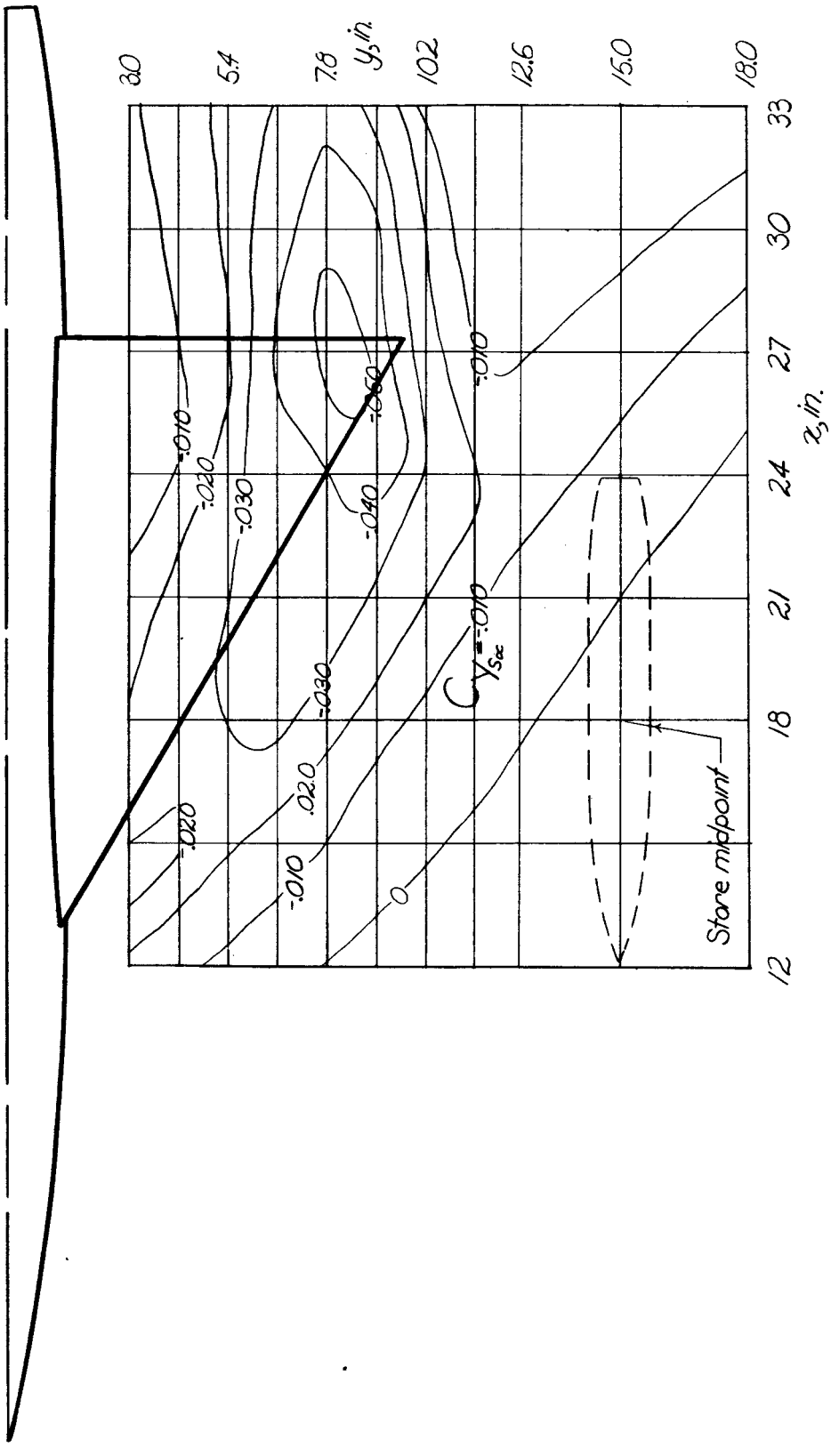

Figure 43.- Contour plot of slope of store side force with α. $z = 2.09$ inches.

[redacted]

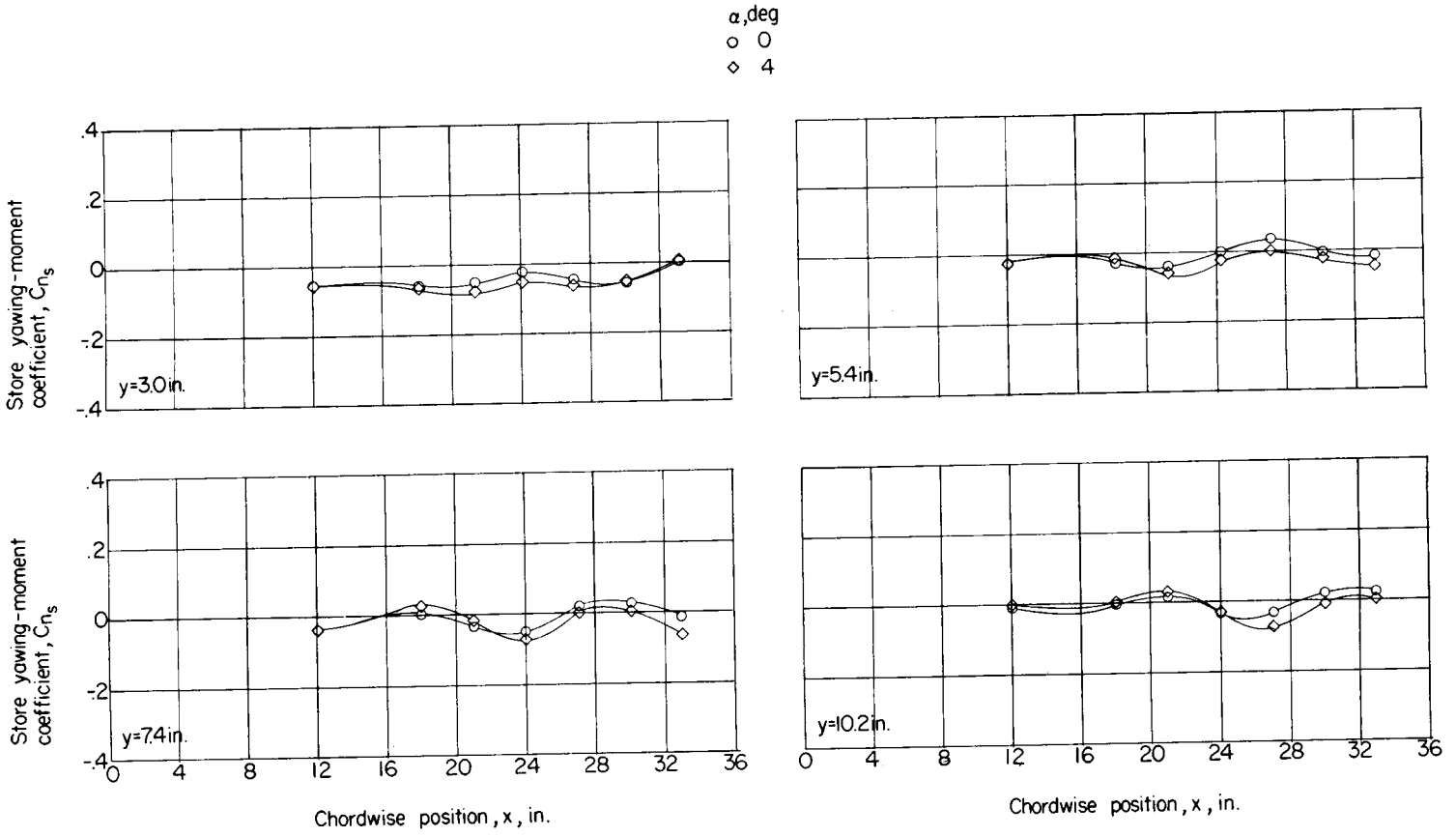

Figure 44.- Effect of angle of attack of wing-fuselage combination on store yawing moment (values recalculated about store midpoint). z = 2.09 inches.

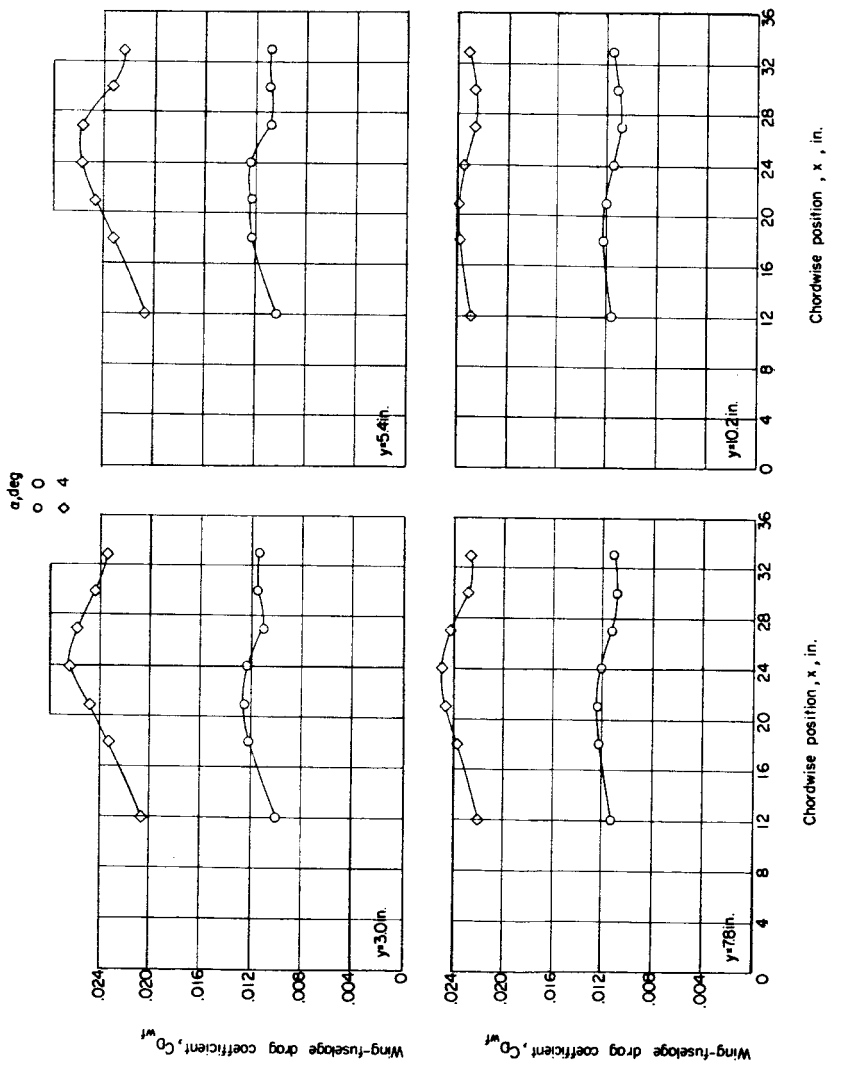

Figure 45.- Effect of angle of attack of wing-fuselage combination on wing-fuselage drag. z = 2.09 inches.

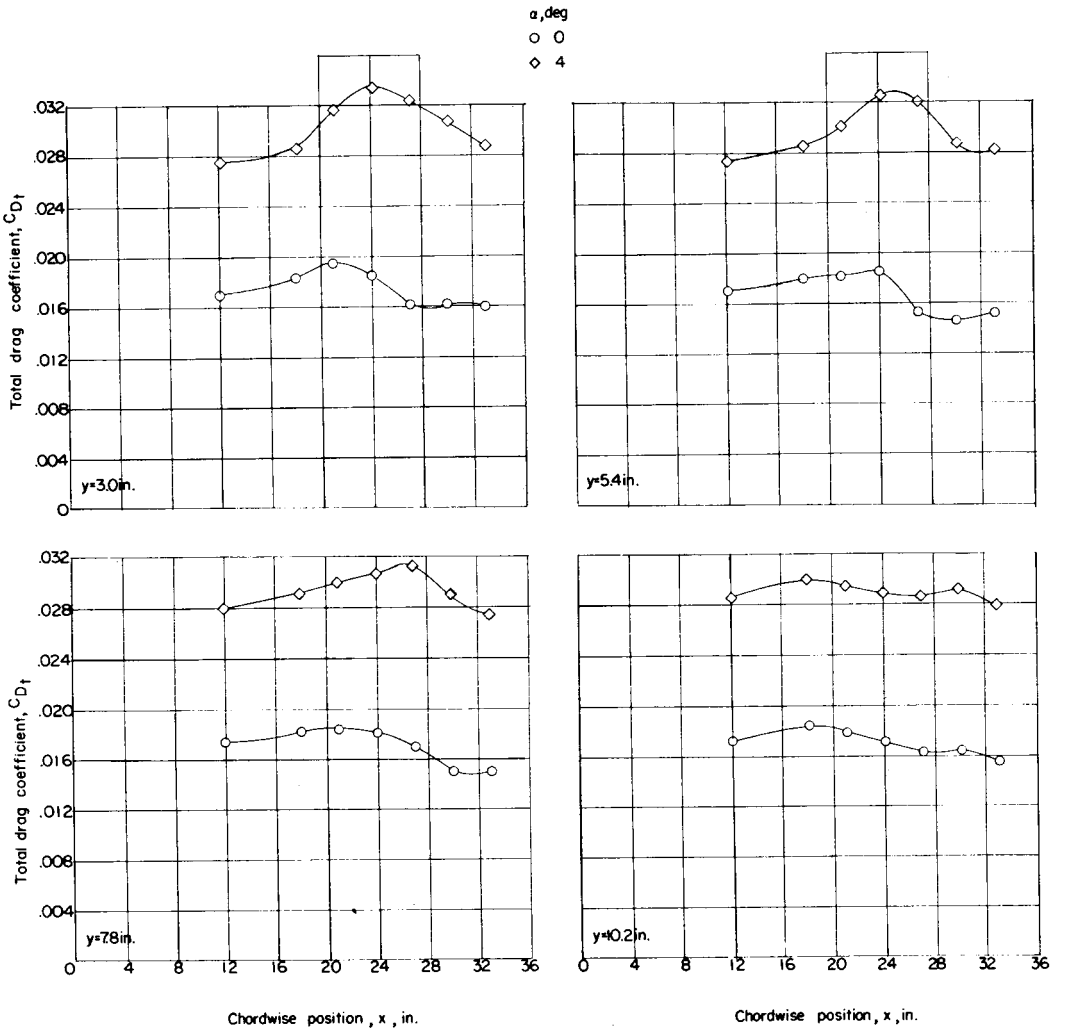

Figure 46.- Effect of angle of attack of wing-fuselage combination on total drag. z = 2.09 inches.

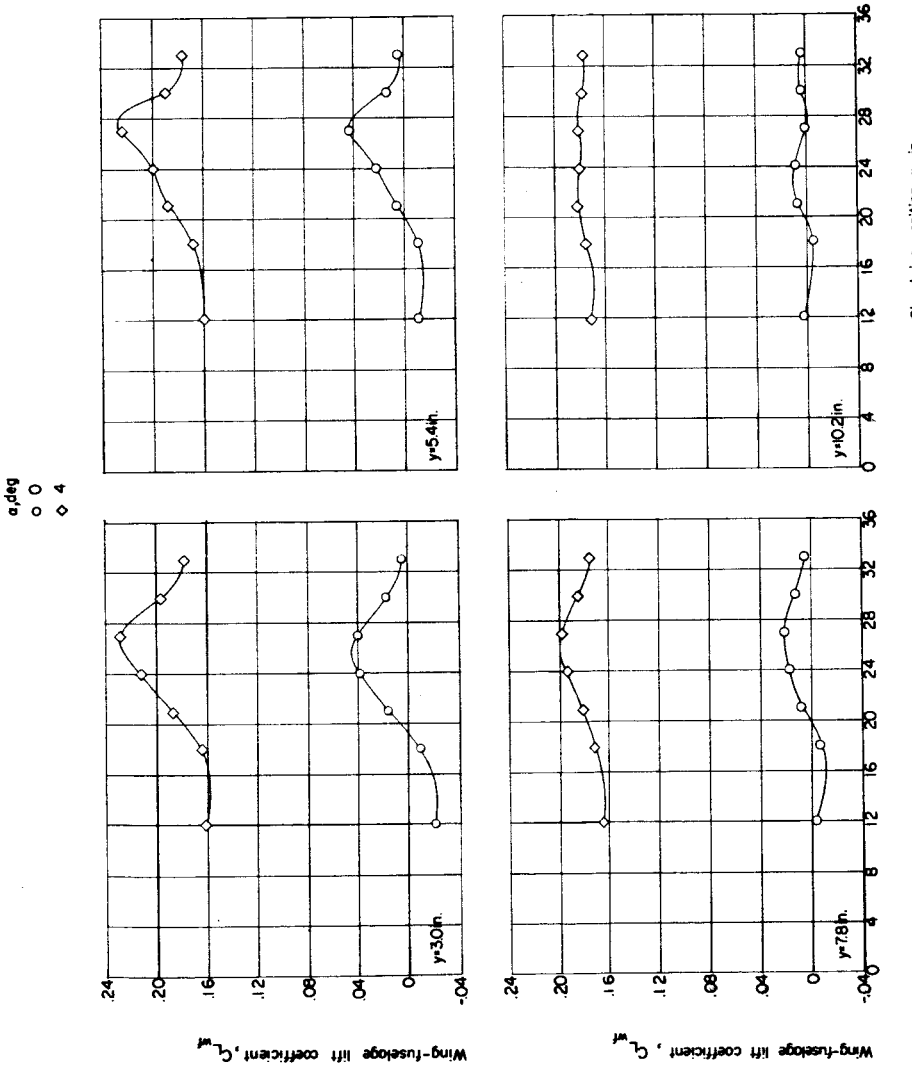

Figure 47.- Effect of angle of attack of wing-fuselage combination on wing-fuselage lift. z = 2.09 inches.

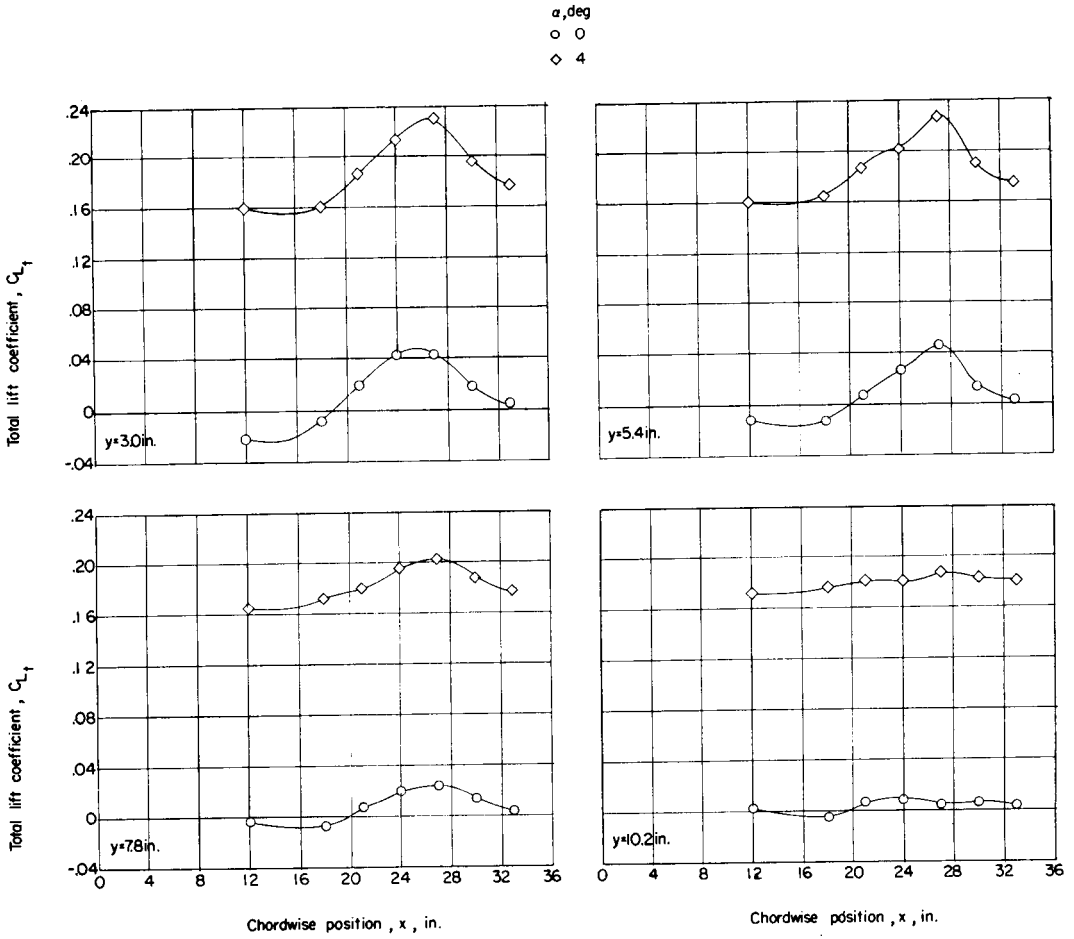

Figure 48.- Effect of angle of attack of wing-fuselage combination on total lift. z = 2.09 inches.

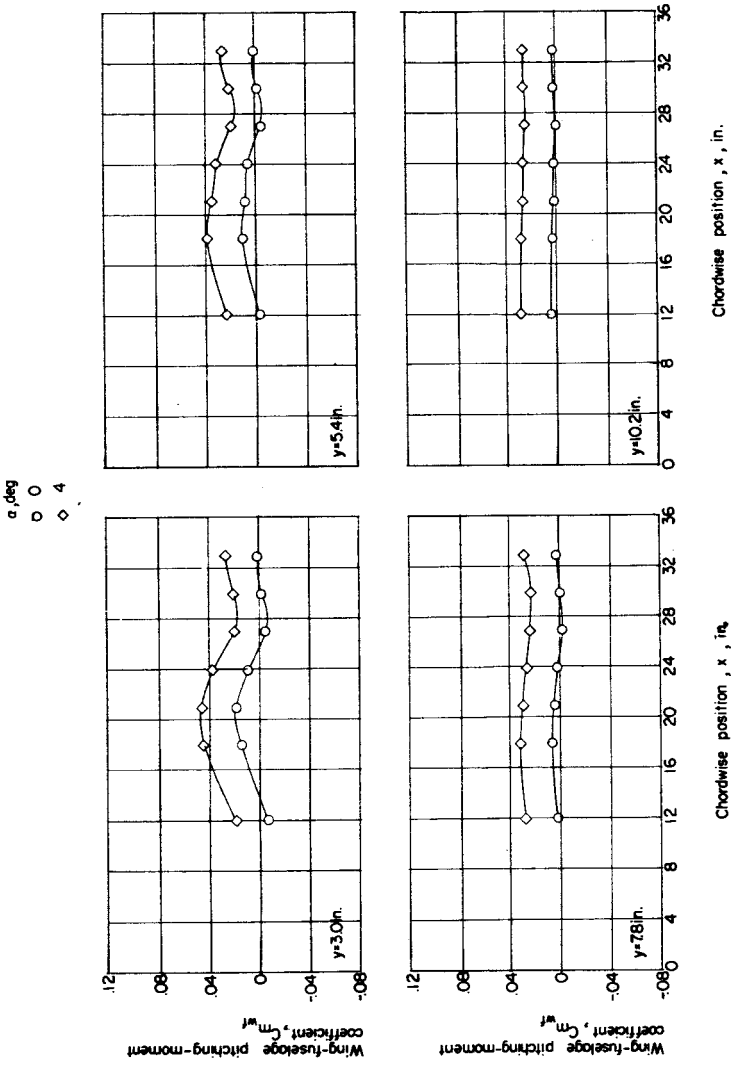

Figure 49.- Effect of angle of attack of wing-fuselage combination on wing-fuselage pitching moment. z = 2.09 inches.

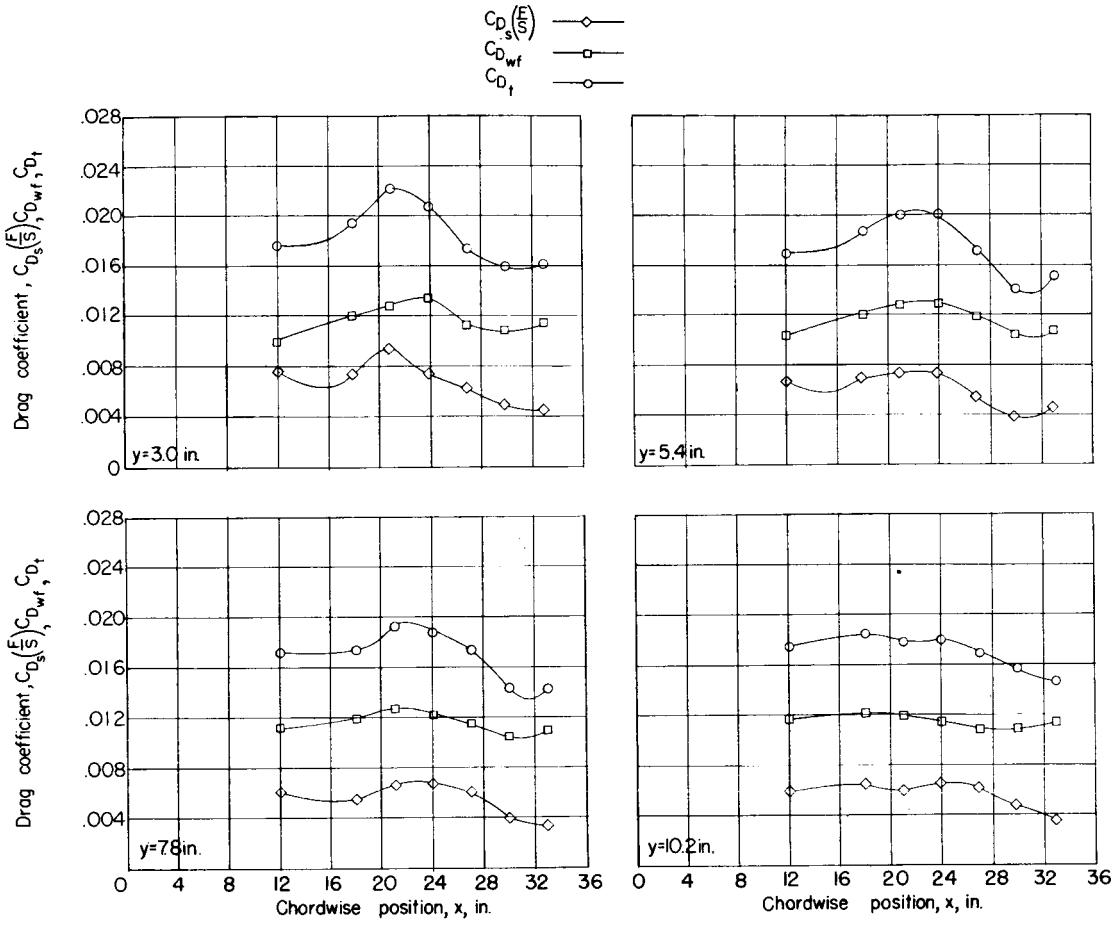

Figure 50.- Relative contribution of store drag and wing-fuselage drag to total drag. z = 1.15 inches; $\alpha = 0^{\circ}$.

[redacted]

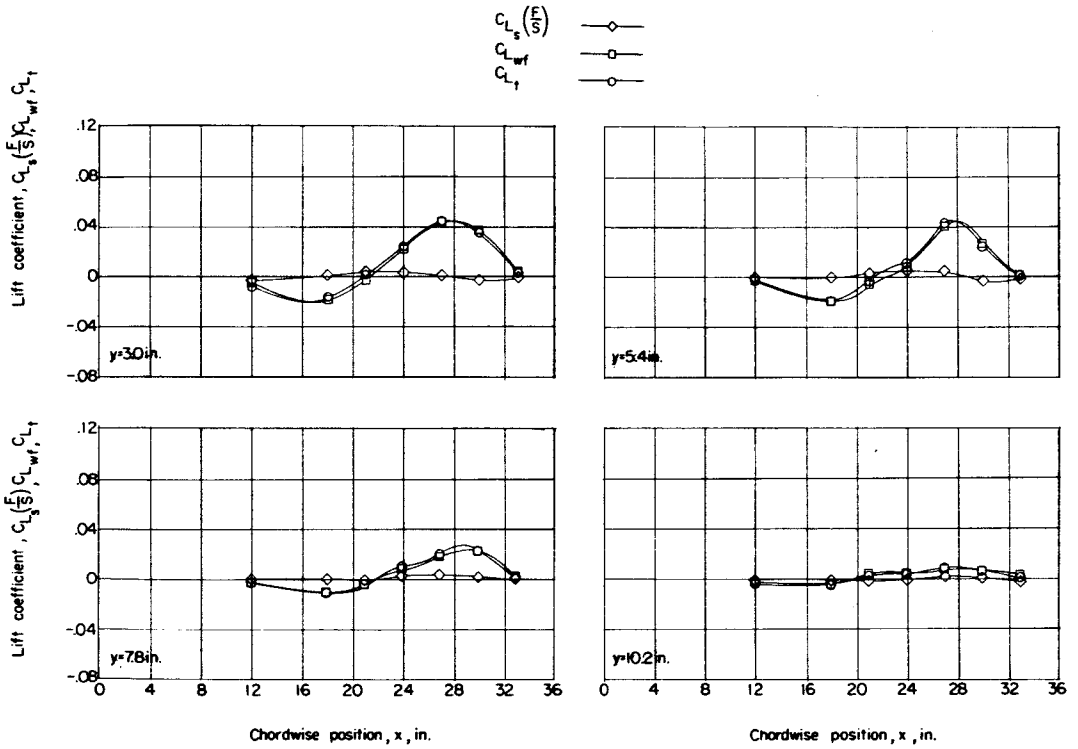

Figure 51.- Relative contribution of store lift and wing-fuselage lift to total lift. z = 1.15 inches; $\alpha = 0^{o}$.

[redacted]

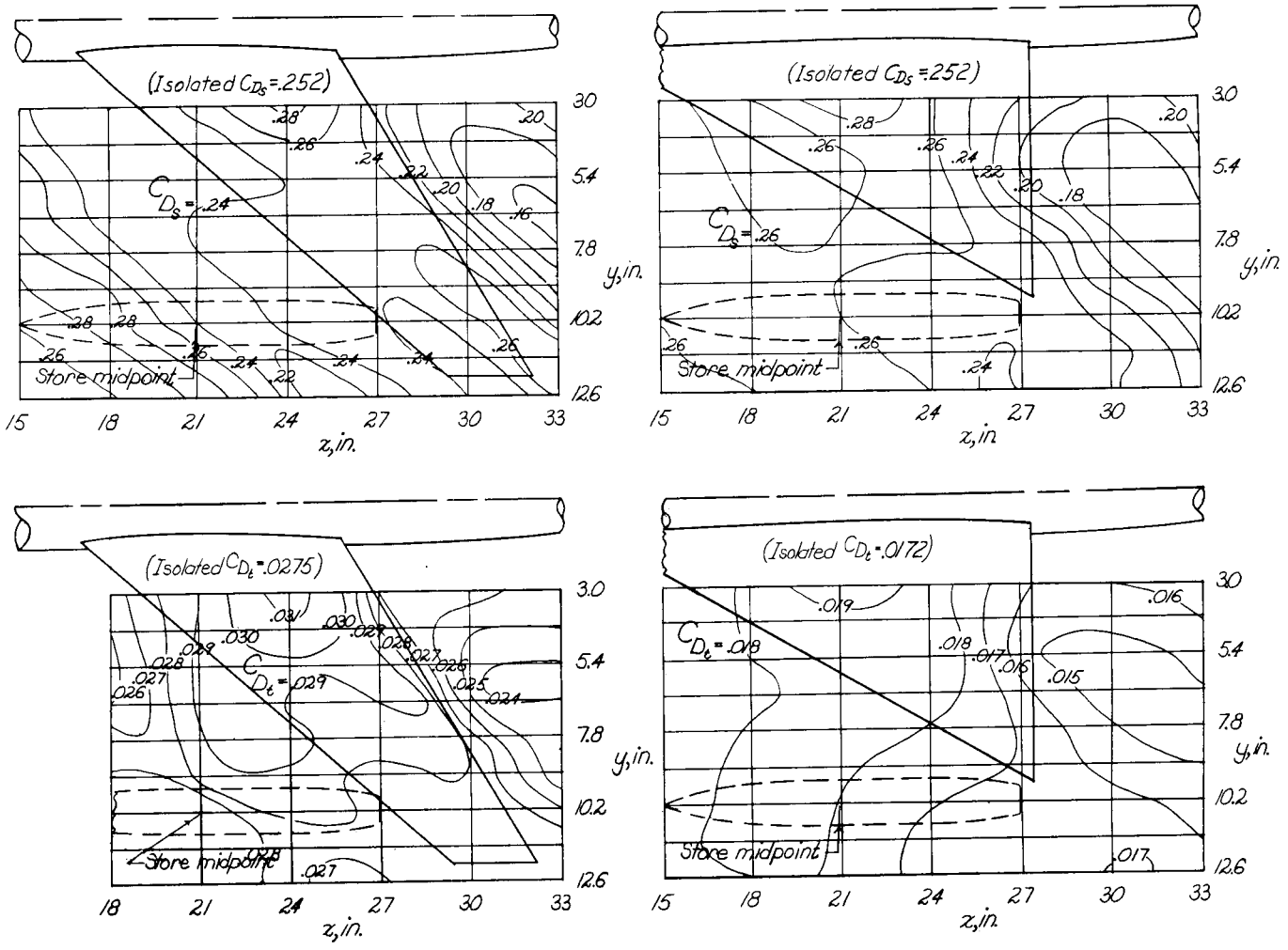

Figure 52.- Comparison of store-drag and total-drag contour plots for the swept wing (ref. 2) and the delta wing. z = 2.09 inches; $\alpha = 0^{\circ}$; M = 1.61.

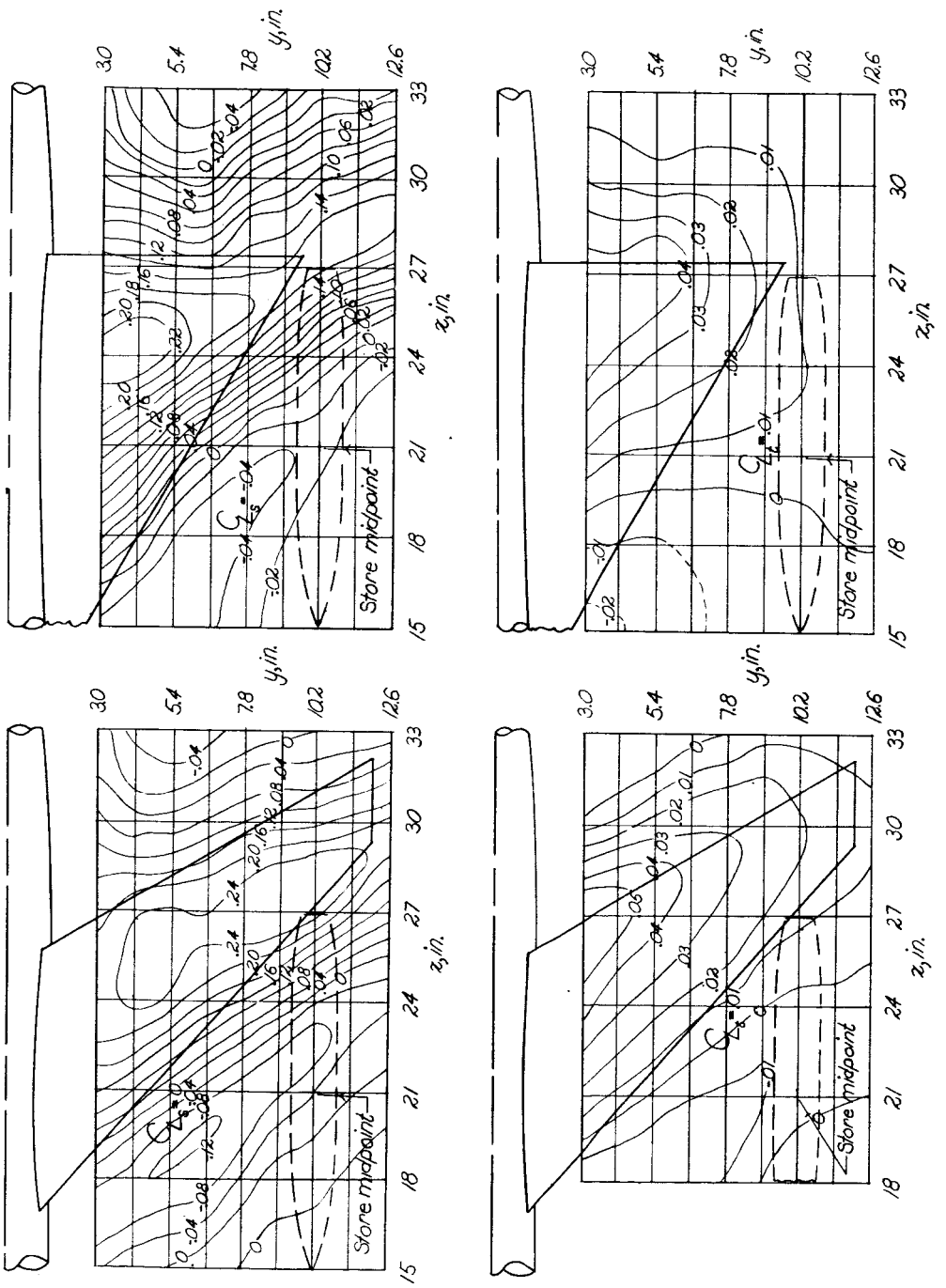

Figure 53.- Comparison of store-lift and total-lift contour plots for the swept wing (ref. 3) and the delta wing. z = 2.09 inches; $\alpha = 0^\circ$; M = 1.61.